X-Ray Bursts

WALTER H. G. LEWIN[1,2,3], JAN VAN PARADIJS[2,3] and RONALD E. TAAM[4]

[1] *Massachusetts Institute of Technology, Physics Department, Center for Space Research, MIT 37–627, Cambridge, MA 02139, USA*
[2] *Astronomical Institute "Anton Pannekoek", University of Amsterdam, and Center for High Energy Astrophysics, Kruislaan 403, 1098 SJ Amsterdam, The Netherlands*
[3] *Institute of Space and Astronautical Sciences, 3–1–1 Yoshinodai, Sagamihara-shi, 229 Japan*
[4] *Department of Physics and Astronomy, Northwestern University, 2145 Sheridan Rd., Evanston, IL 60208, USA*

(submitted October 1992)

Table of Contents

Space Science Reviews **62:** 223–389, 1993.

1. Introduction

1.1. Progress during the Past Decade

Since the last comprehensive reviews on X-ray bursts were written about a decade ago by Lewin and Joss (1981, 1983), many new data have become available on type I bursts (thermonuclear flashes on the surface of a neutron star) and type II bursts from the Rapid Burster (spasmodic accretion) largely from observations with Tenma, EXOSAT, and Ginga. Also much theoretical work has been done during the last decade. (i) The number of type I burst sources, all of which are low-mass X-ray binaries (LMXB), has increased from ~32 to ~40 (see Chapter 9). (ii) Photospheric radius expansion of the neutron star atmosphere during very strong type I X-ray bursts has been well established and has led to the possibility, at least in principle, of measuring both the mass and radius of neutron stars thereby gaining information about the equation of state of neutron star matter (Sect. 3.4 and 4.5). (iii) A 4.1 keV absorption line was detected in several type I burst spectra from different sources, the origin of which is unclear (Sect. 3.3, 4.6.1, 5.5). (iv) Following the discovery of the intensity-dependent quasi-periodic oscillations (QPO) in the X-ray flux of the bright LMXB GX 5–1 in 1984, the examination of power density spectra and color-color diagrams of a dozen LMXB led to a classification of "Z" and "atoll" sources; it appears that burst sources are largely (but not exclusively) atoll sources, and that several type I burst properties depend on the spectral state of the source (Sect. 2.5 and 3.8). (v) The evolutionary connection between LMXB and msec radio pulsars has come into focus during the past decade, and (vi) new ideas have evolved about the magnetic-field decay of neutron stars in LMXB (Sect. 2.4). (vii) QPO were detected in type II bursts (first in 1982) as well as in the persistent emission of the Rapid Burster (Sect. 7.10). (viii) Several new peculiarities have been detected in the type II bursts and in the persistent emission from the Rapid Burster (Sects. 7.5 and 7.7). (ix) Much theoretical work was done during the past decade on neutron star model atmospheres, on the interpretation of the burst spectra (Chapter 5), and on the theory of the thermonuclear flashes themselves (Chap. 6). (x) Little progress was made in understanding the behavior of the Rapid Burster (Chapter 8).

Recent theoretical work (Bildsten *et al.* 1992) suggests the possibility for the significant depletion of CNO elements by nuclear spallation reactions which may

have an important impact on models for type I bursts.

1.2. The Content of this Review

This review is largely based on results that were published before January 1, 1992. We will start with a brief history with the highlights that shaped the present ideas (Sect. 1.3). This will be followed by a chapter describing the characteristics of galactic bulge sources of which the burst sources are a subset. In Chapter 3 we discuss the properties of type I bursts in detail. In Chapter 4 we discuss the various methods, using type I X-ray bursts, to derive constraints on the mass-radius relation of neutron stars in burst sources. The spectra of type I bursts are discussed in Chapter 5 and the theory of the bursts in Chapter 6. The Rapid Burster is separately discussed in Chapter 7 and the rather limited theory of the type II bursts and our understanding of the unique behavior of the Rapid Burster are discussed in Chapter 8. Chapter 9 contains a description of some selected important features for each of the known burst sources (e.g., orbital periods, optical identifications, globular-cluster membership, distances, nature of the companion, ...).

1.3. Brief History – Highlights

X-ray bursts were discovered in 1975 independently by Grindlay *et al.* (1976a) and Belian, Conner and Evans (1976). Grindlay *et al.* (1976a) observed two bursts from a previously known X-ray source in the globular cluster NGC 6624. In February 1976, two additional burst sources were found by Lewin *et al.* (1976b) within a few degrees of the galactic center; the presence of a third burst source was suspected and searched for in early March 1976. It was found (Lewin 1976b) and another extraordinary source, only $\sim 0.5^\circ$ away, was discovered which produced about thousand bursts per day (Lewin *et al.* 1976c); it was later called the Rapid Burster. The bursts from the Rapid Burster behaved like a relaxation oscillator: the higher the fluence of a burst, the longer the waiting time to the next burst. In March 1976 the Rapid Burster was found to be located in a previously unknown, highly reddened globular cluster (Liller 1977). The activity of the Rapid Burster stopped by mid April 1976. About a year later, White *et al.* (1978a) observed the source to be active again. Many active periods of the Rapid Burster (each lasting several weeks) have been observed since then (see Fig. 7.1).

Within a year, over 20 burst sources were found, largely due to observations with SAS–3 and OSO–8. At first, several models of instabilities in the accretion flow were proposed to explain the bursts. It was also proposed that burst sources were black holes of a few hundred solar mass at the center of globular clusters (e.g., Grindlay and Gursky, 1976a; Forman and Jones 1976; Grindlay 1978) but this idea was soon rejected: (i) the distribution of the burst sources was unlike that of globular clusters (Lewin *et al.* 1977b) and (ii) the measured blackbody radii during bursts strongly indicated that the bursts are produced by neutron stars (Swank *et al.* 1977; Hoffman, Lewin and Doty 1977a,b; Van Paradijs 1978).

Maraschi and Cavaliere (1977) and independently Woosley and Taam (1976) were the first to discuss the possibility that the X-ray bursts were due to thermonuclear flashes on the surface of accreting neutron stars. [Dr. L. Maraschi suggested this in early February 1976 when she was visiting MIT at the time that the galactic center region was observed with SAS–3; many X-ray bursts were then observed (Lewin 1976a; Lewin *et al.* 1976b). Several years earlier, before the discovery of X-ray bursts, Hansen and Van Horn (1975) had made pioneering investigations into thermonuclear instabilities in the surface layers of accreting neutron stars.] However, after the discovery of the Rapid Burster in early March, 1976, it became clear that the rapidly repetitive bursts could not be due to thermonuclear flashes (see the discussions in Lewin *et al.* 1976c, and Woosley and Taam 1976); if they were, a very high flux of persistent X-ray emission due to the release of gravitational potential energy should be present, and this was not observed. Thus the thermonuclear-flash model could not explain all burst phenomena and that was not in its favor (see e.g., Lewin and Joss 1977).

A break came in the fall of 1977 when Hoffman, Marshall and Lewin (1978a) discovered that the Rapid Burster emits two very different kinds of bursts. They introduced the classification of type I and type II bursts and suggested that the rapidly repetitive type II bursts are due to accretion instabilities and that the type I bursts are due to thermonuclear flashes. Thus in the case of the Rapid Burster, the accretion onto the neutron star is spasmodic, giving rise to the type II bursts, and this makes the source unique. Detailed calculations by Joss (1978) and Taam and Picklum (1979) strengthened the idea that thermonuclear flashes on the surface of neutron stars produce type I bursts. Effects of nonthermal equilibrium and thermal inertia effects were stressed by Taam (1980) and compositional inertia effects by Ayasli and Joss (1982) and Woosley and Weaver (1985). More recent work by Bildsten *et al.* (1992) points out the possibility for a reduction of the CNO nuclei due to the interaction of the accretion flow with the neutron star atmosphere and calls into question the pure helium flash model for the accretion of hydrogen rich matter.

In the summer of 1977, 1735–44 was the first burst source to be optically identified by McClintock *et al.* (1978); its optical spectrum was very similar to that of Sco X–1. This was also the first burst source from which in the summer of 1978 a simultaneous optical and X-ray burst was observed (Grindlay *et al.* 1978; McClintock *et al.* 1979) after an extensive world-wide coordinated burst watch in 1977 failed to detect any radio, infrared or optical burst coincident with an observed X-ray burst (see Sect. 3.9.1).

It was long suspected that burst sources are low-mass X-ray binaries. Direct evidence for this was obtained in 1980 and 1981: (i) the quiescent optical counterparts of the transient (burst) sources Cen X–4 and Aql X–1 were found to be low-luminosity late-type stars (Van Paradijs *et al.* 1980; Thorstensen, *et al.* 1978; Koyama *et al.* 1981), (ii) an orbital period of $\sim$3.8 h was found for the burst source 1636–53 (Pedersen, Van Paradijs and Lewin 1981).

Photospheric radius expansion of the neutron star atmosphere, due to radiation pressure during a strong X-ray burst, became well established in 1984 (see Sect. 3.4). It led to the possibility, at least in principle, of obtaining both the mass and the radius of the neutron star and thereby gaining information about the equation of state of neutron star matter (see Sect. 4.5).

In that same year, a 4.1 keV absorption line was found in a type I burst from 1636–53 (Waki *et al.* 1984). It was suggested that this is a gravitationally redshifted resonance line of He-like iron (from the surface of the neutron star) in which case the redshift "z" would be 0.6 which is high, though perhaps not impossible. Since that time, absorption lines at 4.1 keV have been observed in at least 7 bursts from 3 different sources. The redshift interpretation as solely gravitational in origin is now in doubt (Magnier *et al.* 1989 and references therein). Recent work by Pinto, Taam and Laming (1992) suggests that the line shift is due to a combination of Doppler and gravitational redshifts.

Due to the long orbit of EXOSAT (~80 h) it became possible (1983–86) to compare burst characteristics with burst intervals up to tens of hours. [Observations prior to EXOSAT were plagued by Earth occultations for ~30 min every ~95 min.] It was found that for the three burst sources that were extensively observed with EXOSAT, the energy in a type I burst is largely determined by the interval since the previous burst (Lewin *et al.* 1987a), thus by the amount of time that accretion occurred, *independent* of the accretion rate. The accretion rates differed by a factor of ~30 (Van Paradijs, Penninx and Lewin 1988a). This means effectively that the time-averaged luminosity in bursts is independent of the time-averaged luminosity in the persistent emission between the bursts (thus of the accretion rate). This is a puzzling result which perhaps suggests that thermal and compositional inertia effects are operating to determine the ignition conditions of the nuclear fuel (see Sect. 3.8).

The discovery of intensity-dependent quasi-periodic oscillations (QPO) in GX 5–1 (Van der Klis *et al.* 1985a), was followed by systematic studies of the power density spectra of many LMXB and the relation to their spectral properties. This led to a classification into "Z" and "atoll" sources (Hasinger and Van der Klis 1989). The power density spectra and the color-color diagrams (i.e., their spectral states) of these two groups differ, and the atoll sources are, on average, less luminous than the Z sources. Most burst sources are atoll sources though at least one (GX 17+2) is a Z source (for a recent review see Van der Klis 1993). Some burst characteristics (among them the burst durations) are strongly correlated with the spectral state (Van der Klis *et al.* 1990); this may indicate that the nuclear fuel composition in the bursts changes as the accretion rate changes.

1.3.1. Burst Nomenclature

Hereafter, type I bursts may be simply called *bursts* and type-I burst sources may be called *burst sources*. However, whenever we discuss type II bursts the "II" will always be mentioned.

2. Characteristics of Burst Sources

The ~40 known burst sources (see Chapter 9) form a subset of the low-mass X-ray binaries (LMXB). The number of known LMXB is ~125 (Van Paradijs 1991, 1993).

2.1. Characteristics of LMXB

LMXB are bright X-ray sources ($> 10^{34}$ erg s^{-1}); they accrete through Roche lobe overflow. Observationally, they distinguish themselves from the $\sim 10^2$ known high-mass X-ray binaries (HMXB, with donor stars $>10\,M_\odot$) in our galaxy by the following characteristics (see, e.g., Lewin and Joss 1981, 1983; Van Paradijs 1983, 1991, 1993; Van Paradijs and McClintock 1993; White, Nagase and Parmar 1993):

- Their star-like optical counterparts are faint (typically $M_v \approx +2$) in contrast to the luminous HMXB which are more than two orders of magnitude brighter. Many LMXB have no known optical counterpart due to severe interstellar absorption. For a review on optical properties, see Van Paradijs and McClintock (1993).
- Their optical spectra (except for transients in quiescence and systems in which the companion is a late-type giant star) are devoid of normal stellar absorption features.
- The ratio of their X-ray to optical luminosities ranges from $\sim 10^2$ to $\sim 10^4$ (except for transients in quiescence). For HMXB this ratio ranges from $\sim 10^{-3}$ to $\sim 10^1$.
- Their X-ray spectra are substantially softer than the spectra of the HMXB.
- They show no periodic X-ray pulsations such as are often observed from highly magnetized, rotating neutron stars in HMXB.
- The majority of them produce X-ray bursts. In contrast, no X-ray bursts have been observed from any of the HMXB or any LMXB that shows pulsations.

All LMXB (except two or three*) are believed to have the above characteristics.

2.2. Mass of the Donor – Evolution

We call a system a LMXB when the mass of the donor star is less than $\sim 1M_\odot$. The mass estimates and mass determinations of the donors in LMXB are often indirect (e.g., through globular-cluster membership and/or the measurement of the orbital period). Fig. 2.1 shows the period distribution of the known LMXB; the burst sources are marked.

For a Roche-lobe filling donor, the donor's average density is uniquely determined by the orbital period (Paczynski 1971; Faulkner *et al.* 1972). If the donor is a low-mass main-sequence star with an approximately linear relation between

* The following two LMXB have hard spectra and they show pulsations: Her X–1 (donor mass $\sim 2.0\ M_\odot$; Nagase 1989) and 1626–67 (donor mass $< 0.06\ M_\odot$; Levine *et al.* 1988). GX 1 + 4 has a hard spectrum and it shows pulsations (Lewin *et al.* 1971; White *et al.* 1976); if the optical identification suggested by Doxsey *et al.* (1977b) is correct, GX 1 + 4 is a LMXB.

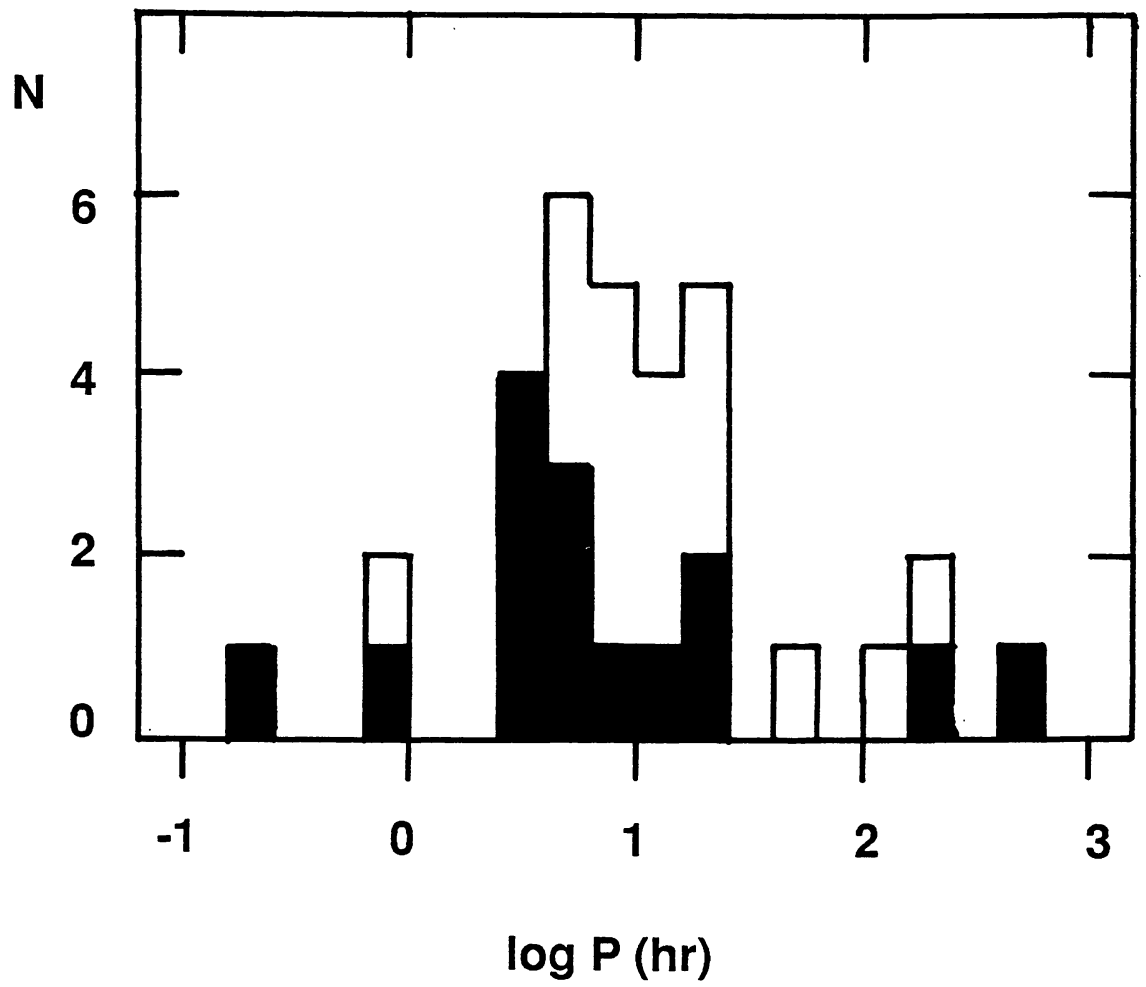

Fig. 2.1. Period Distribution of LMXB; the Bursters are marked.

the mass and the radius, one finds that the mass of the donor is proportional to the orbital period (Warner 1976). As an example, for 1636–53 the orbital period is ~3.80 h (Pedersen, Van Paradijs and Lewin 1981); assuming that the donor is a main-sequence star, its mass is $\sim 0.45\ M_\odot$. If we have strong reasons to believe that the donor has a mass less than $\sim 1\ M_\odot$ (old population), orbital periods in excess of ~10 h indicate that the donor cannot be a main-sequence star; it must be evolved. In the case of Cen X–4 (orbital period ~ 15 h), the companion is probably a stripped giant with a mass between ~ 0.04 and $\sim 0.18\ M_\odot$ (Chevalier *et al.* 1989; McClintock and Remillard 1990). For orbital periods shorter than ~80 min, the donor cannot be a main-sequence star either (Paczynski and Sienkiewicz 1981, 1983). Examples are 1820–30 (orbital period ~11 min; Stella *et al.* 1987a), 1626–67 (orbital period ~41 min; Middleditch *et al.* 1981), and 1916–05 (orbital period ~50 min; White and Swank 1982). The donor masses in these systems are ~0.06–0.08 $M_\odot$ (Stella, Priedhorsky and White 1987a; Rappaport *et al.* 1987), probably $< 0.06\ M_\odot$ (Middleditch *et al.* 1981; Levine *et al.* 1988), and ~0.10–0.15 $M_\odot$, (Nelson *et al.* 1986), respectively.

For assumed conservative mass transfer (i.e., no mass escapes the system and the total angular momentum of the binary system remains constant) from a low-mass to a more massive star, the binary separation must increase and this could terminate the mass transfer. The mass transfer can continue if either the donor expands and continues to fill its Roche lobe or the orbit shrinks. The first possibility applies when the donor has evolved off the main-sequence. Shrinking of the orbit requires a decrease in orbital angular momentum. This is done in the form of gravitational radiation (Kraft *et al.* 1962; Faulkner 1971). However, the angular momentum loss due to gravitational radiation is insufficient to explain mass transfer rates in excess of $\sim 10^{-10}\ M_{\odot}$ per year (Paczynski 1967). It has been suggested that magnetic braking can provide the additional necessary angular momentum loss (Verbunt and Zwaan 1981). Detailed reviews of the evolution of X-ray binaries have recently been given by Bhattacharya and Van den Heuvel (1991) and Van den Heuvel and Verbunt (1993).

2.2.1. Transients

The majority of the known LMXB (and most burst sources) are permanently X-ray active. About 40, however, are transients (Van Paradijs 1991, 1993 and references therein), with typical X-ray active periods of several months. The transient behavior can be recurrent with intervals of order one to tens of years (White, Kaluzienski and Swank 1984; see also Tanaka and Lewin 1993 and references therein). About 12 of these transients produce X-ray bursts during their active phase. For optical properties, see Van Paradijs and McClintock (1993).

2.3. Old Population

The LMXB are concentrated towards the galactic center (Lewin *et al.* 1977b). About 17 are found in globular clusters [2 of which in ω Cen (Verbunt private communication), and 4 in 47 Tuc (Verbunt *et al.* 1993)]; nine of them are known burst sources (Chapter 9). Their locations outside regions of active star formation identify the LMXB and burst sources as members of an old population (see Fig. 2.2). The low mass of the donor stars supports the idea that the LMXB, of which the burst sources are a subset, are an old population.

2.4. Magnetic Fields of Neutron Stars

Neutron stars in LMXB almost certainly have a weak magnetic field compared to the neutron stars in the massive (Population I) binary systems. The absence of X-ray pulsations from LMXB and the fact that type I X-ray bursts never occur in systems which show X-ray pulsations are generally used as arguments for the weak magnetic fields. The pulsations (in most cases observed from the massive binaries) are almost certainly the result of strong ($> 10^{11}$ G) neutron star surface fields in systems where the magnetic dipole axis is not aligned with the rotation axis of the neutron star. To date (February 1992) there are 9 pulsating neutron star binary systems from which a cyclotron absorption line has been detected in the

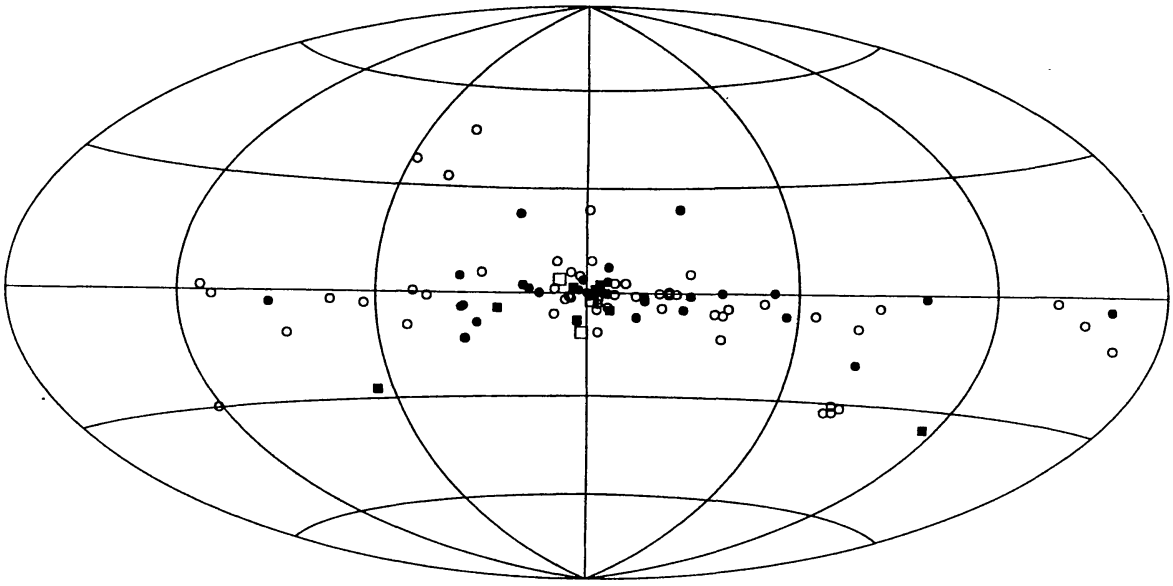

Fig. 2.2. Galactic sky map of LMXB; burst sources and globular cluster sources are specially marked.

X-ray spectrum (Makishima 1992); this indicates magnetic dipole fields of order 10^{12} G (Nagase 1989). Type I X-ray bursts are not expected from such systems as the strong fields funnel the accreted matter to only a very small fraction of the neutron star surface; the effective accretion rate (accretion rate per unit area) is thus very high, and this may suppress the thermonuclear flashes (Joss 1978; Taam and Picklum 1978; Joss and Li 1980).

It was believed for a long time that the magnetic fields of neutron stars decay on a time scale of $\sim 10^7$ yr (Gunn and Ostriker 1969) which provided a natural explanation of why the magnetic fields in old neutron stars in LMXB are relatively weak and why those of young neutron stars in the massive binary systems are so strong. It was also suggested (but this never registered in the West until very recently) that magnetic field decay was the result of accretion, thus, not necessarily due to age (Bisnovatyi-Kogan and Komberg 1974). In this accretion-induced field decay model, the field lines are "buried" below the surface of the neutron star by the accreted matter.

Kulkarni (1986) showed that the neutron star in the millisecond radio pulsar PSR 0655 + 64 (with a magnetic dipole field of $\sim 10^{10}$ G) is much older than one would expect for a magnetic-field decay with an e-folding time of $\sim 10^7$ yr (see also Callanan *et al.* 1990 and Kulkarni *et al.* 1991). Van den Heuvel *et al.* (1986), and Bhattacharya and Srinivasan (1986) showed that the number of observed millisecond radio pulsars was much larger than one would expect for such a magnetic field decay. Verbunt *et al.* (1990) convincingly argued that the neutron star in Her X–1 is very old, yet Her X–1 is a pulsating X-ray source with a magnetic dipole field of a few times 10^{12} G (Trümper *et al.* 1977). They came to the conclusion that an old neutron star can have a very strong magnetic field.

The accretion-induced magnetic field decay model by Bisnovatyi-Kogan and Komberg (1974) was reinvented (Taam and Van den Heuvel 1986; Shibazaki *et al.* 1989; Romani 1990) in the light of the above observational evidence.

Following these developments, it has been suggested by Srinivasan *et al.* (1990) that the magnetic-field strength (and its decay) of a neutron star depends not on the amount of matter accreted on the surface of a neutron star but on the spin history of the neutron star through the coupling of the quantized vortices of rotation and the quantized magnetic flux tubes. A very old neutron star that has always had a very short spin period ($<\sim$ few sec) would always maintain a strong field if it were born with a strong field, but it would have a much weaker field if it had been spun down for a sufficient amount of time to a period of ten seconds or longer. A detailed review (including the history) on magnetic field decay is given by Bhattacharya and Srinivasan (1991, 1993).

2.5. Z AND ATOLL CLASSIFICATION

The relatively bright low-mass X-ray binaries have been divided into two classes: the "Z" sources (to date, October 1992, six sources fall in this group) and the "atoll" sources ($\sim$13 sources have been classified as atoll sources) which are characterized by the Z-like and atoll-like shapes of their X-ray color-color diagrams (Hasinger and Van der Klis 1989).

At their lowest accretion rates (in the horizontal branch), Z sources show $\sim$13–60 Hz quasi-periodic oscillations (QPO) believed to be due to magnetic gating of the accretion flow (Alpar and Shaham 1985; Lamb *et al.* 1985; Shibazaki and Lamb 1987; Lamb 1991; Ghosh and Lamb 1992, and references therein). At higher accretion rates a different type of QPO appears; the frequency is near 6 Hz in the normal branch and can increase up to $\sim$20 Hz in the flaring branch (for reviews on QPO see Lewin, Van Paradijs and Van der Klis 1988; Van der Klis 1989; Van der Klis and Lamb 1993; Van der Klis 1993). The 6-Hz QPO have been interpreted in terms of optical depth variations in the radial flow of accreting matter which produces an oscillation in the degree of Comptonization as the luminosity approaches the Eddington critical luminosity (Fortner *et al.* 1989, 1992). [Sound waves in the rotating accretion disk have also been considered (Alpar *et al.* 1992).] Both types of QPO are absent in atoll sources. In addition to the QPO in Z sources, several broad noise components whose properties are also correlated with the source state are seen in the power spectra of Z as well as atoll sources. These components cover a frequency range between $\sim 10^{-3}$ Hz and 10^2 Hz with a fractional rms variation between $\sim$1% and $\sim$20%.

The two Z sources (Sco X–1 and Cyg X–2) for which an orbital period is known, have long orbital periods, thus an evolved companion (see above). The atoll sources (1636–53, 1820–30, 1735–44 and GX 9 + 9) for which a period is known (Chapter 9; Hertz and Wood 1988; Schaefer 1990), have much shorter orbital periods. The observed differences between Z and atoll sources may therefore be correlated with the stellar type of the donor star, suggesting a link with LMXB

evolution (Hasinger and Van der Klis 1989; see also Lewin and Van Paradijs 1986). The Z sources are on average more luminous than the atoll sources; it is therefore not surprising that the type I burst sources are by and large atoll sources as high accretion rates suppress the thermonuclear flashes (Fujimoto, Hanawa and Miyaji 1981; Ayasli and Joss 1982).

Type I bursts have been observed from the Z source GX 17 + 2 and from 10 of the ~13 known atoll sources. The burst sources Cir X–1 and the Rapid Burster (Chapter 7) can not be classified in either one of these two classes (Rutledge *et al.* 1993).

Some burst characteristics, such as the type I burst duration and the blackbody radius during burst decay, are correlated with the spectral state of the source (Nakamura *et al.* 1989; Van der Klis *et al.* 1990). In Fig. 3.16 we show these correlations in a color-color diagram for the atoll source 1636–53; similar results have been found for 1705–44, and for other burst sources (M. van der Klis, private communication).

3. Type I X-ray Bursts

3.1. Introduction

Type I X-ray bursts (hereafter called X-ray bursts or simply bursts) have been observed from ~40 sources so far. In this chapter we discuss the observed properties of X-ray bursts and their relation to properties of the persistent emission. Individual burst sources are discussed in Chapter 9.

3.2. Burst Profiles

X-ray bursts show a large variety in profiles. This is illustrated in Fig. 3.1, in which we show burst profiles from three different sources. Profiles of bursts from a given source may look quite similar and have characteristic shapes [see e.g. Hoffman, Lewin and Doty (1977b) for 1728–337, and Haberl *et al.* (1987) for 1820–303], but this is by no means a general phenomenon (see Fig. 3.2 and 3.3).

Burst rise times vary from less than a second (e.g., Day and Tawara 1990) to ~10 s (e.g. Gottwald *et al.* 1986), and decay times are in the range of ~10 s (e.g., Lewin *et al.* 1980; Van Paradijs *et al.* 1988b) to minutes (e.g., Tawara *et al.* 1984a; Lewin, Vacca and Basinska 1984). In general, burst profiles depend strongly on photon energy, with decays which are much shorter at high photon energies than at low energies (see Fig. 3.4). This energy dependence of the burst profile corresponds to a softening of the burst spectrum during the decay, which is the result of the cooling of the neutron star photosphere (see Sect. 3.3).

For the transient source 1608–522 Murakami *et al.* (1980a) found that the burst rise times were anti-correlated with the persistent X-ray flux. In general, the burst rise times do not depend in an obvious way on other burst properties, except that most bursts which show evidence for photospheric radius expansion (see Sect. 3.4) have rise times less than ~1 second (see, e.g., Lewin *et al.* 1987a).

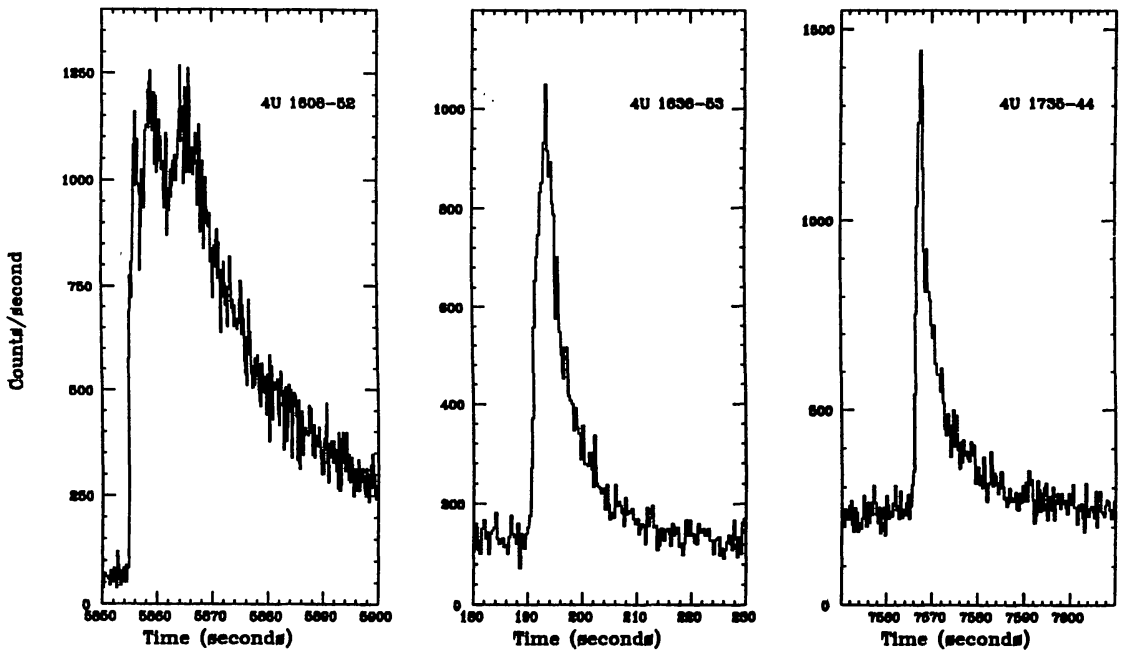

Fig. 3.1. Examples of X-ray burst profiles, as observed with EXOSAT in the ~1–20 keV energy band, from 1608–522 (left panel), 1636–536 (middle panel), and 1735–444 (right panel). The counting rates have not been corrected for dead time and refer to one half of the detector array. The horizontal axes represent time in seconds. The burst start times are: 1986 March 12, UT 22:26:30 (1608–522), 1984 May 8, UT 19:31:36 (1636–536), and 1984 August 23, UT 18:28:28 (1735–444) (courtesy T. Oosterbroek).

Approximately linear relations between the (bolometric) burst fluence, E_b, and the (bolometric) peak burst flux, $F_{\max}$, have been found in several sources (1735–444: Lewin *et al.* 1980; 1636–536: Ohashi *et al.* 1982; Lewin *et al.* 1987a; Ser X–1: Sztajno *et al.* 1983; 1728–337: Basinska *et al.* 1984; see Fig. 3.5). For very strong bursts the $(E_b, F_{\max})$ relation saturates (see, e.g., Basinska *et al.* 1984): the peak luminosity cannot exceed the Eddington limit (see Section 3.4), and an increase in E_b corresponds to a longer burst. For the transient source 1608–522 a linear $(E_b, F_{\max})$ relation was only found when the source was bright. When it was faint $F_{\max}$ was approximately constant (at a value below the highest peak fluxes reached when the source had a high persistent flux); E_b then varied by a substantial factor (Murakami *et al.* 1980a).

In about a dozen sources bursts have been observed with double-peaked profiles, which are particularly distinct at high energies (examples are shown in Fig. 3.6). These burst profiles are caused by photospheric radius expansion due to radiation pressure; they are discussed in more detail in Sect. 3.4. These bursts, which all have very high peak fluxes, should not be confused with the relatively weak bursts with multi-peaked (bolometric) profiles observed from 1636–536 (Sztajno *et al.* 1985; Van Paradijs *et al.* 1986a; see Fig. 3.7 and 3.8); the latter profiles likely reflect a genuine variation in the rate at which thermonuclear energy is generated or released.

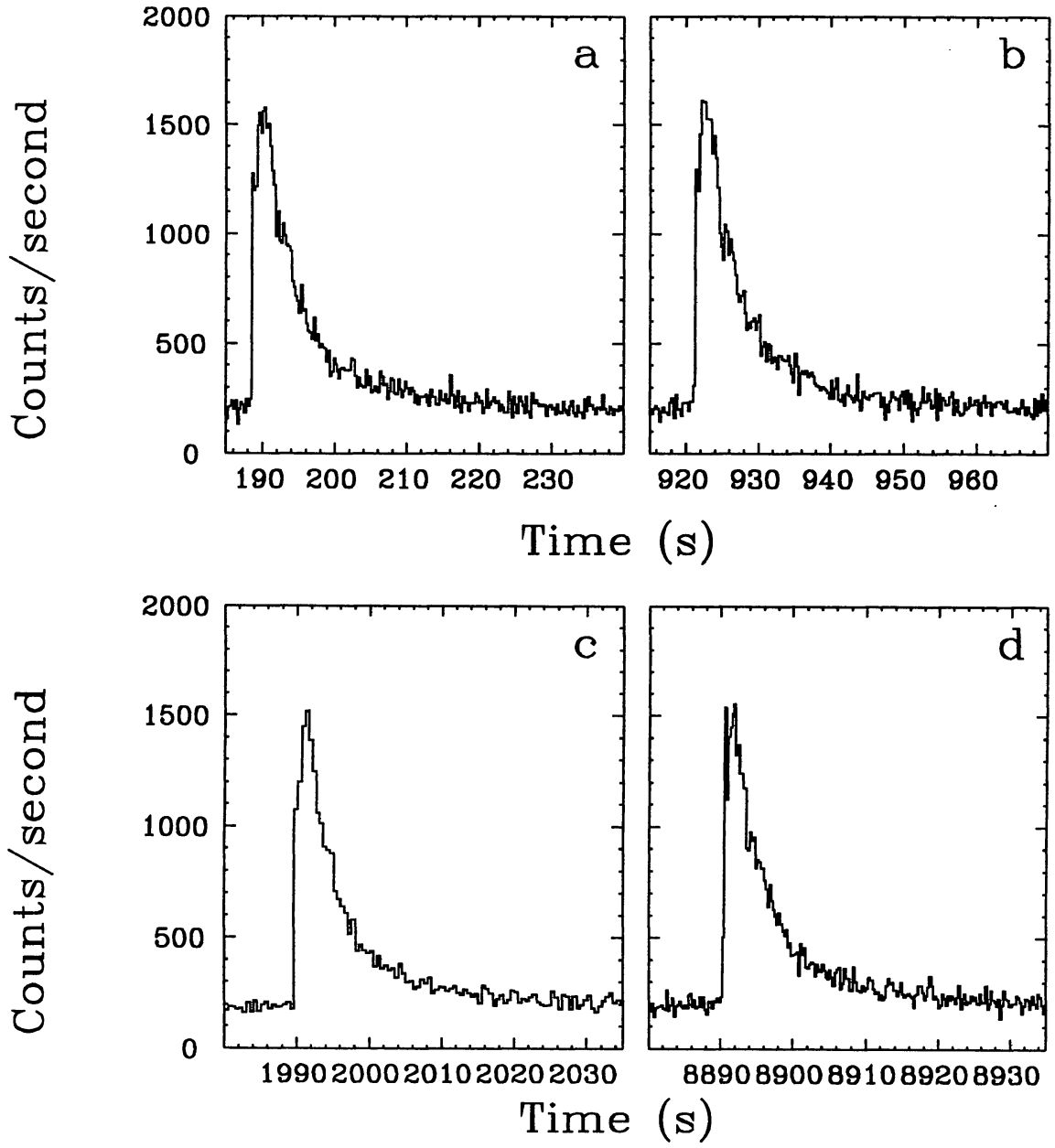

Fig. 3.2. Profiles of four of seven bursts observed from 1820–303 with EXOSAT in the ~1–20 keV band during a 20 hour observation on August 19/20, 1985. The counting rates have not been dead-time corrected. The horizontal axes represent time in seconds. The burst start times are: Aug. 19, UT 12:16:23 (a), Aug. 19, UT 18:42:52 (b), Aug. 19, UT 15:26:52 (c), and Aug. 19, UT 21:55:28 (d). The profiles of all seven bursts were very similar (courtesy T. Oosterbroek).

In some cases a relation has been observed between burst profiles and the persistent emission. Clark *et al.* (1977) observed a gradual decrease of the decay time of bursts from 1820–303, as the persistent X-ray flux increased by a factor of ~5. Murakami *et al.* (1980a) observed 1608–522 during an active phase in April 1979 when the persistent flux was relatively high; the majority of the bursts then had a fast rise (<2 s) and a fast decay (<15 s). Two months later, when

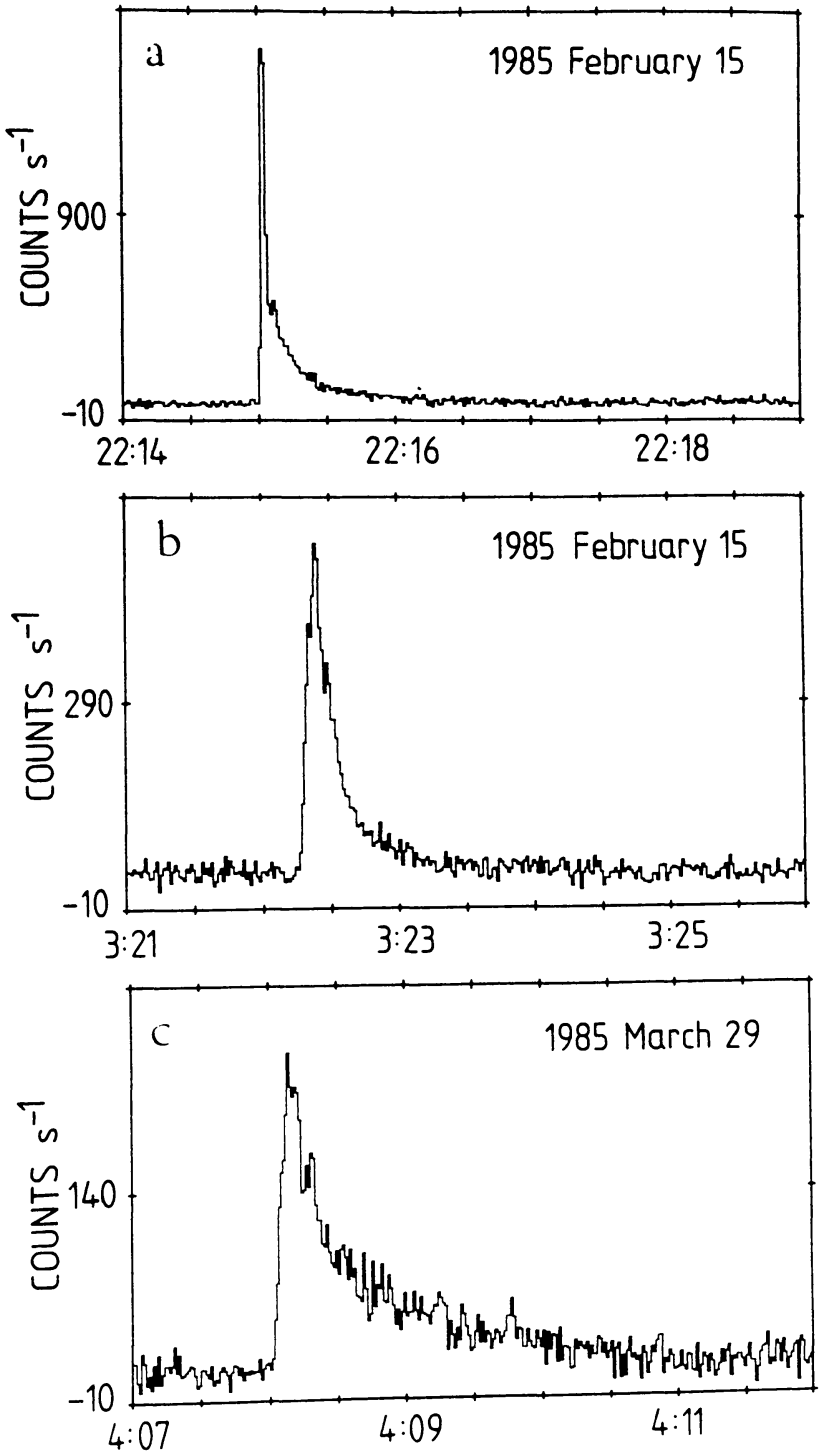

Fig. 3.3. Three bursts (1.5–15 keV) from 0748–676, with very different durations. The horizontal axes are UT (in hh:mm). Burst (a) showed radius expansion during its initial phase. The count rates have not been dead-time corrected (from Gottwald *et al.* 1986).

the persistent flux had decreased by a factor of ~5, the bursts had a slower rise and decay. Also, the maximum observed burst flux was lower at that time (by a factor of ~ 3) than it was during the early part of the active phase. The findings of Murakami *et al.* are supported by later observations of 1608–522 by Nakamura *et*

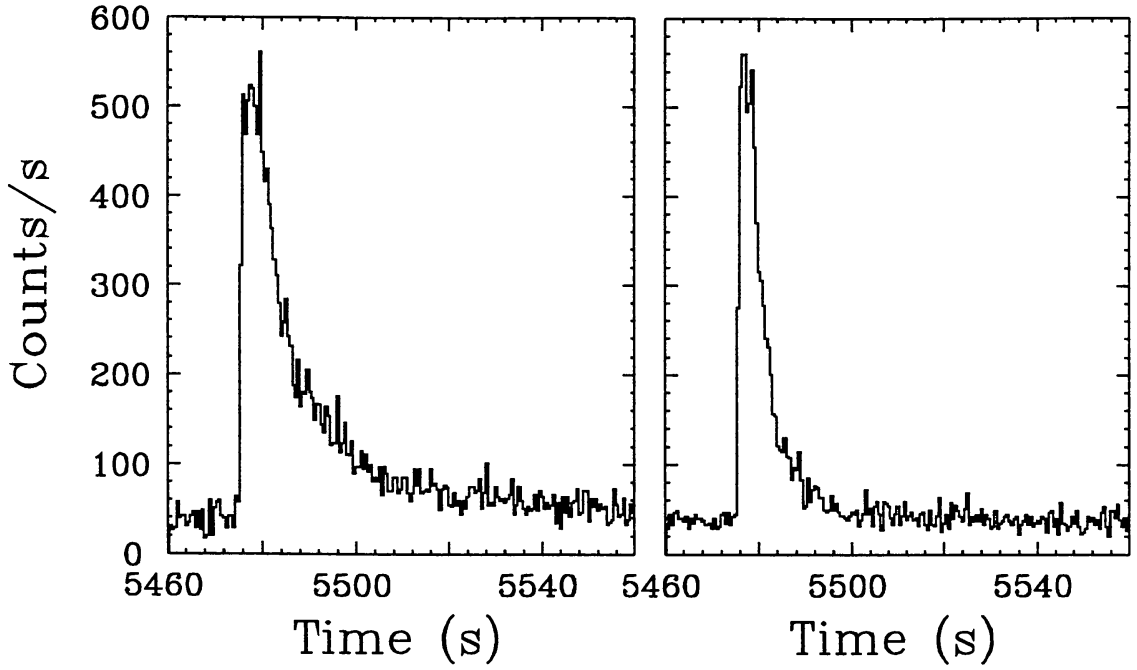

Fig. 3.4. One X-ray burst from 1702–429 observed with EXOSAT in the 1.2–5.3 keV band (left), and the 5.3–19.0 keV band (right). Time is in seconds since 1986 April 8, UT 03:31:31. The softening of the X-ray burst spectrum during decay is apparent as a relatively long tail in the low-energy burst profile (courtesy T. Oosterbroek).

al. (1988). A striking example of a relation between burst profiles and the level of the persistent emission is the case of 0748–676, for which Gottwald *et al.* (1986) found that both the fluence (E_b) and the peak flux ($F_{\max}$) of the bursts increased as the persistent flux increased by about an order of magnitude; the ratio $E_b/F_{\max}$, which is a measure of the effective duration of the burst decreased by a factor of $\sim$3. Van Paradijs, Penninx and Lewin (1988a) found from a statistical study that an anti-correlation between burst duration and the persistent X-ray luminosity is a global property of X-ray burst sources. The relation between burst properties and mass accretion rate is discussed in more detail in Sect. 3.8.

3.3. Burst Spectral Analysis

Most observations of X-ray bursts have been made with proportional counters or gas-filled scintillation counters which produce a signal in the form of counting rates in a number of pulse-height analyzer (PHA) channels. The relation between the PHA channel number and the energy of an incoming photon is not a simple scaling, but can be described by a so-called detector matrix which includes the (energy-dependent) efficiency of the detector and the escape phenomenon (see Fraser 1989). The inversion of this matrix, which would directly convert the observed PHA channel count-rate spectrum into an incident photon spectrum, is an unstable operation. It has therefore become standard procedure to study the spectra of X-ray sources by assuming a particular shape of the incident photon spectrum, and fold

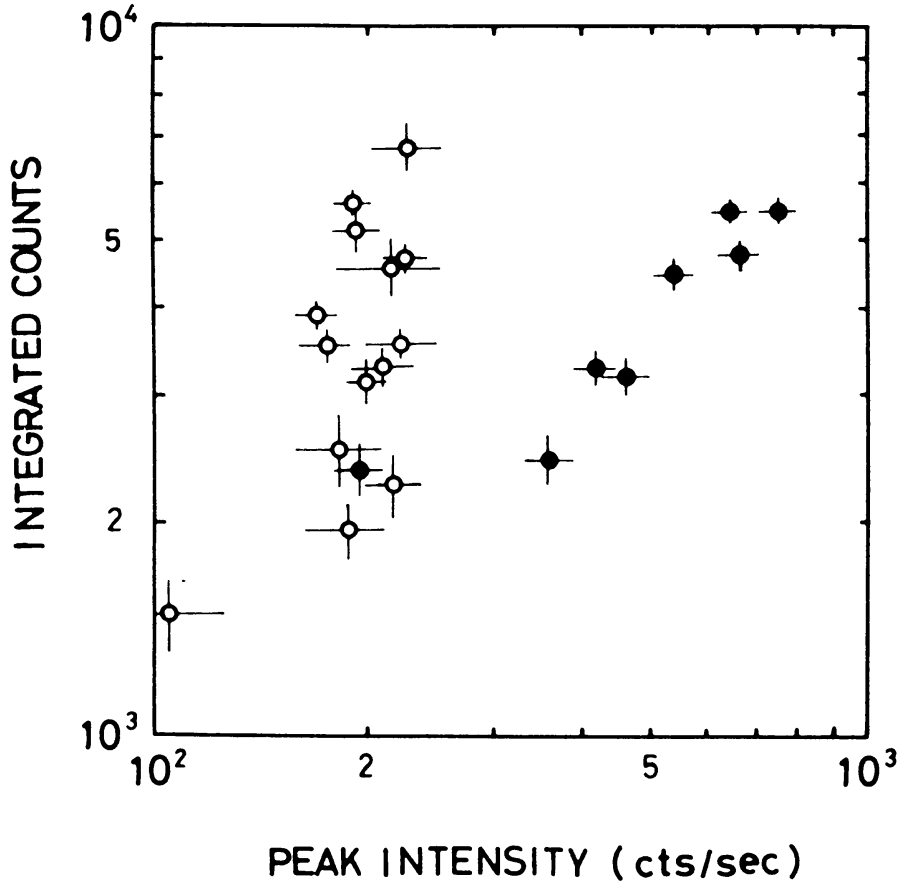

Fig. 3.5a.

Fig. 3.5. Relation between peak burst flux and burst fluence. (a) 1608–522 (Murakami *et al.* 1980a). Filled circles indicate bursts observed during a period when the persistent X-ray flux was high; the burst peak fluxes were then generally high, and variable, and strongly correlated with the burst fluence. Open circles indicate bursts observed when the persistent flux was low, the bursts then had low peak fluxes which did not vary much from burst to burst. (b) 1728–337 (Basinska *et al.* 1984). For weak bursts there is a linear relation between burst peak flux and fluence which saturates for stronger bursts. Panels (c) and (d) show that for 1735–44 and 1837+049 there are linear relations between burst peak flux and burst fluence (from Lewin *et al.* 1980; Sztajno *et al.* 1983).

this spectrum through the detector response matrix to obtain a predicted count-rate spectrum. Whether the assumed incident spectrum describes the observations satisfactorily is then assessed by some quality estimator, generally a least-squares fitting of the predicted count-rate spectrum to that observed. This fitting leads to a determination of parameters of the spectral model, and an estimate of the quality of the fit in terms of a minimum χ^2 value.

Swank *et al.* (1977; see Fig. 3.9) and Hoffman, Lewin and Doty (1977a,b) found that the time-dependent spectra of X-ray bursts are well described by a blackbody spectrum (Planck function):

$$F_{bb}(E)\,\mathrm{d}E = KE^3[\exp(E/kT_{bb}) - 1]^{-1} \tag{3.1}$$

Here E is the energy of the incident photon, T_{bb} is the blackbody temperature (it is customary to use kT_{bb}, expressed in keV), and K is a normalization constant. Most

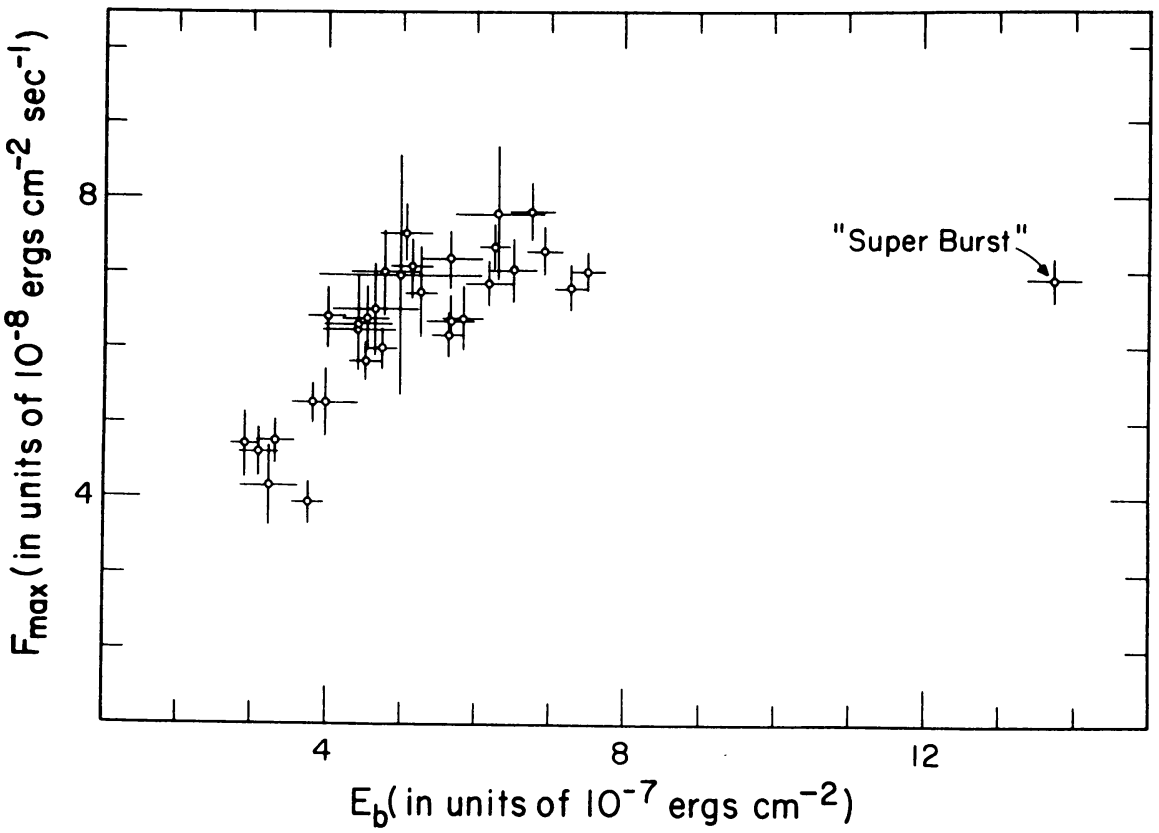

Fig. 3.5b.

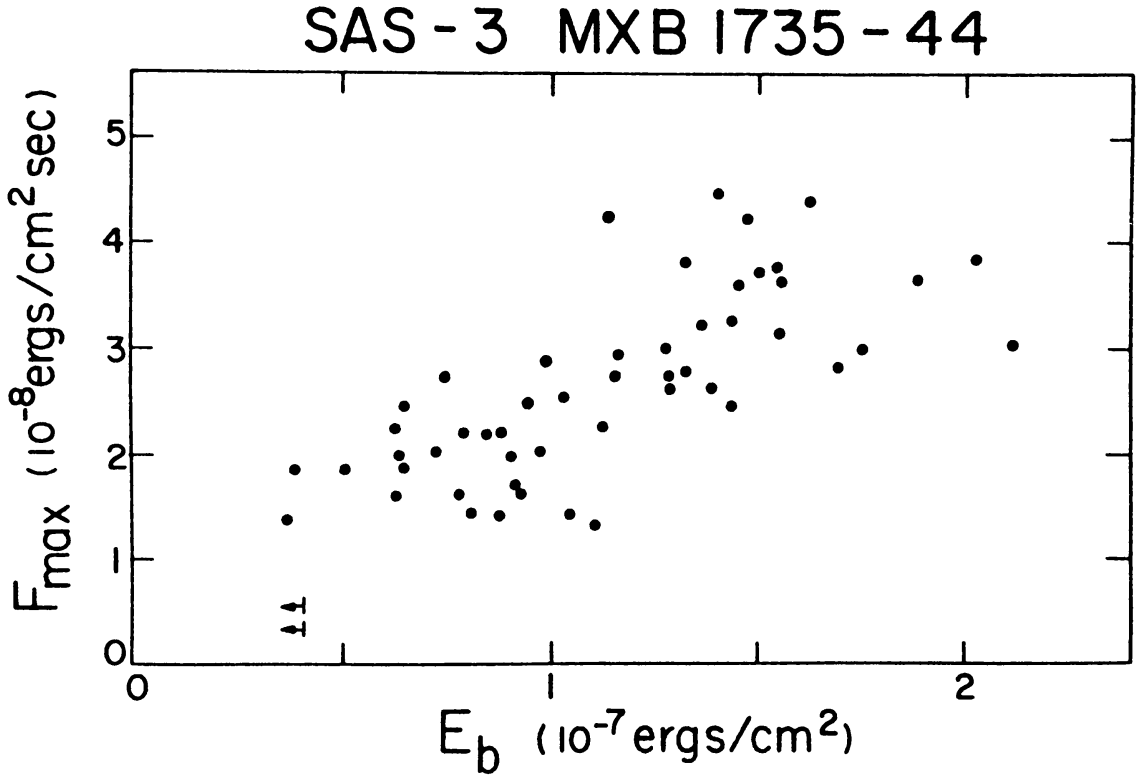

Fig. 3.5c.

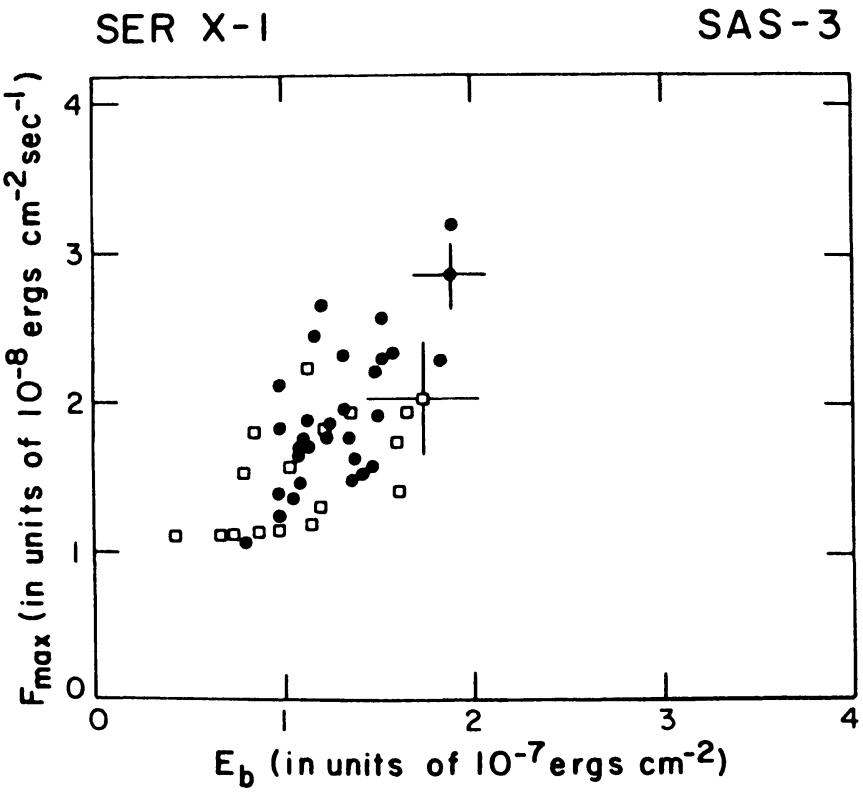

Fig. 3.5d.

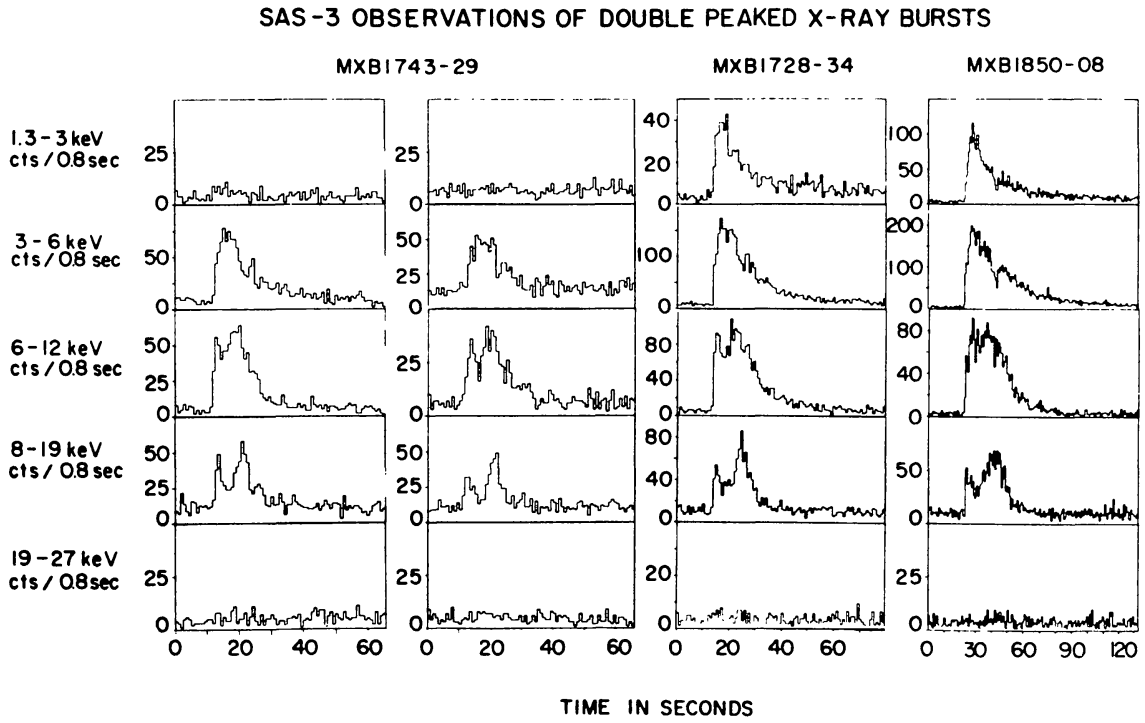

Fig. 3.6. X-ray bursts from three different sources showing energy-dependent double-peaked profiles, indicative of photospheric radius expansion near burst maximum. The X-ray spectrum of MXB 1743–29 (located near the galactic center) is highly cut off below 3 keV due to interstellar absorption. This figure is from Hoffman, Cominsky and Lewin (1980).

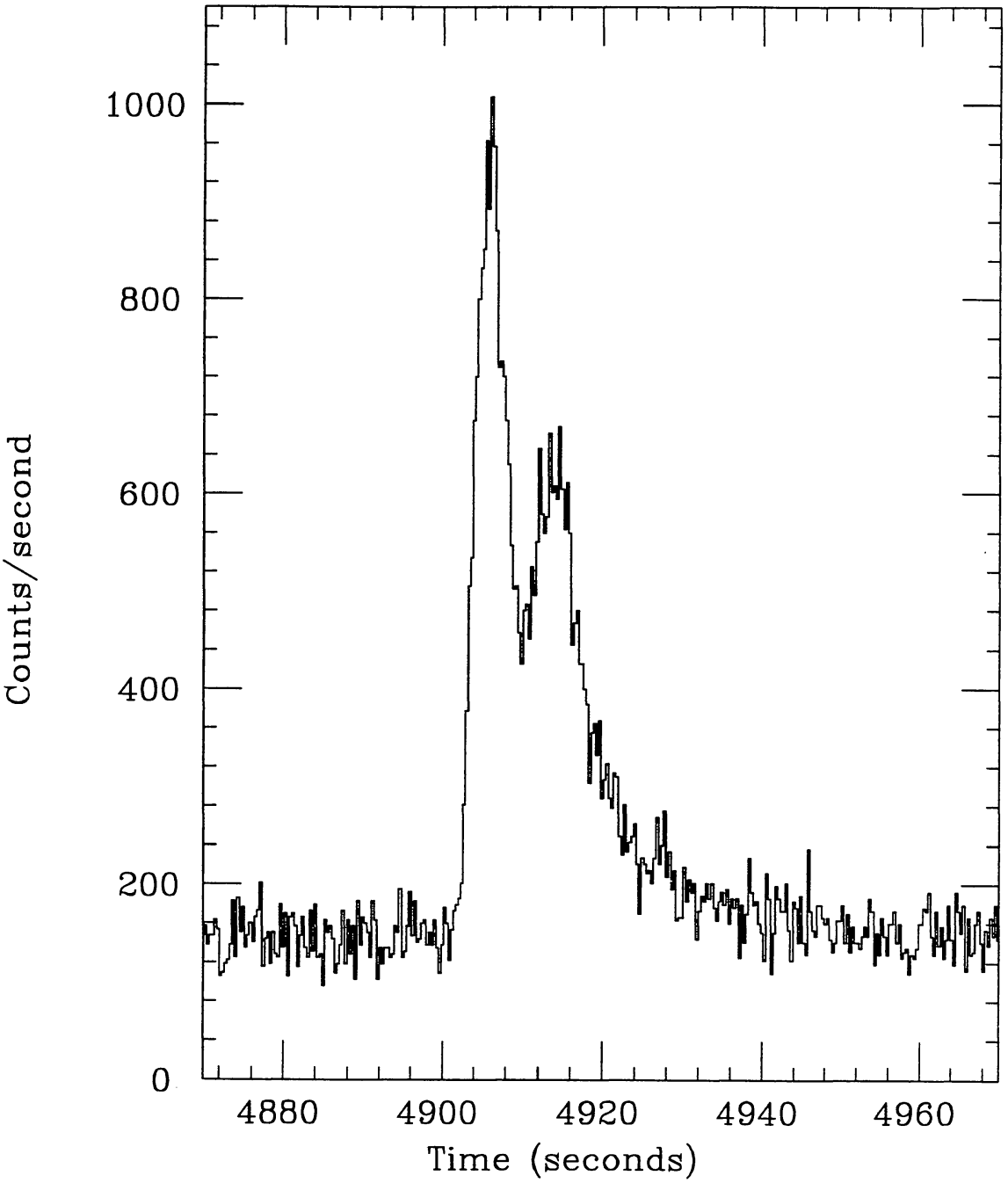

Fig. 3.7. Two examples of bursts from 1636–536 with double-peaked profiles that are visible at all photon energies, and are not caused by photospheric radius expansion (Sztajno *et al.* 1985). These bursts profiles have been observed with EXOSAT, and are displayed for the 1–20 keV range (courtesy T. Oosterbroek).

spectral studies of X-ray bursts made since the earliest results have been based on blackbody spectral fits. In making spectral fits it is customary to subtract the pre-burst persistent emission from the total signal. Since the burst emission may affect the accretion flow it is not obvious that this is correct. However, it is unclear what the effect of the burst on the persistent flux is. For instance, for bursts which at

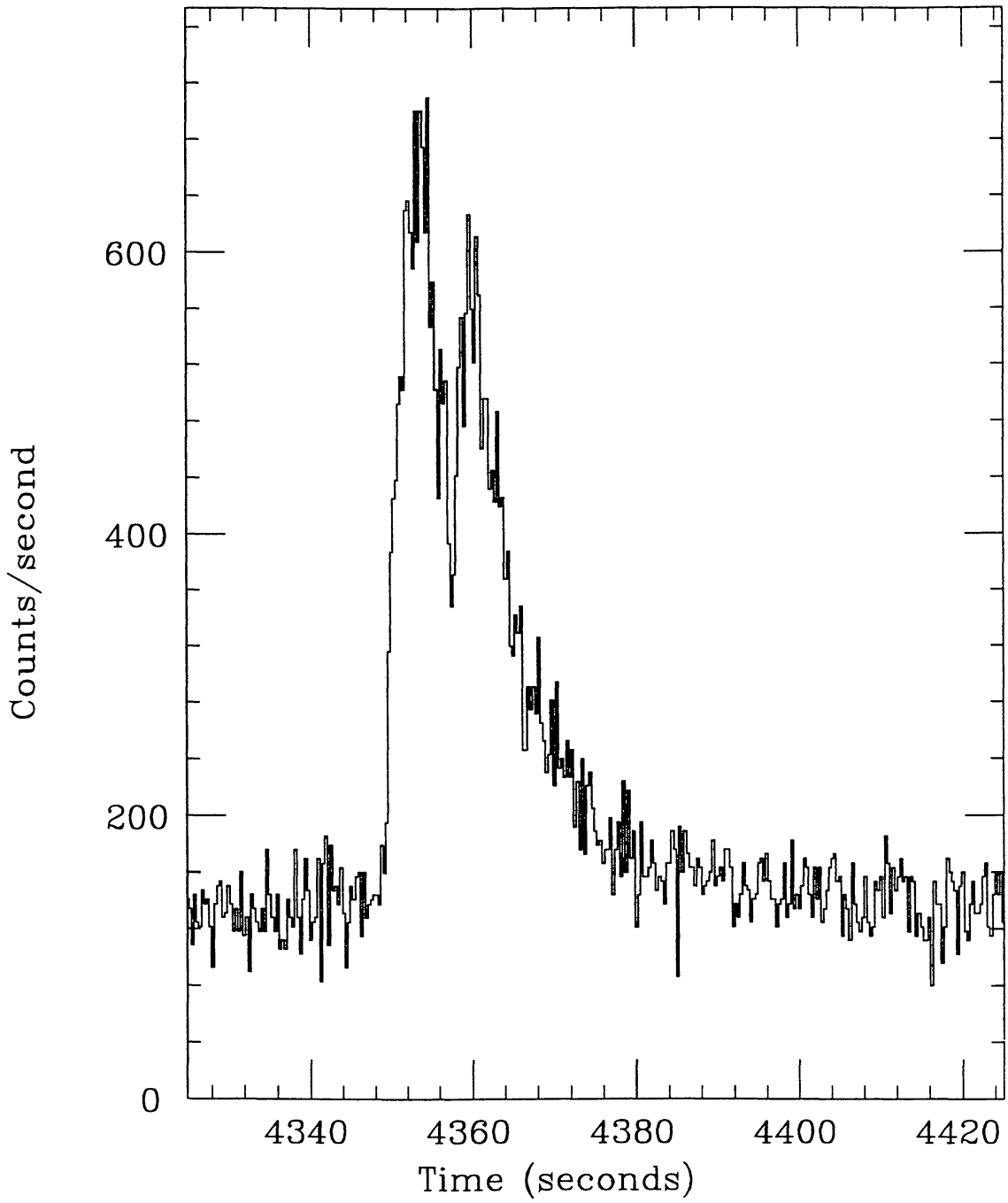

Fig. 3.7 *(continued)*

their peaks reach the Eddington limit (see Sect. 3.4) one might expect a temporary suppression of the accretion; however, it has been argued (Walker and Meszaros 1989) that instead the accretion rate is then enhanced (as long as the luminosity is sub-Eddington), due to increased angular momentum loss of the inflowing matter by radiation drag.

The effect of the energy dependent interstellar absorption is taken into account by a factor of the form $\exp[-\sigma(E)N_{\rm H}]$, where $N_{\rm H}$ is the interstellar hydrogen

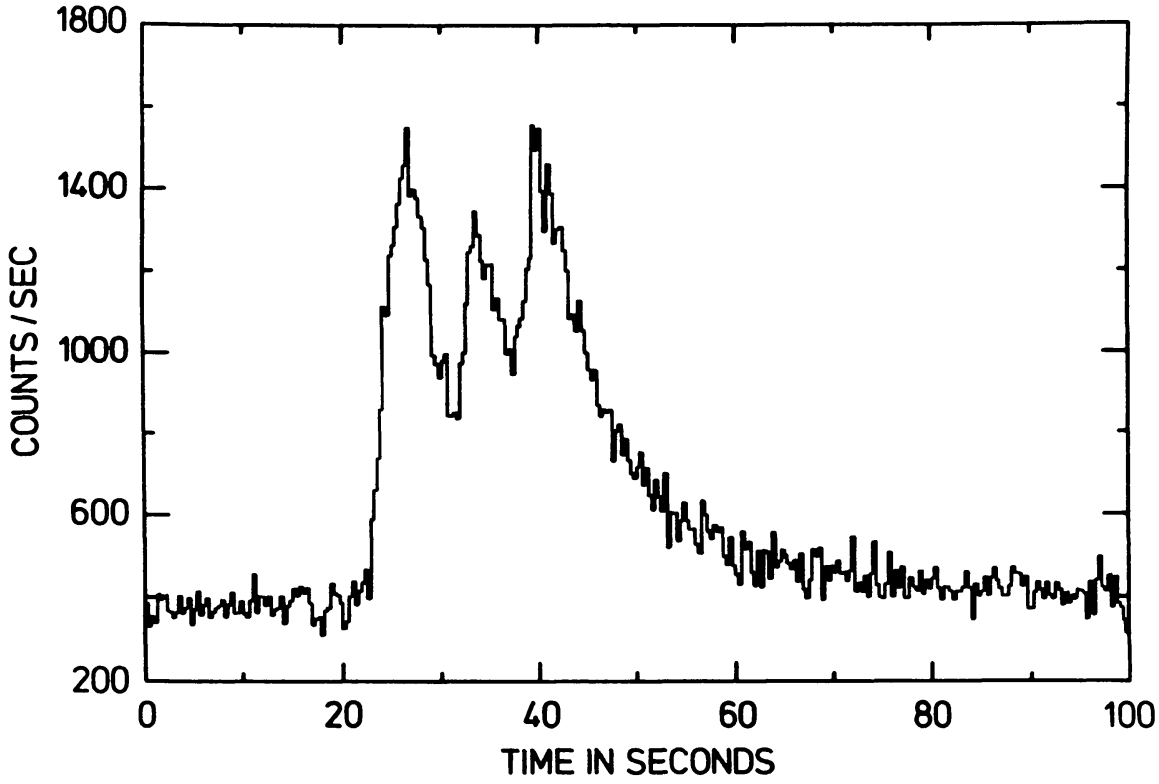

Fig. 3.8. Triple-peaked burst observed with EXOSAT from 1636–536 (from Van Paradijs *et al.* 1986a).

column density between the source and the observer, and $\sigma(E)$ is the absorption cross section per hydrogen nucleus (this depends, of course, on the assumed chemical composition of the interstellar medium; see, e.g., Morrisson and McCammon, 1983). Interstellar absorption of X rays is dominated by photoelectric absorption; its effect on an observed X-ray spectrum therefore appears as a low-energy cut off. The relation between the low-energy cut off, $N_{\rm H}$ and the (optical) interstellar reddening has been studied by Gorenstein (1975), Ryter *et al.* (1975) and Bohlin *et al.* (1978).

The best-fit blackbody temperature can be used to determine the bolometric flux, $F_{\rm bol}$, in the burst by multiplying the flux, observed in the energy range (E_1, E_2) covered by the detector, by a bolometric correction factor $\int_0^\infty F_{bb}(E)\,{\rm d}E / \int_{E_1}^{E_2} F_{bb}(E)\,{\rm d}E$, which is a function of kT_{bb} alone. From the bolometric flux and the blackbody temperature one can determine the apparent blackbody radius, R_{bb}, of the burst emitting region (identified with the surface of a neutron star) through:

$$R_{bb} = d\,(F_{\rm bol}/\sigma T^4)^{1/2} \tag{3.2}$$

Here d is the source distance (see Chapter 4 for a detailed discussion of blackbody radii).

Thus, the result of a typical spectral analysis of an X-ray burst is the variation with time of blackbody temperature, bolometric flux and blackbody radius (see

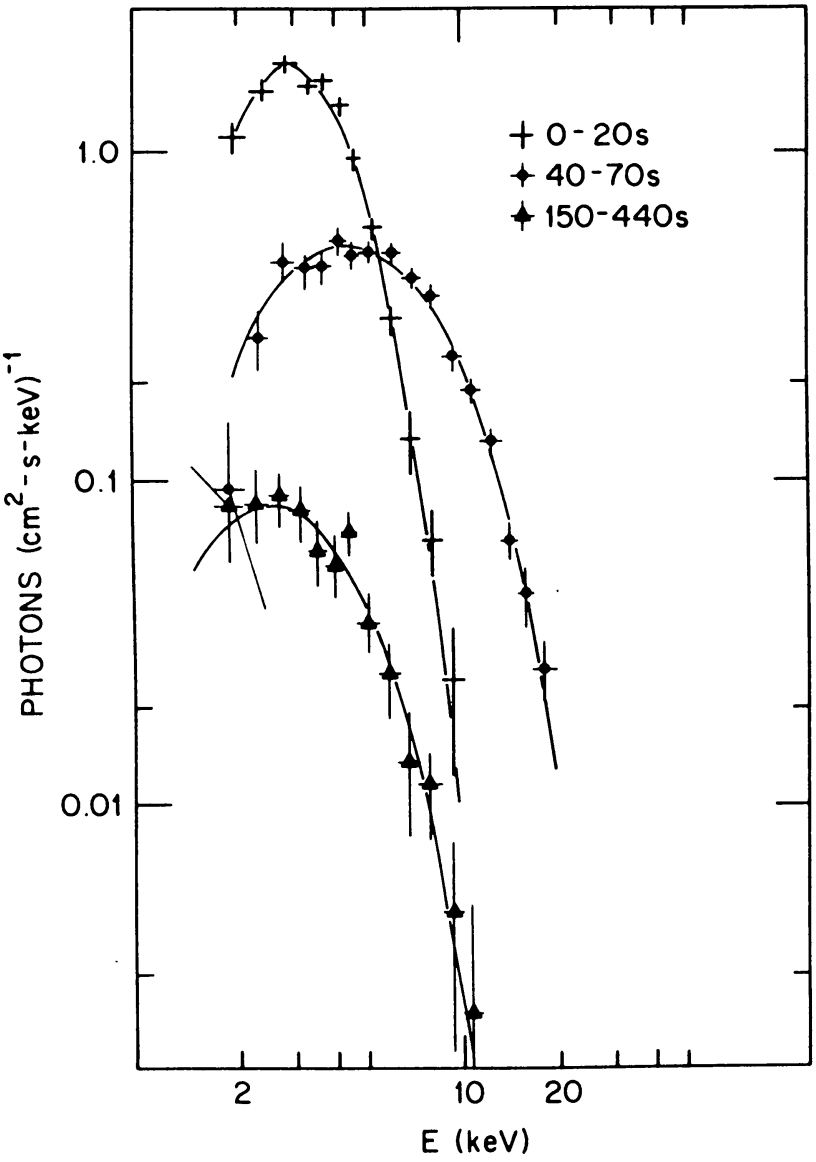

Fig. 3.9. Average spectra, during three time intervals, of a long burst which probably came from 1724–307 in the globular cluster Ter 2. The solid curves are blackbody fits to the data. The values for kT are ~0.9 keV (0–20 s), ~2.3 keV (40–70 s), and ~1.2 keV (150–440 s). For assumed spherical emission and source distance of 10 kpc the blackbody radii were ~100 km during the first 20 s of the burst, and ~15 km thereafter. This figure is from Swank *et al.* (1977).

Fig. 3.10). A useful way to display these results is a diagram of log $F_{\rm bol}$ versus log kT_{bb}; to adhere to astronomical convention (Hertzsprung-Russell diagram) temperature is plotted horizontally, and increases to the left (see Fig. 3.11). During burst decay one finds in general that R_{bb} is approximately constant, i.e. in the Hertzsprung-Russell (HR) diagram the burst is then represented by points located along a straight line ("cooling track") with slope 4. As we discuss in more detail in Sect. 3.4 and Ch. 4, in some bursts photospheric radius expansion occurs due to strong radiation pressure. During the expansion phase the luminosity remains approximately constant. In the HR diagram the burst is then represented by a nearly

horizontal track that runs to the right from the upper part of the cooling track.

It was pointed out by Van Paradijs and Lewin (1985b) that if the neutron star in an X-ray burst source is sufficiently hot to give a significant blackbody (or blackbody-like) contribution to the persistent X-ray flux, blackbody radii obtained from this standard burst analysis contain systematic errors which can be very large near the end of the burst when the burst flux reaches very low values. In this case the burst emission is given by the difference between the emission of two blackbodies; this difference does not have a blackbody energy distribution. They showed that when the burst flux is small the blackbody temperature assigned to its spectrum is directly related to the quiescent (prior to the burst) blackbody temperature T_0 (it looks somewhat like a blackbody with $T_{bb} \sim 1.3T_0$) independent of the burst flux. As a consequence, during the final decay part of the burst the apparent blackbody radius (determined according to Equation (3.1)) becomes artificially very small, and ultimately goes to zero as the burst flux goes to zero. This effect was found to be important in a burst observed from the luminous source GX 17 + 2 (Sztajno *et al.* 1986).

Although blackbody spectra in general provide a good fit to observed burst spectra, evidence for significant deviations from a blackbody has been obtained in some cases. Blackbody temperatures kT_{bb} in excess of 3 keV have been observed for several sources; this is substantially higher than the Eddington temperature, in spite of the fact that burst luminosities are not expected to exceed the Eddington limit (see Sect. 3.4, and Ch. 4); this indicates that the spectra emitted during bursts mimic those of blackbodies at temperatures higher than the effective temperature (see Ch. 5). According to Nakamura *et al.* (1989) burst spectra from 1608–522 show high-energy tails when the persistent flux is relatively low. They interpret this tail as a result of comptonization of the burst emission in a hot plasma surrounding the neutron star. From a detailed analysis of possible high-energy tails in burst spectra observed from 1636–536, Damen *et al.* (1990a) found no evidence for such comptonization. Systematic deviations from a blackbody spectrum, in the form of temperature dependent "bumps" have been found in burst spectra observed during one very long X-ray burst from 2127 + 119 in M15 (Van Paradijs *et al.* 1990a); their interpretation is presently unclear.

A particularly interesting non-Planckian feature in burst spectra was found by Waki *et al.* (1984) who detected absorption lines in X-ray spectra of four (out of 13) X-ray bursts from 1636–536. These lines were observed only during part of these four bursts. Three of the lines occurred at an energy of 4.1 keV, the fourth at 5.7 keV. Waki *et al.* interpreted these lines as redshifted Lyman α lines of helium-like iron atoms. Absorption lines, all occurring at this same energy of 4.1 keV, have also been detected in spectra of three bursts from 1608–522 (Nakamura *et al.* 1988) and one burst from 1747–214 (Magnier *et al.* 1989). Less convincing results have been published by Turner and Breedon (1984), Sztajno *et al.* (1984) and Trümper *et al.* (1985). The lines are strong, with equivalent widths up to ~500 eV; such strong lines are difficult to explain in terms of atomic transitions in the neutron star

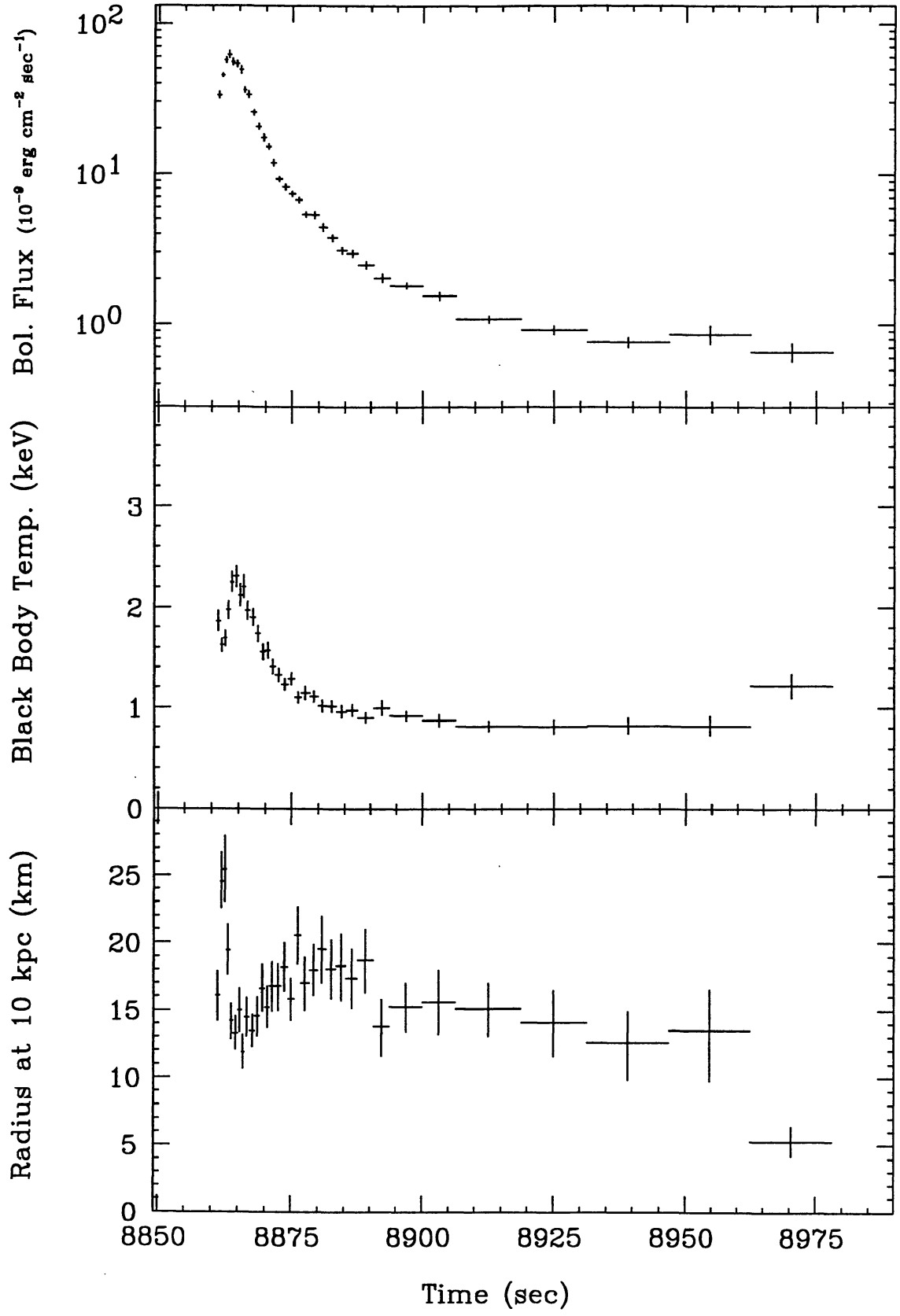

Fig. 3.10. Variation of the bolometric flux, blackbody temperature, and blackbody radius during a burst observed with EXOSAT from 1636–536, as obtained from time-resolved blackbody fittings of burst spectra (see text). (Courtesy T. Oosterbroek).

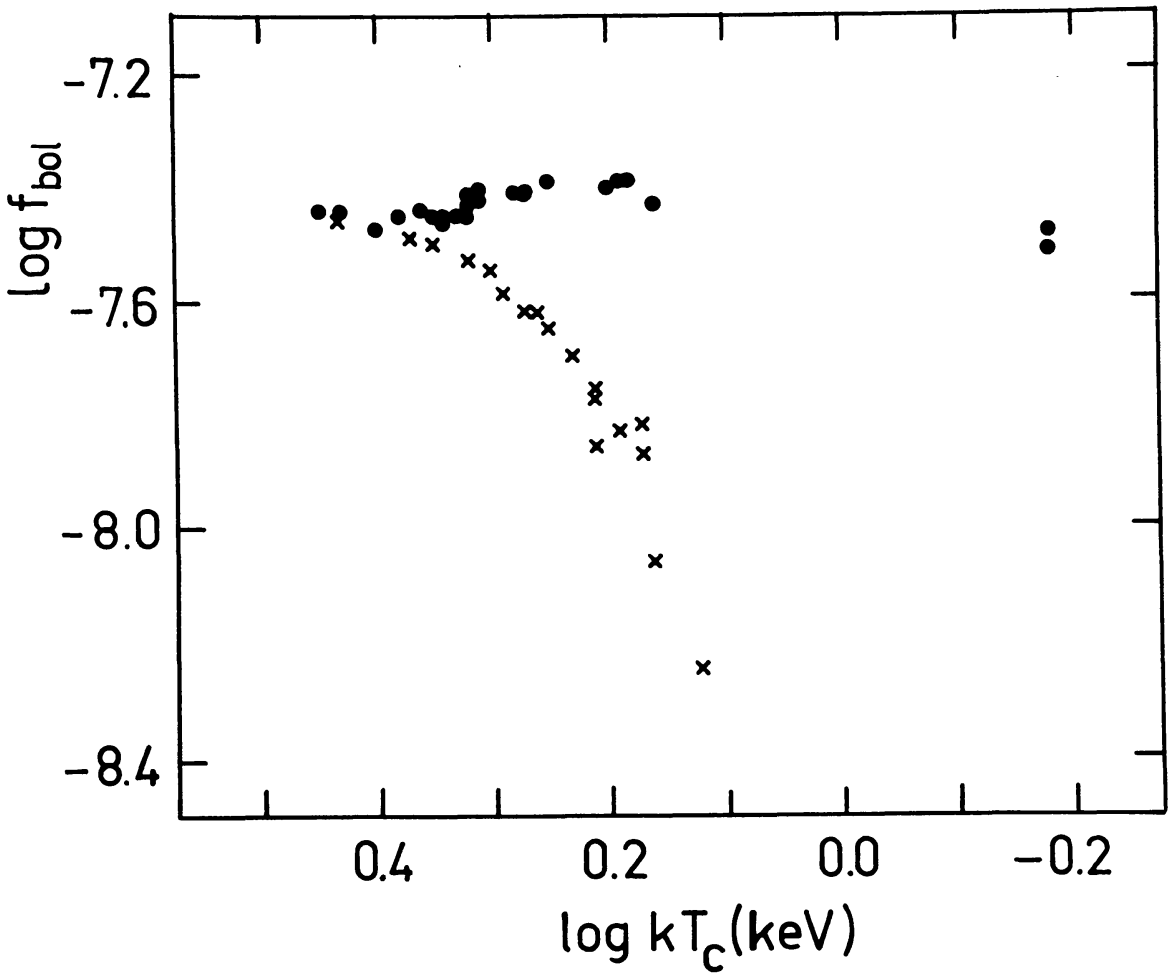

Fig. 3.11. Flux-temperature diagram for an X-ray burst observed with Ginga from 2127+119 in the globular cluster M15. Dots indicate the photospheric expansion/contraction track, the crosses the cooling track. The two dots on the far right (very large radius expansion) are too low in flux (see Sect. 3.4); this is likely caused by the fact that at these very low temperatures only a minute fraction of the flux is sampled in the X-ray band which leads to a large uncertainty in the flux measurement. Notice that the cooling track is not a straight line with slope 4; this reflects deviations from a Planckian curve. This figure is from Van Paradijs *et al.* (1990a).

atmosphere which transfers the burst radiation; it has been suggested (Pinto *et al.* 1992) that they are formed in the accretion flow (see Sect. 5.5).

3.4. Photospheric Radius Expansion

Strong burst-like events, lasting up to 1500 seconds have been observed (Hoffman *et al.* 1978b; Tawara *et al.* 1984a, c; Lewin, Vacca and Basinska 1984; Van Paradijs *et al.* 1990a) which, because of their peculiar profiles and very long duration, were not initially recognized as type I X-ray bursts; Hoffman *et al.* called them fast transients with a precursor. It is possible that the sparsely sampled burst observed by Swank *et al.* (1977), which lasted for a few hundred seconds, is a similar event.

The events (see Fig. 3.12) start with a brief increase of the X-ray intensity (the precursor), which rises rapidly (within a second) and lasts for a few seconds;

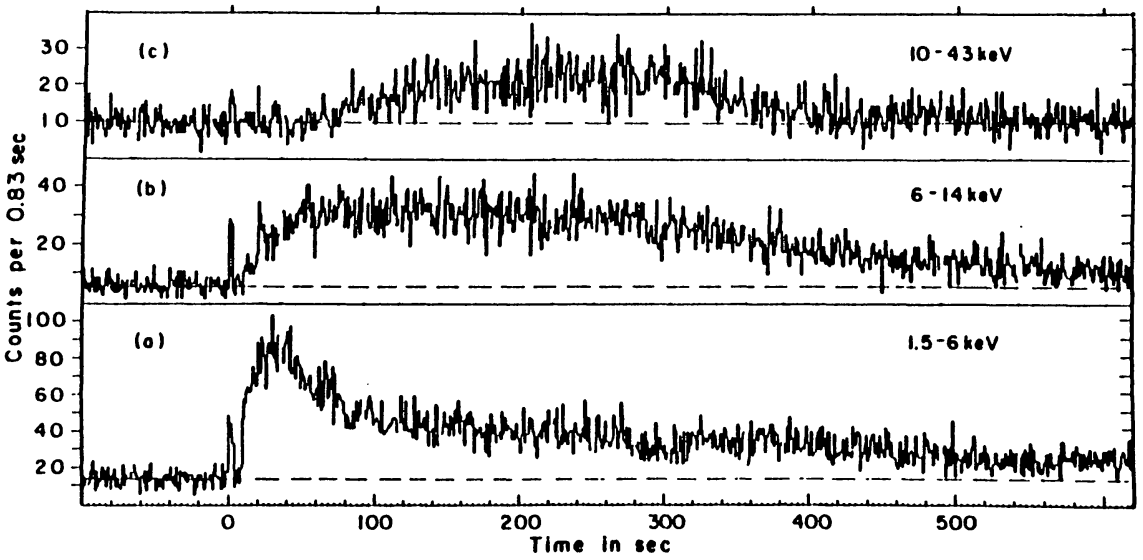

Fig. 3.12. Profile of a very long X-ray burst observed on February 7, 1977 with SAS–3. Before the main event a precursor occurred which was separated from the main event by ~7 s in the (1.5–6 keV) band, and ~60 s in the (10–43) keV band. This profile is the result of very strong radius expansion during the initial phase of the burst (see text). This figure has been adapted from Lewin, Vacca and Basinska (1984).

it is followed by a return to the persistent flux level for a time interval lasting between ~5 and ~10 seconds. After this, the main part of the event starts: a relatively slow increase of the X-ray intensity first appears in the low-energy band and progressively later X rays become visible at higher energies. Thus during the first part of this main event the X-ray spectrum (which can be reasonably well described by a blackbody spectrum) gradually becomes harder. After the blackbody temperature has reached a maximum value (in excess of kT ~2.5 keV) the main event starts to decay with a gradual decrease of the X-ray flux accompanied by a softening of the spectrum, corresponding to the cooling of a blackbody of approximately constant size, similar to what is observed in a "normal" type I X-ray burst.

Tawara *et al.* (1984a) and Lewin, Vacca and Basinska (1984) independently proposed that the precursor and the main event are both part of one very energetic type I X-ray burst during which the luminosity becomes so high (i.e., reaches the Eddington limit), that temporarily the atmosphere of the neutron star, through which the burst radiation is transported, expands due to radiation pressure, possibly through the formation of a stellar-wind outflow of material from the neutron star. After the luminosity decreases below the Eddington limit the photosphere contracts. The observed variation of the blackbody radius during the main parts of these events supports this picture.

Detailed calculations of the effect of a (super-) Eddington luminosity on the structure of a neutron star atmosphere have shown that during the expansion and contraction of the atmosphere the luminosity always remains very close (to within

a percent or less) to the Eddington limit; the excess luminosity is transformed very effectively into kinetic and potential energy of the extended atmosphere (Hanawa and Sugimoto 1982; Taam 1982; Wallace *et al.* 1982; Paczynski 1983a,b; Kato 1983; Ebisuzaki *et al.* 1983; Paczynski and Proszynski 1986; Paczynski and Anderson 1986; Joss and Melia 1987). As discussed in detail in Chapter 4, this theoretical result can be used to constrain the mass-radius relation of neutron stars.

As the photospheric radius, $R_{\rm ph}$, increases at a near constant luminosity, L, the effective temperature, $T_{\rm eff}$, will decrease according to $T_{\rm eff} = (L/4\pi\sigma)^{1/4}$ $(R_{\rm ph})^{-1/2}$. The end of the observed precursor signals that the radius has become so large and, correspondingly, the temperature so low, that X rays are no longer emitted. As the photospheric radius slowly starts decreasing (and the temperature starts increasing) X rays will again be emitted, first at low energies, and later on, as the temperature continues to increase, at higher energies as well. The radius decrease stops when the photosphere has shrunk to its original value after which the neutron star surface cools, but the photospheric radius remains equal to the radius of the neutron star.

Photospheric radius expansion at a luminosity close to the Eddington limit also occurs during classical nova outbursts which are caused by unstable hydrogen burning on the surface of an accreting white dwarf in a mass exchanging low-mass binary (Gallagher and Starrfield 1978; Cordova 1993).

These very long X-ray bursts with "precursors" are related to the bursts with double-peaked profiles, which are particularly prominent at high photon energies (Fig. 3.6; Lewin *et al.* 1976d; Hoffman *et al.* 1979, 1980; Grindlay *et al.* 1980; Vacca, Lewin and Van Paradijs 1986; Haberl *et al.* 1987), but not apparent in burst profiles covering a wide energy range (Fig. 3.2). These energy-dependent double-peaked profiles are also the result of photospheric radius expansion (Hanawa and Sugimoto 1982; Taam 1982; Wallace *et al.* 1982; Paczynski 1983a, b; Ebisuzaki *et al.* 1983; Kato 1983); however, in these cases the radius increase is not very large, and leads only to a temporary shift of the burst emission to lower energy photons within the X-ray band. Only when the radius expansion is very large will the X-ray emission disappear completely; in that case the first peak of the burst profile becomes disconnected from the rest of the burst, i.e., it becomes a "precursor".

X-ray bursts with photospheric radius expansion have so far been observed from 13 sources (see Chapter 9 for more detailed information on these events). Five of these (1724–307, 1746–370, 1820–303, 1850–087 and 2127 + 119) are located in globular clusters, and for them distances can be estimated using optical observations of the cluster. This allows us to evaluate whether the peak luminosities of bursts with radius expansion can be considered standard candles (cf. Van Paradijs 1978; Lewin 1984). We find that except for the bursts from 1746–370 these peak luminosities are 3.0 ± 0.6 (1 standard deviation) $\times 10^{38}$ erg s^{-1} (for assumed isotropic burst emission). The low value for 1746–370 (1.0×10^{38} erg s^{-1}) has been discussed in detail by Sztajno *et al.* 1987).

Sugimoto *et al.* (1984) found that the distribution of burst peak fluxes for

1636–536 is bi-modal, with a gap between $F_{max} \sim 4.0 \times 10^{-8}$ and $\sim 6.5 \times 10^{-8}$ erg cm^{-2} s^{-1} (see Fig. 3.13). Below the gap the F_{max} values range over a factor ~4; the peak fluxes above the gap are consistent with a single value. All the burst above the gap (but none below the gap) show evidence for photospheric radius expansion. These results have been confirmed by subsequent observations (see Fujimoto *et al.* 1987b, 1988; Damen 1990). Sugimoto *et al.* proposed that the peak flux above the gap and the upper bound to the distribution below the gap correspond to the Eddington limit for hydrogen-poor matter, and for matter with cosmic compostion, respectively (see Sect. 4.5.1); these Eddington limits are expected to be in the ratio ~1.7, consistent with the observed ratio of the corresponding peak fluxes. They suggested that during the radius expansion the upper hydrogen-rich layers are ejected from the neutron star surface, thereby exposing the hydrogen-poor layers which were involved in the nuclear processing. There is a finite chance that a radius-expansion burst has a peak flux that lies in the gap (Fujimoto *et al.* 1987b), but this requires some fine tuning of the conditions in the outer layers. [Damen (1990) found that one of 61 bursts observed from 1636–536 with EXOSAT has a peak flux inside the gap]. The distribution of peak fluxes for 1636–536, in particular the existene and location of the gap, has not been observed to change over the years; this indicates that any anisotropy of the burst emission (see Sect. 4.3.2) remains constant.

The double-peaked radius expansion bursts should not be confused with the small number of bursts observed from 1636–536 which showed two (in one case even three) peaks in their bolometric profiles (Sztajno *et al.* 1985; Van Paradijs *et al.* 1986a; see Fig. 3.7 and 3.8). These bursts had peak luminosities substantially less than the Eddington limit, and they showed no evidence for radius expansion. Melia (1987) suggested that these multi-peaked profiles are caused by diffuse scattering of the burst radiation in a burst-induced accretion disk corona. However, Penninx, Van Paradijs and Lewin (1987) showed this is not the case; it is likely that these profiles reflect variations in the rate of generation or release of nuclear energy.

3.5. Burst Intervals

Burst intervals can be regular or irregular on time scales of hours to days (see Fig. 3.14); they range from ~5 minutes to days; burst activity can stop altogether for periods from days to months. Very regular burst behavior has been observed from, e.g., 1658–298 (Lewin 1977), 1820–303 (Clark *et al.*, 1977; Haberl *et al.* 1987) and 1323–619 (Parmar *et al.* 1989a).

The burst occurrence rate is sometimes (but not always) related to the level of persistent X-ray emission. Clark *et al.* (1977) found that the persistent flux of 1820–303 increased by a factor of ~5 while the burst intervals gradually decreased by ~50%. The persistent flux continued to increase, and the bursts stopped completely. According to Priedhorsky and Terrell (1984b) the X-ray flux of 1820–303 shows a long-term (176 days) periodic variation; X-ray bursts have only been observed when the source was in a low state (Vacca, Lewin and Van Paradijs 1986; Stella,

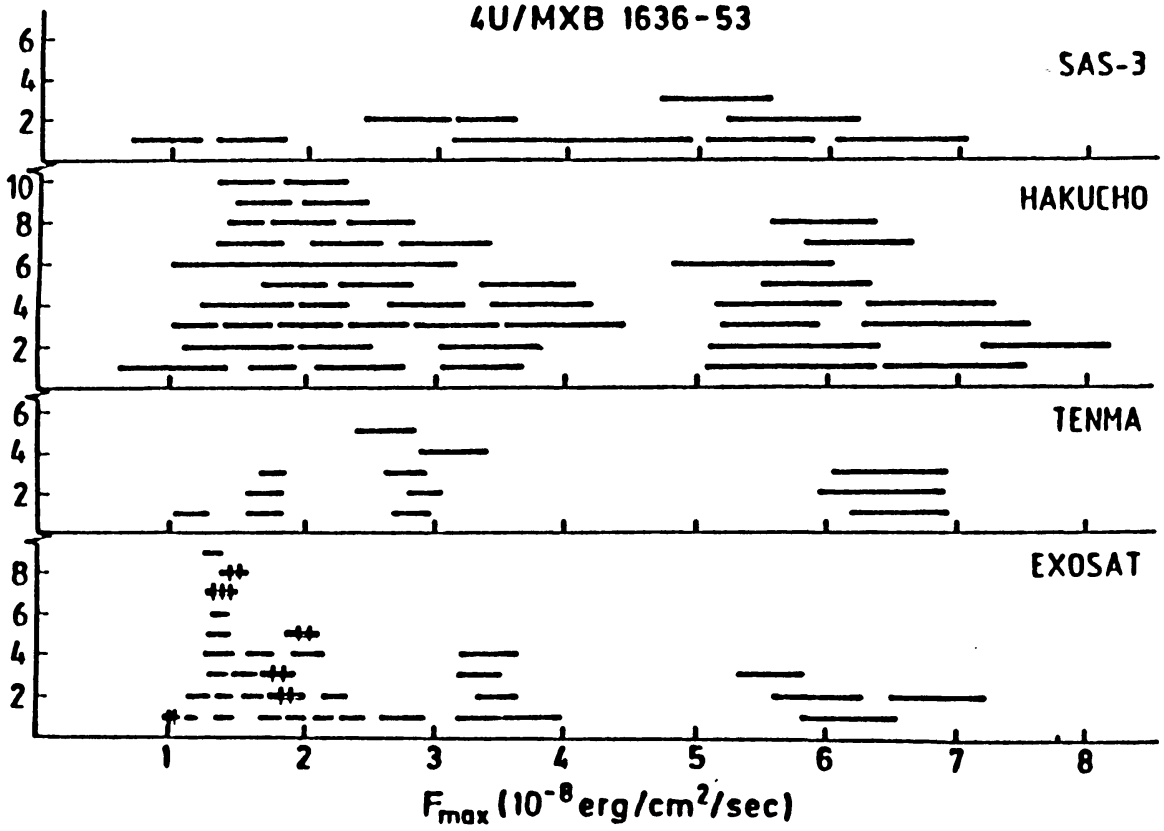

Fig. 3.13. Distribution of maximum burst fluxes from 1636–536, observed with different satellites. For every burst its one-sigma error range is indicated with a horizontal bar. Bars with two and three tic marks indicate bursts with a double-peaked and triple-peaked profile, respectively. (from Fujimoto *et al.* 1988).

Priedhorsky and White 1984; Haberl *et al.* 1987). The transient source 1658–298 produced bursts at very regular intervals of ~2.5 hours when the persistent flux was less than $\sim 5 \times 10^{-11}$ erg cm^{-2} s^{-1} (Lewin, Hoffman and Doty 1976e). When the persistent flux was $\sim 2 \times 10^{-9}$ erg cm^{-2} s^{-1} no bursts were observed (Lewin *et al.* 1978; Share *et al.* 1978). Similar behavior has been observed for the bright source GX 3 + 1 which was found in a burst active state, when its persistent X-ray flux was relatively low (Makishima *et al.* 1983).

Bursts from the transient sources Cen X–4, 1608–522, Aql X–1, and 0748–676 have only been observed when these sources were in the bright state (Matsuoka *et al.* 1980; Murakami *et al.* 1980a; Nakamura *et al.* 1989; Koyama *et al.* 1981; Czerny *et al.* 1987; Gottwald *et al.* 1986). However, this does not contradict the above mentioned anti-correlation between burst occurrence and persistent luminosity. In the case of Cen X–4 and Aql X–1 X-ray bursts occurred when the outburst had already decayed by a substantial factor. In the case of 0748–676 and 1608–522 the persistent flux remained high for a long time after the transient outburst started; when the type I X-ray bursts were observed the persistent X-ray luminosity was at least a factor 10 below the Eddington limit, as measured by the peak fluxes of

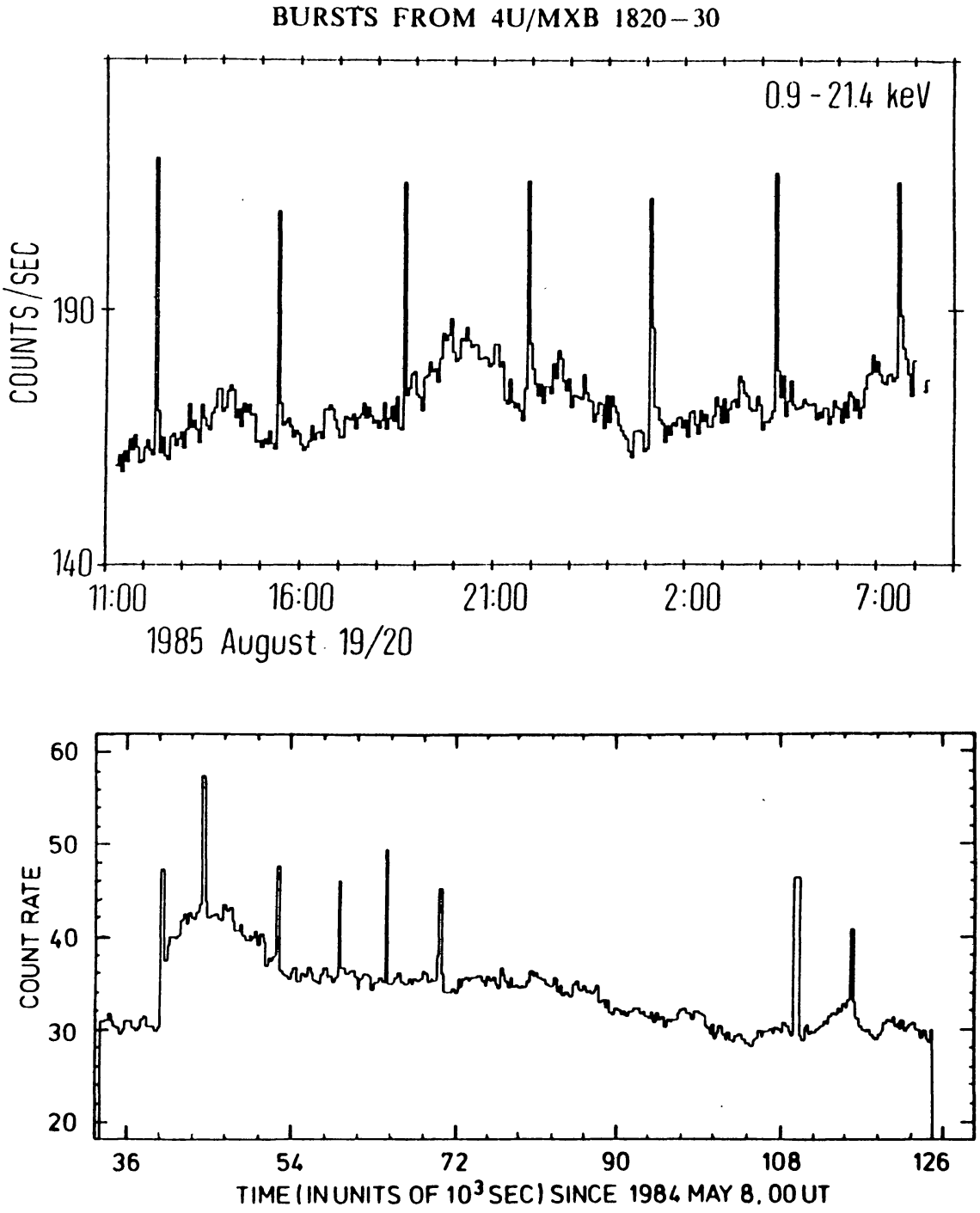

Fig. 3.14. (a) Example of a very regular burst recurrence pattern, observed for 1820–303 (from Haberl *et al.* 1987). (b) Irregular burst recurrence, observed from 1636–536 (from Sztajno *et al.* 1985).

bursts which showed radius expansion (see Sect. 3.4).

In several well studied sources large variations in the observed burst intervals occurred, apparently unrelated to variations in the rate of the accretion that feeds

the bursts (e.g., Ser X–1: Li *et al.* 1977, Sztajno *et al.* 1983; 1735–444: Lewin *et al.* 1980; Van Paradijs *et al.* 1988b; 1728–337: Basinska *et al.* 1984; 1636–536: Lewin *et al.* 1987a). Very irregular burst behavior tends to occur in sources with relatively high persistent X-ray luminosities (Van Paradijs *et al.* 1979a, 1988a; see Sect. 3.7); this may be related to the fact that these persistent luminosities are close to a critical value (near half the Eddington luminosity) above which X-ray bursts do not occur (as expected from some thermonuclear-flash models (Fujimoto *et al.* 1981; Ayasli and Joss 1982). In 1735–444 there is a tendency for the bursts to come in clusters (Lewin *et al.* 1980; Van Paradijs *et al.* 1988b), and it is perhaps possible that in this relatively luminous source the bursts themselves create conditions in the accreted material that quench further burst activity for some time.

Burst intervals as short as ~10 minutes have been observed from 0748–676 (Gottwald *et al.* 1986), 0836–429 (Aoki *et al.* 1993), 1608–522 (Murakami *et al.* 1980b), 1636–536 (Ohashi 1981; Pedersen *et al.* 1982b), 1705–440 (Langmeier *et al.* 1987), 1743–28 (Lewin *et al.* 1976d), and 1745–248 (Inoue *et al.* 1984a). According to current models of thermonuclear flashes (see Chapter 6) these intervals are much too short to replenish, through accretion, a sufficient amount of nuclear fuel to account for the second burst. Thus, one requires the presence of a reservoir of nuclear fuel which survived the previous thermonuclear flash, and can be prematurely rekindled. A considerable amount of hydrogen and helium may survive a flash in the upper layers of the accreted material, where the temperature remains relatively low (see, e.g. Hanawa and Fujimoto 1984). Fujimoto *et al.* (1987b) proposed that this inactive layer can be used as fuel for a "premature" burst, if it can be mixed into the deeper hotter layers (which underwent nuclear processing during the previous burst) where the mixing of fresh fuel may lead to a new instability. Fujimoto *et al.* (1988) suggested a specific mixing mechanism involving differential rotation between the freshly accreted layer and the deeper layers where angular momentum was distributed uniformly by convection during the previous flash.

3.6. Burst Energy and Burst Intervals

For the simplest type of thermonuclear-flash models one would expect that there is a correlation between the time interval since the previous burst and the integrated burst energy: the longer this time interval is, the larger is the amount of nuclear fuel available for the burst.

Hoffman, Lewin and Doty (1977b) were the first to find a possible correlation (for 1728–337) between the burst fluence, E_b, and the time interval, $\Delta\tau$, since the previous burst: the lower the observed burst frequency was, the larger was the fluence. This was confirmed by later more extensive observations of this source (Basinska *et al.* 1984). Lewin *et al.* (1980) found evidence for a correlation between the average burst interval and the burst fluence for 1735–444. Hoffman *et al.* (1980) suggested, based on statistical evidence, that the very strong bursts (with double-peaked profiles; see Sect. 3.4) came after long waiting times. For optical bursts from

1636–536 Pedersen *et al.* (1982b) found a clear correlation between the fluence and the interval since the previous optical burst.

Prior to EXOSAT all X-ray satellites were in near-Earth orbits, and X-ray burst studies were hampered by the limitation in the duration of uninterrupted observations: most sources were occulted by the Earth for ~30 minutes every ~100 minute orbit, and unless burst intervals were less than ~1 h, or the bursts occurred periodically, the measurement of burst intervals were very uncertain. The 91 h orbital period of EXOSAT made it possible to determine burst intervals of up to tens of hours and to study in detail the relation between burst fluence and burst intervals.

Extensive studies of the $(E_b, \Delta\tau)$ relation have been made with EXOSAT for 1636–536 (Lewin *et al.* 1987a; Damen 1990), 1735–444 (Van Paradijs *et al.* 1988b) and 0748–676 (Gottwald *et al.* 1986; 1987a). For all three sources one finds globally that the longer the burst interval, the higher is the burst fluence; because of the correlation between burst fluence and peak flux the same is also true for the latter quantity (see Fig. 3.15). The scatter around these relations is, however, substantial. For time intervals below a value, that ranges between ~1 hour for 1735–444 and ~6 hours for 1636–536, the $(E_b, \Delta\tau)$ relation is approximately linear; for longer intervals the burst fluence does not increase much any more. Gottwald *et al.* (1987a) pointed out that for 0748–676 the linear relation between E_b and $\Delta\tau$ leads to a positive value for E_b $(2 \pm 0.5 \times 10^{-8}$ erg cm$^{-2})$ at $\Delta\tau = 0$; this reflects the occurrence of X-ray bursts after very short waiting times (see Sect. 3.5).

Bursts that come after very long waiting times tend to show photospheric radius expansion, and some of the flattening of the $(E_b, \Delta\tau)$ relation may therefore be explained in terms of the energy consumed in mass ejection. The flattening may also be explained by a growing leak of nuclear fuel, e.g. due to steady nuclear burning during the intervals between bursts (Lewin *et al.* 1987a; Fujimoto et al. 1987b). For 1636–536 it may be possible to explain the energy leak simply in terms of continuous stable hydrogen burning through the CNO cycle (Fujimoto *et al.* 1987b). However this explanation is unlikely to work for 1735–444 (Van Paradijs *et al.* 1988b). For this source the α-value (see Sect. 3.7) for bursts which come after an interval of less than an hour (α ~250) are consistent with the values expected for thermonuclear flashes in which only helium participates. The very high α-values for the bursts that occurred after very long time intervals indicate that prior to these bursts both hydrogen and helium are stably burning (cf. Van Paradijs *et al.* 1979a). The rapid transition to very long burst intervals (in which helium is stably burnt) is not accounted for by present models of thermonuclear flashes on the surface of a neutron star (cf. Fujimoto *et al.* 1987a,b).

3.7. Burst Energetics and the Persistent Flux

The fuel for the thermonuclear flashes that give rise to X-ray bursts was accreted on the surface of the neutron star prior to the burst. The accretion of one gram of

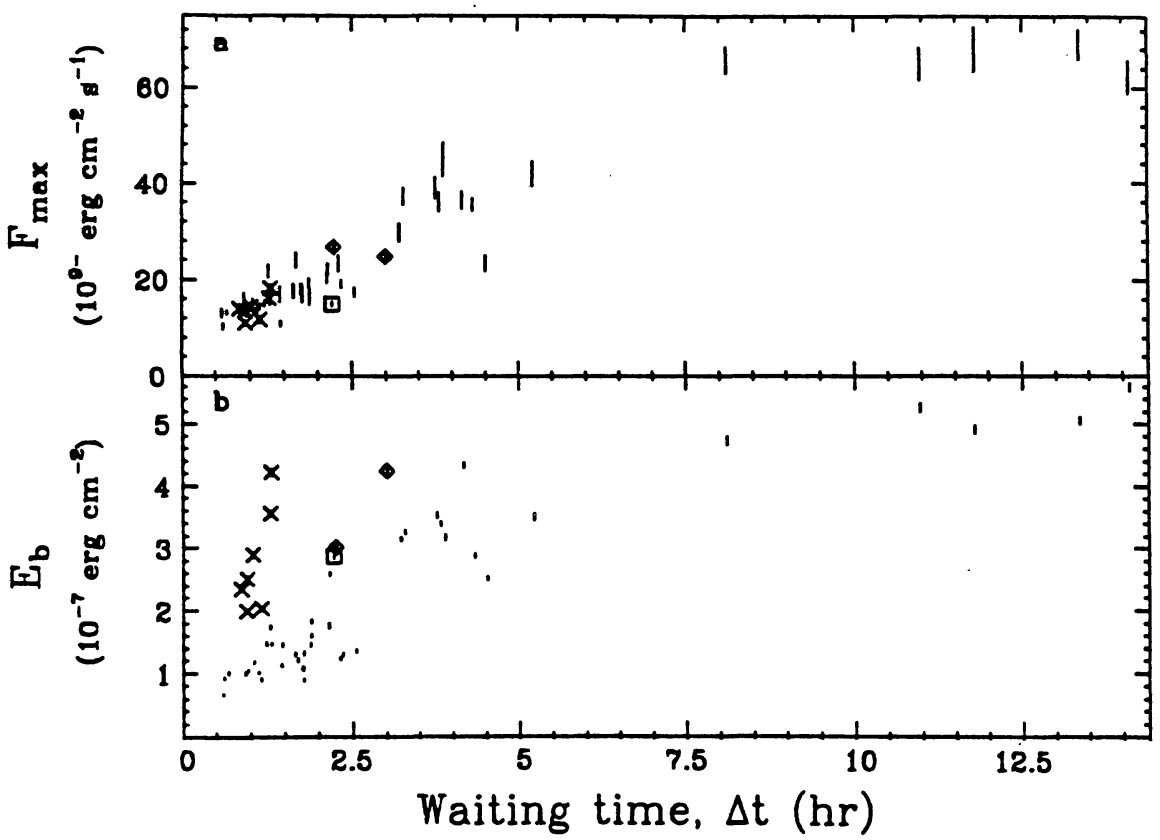

Fig. 3.15. Dependence of burst peak fluxes (top panel) and burst fluences (bottom panel) on the waiting time since the previous burst, for 1636–536. Crosses and diamonds indicate bursts that occurred during "island" states in 1983 and 1985, respectively; the square indicates a burst that had a triple-peaked profile (see Fig. 3.8). This figure has been adapted from Damen (1990).

material leads to the emission of an amount of energy equal to $\varepsilon_G = GM_*/R_*$ (where M_* and R_* are the mass and radius of the neutron star). For "canonical" values $M_* = 1.4\ M_\odot$ and $R_* = 10$ km one finds $\varepsilon_G = 1.8 \times 10^{20}$ erg g^{-1} = 180 MeV/nucleon= $0.2c^2$. The amount of energy liberated in thermonuclear burning depends on the composition of the fuel. In the transformation of pure hydrogen into iron-peak elements the total available nuclear energy is 8.4 MeV/nucleon $\sim 8 \times 10^{18}$ erg g^{-1} $\sim 0.009c^2$; for helium this amount is $\varepsilon_N = 1.7$ MeV/nucleon $\sim 1.6 \times 10^{18}$ erg g^{-1} $\sim 0.002c^2$ (Clayton 1968). This energy is liberated in the form of kinetic energy and γ photons (this energy emerges in the X-ray burst) and neutrinos. The fraction ultimately emitted in X-ray photons depends on the detailed path in the nuclear-reaction network via which the iron-peak elements are reached; it is roughly $0.007c^2$ (6×10^{18} erg g^{-1}) and 0.002 c^2 ($\sim 1.6 \times 10^{18}$ erg g^{-1}) for hydrogen and helium, respectively.

In the simplest version of the thermonuclear-flash model in which all accreted matter is processed in flashes, one therefore expects that the ratio of the average luminosity emitted in the persistent X-ray emission (L_p) to that emitted in X-ray bursts (L_b; the average is taken over the time interval since the previous burst)

equals $L_p/L_b = \varepsilon_G/\varepsilon_N \sim$(25–100) $(M_*/M_\odot)/(R_*/10$ km); the lower and upper value of the range correspond to hydrogen and helium burning, respectively. For assumed isotropy of both the burst and persistent X-ray emission this equals the observed ratio (indicated by α) of the average persistent X-ray flux to the average flux emitted in bursts (this value may be somewhat modified because of the limited passband of most X-ray observations, typicaly 2–10 keV).

Hoffman, Marshall and Lewin (1978a) observed that the ratio of the average fluxes emitted in the type II and type I bursts from the Rapid Burster was $\sim$120; this led to their recognition that the type II bursts are caused by accretion instabilities, which removed a major stumbling block to the acceptance of the thermonuclear flash model for (type I) bursts (see Sect. 1.3).

Observed values of α range from $\sim$10 to $\sim 10^3$, with a maximum in the distribution of α values near 10^2, roughly as expected for the thermonuclear-flash model. The α ratio varies with the persistent luminosity of the source; this is discussed in Sect. 3.8.

The observed values of α can differ substantially from the above estimates for several reasons. Prior to the occurrence of an X-ray burst, steady burning of the accreted fuel may occur in which case the observed value for α may reach arbitrarily high values (see e.g. Van Paradijs *et al.* 1988b). In case part of the nuclear fuel survives an X-ray burst, fuel is available for a subsequent burst, and low values for α are observed (in, e.g., 0748–676, see Gottwald *et al.* 1987a).

3.8. Dependence of Burst Properties on Accretion Rate

As mentioned in Sect. 3.2 and 3.5, in a number of sources a correlation has been observed between burst profiles (and intervals) and the persistent X-ray flux F_p. A striking example is the transient source 0748–676, for which Gottwald *et al.* (1986; 1987a) obtained the following results:

(i) The burst frequency was anti-correlated with F_p; it varied from 0.75 h^{-1} to 0.12 h^{-1} as F_p varied from $\sim 3 \times 10^{-10}$ to $\sim 10^{-9}$ erg cm^{-2} s^{-1}. A similar anti-correlation has been observed in some other transients (e.g., 1658–298, see Lewin *et al.* 1978), but not in others (e.g., 1608–522, see Murakami *et al.* 1980a). This anti-correlation may be similar to that observed in some luminous persistent sources, such as 1820–303 (Clark *et al.* 1977) and GX 3+1 (Makishima *et al.* 1983); in these sources burst activity ceased altogether when the persistent flux was above a certain 'critical' level (as follows from some models of thermonuclear flashes, see e.g. Fujimoto *et al.* 1981; Ayasli and Joss 1982).

(ii) The average ratio, α, of the total energy emitted in the persistent flux to that emitted in bursts (see Sect. 3.7) increased strongly with F_p, from $\sim$12 to $\sim$75 over the range given above.

(iii) Over the above range in F_p the average burst fluence E_b increased by a factor of 2, the maximum peak flux, $F_{\max}$, increased by a factor of $\sim$10, and the average burst duration $\tau = E_b/F_{\max}$ decreased from $\sim$25 s to $\sim$6 s.

(iv) The blackbody radius of the burst emitting region depends strongly on F_p

(see Sect. 4.7 and 5.4).

An anti-correlation between burst duration τ and the persistent flux was also found for 1608–522 by Murakami *et al.* (1980a) who made a distinction between 'fast' and 'slow' bursts (cf. Matsuoka 1985). Van der Klis *et al.* (1990) found for bursts from 1636–536 and 1705–440 that τ is strongly correlated with the spectral state of the persistent X-ray emission (as indicated by the position in the X-ray color-color diagram, see Fig. 3.16); this correlation is much better than with F_p (Damen *et al.* 1989; see also Nakamura *et al.* 1989). Van der Klis *et al.* (1990) found a similar result for the blackbody radii obtained for these bursts. Following the results of Hasinger and Van der Klis (1989), Van der Klis *et al.* interpreted this as evidence that it is the mass accretion rate that controls the burst duration and the blackbody radius (e.g. through its influence on the structure of the outer envelope of the neutron star, or the angular dependence of the X-ray emission); if their interpretation is correct the observed persistent X-ray flux is not always a good measure of the accretion rate.

Van Paradijs, Penninx and Lewin (1988a) investigated the relation between important burst parameters and the persistent X-ray luminosity, which they took to be a measure of the accretion rate (see, however, Hasinger and Van der Klis 1989). Guided by the notion (see Section 3.4, and references therein) that the peak luminosity of X-ray bursts that show photospheric radius expansion equals the Eddington luminosity, they assumed this peak luminosity is a standard candle (see also Van Paradijs 1978; Van Paradijs *et al.* 1979a); this assumption is probably correct to within a factor of 2 for most (if not all) sources. This makes it possible to define a relative distance scale and leads to the following expression for the persistent X-ray luminosity L_p:

$$L_p = L_0(\xi_p/\xi_b)\gamma \tag{3.2}$$

Here ξ_p and ξ_b are anisotropy factors for the persistent and burst emission, respectively (see Equation (4.9)), and γ is the ratio of the observed persistent flux, F_p, to the net peak flux (not including the persistent emission), $F_{\rm re}$, of bursts with radius expansion. Their results have been summarized in Fig. 3.17 and 3.18 which show the γ-dependence of the burst duration $\tau(= E_b/F_{\rm max})$ and the α-value, respectively.

From Fig. 3.17 it appears that τ is anti-correlated with γ over the whole observed range of γ. It varies between 30 s and a few minutes at $\log \gamma \sim -2$, and $\sim$5 s at $\log \gamma \sim -0.5$. The average (γ, τ) relation is rather tight and encompasses both the bursts with radius expansion (Sect. 3.4) and the more common X-ray bursts quite well. There is no evidence for a clear separation of bursts into two groups, one with long and another with short durations (cf. Murakami *et al.* 1980a; Matsuoka 1985). In the framework of thermonuclear-flash models this decrease of τ with γ indicates that hydrogen becomes less important in the energetics of the bursts as the mass accretion rate increases (see Section 3.7 and Chapter 6).

The average values of α are strongly correlated with γ, with $\log \alpha$ varying

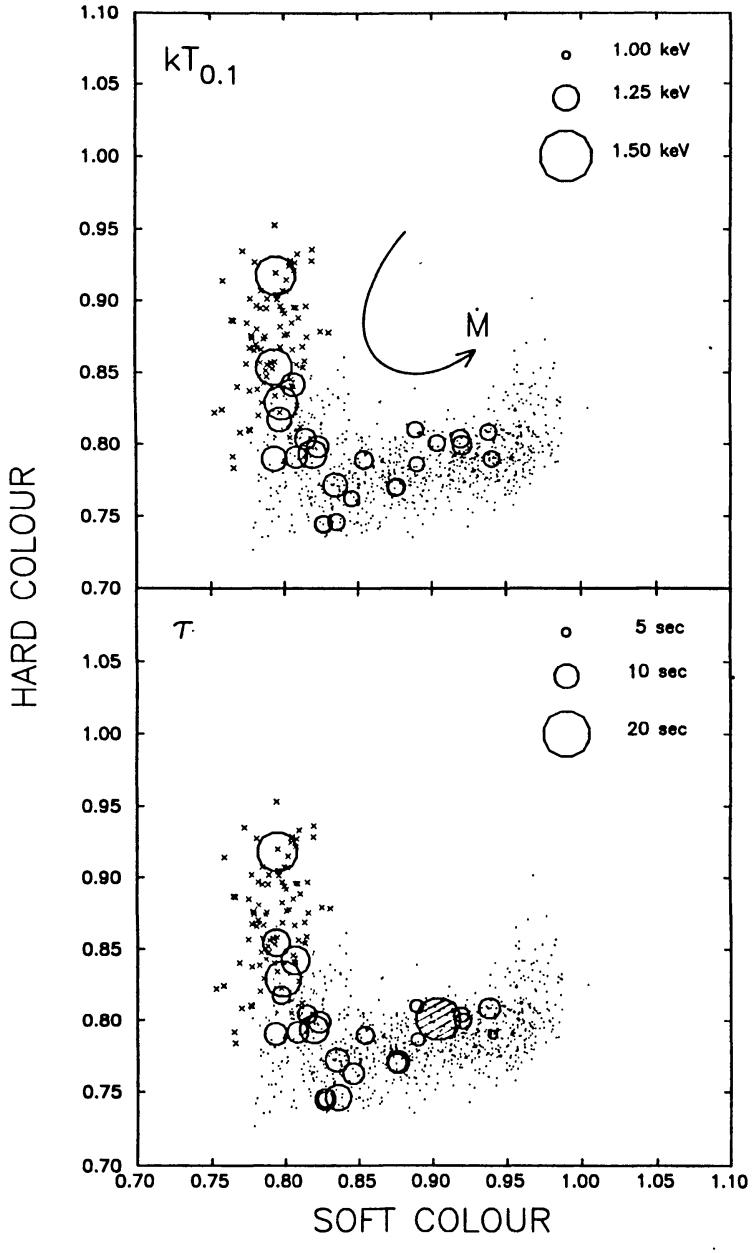

Fig. 3.16. X-ray colour-colour diagrams (small symbols) for 1636–536, with X-ray bursts superposed (large symbols). Each colour measurement corresponds to 200 s of data. The hard colour is the ratio of the count rates in the 6.1–20.5 keV and 4.5–6.1 keV bands, the soft colour that of the 2.9–4.5 and 0.9–2.9 keV bands. Crosses and dots indicate "island" and "banana" states, respectively, as determined from the X-ray variability characteristics. The position of a large circle indicates the average colours of the persistent emission just before and after the burst; the size of the circle indicates the temperature $kT_{0.1}$ when the burst flux is 10% of the Eddington flux (top panel) or the burst duration (bottom panel). The hatched circle in the lower frame indicates the burst with a triple-peaked profile; apart from this burst there is a strong correlation between the source state, and both the temperature $kT_{0.1}$ and burst duration. The direction in which $\dot{M}$ is believed to increase is indicated. This figure is from Van der Klis *et al.* (1990).

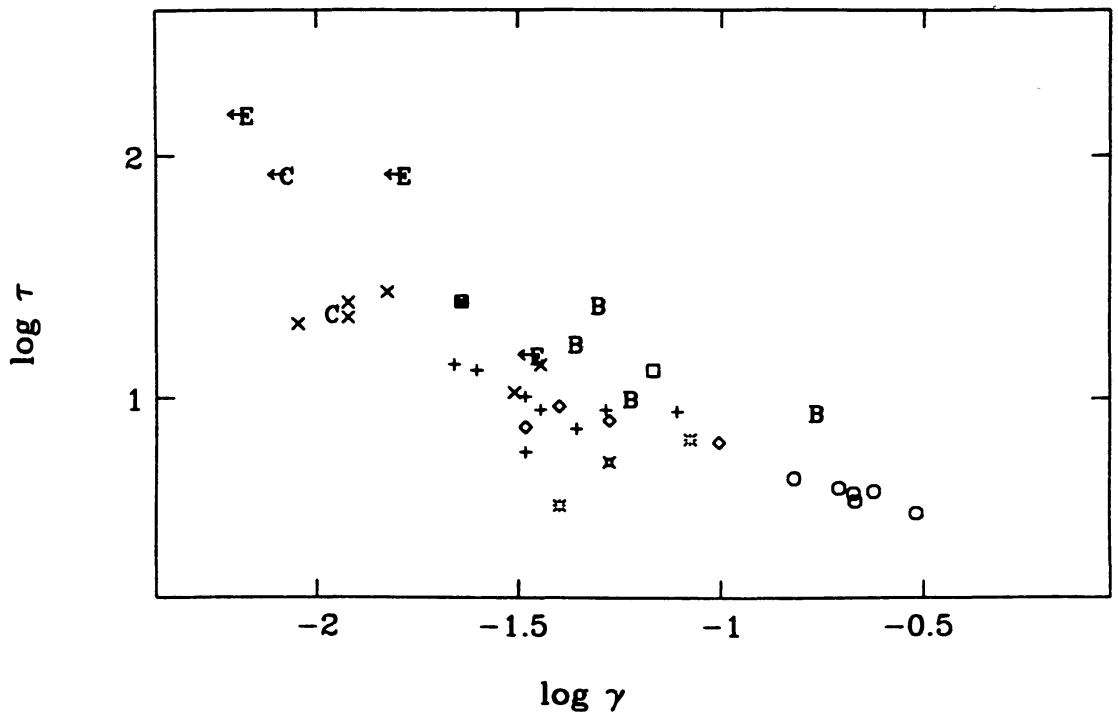

Fig. 3.17. Relation between burst duration τ and the persistent X-ray luminosity, represented by the ratio γ of the persistent X-ray flux to the Eddington flux, for burst sources that produced bursts with photospheric radius expansion. The symbols represent different sources as follows: 0748–676 (×), 1516–569 (□), 1608–522 (B), 1636–536 (+), 1715–321 (E), 1724–307 (C), 1728–337 (◊), 1735–444 (o), 1746–370 (¤), 1820–303 (∗). This figure is from Van Paradijs, Penninx and Lewin (1988a).

from ∼1 to > 3 for log γ varying from ∼ –2 to –0.5 (see Fig. 3.18); this confirms the result of Gottwald *et al.* (1986) for 0748–676, for a much larger interval in γ. The global (α, γ) relation is in qualitative agreement with the above-mentioned decreasing importance of hydrogen in the energetics of the bursts as the mass accretion rate increases. However, a more detailed analysis of the results shows that the ratio α/γ, which is proportional to the time-averaged burst luminosity, is approximately constant, i.e. independent of the rate at which nuclear fuel is accreted (Van Paradijs, Penninx and Lewin 1988a). This rather surprising result can be illustrated by a comparison of the relations between burst energy (not fluence) and waiting time Δt since the previous burst on the one hand, and on the other hand that between burst energy and integrated persistent luminosity during that interval Δt (see Fig. 3.19). Within the framework of the assumptions made by Van Paradijs, Penninx and Lewin (1988a) the burst energy is proportional to the quantity $U_b = E_b/F_{\rm re}$; the integrated persistent luminosity is proportional to $U_p = \gamma\Delta t$. From Fig. 3.19 it appears that over a large range in γ the (U_b, Δt) relation is fairly unique, whereas the (U_b, U_p) relation resembles a scatter diagram. If the persistent flux were a measure of the accretion rate this would lead to the rather surprising conclusion that, independent of the accretion rate, after a given waiting time Δt, burst sources produce bursts with approximately the same (average) energy. This would suggest that continuous stable burning of a sizeable

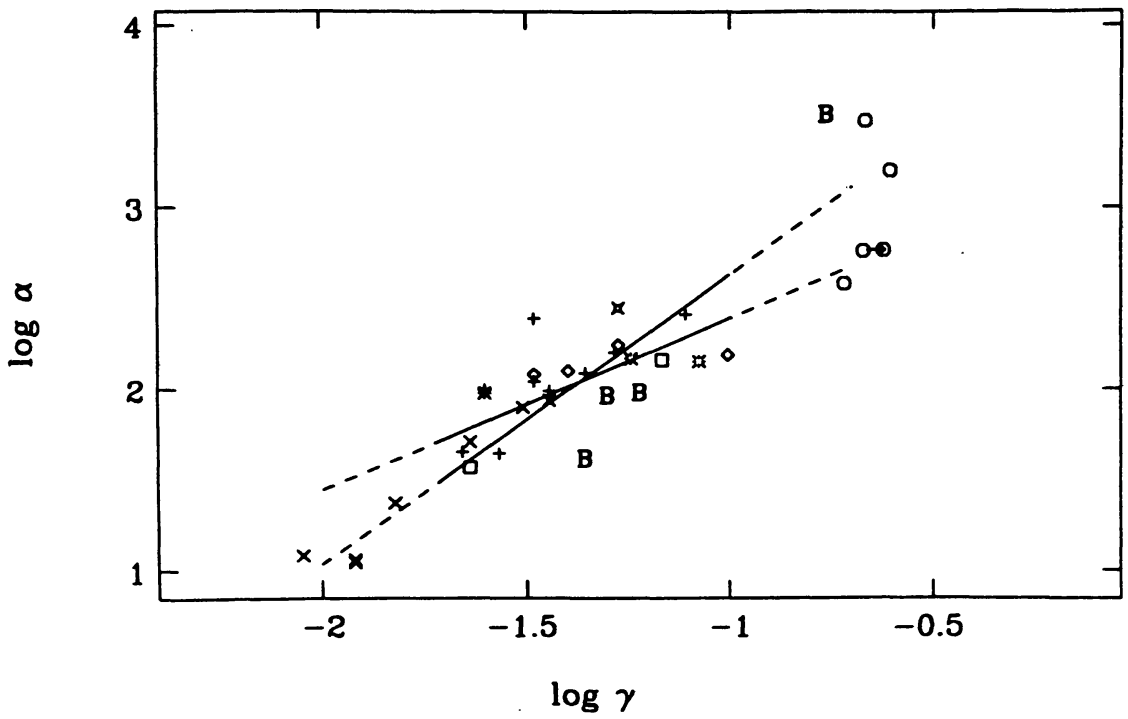

Fig. 3.18. Relation between log γ and log α for burst sources that have produced X-ray bursts with radius expansion. The symbols are explained in the caption of Fig. 3.17. The figure contains two straight lines. One represents a least-squares fit to the data in the interval $-1.7 < \log\gamma < -1.0$. The other (the steeper of the two) is the long axis of the dispersion ellipse of a bivariate (log α, log γ) distribution of the same data points. This figure is from Van Paradijs, Penninx and Lewin (1988a).

fraction of the accreted nuclear fuel occur not only in luminous X-ray burst sources (see Sect. 3.6), but in less luminous sources as well; this fraction would be a rather gradual function of the mass accretion rate.

3.9. Observations at Other Wavelengths

3.9.1. Optical Bursts

Between 1977 and 1980 several campaigns of coordinated optical and X-ray observations of burst sources were organized by the SAS–3 group. During the 1977 "burstwatch" optical observations were made of 1837 + 049 (Ser X–1) when X-ray bursts were detected with SAS–3. No optical bursts were detected, with upper limits to the ratio of the fluence $E_{\rm opt}$ in any optical burst to that in the X-ray burst ($E_{\rm X}$) between $\sim 5 \times 10^{-5}$ and $\sim 10^{-4}$ (Abramenko *et al.* 1978; Takagishi *et al.* 1978; Bernacca *et al.* 1979).

During the 1978 campaign the first simultaneous optical/X-ray burst was detected, from 1735–444 (Grindlay *et al.* 1978; see Fig. 3.20). The fluence in the optical burst was $\sim 2 \times 10^{-5}$ that in the X-ray burst; this is too large by $\sim$6 orders of magnitude to explain the optical emission as the low-energy tail of the blackbody X-ray burst emission. The optical burst was delayed by $\sim$3 seconds (McClintock *et al.* 1979). Later in the 1978 campaign an optical burst was detected

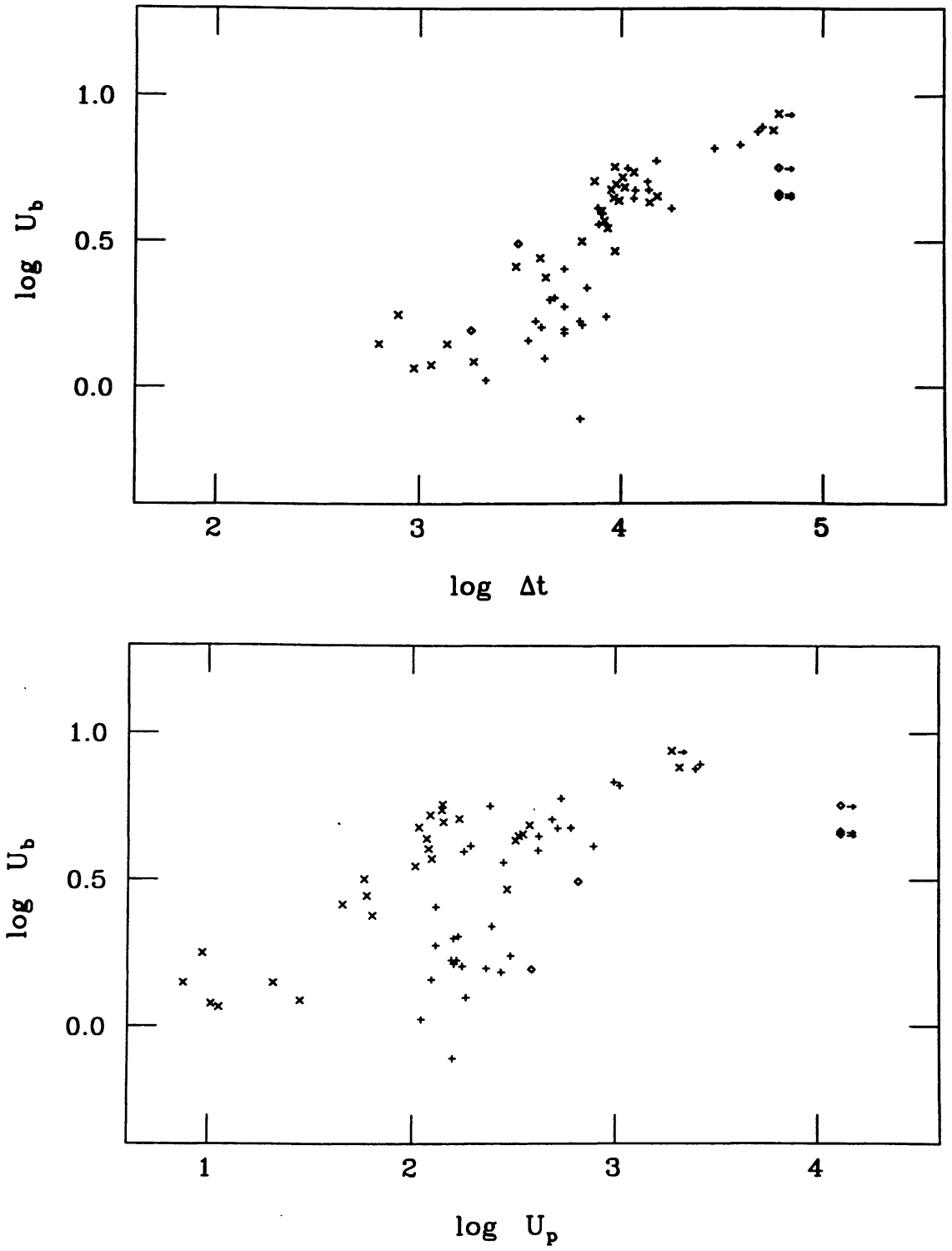

Fig. 3.19. (a) Dependence of the parameter U_b, which is a measure of the integrated burst energy (not fluence) on the waiting time Δt since the previous burst, for 0748–676 (×), 1636–536 (+), and 1735–444 (o), which have log γ values in the range between –2.0 and –0.6. (b) Dependence of the parameter U_b on $U_p = \gamma \Delta t$ for the same sources as in (a). U_p is a measure of the integrated persistent X-ray luminosity (not flux) in the interval since the previous burst. This figure is from Van Paradijs, Penninx and Lewin (1988a).

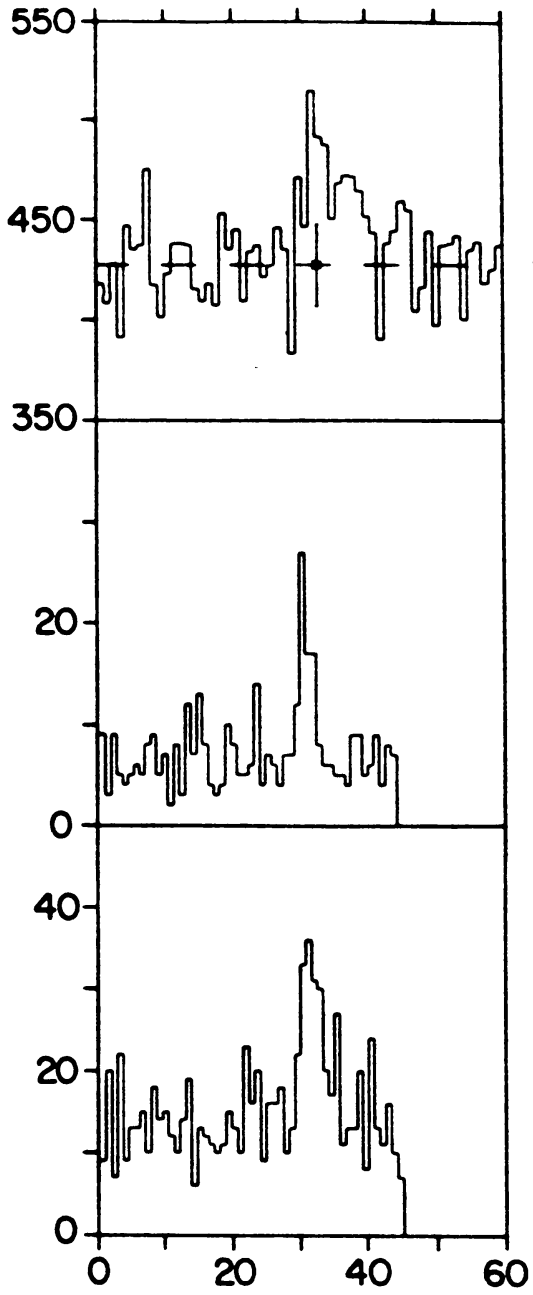

Fig. 3.20. First detected coincident optical/X-ray burst (from the source 1735–444). The top panel shows the optical light curve (arbitrary units) in the 3100–5500 Åband, the middle and bottom panel show the X-ray burst profiles (arbitrary units) in the 5–10 keV and 2.5–5.0 keV bands. The horizontal axis represents the time in sec. This figure has been adapted from Grindlay *et al.* 1978).

from 1837+049 (Hackwell *et al.* 1979), which was delayed by 1.4 ± 0.5 s, and whose ratio $E_{\rm opt}/E_{\rm X}$ ($\sim 3 \times 10^{-6}$) was consistent with the non-detection of bursts from this source the year before (see above).

These results indicated that all optical emission from X-ray burst sources is the result of reprocessing of X-rays in material within a few light seconds from the X-ray source, which is enhanced during an X-ray burst (for reviews see Van Paradijs

1983; Van Paradijs and McClintock 1993). Plausible sites for this reprocessing are an accretion disk around the neutron star and the hemisphere of the secondary star facing the X-ray source (insofar as it is not shielded by the accretion disk). The optical signal will be delayed (and also smeared) as a result of a range of travel-time differences between the X rays that directly go to the observer, and those that first hit the disk, become transformed into optical photons, and then go to the observer. Delay and smearing due to radiative processes are not very important (Pedersen *et al.* 1982a). According to this picture, the X-ray bursts serve as a probe: they illuminate the surroundings of the neutron star which reveal their presence by optical radiation. By comparing the changes in the X-ray and optical signals one can deduce information about these surroundings.

Very extensive simultaneous optical/X-ray burst observations have been made of 1636–536, which was regularly monitored with Hakucho and ESO telescopes during periods of ~6 weeks and ~1 month in 1979, and 1980, respectively. In this period a total of 69 X-ray bursts and 41 optical bursts were detected, ten of which were detected both in the X-rays and optical bands. During none of the optical (X-ray) bursts for which an X-ray (optical) counterpart was not observed were X-ray (optical) observations simultaneously made. The optical observations showed that there is a strong correlation between $E_{\rm opt}$ and $F_{\rm opt,max}$, both of which, in turn, are positively correlated with the time interval since the previous burst; two of the optical bursts occurred at an interval of only 5.5 minutes (Pedersen *et al.* 1982b).

During the 1979 observations five coincident optical/X-ray bursts were detected (Pedersen *et al.* 1982a), for three of which the data were of sufficient quality to make a detailed anaysis. These observations were interpreted in terms of a simple geometric model in which the optical emission (both during and outside bursts) is that of a (single-plate) blackbody, and is caused by reprocessing of X rays in material in the vicinity of the X-ray source. [One of these simultaneous optical/X-ray bursts from 1636–536 was observed in three optical passbands. The analysis of this time-resolved colour information shows that X-ray reprocessing into optical light is reasonably described by a single-temperature blackbody model (Lawrence *et al.* 1983b)]. From their analysis Pedersen *et al.* (1982a) find that the reprocessor has a linear size of ~1.5 lightseconds, independent of detailed assumptions about its geometry. These results put limits on the size of the accretion disk, which are consistent with a binary separation corresponding to the 3.8 hour orbital period (Pedersen, Van Paradijs and Lewin 1981; Smale and Mukai 1988; Van Paradijs *et al.* 1990b).

Matsuoka *et al.* (1984) analyzed the six best-quality cases of the ten coincident optical/X-ray bursts detected from 1636–536 during the 1979 and 1980 campaigns. They find that for five of these optical bursts the delay times are consistent with a single value near 2.5 s; however, for one burst the delay is significantly smaller; this suggests that the reprocessing region is either moving or varying in size. A natural way to account for variations in delay time is to assume that a significant

fraction of the reprocressing occurs in the secondary star. In that case one would expect to see a correlation between the apparent size of the optical emitter and the delay time (both of which vary with the phase of the orbital cycle); however, Matsuoka *et al.* (1984) did not find such correlation. Using an orbital ephemeris for 1636–536, based on optical brightness variations, covering the period between 1980 and 1988, Van Paradijs *et al.* (1990b) find no evidence for a relation between delay time and orbital phase. Also, the variation with orbital phase of the ratio of optical to X-ray burst fluences (and peak fluxes) does not follow the average optical light curve. These results suggest that substantial long-term changes occur in the spatial distribution of reprocessing material in the binary system.

Turner *et al.* (1985) and Trümper *et al.* (1985) each reported the detection of a coincident optical/X-ray burst from 1636–53; these optical bursts were delayed by 0.1 ± 0.1 s, and $\sim$ 3 s, respectively. The delay measured by Turner *et al.* is probably affected by a systematic uncertainty in the timing of the optical data due to a power failure some time before the optical observations (H. Pedersen, private communication).

Mason *et al.* (1980) observed an optical burst from 1254–690; X-ray bursts from this source were observed later with EXOSAT (Courvoisier *et al.* 1986). An optical burst was detected from the recurrent transient source Aql X–1 when it was in outburst (Van Paradijs, Pedersen and Lewin 1981; see also Van Paradijs 1983); Aql X–1 is a known X-ray burst source (Koyama *et al.* 1981).

Mauder (1981) reported the detection of a possible optical burst from Sco X–1; in our opinion this result requires confirmation from independent observations.

3.9.2. Radio and Infrared Observations

Radio observations were made of five X-ray burst sources during the 1977 coordinated burst campaign; no radio bursts were detected (Johnson *et al.* 1978; Ulmer *et al.* 1978; Thomas *et al.* 1979).

Kulkarni *et al.* (1979) and Jones *et al.* (1980) reported the detection of infrared bursts from 1730–335 (Rapid Burster). It is unclear whether these events are real (cf. Apparao and Chitre 1980). Sato *et al.* (1980) did not detect infrared bursts from this object.

Radio bursts from 1730–335 were reported by Calla *et al.* (1979, 1980a,b). No X-ray bursts were seen during simultaneous Hakucho observations (Hayakawa 1981).

Based on extensive X-ray, radio and infrared observations of 1730–335, made during 1979 and 1980, Lawrence *et al.* (1983a) concluded that (i) it is unlikely that the previously reported radio bursts from this source are real; (ii) the reported infrared bursts are harder to dismiss, but difficult to reconcile with the many null observations (see Sect. 7.6).

3.10. Rapid Variability During X-Ray Bursts

In a number of cases rapid variability (time scales less than a second) has been observed during X-ray bursts; in some cases the variations were coherent (i.e., coherence limited by the length of the burst). It is unlikely that these variations can be explained by a single mechanism [see Livio and Bath (1982) for a discussion of models].

Mason *et al.* (1980) found a coherent brightness modulation during an optical burst they observed from 1254–690, at a frequency of 36.40 Hz. We note that the high frequency of this modulation makes it unlikely that the optical burst was associated with a type I X-ray burst; if the optical burst originates from reprocessing of X rays in a region a few light-seconds across the high-frequency oscillation is expected to be washed out by light travel time effects.

Sadeh *et al.* (1982) reported the detection of 12 ms oscillations just before and during one of four X-ray bursts from 1728–337 which they observed with HEAO–1. The period of the oscillations showed a drift from 12.254 ms before the burst to 12.244 ms during the burst. We note that the significance level of this (drifting) periodic signal given by Sadeh *et al.* (99.7%) is likely to be overestimated, since they did not take into account the presence of irregular variability in the signal (as found during this same burst by Hoffman *et al.* 1979).

Murakami *et al.* (1987) detected oscillations with a period of 0.65 s during the phase of photospheric radius expansion of a strong X-ray burst they observed from 1608–522. The oscillation of the low-energy X-ray count rate is anti-correlated with that at high-energy X rays. Murakami *et al.* conclude that these oscillations are caused by oscillations in the photospheric radius which occur at an approximately constant bolometric luminosity. Possibly similar oscillations at a much longer period ($\sim$10 s) which lasted for only a few cycles were found during the phase of photospheric radius expansion of a burst from 2127+119 (Van Paradijs *et al.* 1990a).

Schoelkopf and Kelley (1991) detected a 7.6 Hz oscillation at a 4.1 σ confidence level during an X-ray burst from Aql X–1 observed with Einstein. The coherence of the oscillations was limited only by the length of the data train ($\sim$80 s). They proposed that the 7.6 Hz oscilation reveals the spin period of the neutron star through a relatively small non-uniformity of the surface brightness across the neutron star (corresponding to a temperature difference of $\sim$2%).

4. Mass-Radius Relation of Neutron Stars

4.1. General Remarks

The properties of neutron star matter are described by an equation of state, which together with the Oppenheimer-Volkoff equations can be used to construct models for the interior structure of neutron stars (see e.g. Shapiro and Teukolsky 1983). Since neutron stars can be considered zero-temperature objects these models form

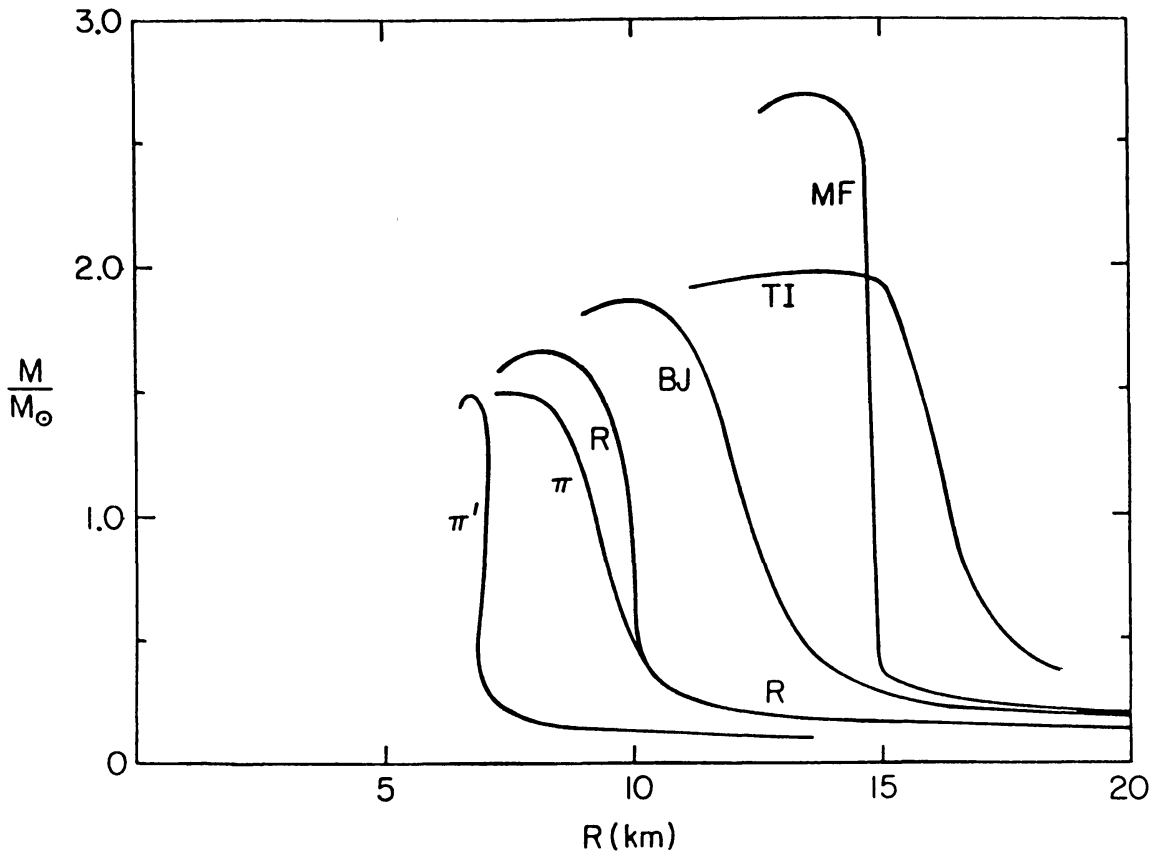

Fig. 4.1. Theoretical mass-radius relations for neutron stars based on various equations of state (from Baym and Pethick 1979).

a one-parameter sequence in which mass and radius depend only on the central density. For a given equation of state one thus obtains a unique relation between mass and radius.

Although the various equations of state are not determined by the compressibility of the matter alone, one conveniently distinguishes between soft and stiff equations of state (corresponding to high and low compressibility, respectively). Globally speaking, for stiffer equations of state the maximum possible neutron-star mass is higher, and for a given value of the mass the radius increases (see Fig. 4.1). Extensive calculations of neutron star models based on a variety of equations of state have been published by Arnett and Bowers (1977), and Datta (1988).

With the possible exception of the short-lived extremely hot boundary layers between colliding nuclei that can be produced in heavy-ion collisions (see e.g. Stock 1989) the supra-nuclear densities encountered in the interior of a neutron star are difficult to reproduce in a laboratory. Therefore, a comparison of measured values of (or constraints on) masses and radii of neutron stars, based on astronomical observations, with theoretical mass-radius relations for neutron star models based on various equations of state, provide an important way to constrain the equation of state of neutron star matter.

Very accurate masses of neutron stars have been determined from general-

relativistic analyses of the pulse arrival times of the binary radio pulsars PSR1913+16 (Taylor and Weisberg 1989) and PSR 1534 + 12 (Wolszczan 1991), and a somewhat less accurate value for PSR 1855+09 (Ryba and Taylor 1991). Pulse arrival time measurements, in combination with radial-velocity observations of their massive companion stars have provided information on neutron star masses for six pulsating high-mass X-ray binaries (Nagase 1989, and references therein). For the LMXB pulsar 1626–67 a (not very accurate) neutron star mass was estimated from timing observations of the X-ray and optical (i.e., reprocessed X rays) pulsations (Middleditch *et al.* 1981). In Fig. 4.2 our present knowledge on neutron star masses has been summarized. Except for Vela X–1 (Van Kerkwijk *et al.* 1993) these results are consistent with a "standard" neutron star mass near 1.4 $M_\odot$; mass differences of more than 0.5 $M_\odot$ between neutron stars cannot at present be excluded.

Observational constraints on the mass-radius relation of neutron stars may be derived (i) from their limiting spin periods (Friedman *et al.* 1986); (ii) from the cooling history of recently formed neutron stars (Tsuruta 1986); (iii) from a measurement of the neutron star magnetic-field strength as obtained from the energy of a cyclotron line in the X-ray spectrum of an X-ray binary pulsar, combined with an interpretation of the spin-up/down behaviour of this pulsar in terms of accretion torques exerted on a magnetized accreting neutron star (Wasserman and Shapiro 1983), (iv) from glitches in pulsar periods (Pines 1991 and references therein), (v) from the neutrino light curve during a supernova explosion, and perhaps (vi) from gravitationally redshifted annihilation lines in γ-ray burst spectra (Liang 1986; see, however, Kluzniak 1989, and Meegan *et al.* 1992).

Information about the equation of state of neutron star matter can be obtained from the neutrino intensity curve in a supernova explosion such as that observed for SN 1987A (Hirata *et al.* 1987; Bionta *et al.* 1987). The radius of the "neutrinosphere" in combination with the binding energy of the neutron star allows, in principle, a test of the various equations of state (Loredo & Lamb 1989, and references therein). Only about two dozen neutrinos were detected from SN 1987A ($\sim 10^{28}$ passed through the Earth); the corresponding uncertainties in the measurements of the neutrinosphere radius and the binding energy of the neutron star are therefore rather large.

Independent information on masses and radii of neutron stars may also be obtained from observations of X-ray bursts. Since these events are caused by the liberation of thermonuclear energy at large optical depth in neutron star surface layers, the interpretation of the spectra of X-ray bursts is little affected by uncertainty about the geometry of the primary burst emission: it comes from a spherical surface. This is very different from the situation encountered, e.g., in interpreting the spectra of the persistent X-ray emission from these sources (compare, e.g., Mitsuda *et al.* 1984; White *et al.* 1988). A remaining question is whether the burst emission is uniformly distributed across the whole neutron star surface. Magnetic fields which are too weak to cause X-ray pulsations may lead to anisotropic accretion onto the neutron star, and give rise to a non-uniform surface distribution of the

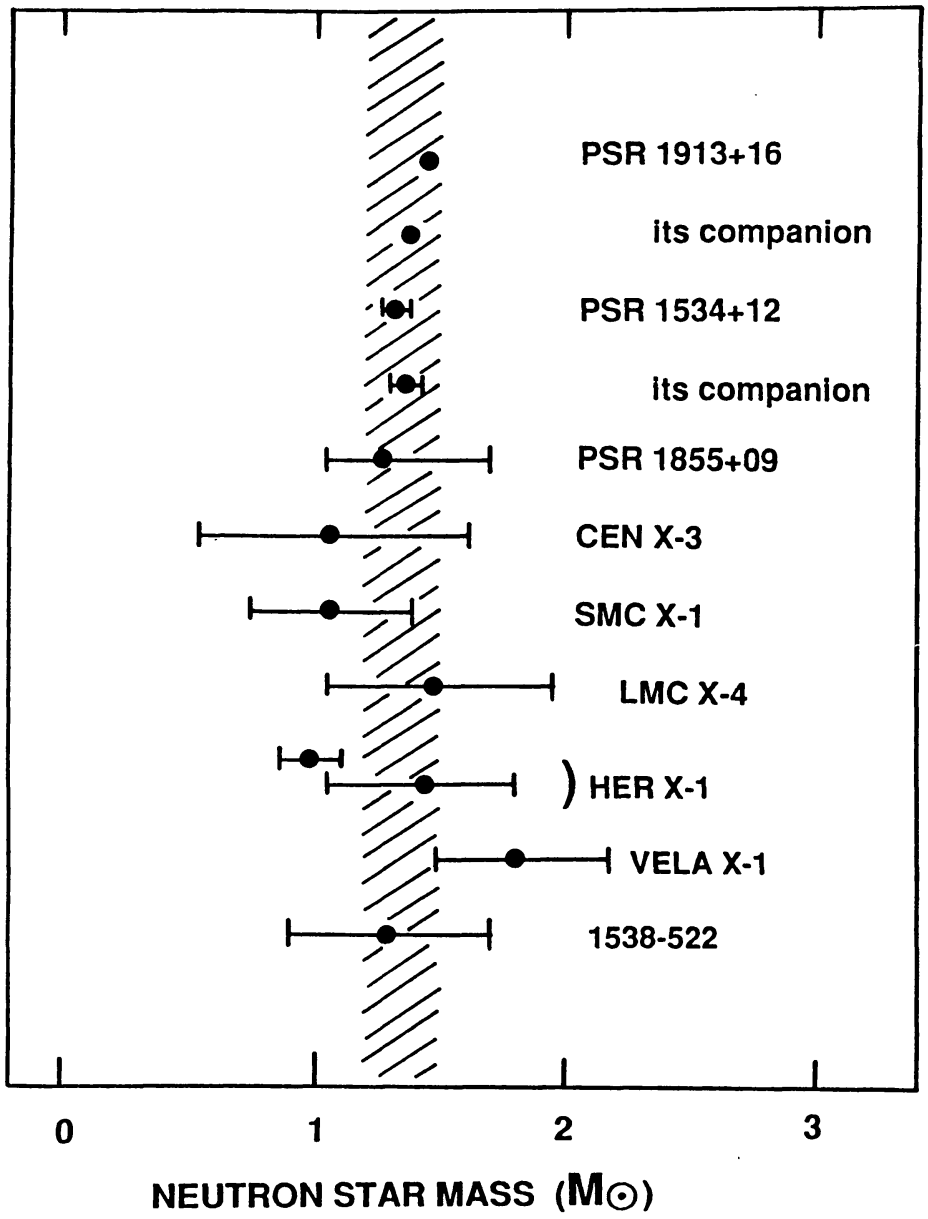

Fig. 4.2. Summary of our empirical knowledge of masses of neutron stars. Five of the neutron star masses have been obtained from general-relativistic analyses of the pulse arrival times of binary radio pulsars (Taylor and Weisberg 1989; Ryba and Taylor 1991; Wolszczan 1991). The neutron star masses for the six X-ray binary pulsars have been obtained from Dennerl (1991: LMC X–4), Nagase (1989: SMC X–1, Cen X–3, Her X–1), Rappaport and Joss (1983: Her X–1), Van Kerkwijk *et al.* (1993: Vela X–1), and Reynolds *et al.* (1992: 1538–522). Error bars indicate 95% confidence limits; they are smaller than the size of the dots for PSR 1913+16 and PSR 1534+12. Note, that for Her X–1 two mass ranges are indicated, one based on an analysis of Doppler shifts of optical pulsations (Rappaport and Joss 1983), and another based on the radial-velocity variations of the secondary (Nagase 1989).

nuclear fuel. This non-uniformity is determined by the ratio of the time scale for diffusion of plasma across the magnetic field lines and the time interval between X-ray bursts. According to the analysis of Hameury *et al.* (1983) this ratio is $\ll 1$ for magnetic fields of the order of 10^9 G, believed to apply to the neutron stars that

emit X-ray bursts (see e.g. Hasinger and Van der Klis 1989). Thus, the assumption that the X-ray bursts originate from a spherical surface would seem a reasonable approximation.

In this chapter we review the various methods which have been used to interpret observations of X-ray bursts in terms of the mass-radius relation of neutron stars; they are all based on the assumption that the whole neutron star surface participates uniformly in the burst emission.

4.2. Blackbody Radii of Neutron Stars

Early studies of the spectra emitted during X-ray bursts showed that these are well described by Planck curves, with a decreasing temperature during the decay phase of the burst (Swank *et al.* 1977; Hoffman, Lewin and Doty 1977a, b; see Sect. 3.3). This interpretation was supported by the observation that during the decay of the bursts the shape of the burst spectrum was approximately Planckian, and the observed flux, F_∞, varied approximately as the 4th power of the observed blackbody temperature $T_{c\infty}$ (the subscript c indicates "color"; the subscript ∞ indicates that the observation is made at a very large distance from the neutron star). This result implies that during a burst one observes an approximately constant burst emitting area. For an assumed uniform spherical blackbody emitter of radius R_∞, at a distance d, we have:

$$L_{b\infty} = 4\pi(R_\infty)^2\sigma(T_{e\infty})^4 = 4\pi d^2 F_{b\infty} \tag{4.1}$$

here L stands for luminosity, and the subscripts b and e stand for "burst" and for "effective", respectively. The quantity $F_{b\infty}$ is the bolometric flux, which is generally not directly measured. Therefore, in the following we will assume that a bolometric-correction factor has been applied to the flux observed in the X-ray band. In general, this correction factor is close to unity (but always > 1); it varies throughout the burst as the spectral shape changes.

If one knows an approximate source distance, the values of R_∞ then follow from the flux measurements, and from the associated blackbody temperatures (it is here assumed that $T_{c\infty} = T_{e\infty}$; this point is addressed below and, more extensively, in Chapter 5). For a distance of $\sim$10 kpc, suggested by the sky distribution of burst sources (Lewin *et al.* 1977b; see also Chapter 2), Swank *et al.* (1977) and Hoffman, Lewin and Doty (1977a,b) found radii, R_∞, roughly comparable to those expected for a neutron star.

Van Paradijs (1978) found that the blackbody radii obtained from different bursts from one source were the same to within their accuracy (see also Ohashi 1981). He used the idea that the average peak luminosity of X-ray bursts might be a "standard candle", and found that for an assumed standard-candle equal to the Eddington limit for a 1.4 $M_\odot$ object (with a hydrogen rich envelope), the radii (R_∞) of all sources were consistent with a single value, near 7 km. The standard candle idea may turn out to be correct, but only for the most luminous bursts which

produce radius expansion of the photosphere of the neutron star (cf. Lewin 1984; see also Sect. 3.4).

In principle, observations of type I bursts provide information on both the mass and radius of a neutron star (Van Paradijs 1979; Goldman 1979; Hoshi 1981; Marshall 1982). In the remainder of this chapter we summarize the presently available methods that can be applied to extract this information; these are based on measurements of the Eddington luminosity, of the angular diameter of the neutron star, and of the gravitational redshift at its surface. In our discussion we will emphasize the present limitations of these methods.

4.3. Observations of Burst Spectra during Burst Decay

Before observations of X-ray burst spectra can be utilized to derive information on neutron star properties a number of complicating issues have to be addressed. These include:

(1) Gravitational redshift of photons emitted from the neutron star surface.

(2) In Equation (4.1) it is assumed that the burst emission is isotropic; this may not be the case.

(3) The source distance must be known.

(4) The burst spectrum is probably not a Planck function.

We will discuss each of these points separately.

4.3.1. The Effect of Gravitational Redshift

According to the theory of general relativity (see e.g. Thorne 1977) the energy of each photon, and also the rate at which they are detected, depend on the gravitational potential. Consequently, the luminosity and temperature of a blackbody emitter observed locally at the surface of the neutron star (indicated by a subscript $_*$), and those observed by a distant observer (subscript $_\infty$) are related by:

$$L_{b\infty} = L_{b*}(1 + z_*)^{-2} \tag{4.2a}$$

$$T_{e\infty} = T_{e*}(1 + z_*)^{-1} \tag{4.2b}$$

with the gravitational redshift factor $1 + z_*$ given by

$$1 + z_* = [1 - 2GM/(R_* c^2)]^{-1/2} \tag{4.3}$$

Here M is the gravitational mass of the neutron star, and R_* is its radius as measured by a local observer on the neutron star surface. For isotropic radiation, and a Planckian spectrum, this local observer would relate the burst luminosity L_{b*} and effective temperature T_{e*} according to:

$$L_{b*} = 4\pi(R_*)^2 \sigma (T_{e*})^4 \tag{4.4}$$

Using the relations (4.1) to (4.4) we find

$$R_\infty = R_*(1 + z_*) \tag{4.5a}$$

$$= R_*[1 - 2GM/(R_* c^2)]^{-1/2} \tag{4.5b}$$

$$= R_*(1 - R_g/R_*)^{-1/2} \tag{4.5c}$$

Here R_g is the Schwarzschild radius

$$R_g = 2GM/c^2 \approx 3(M/M_\odot)\ \text{km} \tag{4.6}$$

The above equations are strictly valid only for non-rotating neutron stars (Schwarzschild metric). However, they are good approximations for neutron star rotation periods larger than a few milliseconds.

Equation (4.5) shows that an observation of the radius (by a distant observer) according to Equation (4.1) gives a relation between the mass M and the radius R_* of the neutron star (Van Paradijs 1979). It is here assumed, for simplicity, that the source distance d (see Equation (4.1)) is known, and that the radiation is emitted isotropically.

It follows from the Schwarzschild metric (this is independent of the equation of state for neutron star matter) that Equation (4.5) does not hold when $R_* < 1.5\ R_g$. This results from the fact that, when $R_* < 1.5\ R_g$, only photons emitted within an angle δ from the outward radial direction can escape to infinity, where δ is given by

$$\sin\delta = (1.5\sqrt{3})(R_g/R_*)(1 - R_g/R_*)^{1/2} \tag{4.7}$$

(Misner *et al.* 1973). For isotropic radiation (such as blackbody emission) the fraction of the emission that escapes is given by $\sin^2\ \delta$. For a distant observer the number of photons is thus reduced. However, the energy distribution of the escaping photons (and therefore T_∞) does not change [this implies that Equation (4.2b) still holds, but Equation (4.2a) does not]. The net result is that then

$$R_\infty = (1.5\sqrt{3})R_g \approx 7.68(M/M_\odot)\ \text{km}\ (R_g < R_* < 1.5R_g) \tag{4.8}$$

The radius R_* of neutron stars is likely to be larger than $1.5\ R_g$ (see e.g. Arnett and Bowers 1977); therefore, in practice we do not have to "worry" too much about this effect.

In Fig. 4.3 we show the M–R_* relation for three values (5, 10, and 15 km) of R_∞. For a given value of M, R_∞ has a minimum value given by Equation (4.8). Conversely, for a given observed radius R_∞, the mass of the neutron star cannot be larger than $(R_\infty/7.68\ \text{km})\ M_\odot$.

4.3.2. Spherical Symmetry – Anisotropy

Only in case the burst emission is isotropic can we make the conversion from flux to luminosity according to Equation (4.1). Even if the burst emission from the neutron star surface were initially isotropic, it is quite possible that at large distances from the neutron star it is not (see, e.g., Lapidus and Sunyaev 1985;

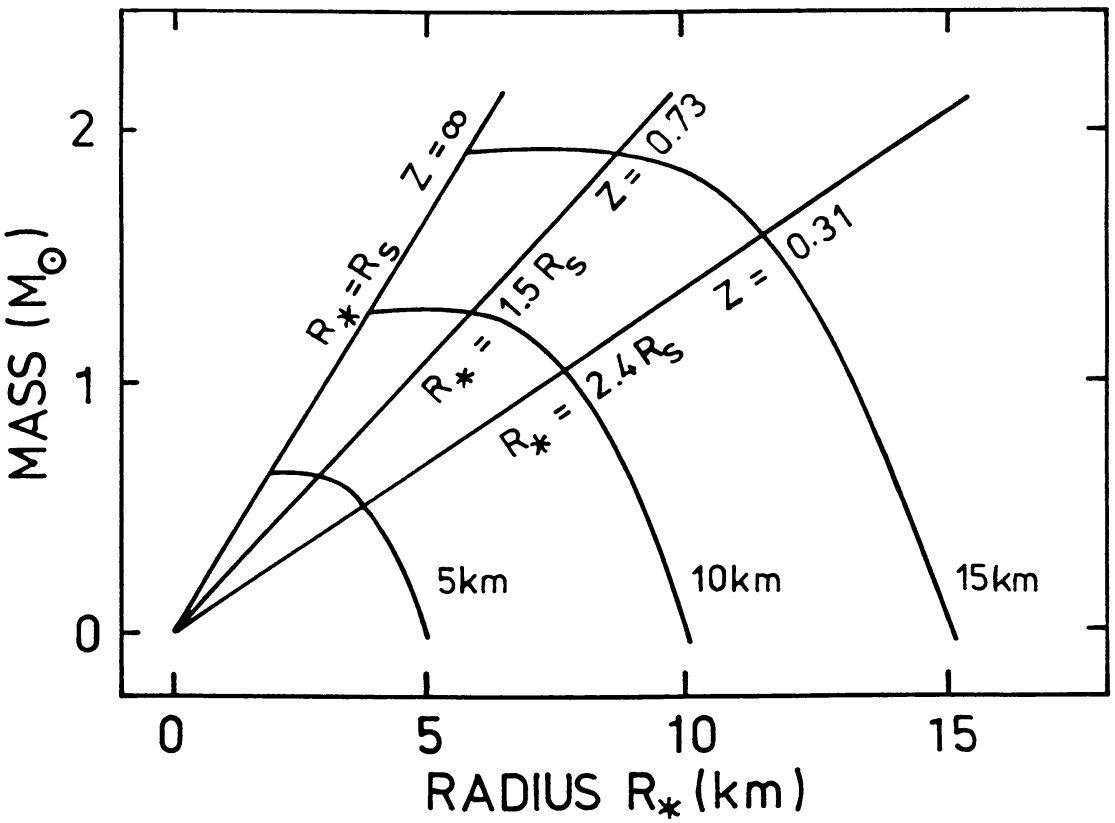

Fig. 4.3. Mass-radius relation for three hypothetical values of the blackbody radius R_∞ (5, 10, and 15 km). For clarity, we have not indicated error regions resulting from the uncertainties in the measurements. The straight lines indicate radii R_*, equal to the Schwarzschild radius R_S, 1.5 R_S, and 2.4 R_S (in the text we use R_g instead of R_S). The latter could, for example, result from an analysis of a burst with radius expansion (see text), or from the determination of the gravitational redshift of an observed spectral feature. For a given mass, the observed blackbody radius, R_∞, has a minimum value $(1.5\sqrt{3})\ R_g$; conversely, for a given blackbody radius R_∞ the mass cannot be larger than R_∞ (km)/7.7 $M_\odot$.

Fujimoto 1988). The anisotropy is expected to depend on the properties of the accretion disk (e.g. its thickness), on the presence of an accretion disk corona, and on the inclination angle of the system. Unfortunately, our knowledge on anisotropy in LMXB is poor. Following Sztajno *et al.* (1987) an anisotropy factor ξ_b can be introduced, according to:

$$L_{b\infty} = 4\pi(R_\infty)^2\sigma(T_{e\infty})^4 = 4\pi d^2 \xi_b F_{b\infty} \tag{4.9}$$

Possible absorption of the burst radiation is also included in ξ_b. If the observed flux is lower than it would be in the absence of anisotropy (or absorption), $\xi_b > 1$; if it is higher, $\xi_b < 1$. In what follows, we assume that ξ_b is constant during the burst. This is not necessarily so, as the anisotropy could, in principle, change during the burst (Melia 1987; see, however, Penninx, Van Paradijs and Lewin 1987).

As pointed out by Lewin *et al.* (1987a) observations of the burst peak flux distribution for 1636–536, which shows a distinct gap, indicate that the unknown burst anisotropy does not change significantly on long time scales. This follows

from the fact that the distribution, particularly the location of the gap, and the peak fluxes of all bursts that cause radius expansion, do not change over the years (see Fig. 3.13).

4.3.3. Source Distances

In general, distances to burst sources are not accurately known. Only in the cases of burst sources located in globular clusters is it possible to use independent information to estimate the distance. For the burst sources 1820–303 (in NGC 6624), 1746–371 (in NGC 6441) and 2127 + 119 (in M15) the distances are reasonably well known.

As we will discuss in Sect. 4.5, the quantity $d^2\xi_b$ (see Equation (4.9)) can be eliminated for X-ray bursts during which photospheric radius expansion occurs.

4.3.4. Non-Planckian Burst Spectra

As we discuss in some detail in Chapter 5 there is good evidence that, in spite of the fact that the observed burst spectra can often be reasonably well fitted with a Planck function, hot neutron stars during X-ray bursts are not well described by blackbodies. However, with neutron star model atmospheres it is – at least in principle – possible to transform the observed colour temperature, that describes the shape of the spectrum, to effective temperature. Based on such models one expects that the colour temperature is higher, typically by a factor 1.5, than the effective temperature (which one would have obtained from the spectral fit if the source were a Planckian emitter). Then a "corrected" value for the blackbody radius R_∞ can be obtained. This approach has been taken in several investigations (see Sect. 4.6).

4.4. Gravitational Redshift from Discrete Features in X-Ray Burst Spectra

If a discrete feature were present in a burst spectrum during times that the radiation comes from the neutron star surface, and if this feature could be identified, one would have a direct measure of the gravitational redshift $(1 + z_*)$ of the neutron star surface (Burbidge 1963; Van Paradijs 1982), and thus of the ratio M/R_* (see Equation (4.3)). Absorption dips in burst spectra have been observed by Waki *et al.* (1984) in four bursts from 1636–536, by Nakamura *et al.* (1988) in three bursts from 1608–522, and by Magnier *et al.* (1989) in one burst from 1747–214 (see Fig. 4.4). Apart from one absorption line near 5.7 keV, observed in a burst from 1636–53 during photospheric radius expansion (Waki *et al.* 1984), all other lines are consistent with one energy 4.1 ± 0.1 keV. Waki *et al.* (1984) suggested that the 4.1 keV lines are due to a gravitationally redshifted resonance line of a highly ionized atomic species, formed in the neutron star atmosphere. Magnier *et al.* (1989) pointed out that if this interpretation is correct, the coincidence of the line energies in three sources leads to the surprising conclusion that the masses of the neutron stars are the same to within $\sim 5\%$, in spite of the fact that they are generally

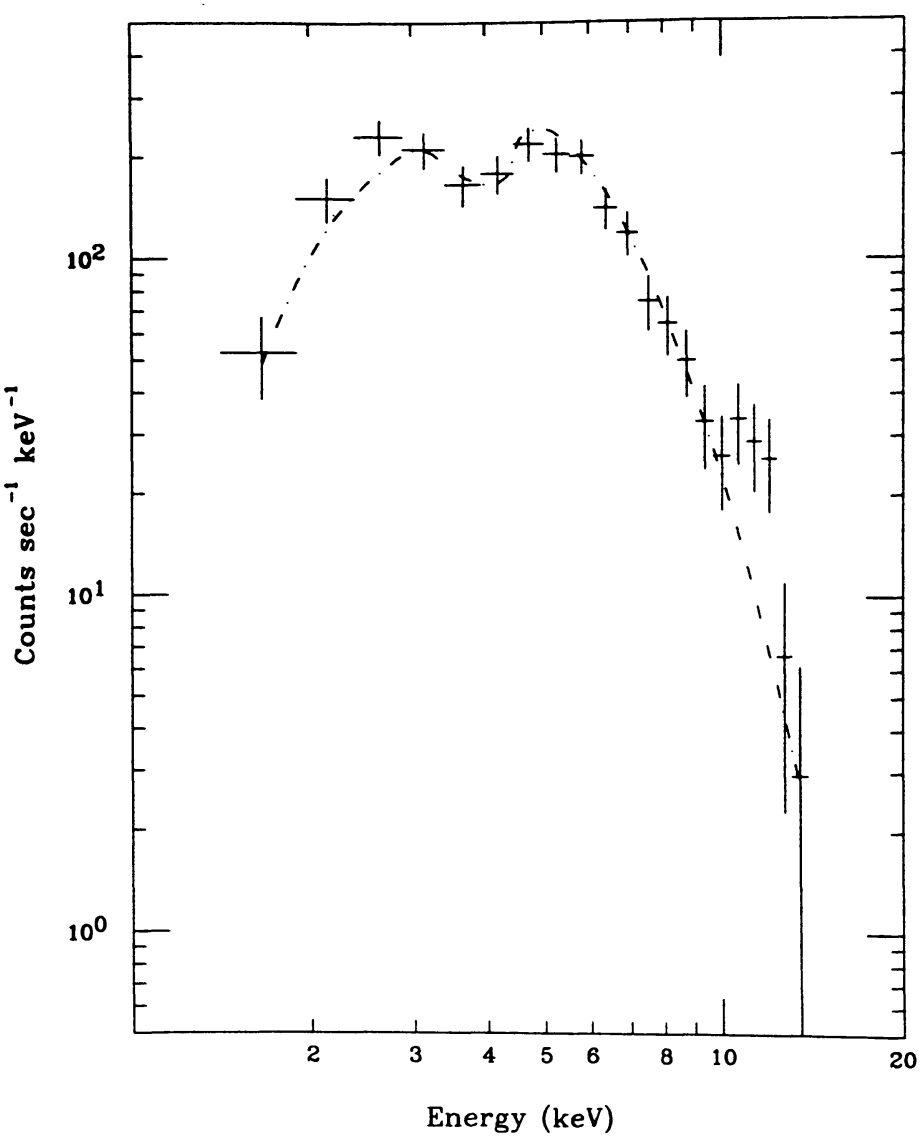

Fig. 4.4. X-ray spectrum, observed during a burst from the source 1747–214, showing evidence for a discrete spectral feature. The dashed line is a fit to a single blackbody spectrum with an absorption line near 4.1 keV (from Magnier *et al.* 1989).

believed to accrete a few tenths of a solar mass during their lifetime as an X-ray source; this may imply that this lifetime has been greatly overestimated. Pinto *et al.* (1992) explain the line as a combined effect of Doppler shift of infalling matter and gravitational redshift. The implications of these observations for the mass-radius relation of neutron stars are discussed in Sect. 4.6.1 (see also Chapter 5).

4.5. Bursts with Photospheric Radius Expansion

4.5.1. The Eddington Luminosity

During very strong bursts the neutron star photosphere expands as a result of radiation pressure (see Sect. 3.4). According to model calculations, during the expansion and contraction phase of the photosphere the luminosity, as measured by a local observer in the photosphere, remains extremely close to the Eddington luminosity,

i.e. the luminosity at which the outward radiation force equals the inward force of gravity (Kato 1983; Ebisuzaki *et al.* 1983; Paczynski 1983a,b; Paczynski and Anderson 1986; Joss and Melia 1987). Since the (theoretical) outflow velocities of the photosphere are much smaller than the speed of light the difference between the luminosities, as measured by an observer moving with the photosphere, and by a stationary observer at the same radial distance, respectively, can be neglected. During the expansion and contraction phase, at photospheric radius R, the Eddington luminosity, as measured by a local observer is:

$$L_{\rm Edd}(R) = (4\pi cGM/\kappa)[1 - 2GM/(Rc^2)]^{-1/2} \tag{4.10a}$$

The Eddington luminosity as measured by a distant observer is:

$$L_{\rm Edd\infty} = (4\pi cGM/\kappa)[1 - 2GM/(Rc^2)]^{1/2} = 4\pi d^2 \xi_b F_{\rm Edd\infty} \tag{4.10b}$$

Here κ is the electron scattering opacity during the expansion phase; in the low-temperature limit it is given by

$$\kappa = 0.2(1 + X)\ {\rm cm^2/g} \tag{4.11}$$

where X is the hydrogen fraction (by mass) of the photospheric matter (for cosmic composition $X = 0.73$). It is likely that the atmosphere of the neutron star during expansion is hydrogen-poor (i.e. $X = 0$, see Sugimoto *et al.* 1984). The quantity $(4\pi cGM/\kappa)$, i.e. the non-relativistic Eddington limit is given by

$$4\pi cGM/\kappa = 2.50 \times 10^{38}(M/M_\odot)(1 + X)^{-1}\ {\rm erg\ s^{-1}} \tag{4.12}$$

In some cases (see below) it may be necessary to take into account the temperature dependence of the electron scattering opacity, which is due to the fact that for very high temperatures the scattering electrons become relativistic. This dependence can be described by the following approximation, valid for the low-density limit appropriate to neutron star atmospheres, due to Paczynski (1983a, b):

$$\kappa = \kappa_0[1 + (\alpha T)^{0.86}]^{-1} \tag{4.13a}$$

where κ_0 is the opacity given in Equation (4.11), and $\alpha = 2.2 \times 10^{-9}\ {\rm K^{-1}}$; this can be written as

$$\kappa = \kappa_0[1 + (kT/39.2\ {\rm keV})^{0.86}]^{-1} \tag{4.13b}$$

Notice that in Equation (4.10a, b) R is not R_*, but rather the radius of the photosphere, which at maximum expansion can be many times the stellar radius (see Sect. 3.4).

Burst observations during the radius expansion phase can be used in two ways to obtain information on the neutron star (see Fig. 4.5). The first is based on a combination of these observations with those during the cooling phase of the burst; this leads to the elimination of the quantity $\mathrm{d}^2\xi_b$. The second method uses the fact that the Eddington limit depends on the radius of the photosphere through the redshift factor, which leads to a method to determine this redshift.

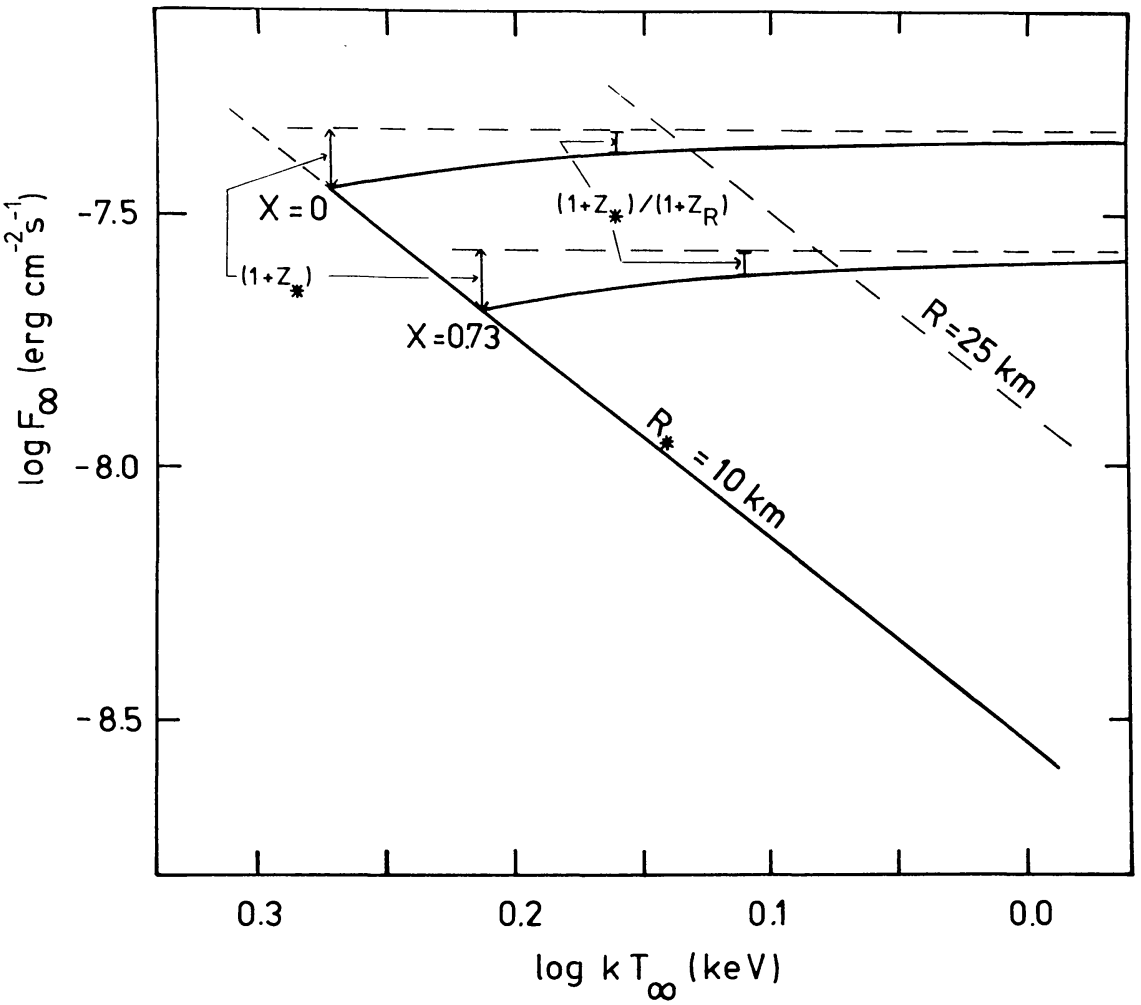

Fig. 4.5. Schematic diagram of the flux F_∞ versus the blackbody colour temperature kT_∞, showing how the gravitational redshift can be determined from the variation of the Eddington luminosity during photospheric radius expansion. The straight line (cooling track) is for a sphere with constant radius; the slope of this line is 4. The slanted dashed line holds for a sphere with a 2.5 times larger radius. Two points are indicated at which the luminosity equals the Eddington luminosity for cosmic (hydrogen content by number $X = 0.73$) and for hydrogen-poor ($X = 0$) compositions; the expansion-contraction tracks are the two solid curves. The redshift factors, $1 + z_*$, are indicated (assuming no change in the composition and in the anisotropy). This figure is from Damen *et al.* (1990b).

4.5.2. The Eddington Temperature

When, just at the end of the phase of photospheric contraction, the radius of the photosphere equals the stellar radius again (we call this "touchdown"), the luminosity is still Eddington-limited, and we have:

$$L_{\mathrm{Edd}*}(R = R_*) = (4\pi cGM/\kappa)(1 - 2GM/R_*c^2)^{-1/2} \tag{4.14a}$$

and

$$L_{\mathrm{Edd}\infty}(R = R_*) = (4\pi cGM/\kappa)(1 - 2GM/R_*c^2)^{1/2} \tag{4.14b}$$

for observers at the stellar surface, and at very large distances from the neutron star, respectively. At "touchdown" the effective temperature of the neutron star reaches a maximum value, $T_{\mathrm{Edd}*}$, given by

$$T_{\mathrm{Edd}*} = (cG/\kappa\sigma)^{1/4}(M/R_*^2)^{1/4}(1 - 2GM/R_*c^2)^{-1/8} \tag{4.15a}$$

In case the neutron star radiates as a blackbody, the corresponding colour temperature, as measured by a distant observer, is given by (Goldman 1979; Marshall 1982):

$$kT_{\mathrm{Edd}\infty} = (2.10\,\mathrm{keV})\,(M/M_\odot)^{1/4}(R/10\,\mathrm{km})^{-1/2} (1 - 2GM/R_*c^2)^{3/8}(1 + X)^{-1/4} \tag{4.16}$$

(note that here the temperature dependence of κ has not been included).

According to Equation (4.16) an observed value of the Eddington (effective) temperature corresponds to a mass-radius relation for the neutron star. This value may be obtained from the observed Eddington (colour) temperature if a value is assumed for the ratio of colour to effective temperatures at the Eddington limit, or from a fit of the observed cooling track in the flux-temperature diagram to a theoretical relation between the ratio $T_{c\infty}/T_{\mathrm{Edd}\infty}$ and the ratio $L_{b\infty}/L_{\mathrm{Edd}\infty}\ (R = R_*) = F_{b\infty}/F_{\mathrm{Edd}\infty}\ (R = R_*)$. It should be noted that Equation (4.16) is equivalent to the expression for the quantity B discussed below.

4.5.3. Combined Analysis of the Expansion and Cooling Phases of Bursts

When the flux is measured during that part of the expansion phase where $R \gg R^*$ the gravitational redshift factor in Equation (4.10b) is 1.0 to good approximation, and we have:

$$L_{\mathrm{Edd}\infty}(R \gg R_*) \approx 4\pi cGM/\kappa = 4\pi d^2 \xi_b F_{\mathrm{Edd}\infty}(R \gg R_*) \tag{4.17}$$

When the anisotropy does not change during the burst, we can combine Equation (4.17) with Equation (4.9) for the blackbody radius, to eliminate the quantity $d^2\xi_b$; we then find, using Equation (4.5):

$$F_{b\infty}/F_{\mathrm{Edd}\infty}(R \gg R_*) = R_*^2(1 - R_g/R_*)^{-1}\sigma(T_{e\infty})^4(\kappa/cGM) \tag{4.18a}$$

We note that the simplification of negligible redshift is not strictly necessary (see e.g. Fujimoto and Taam 1986; Sztajno *et al.* 1987; Van Paradijs and Lewin 1987), and in some cases (see Sect. 4.5.4.) not even acceptable. One can likewise combine Equation (4.9) with Equation (4.14b) for the Eddington limit at the end of the photospheric radius contraction phase, when the photosphere has just reached the stellar surface ("touchdown"), to obtain:

$$F_{b\infty}/F_{\mathrm{Edd}\infty}(R = R_*) = R_*^2(1 - R_g/R_*)^{-3/2}\sigma(T_{e\infty})^4(\kappa/cGM) \tag{4.18b}$$

Equations (4.18a, b) express relations between the mass M of the neutron star and its radius R_*, which are independent of the source distance and the anisotropy of the burst emission. We stress here again that in deriving Equation (4.18a, b) the anisotropy has been assumed to be the same during the expansion and cooling phases of the burst. "Observables" are: $F_{b\infty}$, $F_{\mathrm{Edd}\infty}$ $(R \gg R_*)$ [or $F_{\mathrm{Edd}\infty}$ $(R = R_*)$], and $T_{e\infty}$ (the conversion from the observed colour temperature $T_{c\infty}$ to the effective temperature $T_{e\infty}$ is discussed in detail in Chapter 5). A measurement of these three observables leads to a measurement of either the quantity $A = [cG/\sigma(T_{e\infty})^4]$ $[F_{b\infty}/F_{\mathrm{Edd}\infty}$ $(R \gg R_*)]$, or of the quantity $B = [cG/\sigma(T_{e\infty})^4]$ $[F_{b\infty}/F_{\mathrm{Edd}\infty}$ $(R = R_*)] = A[1 - 2GM/(c^2 R_*)]^{-1/2}$; here:

$$A = R_*^2[1 - 2GM/(c^2 R_*)]^{-1}(\kappa/M) \quad (R_* \geq 1.5R_g) \tag{4.19a}$$

For $R_* < 1.5\ R_g$ (see Equation (4.8)), the quantity A becomes:

$$A \approx (7.78\ M/M_\odot \text{ km})^2\ (\kappa/M) \quad (R_* < 1.5\ R_g) \tag{4.19b}$$

In the latter case, for a given value of A, M is independent of R_*. In Fig. 4.6 we show in the M–R_* diagram two curves for two different values of κ (0.20 and 0.34 cm^2/g), for a typical observed value for $A = 10^{-22}$ $(\pm\ 15\%)$ cm^4/g^2.

Equation (4.18), in which the distance is absent, is essentially an expression of the unchanging angular size of the burst source (i.e., R_∞/d). Thus, as one moves along one of the curves in Fig. 4.6, the angular size of the burst source remains constant, but R_∞ and d change; this is not the case for the curves in Fig. 4.3.

During the decay phase of bursts from one source, which has shown at least one burst with radius expansion, one can make several measurements of both the flux and the associated blackbody temperature. For blackbody emission from a spherical object with a constant radius, the ratio $F_{b\infty}/(T_{e\infty})^4$ remains constant. Therefore, one derives the average value for several measurements during burst decay, and this value with its associated error is used to construct allowed regions in the M–R_* diagram (see Sect. 4.6).

In the above analysis the effect of a non-Planckian shape of the burst spectrum can be taken into account if a relation between the observed colour temperature T_c and the effective temperature T_e can be established. Simple analytical relations, derived from the results of model-atmosphere calculations (see also Ch. 5), have been proposed by Sztajno *et al.* (1987) and Ebisuzaki and Nakamura (1988). These can be used to either derive a new analytical relation between M and R_*, analogous to Equation (4.19a, b), in terms of observable quantities (see e.g. Fujimoto and Taam 1986; Sztajno *et al.* 1987), or to transform each individually pair of measured values $[T_{c\infty}, F_{b\infty}]$ to a pair $[T_{e\infty}, F_{b\infty}]$, and then use Equation (4.19a, b).

4.5.4. Gravitational Redshift from the Variation of the Eddington Flux during Radius Expansion

As can be seen from Equation (4.10b) the Eddington luminosity, as measured by a distant observer, depends not only on the mass, but also on the radius of the

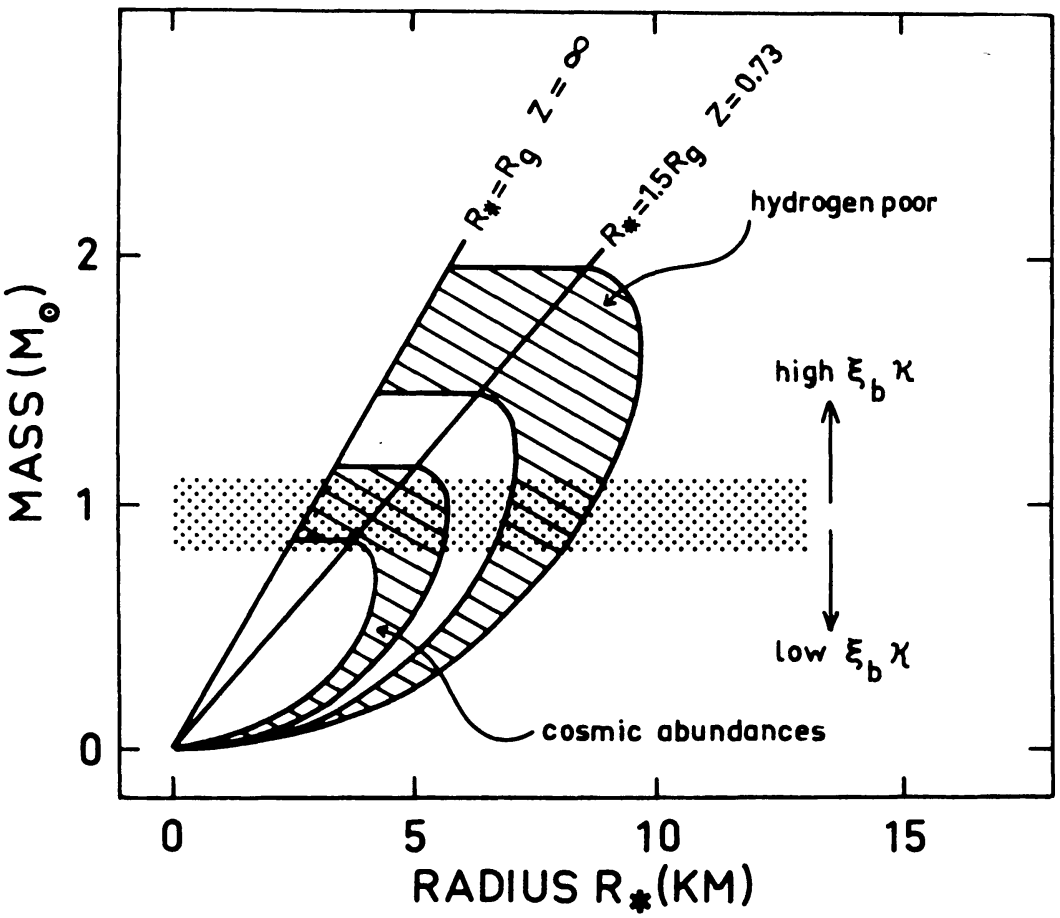

Fig. 4.6. Mass-radius relation resulting from the observation of an X-ray burst with radius expansion. We have assumed, for the purpose of illustration only, that the quantity A in eq. (4.19) is in the range $(0.85–1.15) \times 10^{-22}$ cm^4 g^{-2} (see text). The allowed regions in this diagram for assumed hydrogen poor ($\kappa = 0.2$ cm^2 g^{-1}) and cosmic ($\kappa = 0.34$ cm^2 g^{-1}) compositions are indicated by the hatched areas. The horizontal (shaded) band indicates schematically the constraint on the mass obtained from the measured Eddington flux ($R \gg R_*$) for a source with known distance. The width of the band reflects uncertainties in the measurements. The position of the band depends on both κ and on the anisotropy ξ, as schematically indicated (from Damen *et al.* 1990b).

emitting object through a gravitational-redshift factor. As pointed out by Paczynski and Anderson (1986) this dependence allows in principle a determination of the gravitational redshift at the surface of the neutron star by comparing the Eddington fluxes as observed when the photospheric radius is very large and when the contraction phase has just ended (see Fig. 4.5).

In its simplest version of the method it is assumed that during the radius expansion the radius of the photosphere is so large that then the gravitational redshift can be neglected. Then the Eddington luminosity is given by Equation (4.17), *viz.*

$$L_{\mathrm{Edd}\infty}(R \gg R_*) \approx 4\pi cGM/\kappa = 4\pi d^2 \xi_b F_{\mathrm{Edd}\infty}(R \gg R_*) \qquad (4.17)$$

At "touchdown" we have:

$$L_{\mathrm{Edd}\infty}(R = R_*) = (4\pi cGM/\kappa)(1 - 2GM/R_* c^2)^{1/2}$$

$$= 4\pi d^2 \xi_b F_{\mathrm{Edd}\infty}(R = R_*) \tag{4.14b}$$

By dividing these equations one sees that the ratio of the Eddington fluxes, observed when the radius expansion is large, and when the photospheric radius equals the stellar radius, respectively, gives the gravitational redshift at the surface of the neutron star, and therewith the ratio M/R_*. (Note that again it is assumed here that the anisotropy remains the same during the burst). A measurement of M/R_* limits the allowed values of M and R_* to a straight line in the M–R_* diagram. This constraint can be used in conjunction with the region in the M–R_* diagram that can be obtained from the combination of data, for the expansion and cooling phase of a burst, described in Sect. 4.5.3, to derive mass and radius separately.

As discussed in detail by Damen *et al.* (1990b), in this comparison of Eddington fluxes one has to take into account the possibility that the photospheric radius R may not be large enough for the approximation $z(R) = 0$ to be valid. In addition, it is important to take the temperature dependence of the electron scattering opacity (Equation 4.12a, b) into account. This "correction" to the Eddington luminosity is rather small (it amounts to ~10%, at $kT = 3$ keV); however, its variation during a typical radius expansion (~5%) is not very small compared to z_*, and since this variation with radius is monotonous, it must be taken into account.

Following Damen *et al.* (1990b) and Van Paradijs *et al.* (1990a) one obtains for the ratio, ζ_∞, of the observed Eddington fluxes the expression:

$$\begin{aligned} \zeta_\infty &= F_{\mathrm{Edd}\infty}(R > R_*)/F_{\mathrm{Edd}\infty}(R = R_*) \\ &= f\,(R, R_*)(1 + z_*)/(1 + z_R) \end{aligned} \tag{4.20a}$$

or

$$(1 + z_*)/(1 + z_R) = \psi_\infty = \zeta_\infty / f\,(R, R_*) \tag{4.20b}$$

with

$$f\,(R, R_*) = [1 + (\alpha T_R)^{0.86}]/[1 + (\alpha T_*)^{0.86}] \tag{4.20c}$$

We can approximate Equation (4.20b) by

$$\psi_\infty = \zeta_\infty[1 + (\alpha T_*)^{0.86} - (\alpha T_R)^{0.86}] \tag{4.21}$$

which, using $T_R/T_* = (T_{R,\infty}/T_{*,\infty})(1+z_R)/(1+z_*) \cong (T_{R,\infty}/T_{*,\infty})/\zeta_\infty$, leads to

$$\begin{aligned} \psi_\infty = \zeta_\infty &[1 + (\alpha T_{*,\infty})^{0.86}(1 + z_*)^{0.86}] \\ &-\zeta_\infty^{0.14}(\alpha T_{*,\infty})^{0.86}(1 + z_*)^{0.86}(T_{R,\infty}/T_{*,\infty})^{0.86} \end{aligned} \tag{4.22}$$

The calculation of ψ_∞ can proceed in two steps. In the first step the temperature dependence of κ is neglected, i.e. one sets $\psi_\infty = \zeta_\infty$, to obtain a first estimate of $(1 + z_*)$ through

$$(1 + z_*)^2 = (\psi_\infty^2 - \chi^{-1})/(1 - \chi^{-1}) \tag{4.23}$$

with $\chi = R/R_*$. This value can then, in the second step, be used in the r.h.s. of Equation (4.22), to obtain a better estimate of ψ_∞ in which the temperature dependence of κ is included. In applying this procedure to a burst observed from the globular cluster M15, Van Paradijs *et al.* (1990a) found that after one iteration the procedure had converged satisfactorily.

The quantity χ in Equation (4.23) is related to the ratio χ_∞ of the photospheric radii, measured by a distant observer, through

$$\chi = R/R_* = (R_\infty/R_{*,\infty})(1 + z_*)/(1 + z_R) = \chi_\infty \zeta_\infty \tag{4.24}$$

To account for the fact that the burst spectra during radius expansion deviate from a Planck curve Damen *et al.* (1990b) assumed that the effect of this can be described by a spectral hardening factor $t_\infty = T_{c\infty}/T_{e\infty}$, which during the radius expansion phase varies with $T_{c\infty}$ in the same way as is observed during the cooling phase of the burst. During the cooling phase the spectral hardening factor t is proportional to $\theta_\infty = T_{c\infty}/(F_{b\infty})^{1/4}$ (see Chapter 5). Then one has

$$\chi_\infty = \chi_{bb\infty}[t_\infty(R > R_*)/t_\infty(R = R_*)]^2 \tag{4.25}$$

To estimate how sensitively the results depend on this assumption Damen *et al.* (1990b) also made the alternative assumption that t is constant during radius expansion (then $\chi_\infty = \chi_{bb\infty}$).

To summarize, the derivation of the gravitational redshift from the variation of the observed Eddington flux during photospheric radius expansion comprises the following steps. (i) Determine the ratio, $\chi_{bb\infty}$, of the blackbody radii at some instant during radius expansion and during touchdown. (ii) From the observed colour temperatures during radius expansion and at touchdown derive the ratio $t_\infty\ (R > R_*)/t_\infty\ (R = R_*)$, and find χ_∞, using Equation (4.25). Alternatively, assume $\chi_\infty = \chi_{bb\infty}$. (iii) Use the observed ratio, ζ_∞, of Eddington fluxes to derive χ, using Equation (4.24). (iv) Finally, the values of χ and ζ_∞, together with the observed temperatures during radius expansion and at touchdown, determine the gravitational redshift by an iterative solution of Equation (4.22).

4.6. Results

4.6.1. Absorption Lines in Burst Spectra

Based on the fact that iron is the most abundant element with resonance lines above 4 keV, and in view of the relevant temperatures in the neutron star atmosphere, Waki *et al.* (1984) suggested that the 4.1 keV line they observed in some bursts from 1636–536 is the redshifted resonance line of helium-like iron (Fe^{25+}), whose laboratory energy is 6.7 keV. The corresponding gravitational redshift $1 + z_* = 1.6$, i.e. $R_* = 1.6\ R_g$.

This is a rather small radius, and Fujimoto (1985) therefore proposed that a part of the observed redshift is due to the rapid rotation of the (previously accreted)

neutron star atmosphere, so that transverse Doppler shift must be combined with gravitational redshift. Assuming that this rotation is Keplerian, Fujimoto (1985) found that the radius constraint can be relaxed to $R_* = 2.4R_g$. However, one would then also expect significant line broadening due to the combined red- and blue-shifted lines from the rotating matter (cf. Kapoor and Datta 1984). Based on the upper limit to the width of the 4.1 keV line of 500 eV for 1636–536 (Waki *et al.* 1984) alone this possibility cannot be excluded; however, combined with the upper limits on the line widths of 320 eV for 1608–522 (Nakamura *et al.* 1988), and 800 eV for 1747–214 (Magnier *et al.* 1989), the suggestion of Fujimoto (1985) must be rejected, since it would require an inclination angle of roughly less than 15° for all three systems. The suggestion by Pinto *et al.* (1992) is more promising. The interpretation of the 4.1 keV line as an atomic transition in the atmosphere of a neutron star is further discussed in Sect. 5.5.

4.6.2. Mass-Radius Constraints from Blackbody Radii and Eddington Fluxes

Most studies of X-ray bursts have included a determination of the blackbody radius, based on Equation (4.1). The derived values are generally of the order of 10 km, for assumed source distances near 10 kpc. We refer to the Appendix for references to studies of individual sources.

Fujimoto and Taam (1986) were the first to apply a combined analysis of burst data obtained by Inoue *et al.* (1984b) with Tenma during the phases of radius expansion and cooling (see Sect. 4.5.3) to estimate the mass and radius of the neutron star in 1636–536. They assumed that the ratio of colour to effective temperature has a constant value (equal to 1.4), and combined the blackbody radius thus obtained with the Eddington flux observed at touchdown to derive the quantity $B = A(1 - R_*/R_g)^{-1/2}$ where A is given by Equation (4.19a), i.e., non-escape of photons for $R_* < 1.5\ R_g$ was neglected. Fujimoto and Taam (1986) did not take into account that the burst emission could be anisotropic. They assumed that the neutron star radius equals 2.4 Schwarzschild radii, based on Fujimoto's (1985) interpretation of the 4.1 keV absorption line (see Sect. 4.6.1). From their analysis they concluded that the mass and radius of the neutron star in 1636–53 are in the ranges (1.28–1.65) $M_\odot$, and (9.1–11.3) km, respectively (see Fig. 4.7). If the redshift of the 4.1 keV line were attributed solely to gravitational redshift their values would have been $\sim 1.7\ M_\odot$, and ~8 km, respectively.

Ebisuzaki (1987) applied a similar analysis to these data which differed from the analysis of Fujimoto and Taam (1986) mainly in the assumed relation between colour temperature and effective temperature. Attributing the energy shift of the 4.1 keV line to gravitational redshift alone, and assuming that the line is due to highly ionized iron, he derived $M = 1.9 \pm 0.1\ M_\odot$, and $R_* = 9 \pm 1$ km. (The alternatives that the line is due to Cr or Ti were also considered by Ebisuzaki). Possible anisotropy of the burst emission was not included in this analysis.

Sztajno *et al.* (1987) analyzed two radius-expansion bursts from 1746–370, located in the globular cluster NGC 6441 for which the distance is reasonably

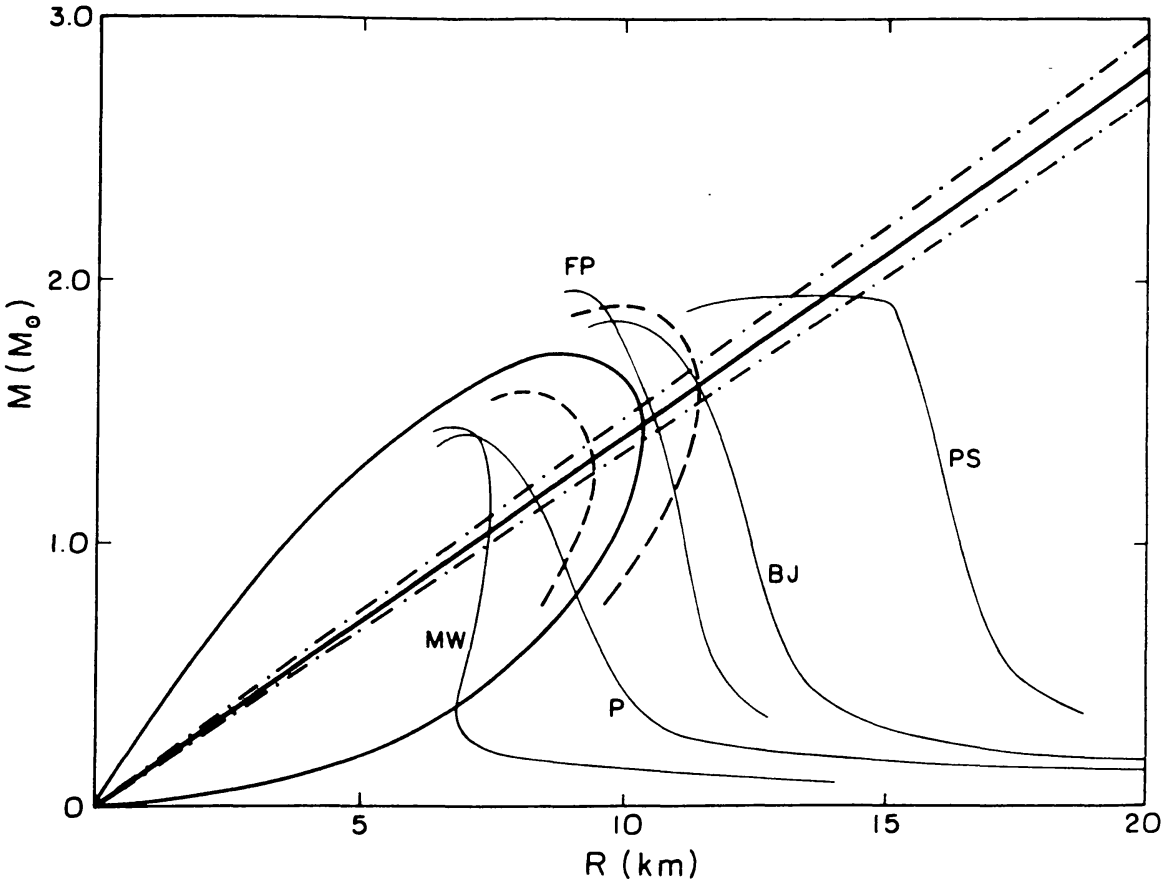

Fig. 4.7. Constraints on the mass-radius relation for the neutron star in 1636–536, obtained from an analysis of a burst with photospheric radius expansion, and a particular interpretation of the 4.1 keV absorption line as the Lyα line of helium-like iron which underwent gravitational and transverse-Doppler redshifts (from Fujimoto and Taam 1986). The left part of the "leaf-like" curve is not correctly drawn; it is drawn correctly in Fig. 4.6. A recent, more plausible interpretation for the 4.1 keV absorption lines have been given by Pinto *et al.* (1992).

well determined. They combined data obtained during the radius expansion and decay of the burst, using Equation (4.17) and (4.19a), and used an approximate analytical approximation to the theoretical results of London *et al.* (1986) to relate colour temperature to effective temperature. Their results (see Fig. 4.8) indicate that whether or not a particular equation of state is acceptable depends on the value of the anisotropy parameter ξ_b (see Equation (4.9)).

The same analysis was applied by Van Paradijs and Lewin (1987) to data obtained by Haberl *et al.* (1987) for bursts from 1820–303 in the globular cluster NGC 6624, for which the distance is relatively well determined. They find that in the likely case that the outer layers of the neutron star are hydrogen-poor (see, e.g., Rappaport *et al.* 1987) none of the current equations of state can be excluded (for a hydrogen-rich case only very soft equations of state are allowed).

Chevalier and Ilovaisky (1990) derived constraints on the mass and radius of the neutron star in 1906 + 000 using an estimate of the gravitational redshift from the variation of the Eddington flux during radius expansion. They assumed that at

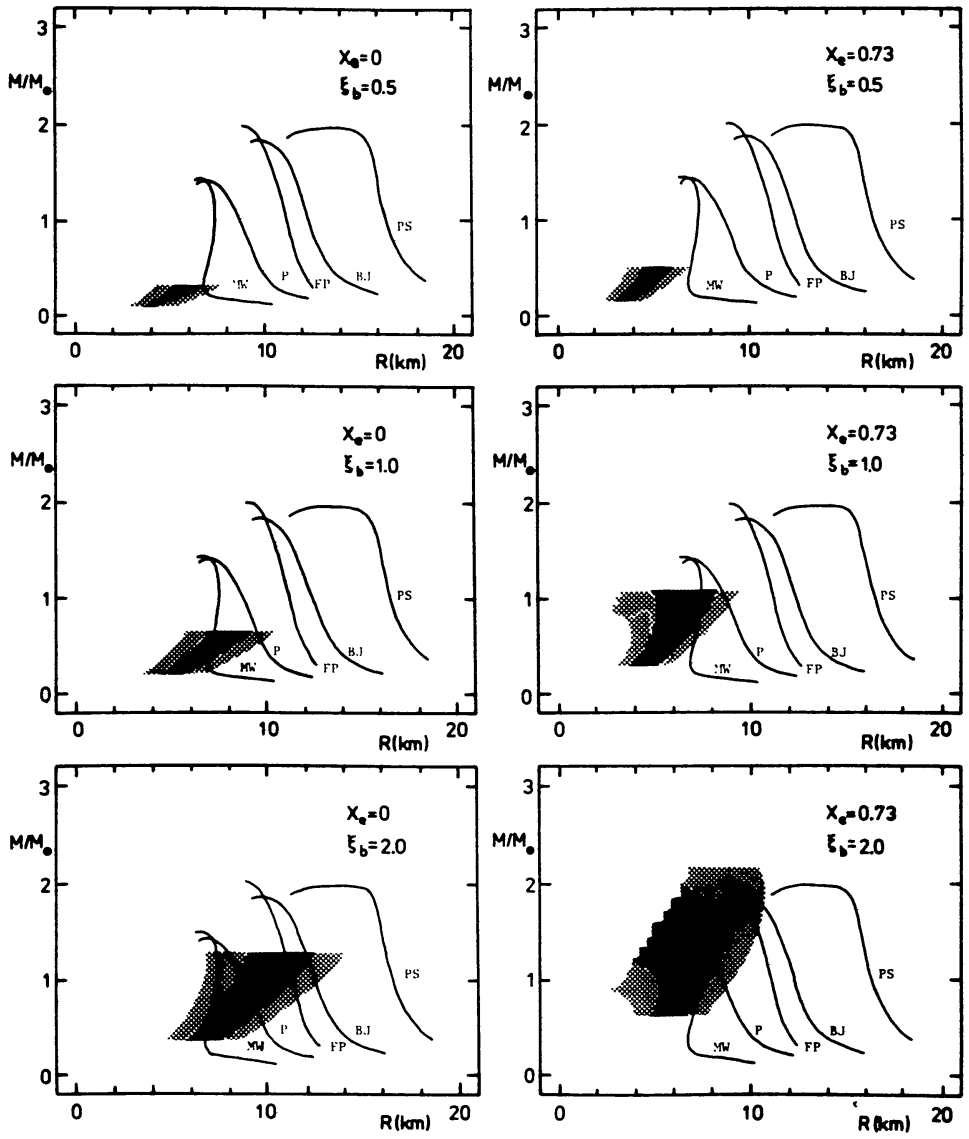

Fig. 4.8. Constraints on the mass-radius relation for the neutron star in 1746–370, from an analysis of a burst with photospheric radius expansion, for various assumed values of the hydrogen content of the photosphere, and the anisotropy factor of the burst emission (from Sztajno *et al.* 1987).

the maximum of the radius expansion the gravitational redshift is unity, and made a straightforward combination of Equation (4.14b) and (4.17). They combined this result with an estimate of the Eddington (effective) temperature (Equation (4.16)) from a fit of the cooling track to a theoretical relation between $T_{c\infty}/T_{\mathrm{Edd}\infty}$ and the luminosity in units of the Eddington luminosity. They prefer a solution for the case that the neutron star envelope is hydrogen-rich and then find a mass M in the range (1.2–2.1) $M_\odot$, and a radius between 9.8 and 12.8 km.

Kaminker *et al.* (1989, 1990) analyzed X-ray bursts observed with ASTRON from 1728–337 and 1730–335 (the Rapid Burster). They used an isothermal scattering atmosphere to describe the shape of the X-ray burst spectra to infer constraints on the neutron stars in these systems.

Damen *et al.* (1990b) attempted to determine the gravitational redshift of neutron stars from the variation of the observed Eddington flux during photospheric radius expansion (see Sect. 4.5.4.) using EXOSAT observations of the systems 0748–676, 1636–536, 1735–444, and 1820–303. They find that this method is quite sensitive to systematic errors, due to possible variations during the photospheric expansion of (i) the persistent X-ray emission, (ii) the photospheric composition, and particularly (iii) the shape of the X-ray burst spectrum. They concluded that the measured values of the redshift for these sources are too uncertain to put significant constraints on neutron star properties.

One very energetic burst observed with Ginga from 2129 + 119 in the globular cluster M15 was analyzed by Van Paradijs *et al.* (1990a). They determined the gravitational redshift from the variation of the Eddington flux during radius expansion (using Equation 4.21 to 4.25). They then used this result to "correct" the Eddington flux for the redshift factor, and applied the combined analysis of the cooling track and radius expansion data, described in Sect. 4.5.3. Thus they obtained three independent pieces of information which, for a chosen composition, allowed a determination of mass, radius and the quantity $d^2\xi_b$ (see Equation (4.9)) separately (see Fig. 4.9). Van Paradijs *et al.* (1990a) found evidence for systematic deviations of the burst spectra from Planckian functions, in the form of spectral "bumps", which they conclude pose a significant limitation to our ability to derive firm numbers of neutron star masses and radii from X-ray burst observations (see also Sect. 5.4).

4.7. Problem Areas

As emphasized above, all work discussed in this chapter has been based on the assumption that during a burst the whole neutron star surface participates uniformly in the burst emission. Early work, which showed that the apparent blackbody radii did not vary significantly between bursts from one source, independent of their profiles (Van Paradijs 1978; Lewin *et al.* 1980; Ohashi 1981), supported this assumption.

The first evidence for differences between the blackbody radii, R_∞, measured during the decay of bursts from one source, was presented by Matsuoka (1986). He found that the locations of the cooling tracks in the flux-temperature diagram for radius-expansion bursts from 1636–53 were different from those of bursts that did not show radius expansion. Matsuoka also superposed cooling tracks for radius-expansion bursts from different sources, by assuming that the Eddington flux $F_{\mathrm{Edd}\infty}$ $(R = R_*)$ corresponds to a fixed luminosity level [see Equation (4.14b)], and found that these cooling tracks for 1728–337 and 1636–536 differed significantly.

Further evidence that the blackbody radii measured for one source are not always the same was found by Gottwald *et al.* (1986) for 0748–676. They showed that in this source R_∞ varied by up to a factor of 3 for a given value of the colour temperature $T_{c\infty}$ (see Fig. 4.10). A surprising result was, that these radius variations showed a very strong positive correlation with variations of the persistent flux (see

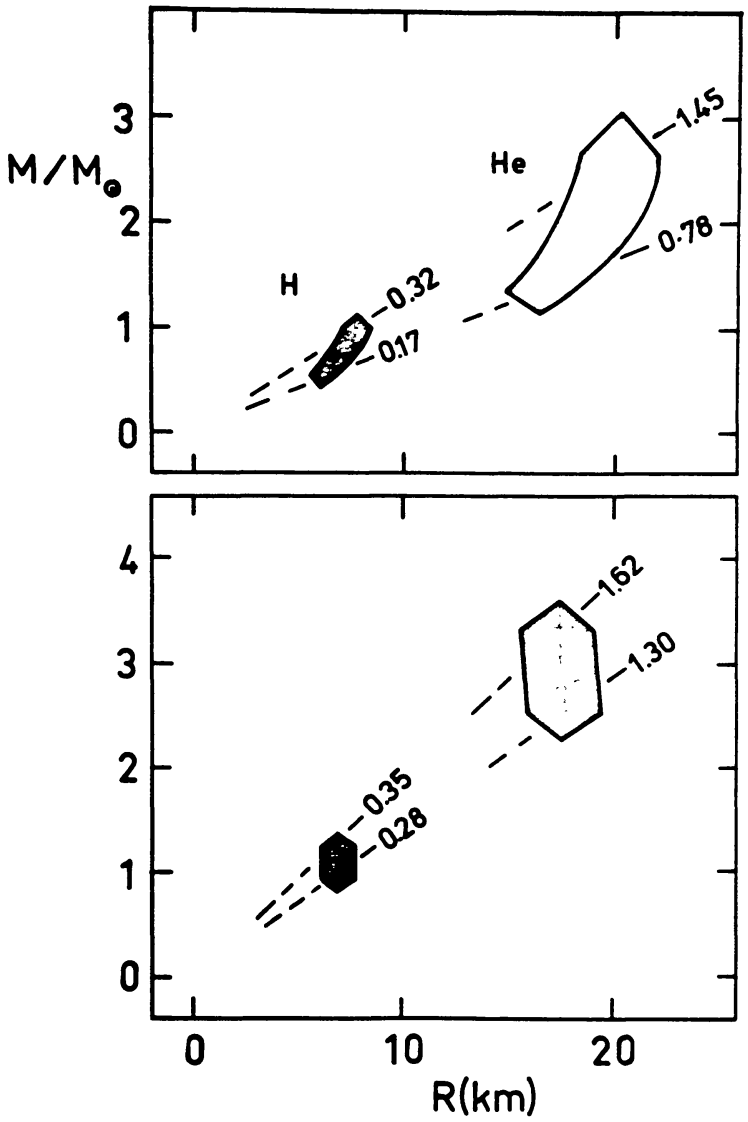

Fig. 4.9. Mass-radius diagram for the neutron star in 2127 + 119. The radius R in the figure is R_* as used in the text. The enclosed areas are allowed regions for assumed cosmic and hydrogen-poor compositions of the neutron star atmosphere, as indicated with "H" and "He" respectively. The numbers in the figure indicate the values derived for the anisotropy factor ξ_b (see text). The upper panel shows the results which are based on the assumption that during the radius expansion track the ratio of colour temperature to effective temperature does not vary. The regions shown in the lower panel were derived under the assumption that during the radius expansion this ratio varied similarly as during the cooling track. This figure is from Van Paradijs *et al.* (1990a).

Fig. 4.11). A very similar correlation between the persistent flux and blackbody radius was found by Gottwald *et al.* (1989) for 1705–440.

Damen *et al.* (1989) carried these analyses one step further by showing (see Fig. 4.12) that for 1636–536 there is a strong correlation between the location of the cooling track of a burst (as measured by the temperature $kT_{0.1}$ at the moment that the burst flux has decayed to 10% of the Eddington flux) and the burst duration τ (defined as the ratio of burst fluence to peak burst flux). The same correlation is also present in the results published by Gottwald *et al.* (1989) for 1705–440.

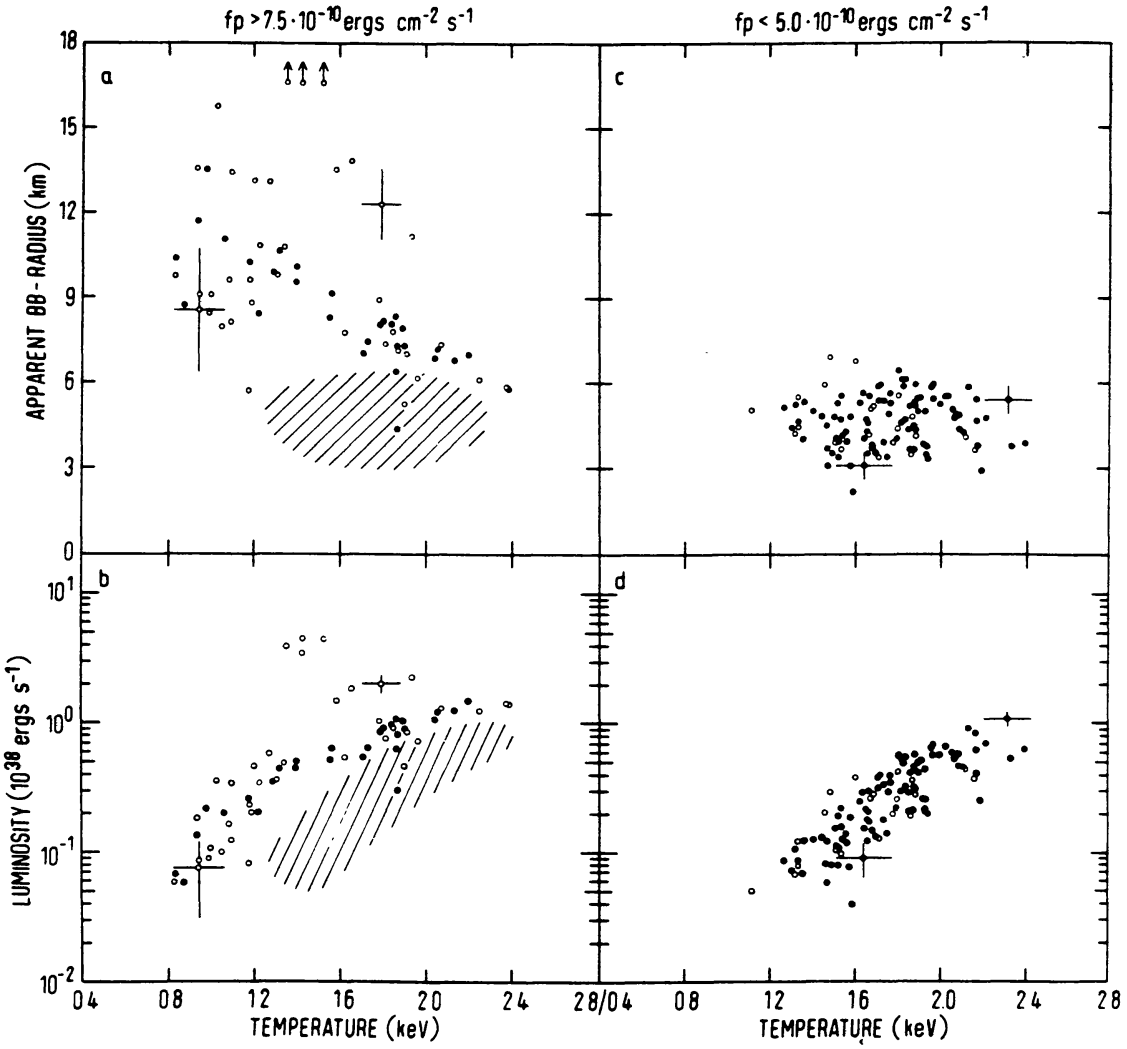

Fig. 4.10. Flux-temperature diagrams (bottom panels b, d) for bursts from 0748–676, and the corresponding diagrams (top panels a, c) of blackbody radius vs temperature. The left (a, b) and right (c, d) panels show results for bursts which occurred when the persistent X-ray flux was $< 5 \times 10^{-10}$ and $> 7.5 \times 10^{-10}$ erg cm^{-2} s^{-1}, respectively. Hatched areas in panels (a, b) indicate the mean location of points in panels (c, d). The open and filled circles indicate bursts with and without initial expansion of the photosphere, respectively. In panel (a) the arrows indicate lower limits to three radii measured during the expansion phase. This figure is from Gottwald *et al.* (1986).

Damen *et al.* (1989) did not find a correlation between $kT_{0.1}$ and the persistent flux of 1636–536; subsequent work by Van der Klis *et al.* (1990) showed that there is a good correlation between both τ and $kT_{0.1}$ and the location of the source in a "colour-colour" diagram for the persistent X-ray emission (see Fig. 3.16). Their interpretation is that there probably is a good correlation between the accretion rate and τ and $kT_{0.1}$, but that the persistent X-ray flux is not a good measure of relatively small variations of the accretion rate.

Three possible explanations could, in principle, be given for these variations in the apparent sizes of burst emitting regions. In the first place these variations could be due to variations in the anisotropy of the burst emission. However, the

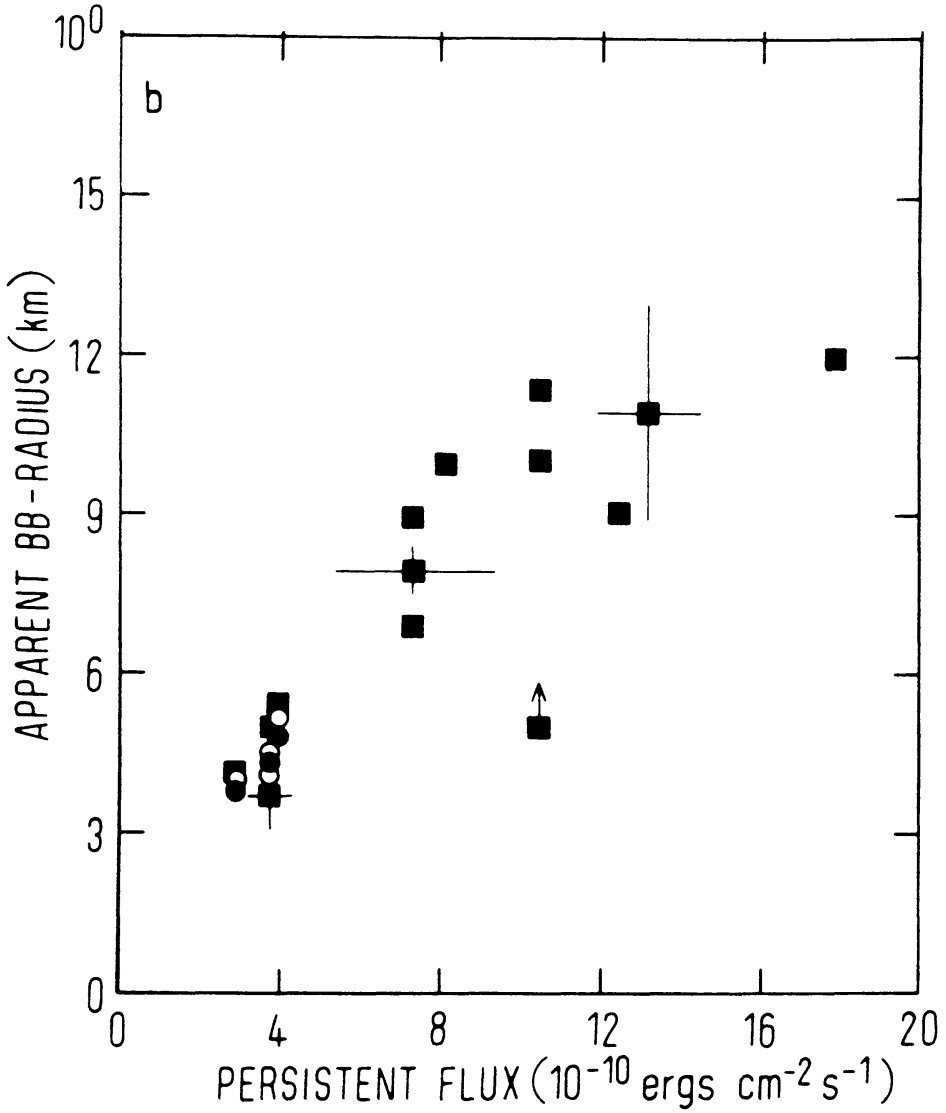

Fig. 4.11. Dependence of the blackbody radius R_∞ (averaged values per burst) on the persistent X-ray flux, for 0748–676. Squares indicate single bursts, filled and open circles indicate the first and second bursts of a pair that occurred less than 20 minutes apart (from Gottwald *et al.* 1986).

required changes in the anisotropy parameter ξ_b are quite large (factors of 4 and 20, for 1636–536, and 0748–676, respectively). Such large variations cannot be easily reconciled with the observed linear relation between peak burst flux and waiting time before the bursts, and with the observed gap in the peak burst flux distribution of 1636–53 (see Sect. 3.4), which would disappear if ξ_b changed by a factor of 1.3 or more between bursts.

A second possible explanation is that the radiating area is not the same for all bursts. However, the same argument concerning the distribution of peak fluxes can be used against this possibility. In addition, there is no obvious reason why there would be an anti-correlation between the burst duration and the radiating area.

The third explanation for the apparent radius variations is based on assumed

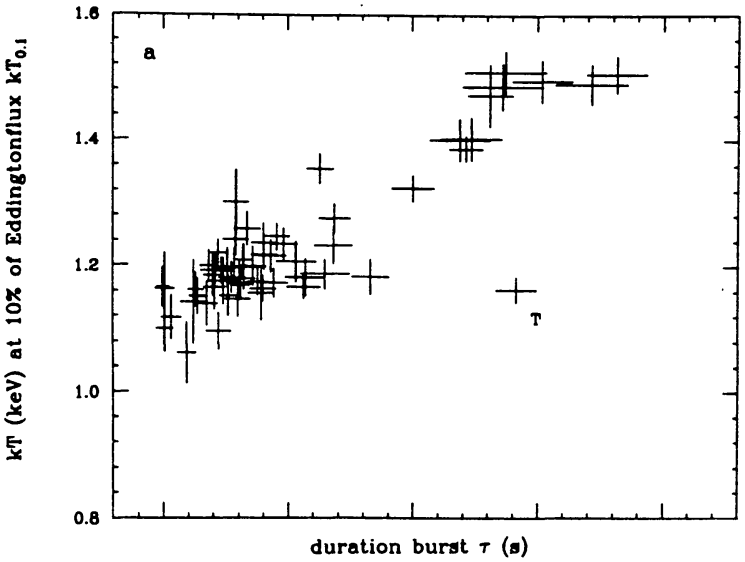

Fig. 4.12. Relation between the duration τ of X-ray bursts and the fitted blackbody temperature, $kT_{0.1}$, at the moment that the flux had decreased to 10 percent of the Eddington flux, for 1636–536. The one point indicated with "T" represents the triple-peaked burst observed for this source (see also Fig. 3.8). This Figure is from Damen *et al.* (1989).

non-Planckian properties of the burst spectra which, in principle, would allow for variations in the relation between colour temperature and effective temperature. Matsuoka (1986) suggested that the spectral changes could be caused by comptonization of the burst emission by hot plasma outside the neutron star. In the case of 1608–522 (Mitsuda *et al.* 1989; Nakamura *et al.* 1989) there is evidence that such comptonization, which gives rise to a high-energy tail in both the burst spectra and the persistent spectra, occurs and becomes more important as the persistent flux decreases. However, variations in a high-energy Compton tail are unlikely to cause the changes in R_∞ observed in 1636–536, since no evidence for such high-energy tails was found for this source by Damen *et al.* (1990a).

Matsuoka (1986) suggested that non-Planckian effects on burst spectra could also affect the cooling tracks in the flux-temperature diagram, through a dependence of the burst spectrum on the chemical composition of the neutron star atmosphere. According to the models of Ebisuzaki and Nomoto (1986) the shape of burst spectra depends on the hydrogen content (measured by the hydrogen mass fraction, X) such that the apparent blackbody radii decrease as X increases. This dependence of R_∞ on the hydrogen content is of particular interest, in view of the evidence that the burst duration τ depends on the chemical composition of the flashing layer, in the sense that τ increases with X (Fujimoto *et al.* 1981; Van Paradijs *et al.* 1988a, and references therein). Bursts which are due to helium flashes in a hydrogen-rich environment last longer than pure helium bursts, due to the relatively long time scales involved in proton-capture processes. Thus, both the burst duration and the location of the cooling track are expected to change with hydrogen content in a way that is consistent with the direction of the $(\tau, kT_{0.1})$ relation found by Damen *et al.* (1989). However, it is not immediately clear that variations in the chemical

composition of the flashing layer (at scattering optical depths $\tau_{sc} \sim 10^8$) and those in the atmosphere ($\tau_{sc} \sim 1$) are related. They could possibly be connected by a mixing of the material in the flashing layer and the neutron star atmosphere during a burst.

Although variation in the hydrogen content may thus provide a qualitative explanation for the correlated variations of R_∞ and τ, it should be noted that the amplitude of the radius variations, which are about a factor 2 in 1636–536, and even larger in 0748–676, substantially exceed the changes expected on the basis of the models (Ebisuzaki 1987; Ebisuzaki and Nakamura 1989).

4.8. Conclusions

The results discussed in this chapter show that X-ray bursts may provide a means to obtain information on both the mass and radius of neutron stars. To us it appears that the main factor which presently prevent the derivation of firm numbers on these quantities is our limited understanding of the spectra of X-ray bursts. In particular, the deviations of burst spectra from a smooth spectral function found for bursts from 2127 + 119, and the dependence of apparent blackbody radii on burst duration (and, indirectly, probably on accretion rate), indicate that our understanding of X-ray burst spectra is incomplete (see Sect. 4.6). Progress in this respect may depend on the availability of improved spectral resolution of X-ray burst observations (such as expected from the Japanese satellite ASTRO-D, due for launch in 1993), and from detailed theoretical studies of neutron star atmospheres, including the possible effects of magnetic fields.

5. X-Ray Spectra of Hot Neutron Stars

5.1. Introduction

Studies of the spectral energy distribution of photons emitted by hot neutron star atmospheres were first made in the 1960's, stimulated by the idea (Chiu 1964; Chiu and Salpeter 1964; Finzi 1964) that the discrete X-ray sources which were then just discovered (Giacconi *et al.* 1963) are young hot neutron stars formed in recent supernovae.

Following the initial calculations of the thermal structure of the outer envelope of cooling neutron stars by Morton (1964) more detailed studies of the spectra were made by Orszag (1965), who found that for effective temperatures in the range (5–10) $\times 10^6$ K these spectra may contain discontinuities due to bound-free edges of abundant elements. Based on an approximate curve-of-growth analysis Onyejuba and Gaustad (1967) suggested that neutron star spectra may also contain spectral lines of abundant elements.

As noted by Burbidge (1963) the wavelengths of discrete spectral features in the radiation emitted from the near vicinity of neutron stars will be gravitationally redshifted. Measurement of the wavelengths of identifiable features would then provide the possibility to determine the gravitational redshift and therefore the

ratio of mass, M, to radius, R_*, of the neutron star (Chiu and Salpeter 1964; see Sect. 4.4 and 5.5), according to $1 + z_* = (1 - 2GM/R_*c^2)^{-1/2}$.

As a result of the measurement of the finite extent of the X-ray source associated with the Crab Nebula (Bowyer *et al.* 1964), and the non-Planckian shape of the X-ray spectra of this source (Clark 1965) and of Sco X–1 (Giacconi *et al.* 1965) it soon became clear that thermal radiation from the surface of a hot neutron star does not provide a good model for the discrete X-ray sources. Meanwhile, accretion onto a compact star had been suggested as a model for powerful X-ray sources (Zel'dovich 1964; Salpeter 1964; Shklovsky 1967; see also Burbidge 1972, and Ginzburg 1990). The idea of thermal emission from a neutron star surface disappeared from discussions about galactic X-ray sources [with the notable exception of a paper by Margon *et al.* (1971) on the source GX 340 + 0], and for some years studies of the structure of neutron star atmospheres and of the spectra of hot neutron stars were not pursued.

The study of the thermal emission from hot neutron star atmospheres received new impetus from the Einstein imaging observations of isolated cooling neutron stars (radio pulsars and young neutron stars inside supernova remnants), and observations of X-ray bursts. The former observations have led to upper limits on the luminosity of neutron stars of known age which seem to be inconsistent with the standard theory of neutron star cooling [see Tsuruta (1986) for a review of this subject]. Important developments in this area may be expected from current ROSAT observations (see, e.g., Finley *et al.* 1992). Model atmosphere calculations have been made by Romani (1987) for effective temperatures ($kT_{\rm eff}$) in the range 0.01 to 0.3 keV, and a range of chemical compositions, to explore the possibility that this inconsistency is caused by deviations of the spectra of these cooling neutron stars from that of a blackbody (the relevant temperature range for the interpretation of X-ray burst spectra is higher, $kT_{\rm eff} \sim 1$ to 3 keV). Model atmospheres in which the effects of a strong magnetic field have been included have been made by Van Riper (1988).

It was first pointed out by Swank *et al.* (1977) that the spectrum of an X-ray burst they observed with OSO–8 was best described by a Planckian model with a time-dependent temperature (kT) ranging between 0.9 and 2.3 keV. Their result was confirmed by Hoffman, Lewin and Doty (1977a, b) for bursts observed with SAS–3 from the sources 1728–337 and 1636–536. The interpretation of X-ray burst spectra in terms of a blackbody of varying temperature was supported by the fact that during the decay the burst flux varied approximately as the fourth power of the blackbody temperature, which implies a constant area of the blackbody emitter. The size of a blackbody emitter, assumed to be spherical, can be expressed as a blackbody radius R_{bb} given by

$$R_{bb}^2 \sigma T^4 = d^2 F_X \tag{5.1}$$

Here d is the distance to the source, and F_X and T are the (time-varying) X-ray flux and (fitted) blackbody temperature, respectively (no correction for gravitational

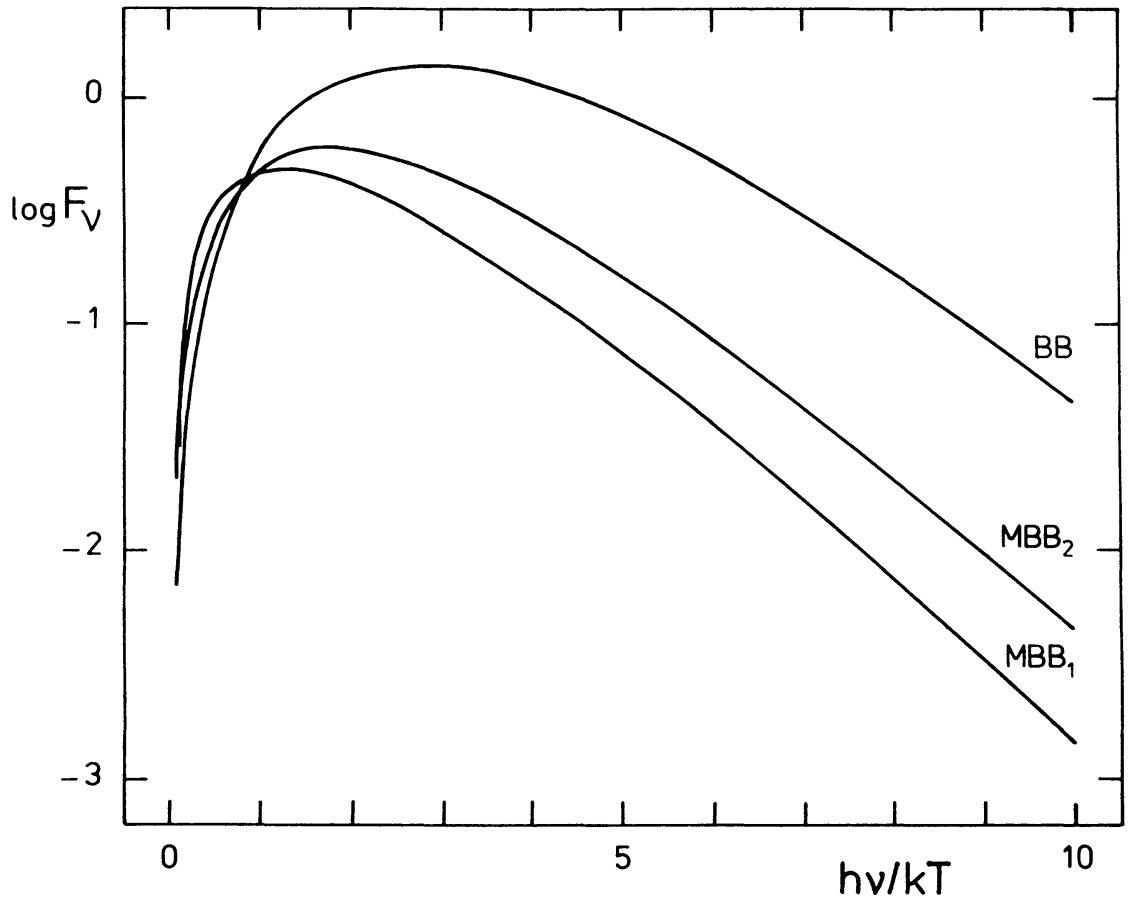

Fig. 5.1. Spectral energy distributions for a blackbody (BB), and for two versions of a modified blackbody (MBB1 and MBB2, see text), as a function of the dimensionless parameter $x = h\nu/kT$. The three functions have been mutually shifted vertically by arbitrary amounts (from Van Paradijs 1985).

redshift included; see Sect. 4.3.1). Hoffman, Lewin and Doty (1977a, b) found that for distances $d \sim 10$ kpc (suggested by the concentration of the burst sources in the direction of the galactic center, Lewin *et al.* 1977b; see Fig. 2.1) the sizes of the burst emitting regions are comparable to the radius of a neutron star . (During the burst observed by Swank *et al.* photospheric radius expansion occurred, see Sect. 3.4).

In conjunction with the success of the thermonuclear-flash model in describing the global properties of X-ray bursts (Woosley and Taam 1976; Maraschi and Cavaliere 1977; Joss 1977, 1978; see Chapter 6), and the discovery that the Rapid Burster emitted two types (I and II) of very different bursts (Hoffman, Marshall and Lewin 1978a), these results provided persuasive arguments leading to the conclusion that type I burst sources are neutron stars. Furthermore, these results suggested that studies of X-ray bursts might be a useful starting point for attempts to constrain the mass-radius relation of neutron stars (Van Paradijs 1978, 1979; see Chapter 4).

Apart from the uncertainty in determinations of distances to X-ray burst sources,

a key question in such a study concerns the shape of X-ray burst spectra. Blackbody emission has the convenient property that it is completely described by just one parameter, the temperature. As a consequence blackbody spectra can be discussed in a transparent way, particularly in conjunction with an assumed spherical geometry. This is apparent in the above expression for the blackbody radius (which is a statement about the temperature dependence of the surface emissivity); it is even clearer when we consider the effect of gravitational redshift on blackbody spectra which provides a reference point for similar analyses of more realistic models of X-ray burst spectra (Goldman 1979; Van Paradijs 1979; Hoshi 1981; Marshall 1982).

There are good indications that neutron stars are not good blackbody emitters. From blackbody fits to burst spectra during the peaks of bursts temperatures have been found up to $\sim$3 keV in a number of sources (see Sect. 3.3) which is far above the value expected at the Eddington limit (< 2 keV; this includes a correction for general-relativistic effects, see Marshall 1982; see also Sect. 4.5.2). If neutron stars would radiate as blackbodies this would imply that the burst fluxes are substantially above the Eddington limit; this is difficult to reconcile with theoretical models which show that as the Eddington limit is reached, expansion of the neutron star photosphere occurs in which the luminosity remains very close to the Eddington limit (see Sect. 3.4).

In this chapter we briefly review studies which have been made to improve on the blackbody assumption by incorporating radiation transfer effects in the calculation of the energy distribution of the emission from a hot neutron star surface. Most of these studies have hitherto been confined within a framework of plane-parallel geometry (i.e. thin layers on a neutron star surface), which is a good approximation unless the luminosity is very close to the Eddington limit.

5.2. Modification of Blackbody Emission by Electron Scattering

For temperatures and densities characteristic of neutron star atmosphere ($T \sim 10^7$ K, $N_e \sim 10^{23}$ cm^{-3}) the opacity is dominated by electron scattering, with a minor contribution from free-free and bound-free absorption (cf. Rybicki and Lightman 1979). Under these circumstances the energy distribution of the emitted radiation can deviate substantially from that of a blackbody.

A simple way to estimate the expected effect of scattering is by considering a semi-infinite uniform isothermal layer in which the interaction of radiation and matter consists of coherent scattering and pure absorption. We indicate the coefficients for scattering and absorption by σ and κ, respectively, and by ε their ratio κ/σ. In the case that scattering dominates the opacity, the photon transport can be described as a random-walk process, which after a possibly large number of scatterings is terminated by photon destruction due to thermal absorption. For small values of ε, the average number, N, of scatterings is given by $N \sim (\sigma + \kappa)/\kappa \sim \varepsilon^{-1}$. The r.m.s. distance over which the photons have diffused through the medium after N scatterings is approximately $N^{1/2}$ scattering mean free paths, corresponding to

an optical-depth interval $\tau \sim N^{1/2} \sim \varepsilon^{-1/2}$. During this random walk the total length of the individual free paths the scattering photons have travelled through the medium (not always in the same direction) equals N mean free paths. Therefore, the average diffusion speed of the photons through the medium is smaller than the speed of light by a factor $N^{-1/2} \sim \varepsilon^{1/2}$. According to this picture photons which escape from the medium have (on average) been created (through thermal emission) at an optical depth $\tau \sim \varepsilon^{-1/2}$ (this is called the thermalization depth $\tau_{\rm th}$), and the rate at which they leave the medium is smaller than the thermal (Planckian) emissivity by a factor $\varepsilon^{1/2}$; in other words, the presence of scattering has led to a decrease of the surface emissivity.

These qualitative considerations are supported by more detailed calculations. From a solution of the transfer equation in the Eddington approximation, with the assumption that the electron scattering is coherent, one obtains the following well-known results (see Mihalas 1978; we have retained the dependence on frequency ν):

(i) The surface value of the source function S_ν is given by $S_\nu(\tau_\nu = 0) = [\varepsilon_\nu^{1/2}/(1 + \varepsilon_\nu^{1/2})]\ B_\nu(T)$. Here B_ν is the Planck function. The source function approaches the Planck function B_ν at optical depths $\tau_\nu \sim \varepsilon_\nu^{-1/2}$ (thermalization depth, indicated by $\tau_{\rm th}$).

(ii) At the surface the flux is given by $H_\nu(\tau_\nu = 0) = 3^{1/2}\ J_\nu\ (\tau_\nu = 0)$, which for small values of ε_ν is approximately equal to $3^{1/2}\ S_\nu\ (\tau_\nu = 0)$.

Thus, for small values of ε_ν, i.e. when electron scattering dominates the opacity, the emissivity of the medium is reduced with respect to the Planck function by a factor $\sim \varepsilon_\nu^{1/2}$. Since the contribution of free-free absorption to the opacity is approximately proportional to ν^{-3} this effect is stronger at higher frequencies. The spectrum emitted by such an isothermal medium (with only free-free and Thomson scattering opacities) is often referred to as modified blackbody emission (cf. Rybicki and Lightman 1979).

In the literature on X-ray burst spectra two versions of such a modified blackbody have been used, the one described above (indicated by MBB1), and another one (MBB2) in which the isothermal layer is not uniform, but has an exponential density distribution with a fixed scale height (Zel'dovich and Shakura 1969). In case the opacity comprises free-free absorption and Thomson scattering, the spectral distributions of these modified blackbodies can be written in terms of the dimensionless parameter $x = h\nu/kT$ as:

$$f_{\rm MBB1}(x) = x^{3/2} e^{-x/2} (e^x - 1)^{-1/2} \tag{5.2}$$

$$f_{\rm MBB2}(x) = x^2 e^{-x} (1 - e^{-x})^{-2/3} \tag{5.3}$$

For comparison, the blackbody distribution is given by

$$f_{bb}(x) = x^3 (e^x - 1)^{-1} \tag{5.4}$$

The frequency dependence of these three spectral distributions is illustrated in Fig. 5.1, which clearly shows the reduced emissivity of the modified blackbodies at high frequencies.

The transfer of a radiative flux through a medium (e.g. the outer layers of a neutron star during an X-ray burst) is connected with the existence of a temperature gradient in the medium (more precisely: a gradient of the source function). This affects the shape of the emitted spectral energy distribution, since the temperature (and thus the Planck function) at the thermalization depth becomes frequency dependent. Generalizing the above results for an isothermal medium, one can write approximately (Castor 1974; Madej 1974; Van Paradijs 1982):

$$H_\nu(\tau_\nu = 0) \sim \varepsilon_\nu^{1/2} B_\nu[T(\tau_\nu = \varepsilon_\nu^{-1/2})] \tag{5.5}$$

This expression is actually the Eddington-Barbier approximation [$H_\nu \sim S_\nu(\tau_\nu \sim 1)$] for the emergent flux (Castor 1974). As a consequence, at higher frequencies (i.e. smaller values of ε_ν) the larger depth and higher temperature at which thermalization occurs may counter-balance the surface decrease of the source function, and instead lead to a high-energy excess in the X-ray burst spectrum (Van Paradijs 1982).

A simplified analysis of this effect on the spectral energy distribution has been given by Madej (1974), who assumed a constant value for ε. His results show the expected spectral hardening for small values of ε. However, since he assumed ε to be frequency-independent the effect of the temperature gradient on the spectral shape enters only through the frequency dependence of the Planck function. An analysis of X-ray burst spectra, based on Madej's results, has been made by Czerny and Sztajno (1983).

The first detailed calculation of the spectra emitted by hot neutron stars, taking into account the temperature gradient in the atmosphere, and the strong frequency dependence of ε_ν was made by Van Paradijs (1982) who stressed that the applicability of the above-mentioned models to a detailed interpretation of X-ray burst spectra is limited by the fact that electron scattering is not a coherent process, but is accompanied by an exchange of energy between photons and electrons (Compton effect, see, e.g., Rybicki and Lightman 1979). This modifies the spectrum through a frequency redistribution of photons, and provides another coupling between matter and radiation (besides absorption processes) which affects the temperature structure of the atmosphere.

The average number of scatterings between the thermalization depth and the stellar surface is approximately $\tau_{\rm th}^2$. Since $\tau_{\rm th}$ increases with photon energy it is expected that comptonization is more important the higher the photon energy is. Furthermore, since the free-free opacity scales with temperature T approximately as $T^{-1/2}$, one expects (for a given photon energy) the thermalization depth to increase with luminosity (i.e. effective temperature), and therefore also the comptonization of the X-ray spectrum to become more important with increasing luminosity. This expectation is confirmed by detailed numerical and analytical calculations (London

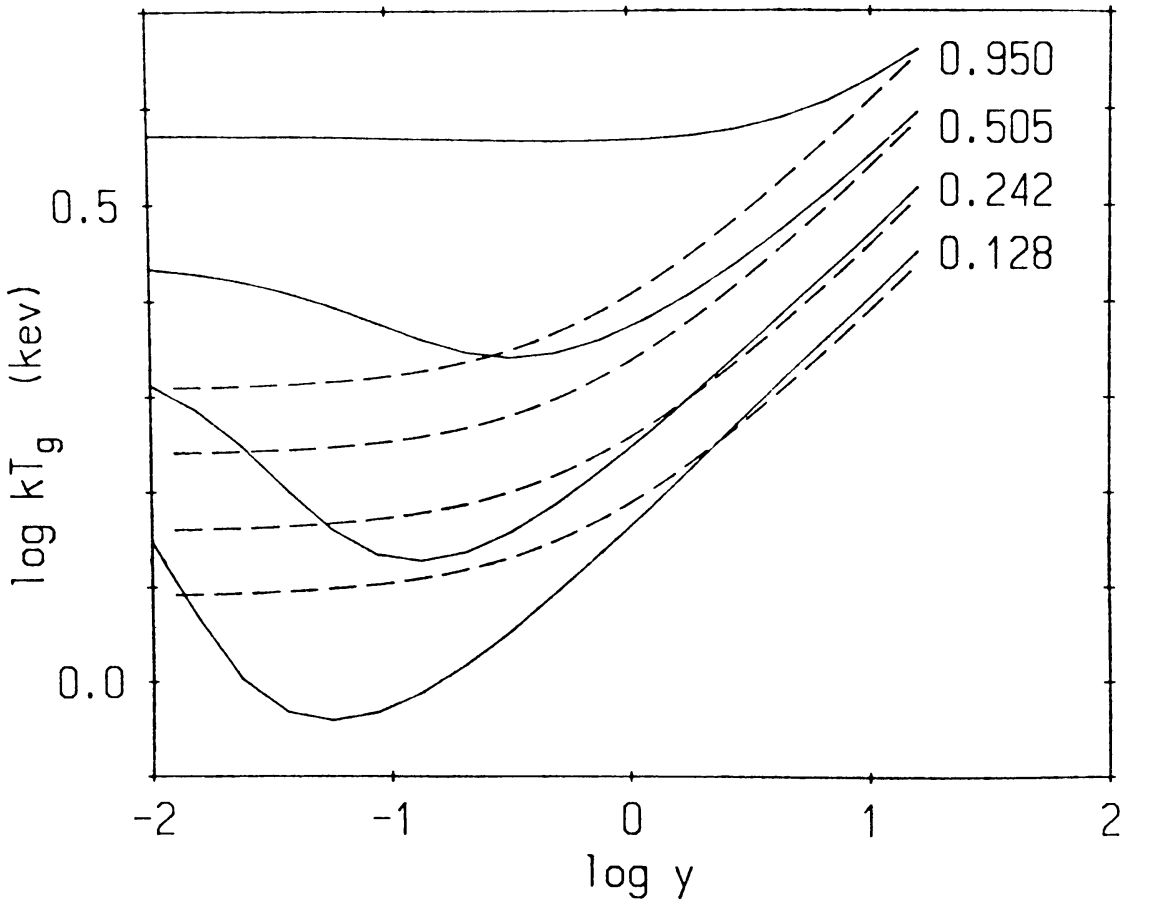

Fig. 5.2. Temperature as a function of electron-scattering optical depth for four neutron star atmospheres, each indicated by their luminosity normalized to the Eddington luminosity. The dashed lines indicate the corresponding temperature distributions for grey atmospheres in the Eddington approximation (from Ebisuzaki 1987).

et al. 1984, 1986; Ebisuzaki and Nakamura 1988; Lapidus *et al.* 1986; Sunyaev and Titarchuk 1986; Babul and Paczynski 1987; Titarchuk 1988; Madej 1989a, 1991; Pavlov *et al.* 1991), which show that the effect of comptonization depends mainly on the ratio, ℓ, of the luminosity to the Eddington limit, and much less on other parameters, such as the surface gravity and chemical composition.

There are two main effects of comptonization. In the first place photons created (mainly by free-free transitions) at the thermalization depth undergo possibly many scatterings in the overlying cooler layers. These photons transfer on average energy to the electrons through Compton recoil. This energy is stored as internal energy which cannot be radiated away efficiently because of the low value of the thermal emission coefficient. As a result the temperature of the outermost layers (above the thermalization depth) increases, and as the luminosity approaches the Eddington limit, these layers tend to an isothermal state with a temperature which is approximately equal to the radiation temperature that describes the energy distribution of the photons created at the thermalization depth (see Fig. 5.2).

In the second place, when the number of scatterings is sufficiently large, the

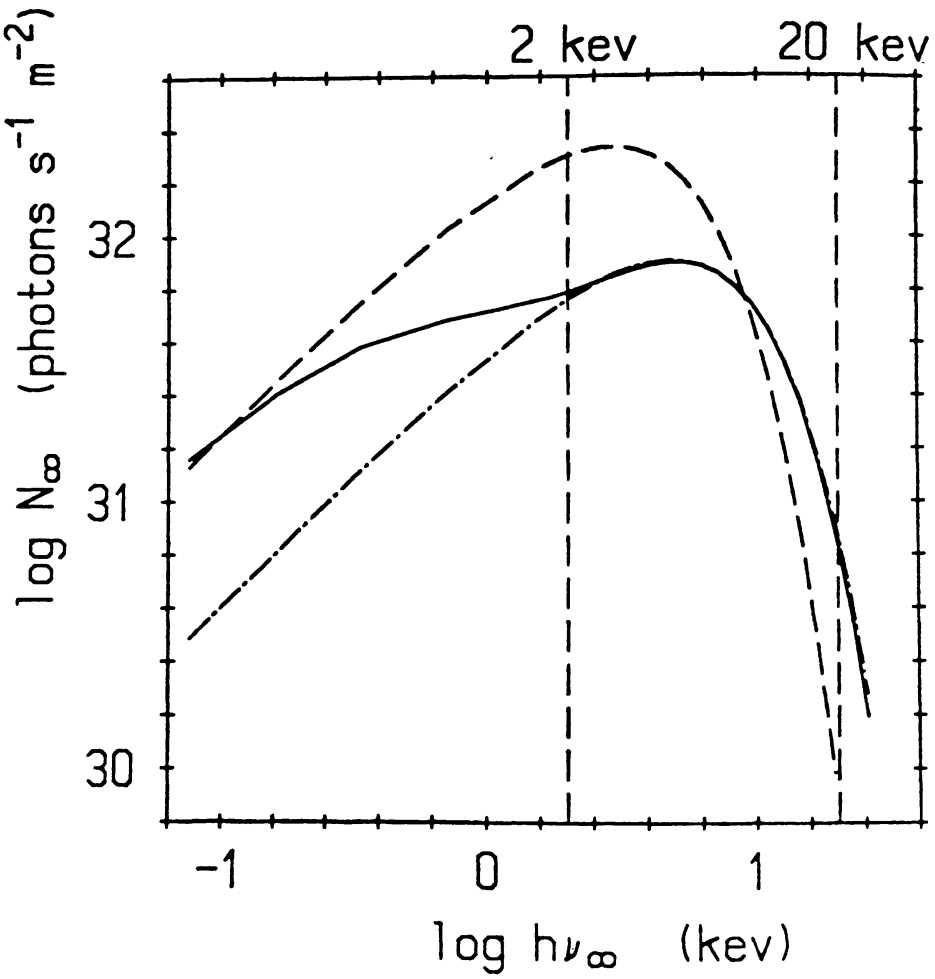

Fig. 5.3. The spectrum of a hot neutron star ($L/L_{\rm Edd} = 0.95$) as observed at large distance. The atmosphere is assumed to be composed of pure helium matter. The mass and radius of the neutron star are 1.4 $M_\odot$ and 10 km, respectively. The spectrum shows a high-energy excess compared to the Planck function at the same effective temperature (indicated by a dashed curve). This figure is from Ebisuzaki (1987).

thermalization depth is not determined any more by the free-free processes but by the exchange of energy between radiation and matter through electron scattering itself (see e.g. Ebisuzaki *et al.* 1984).

As a consequence of the energy transfer from high-energy photons (originating near the thermalization depth) to relatively low-energy electrons in the outermost layers the high-energy excess is diminished compared to the case of coherent electron scattering, although the emergent spectrum is still substantially harder than that of a Planckian spectrum at the effective temperature (see Fig. 5.3). Due to the increase of the surface temperature, an excess (relative to a Planck function fitted near the peak of the emergent spectrum) occurs at energies sufficiently low that the free-free absorption cannot be neglected relative to electron scattering.

5.3. Neutron Star Model Atmospheres

The first detailed numerical calculations of model atmospheres of (non-magnetic) neutron stars that included comptonization were made by London *et al.* (1984, 1986). Since the thermal time scale of the atmosphere is much shorter than the time scale on which the luminosity in an X-ray burst changes (of order a second) London *et al.* assumed that the atmospheres are in radiative equilibrium. This implies that they neglected energy transfer due to convection, which is reasonable, since for bursts in which the Eddington limit is not reached the convection zone that develops after a thermonuclear flash does not extend to the stellar surface. Similarly, for luminosities below the Eddington limit the hydrodynamic time scale is of the order of the free-fall time scale ($\sim 10^{-4}$ s), and the atmospheres are then in hydrostatic equilibrium. This equilibrium breaks down when the luminosity that enters the photosphere from below becomes much larger than the Eddington limit; then a stellar-wind outflow occurs, which causes an increase of the radius of the photosphere of the neutron star (see Sect. 3.4). [As shown by Paczynski (1983a, b) and Paczynski and Anderson (1986), for luminosities at the base of the photosphere only slightly above the Eddington limit extended atmospheres in hydrostatic equilibrium will be formed; this is a general-relativistic effect].

In the opacity, London *et al.* included Compton scattering and free-free and bound-free absorption. The Compton scattering was described with the Kompaneets equation (see Rybicki and Lightman 1979) which implies that the full angular and frequency dependence of the electron scattering has been replaced by a diffusion in frequency space [cf. Madej (1989a) for a discussion of the latter point]. Deviations from local thermodynamic equilibrium were taken into account in the calculation of the ionization equilibrium of Fe^{+24} and Fe^{+25}.

The calculations of London *et al.*, and of other similar calculations (Ebisuzaki *et al.* 1984; Ebisuzaki and Nomoto 1986; Foster *et al.* 1986; Ebisuzaki 1987; Babul and Paczynski 1987; Ebisuzaki and Nakamura 1988; Madej 1991; Pavlov*et al.* 1991), provide quantitative support for the qualitative discussions in Sect. 5.2. This includes the heating of the surface layers above the thermalization depth, and the hardening of the emergent spectrum with respect to a Planck function at the same effective temperature.

The spectral hardening is usually expressed by the ratio, t, of the colour temperature T_c (which describes the shape of the observed spectrum in terms of a blackbody fit) to the effective temperature, $T_{\rm eff}$. This ratio t, which does not vary with distance from the neutron star (i.e., gravitational redshift), depends mainly on the ratio, ℓ, of the luminosity to the Eddington limit (see Sect. 5.2); after this ℓ-dependence has been taken into acount there is little remaining depencence on other parameters, such as surface gravity, or chemical composition (see, e.g. Babul and Paczynski 1987; Titarchuk 1988; Pavlov *et al.* 1991).

In Fig. 5.4 we compare the luminosity dependence of t, as given by Ebisuzaki and Nakamura (1988). In their calculation of the spectral hardening factor Ebisuzaki

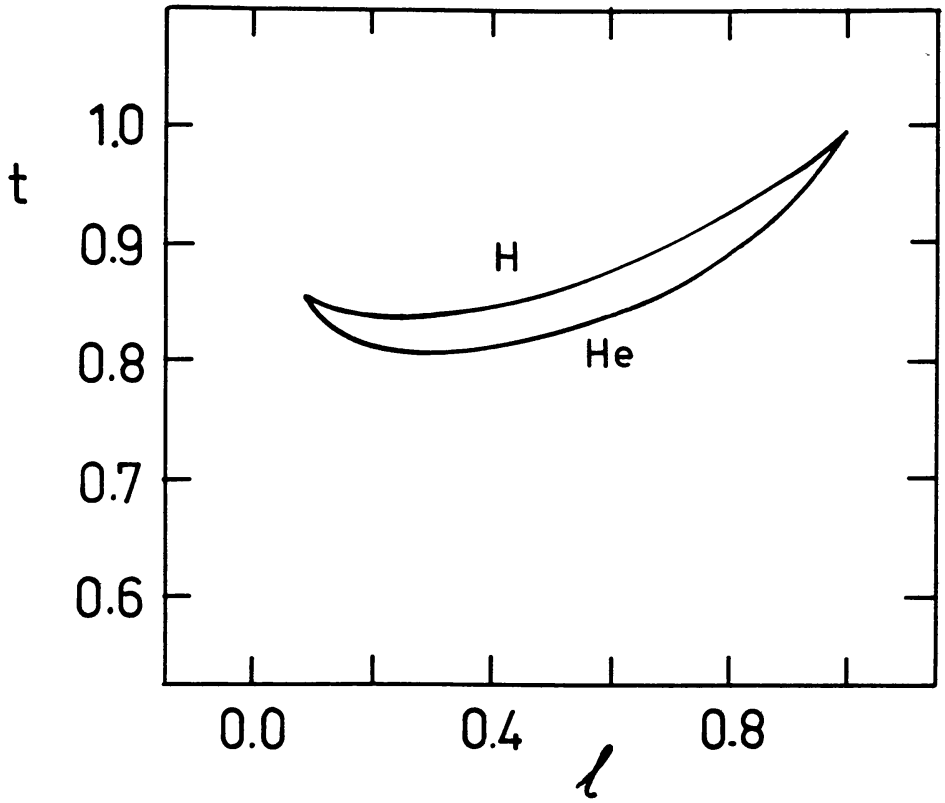

Fig. 5.4. Luminosity dependence of the hardening of spectra emitted by hot neutron stars. The theoretical value of the ratio t of colour temperature kT_c to effective temperature $kT_{\rm eff}$ is plotted as a function of the luminosity ℓ (in units of the Eddington limit); the relation follows analytical fits (Ebisuzaki and Nakamura 1988) to the numerical results of Ebisuzaki (1987). The relation has been normalized to unity at $\ell = 1$. "H" and "He" indicate the results for neutron star atmospheres with cosmic ($X = 0.73$) and hydrogen-poor ($X = 0$) compositions, respectively (from Van Paradijs *et al.* 1990a).

and Nakamura took into account that for a given X-ray burst spectrum the fitted colour temperature depends on the spectral sensitivity of the detector used. Folding the spectra of London *et al.* (1986) through the Tenma GSPC spectral response, Ebisuzaki (1987) found that this gave rise to a systematic decrease of ~8% in the fitted value of T_c, compared to the values listed by London *et al.* (1986). However, a similar analysis by Oosterbroek (1989) for the EXOSAT ME detector response showed a small difference of only ~3%. In our comparison this effect is not included.

As a luminosity parameter we have used the ratio ℓ. This ratio is related to the effective temperature at the stellar surface, $T_{\rm eff*}$ (which is a model parameter used by London *et al.* 1984, 1986) by:

$$\ell = (L_*/L_{\rm Edd*}) = (T_{\rm eff*}/T_{\rm Edd*})^4 \tag{5.6}$$

where the Eddington temperature (as measured at the stellar surface) is given by

$$T_{\rm Edd*} = (cg_*/\sigma\kappa)^{1/4} = (cGM/\sigma\kappa R_*^2)^{1/4}(1 - 2GM/R_*c^2)^{-1/8} \tag{5.7}$$

Here g_* is the gravity acceleration at the stellar surface (which is also a parameter of the models of London *et al.*), κ is the electron scattering opacity, and the other symbols have their customary meaning (see also Sect. 4.5.2).

Ebisuzaki and Nakamura (1988) gave an analytical expression, in which the ratio of the colour temperature $T_{c\infty}$ and Eddington temperature $T_{\mathrm{Edd}\infty}$, as measured by a distant observer, is related to the ratio of the luminosity and the Eddington luminosity for a hydrogen poor composition. Here

$$T_{\mathrm{Edd}\infty} = (cGM/\sigma\kappa R_*^2)^{1/4}(1 - 2GM/R_*c^2)^{3/8} \tag{5.8}$$

is to be interpreted as the colour temperature of a blackbody emitting at the Eddington limit, as observed at a large distance from the neutron star (see Sect. 4.5.1). To relate this analytic expression to a $t(\ell)$ relation we have 'corrected' the values of $T_{c\infty}$ to the values T_{c*} at the neutron star surface by applying a blueshift factor $(1 - 2GM/R_*c^2)^{-1/2}$ using $M = 1.4\ M_\odot$ and $R_* = 10$ km (then $kT_{\mathrm{Edd}\infty} = 1.87$ keV); the corresponding value of $kT_{\mathrm{Edd}*}$ $(= 2.44$ keV) is obtained from Equation (5.7). For a cosmic composition these "Eddington temperatures" are lower by a factor $\sim$0.87.

The results in Fig. 5.4 show that t generally lies between $\sim$1.4 and $\sim$1.7, for luminosities relevant to X-ray burst spectra. For very small luminosities ($\ell < 0.1$) t increases as ℓ decreases. This is a result of the 'blanketing' effect (Mihalas 1978): the strong frequency dependence of the free-free opacity (which is important at low luminosities) leads to a 'backwarming' of the deeper atmospheric layers (from which the high-energy photons can relatively easily escape) and a cooling of the surface layers. For higher luminosities ($\ell > 0.2$) t increases with ℓ because the thermalization depth increases (due to the decreasing importance of free-free opacity), and photons are created at temperatures which are increasingly higher than the effective temperature.

According to Babul and Paczynski (1987) the increase of the spectral hardening with luminosity continues up to the Eddington limit. Based on a relatively simple model, in which the atmosphere is divided into a small number of regions in the frequency versus optical-depth plane according to the relative importance of free-free and electron scattering opacities, they showed that very close to the Eddington limit the color temperature may be as high as twice the effective temperature.

5.4. Comparison with Observed X-Ray Burst Spectra

Early time-resolved spectral analyses of X-ray bursts (Swank *et al.* 1977; Hoffman, Lewin and Doty 1977a,b) indicated that the broad-band characteristics of burst spectra are well described by Planck functions, and these results have *grosso modo* been confirmed by subsequent studies. However, the fact that blackbody fits to burst spectra give good fits (in terms of χ^2) does not necessarily imply that the burst emission is Planckian. The model-atmosphere calculations discussed in Sect. 5.3 showed that, although the spectra emitted by hot neutron star atmospheres are quite

similar to Planckian curves, the colour temperatures of these theoretical spectra are generally substantially higher than the corresponding effective temperatures.

In several cases detailed analyses of observed X-ray burst spectra have provided evidence for deviations of these spectra from blackbodies which cannot be described in terms of only a spectral hardening as explained by these model atmospheres. Nakamura *et al.* (1989) found a high-energy excess (above the fitted blackbody curve) in burst spectra from 1608–522, which they interpreted as evidence for comptonization of photons in a very hot plasma surrounding the neutron star. Day and Dove (1991) have suggested that this excess may be caused by a disk-reflection component in the burst spectrum, analogous to what has been observed in the spectra of some active galactic nuclei. No such excess was found in burst spectra from 1636–536 (Damen *et al.* 1990a). Van Paradijs *et al.* (1990a) found systematic deviations in burst spectra from 2127 + 119 in the form of temperature-dependent bumps, which have not been reproduced in the model atmospheres described in Sect. 5.3. Perhaps we are encountering here the effect of a magnetic field, which may influence an emergent X-ray spectrum through its effect on the atmospheric density distribution and the opacity (see, e.g., Van Riper 1988).

A way to study the possibly non-Planckian nature of burst spectra would be to make use of the basic assumption underlying many analyses of X-ray burst spectra, *viz.* that during the cooling part of the burst the neutron star surface uniformly participates in the burst emission. Then the variation of the flux, F, is caused by a variation of the surface emissivity of the neutron star, i.e. its effective temperature, $T_{\rm eff}$. If during the cooling phase of the burst the neutron star would radiate as a blackbody the cooling track in the flux-temperature diagram would be a straight line with a slope d(log F)/d(log T) = 4. Deviations from a blackbody then show up as a different slope, or curvature, of this cooling track in the flux-temperature diagram, reflecting a variation of the ratio $t = T_c/T_{\rm eff}$. This quantity is proportional to the observed ratio, θ, of the fitted colour temperature ($kT_{c\infty}$) to the one-quarter power of the bolometric flux, $F_{\rm bol\infty}$. In Fig. 5.5 we show the variation of θ, as a function of $\ell (= F_{\rm bol\infty}/F_{\rm Edd\infty})$, for a very strong burst from 2127 + 119 in the globular cluster M15, which showed photosperic radius expansion).

It appears from Fig. 5.5 that relatively high values of θ occur near $\ell = 1$ and $\ell < 0.3$, with a broad minimum in θ near $\ell \sim 0.5$. This is in agreement with the behaviour expected from model atmosphere calculations (see Sect. 5.4), and shows that at high luminosities the dominance of electron scattering causes a major hardening of the spectrum. The increase of θ at low luminosities reflects the increasing importance of the blanketing effect.

Based on this rough similarity between the observed $\theta(\ell)$ variation and the calculated $t(\ell)$ variation it seems safe to conclude that the colour temperatures derived from spectral fits to burst spectra are larger than the effective temperatures by a factor of typically $\sim$1.5, but increasing as ℓ approaches unity; this corresponds to an underestimate of the apparent radius of the neutron star by a factor $\sim$2.

Clearly, the value of t has to be known quite accurately before meaningful

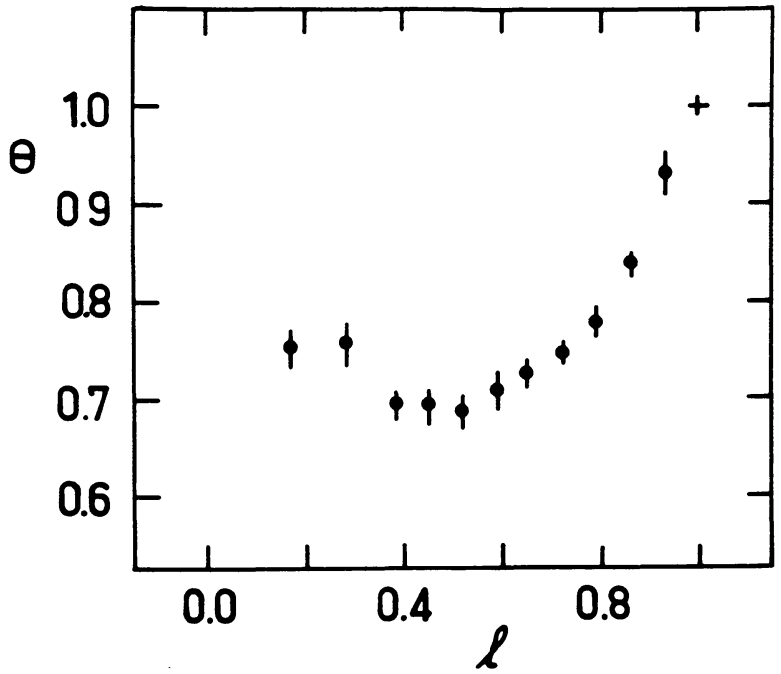

Fig. 5.5. Luminosity dependence of the hardening of spectra emitted by hot neutron stars. The quantity $\theta = kT_\infty\ (F_{\mathrm{bol}\infty})^{-1/4}$, observed during the cooling phase of a burst from 2127 + 119, is plotted as a function of the luminosity ℓ (in units of the Eddington limit). For an emitter of constant area, θ is proportional to the ratio τ of colour temperature to effective temperature. The relation has been normalized to unity at $\ell = 1$ (from Van Paradijs *et al.* 1990a).

conclusions about neutron-star properties can be drawn on the basis of X-ray burst observations. This may not be easy, since apart from the overall agreement with the theoretical $t(\ell)$ variation there are clear differences in detail. In particular, the observations indicate that the minimum in the $\theta(\ell)$ curves [normalized to $\theta(1) = 1$] is deeper than expected from available models. This suggests that close to the Eddington limit the spectral hardening may have been underestimated in the models (cf. Babul and Paczynski 1987).

In addition to differences in the details of observed $\theta(\ell)$ and theoretical $t(\ell)$ relations there are notable differences between some of the $\theta(\ell)$ relations observed for different sources. Such differences, which correspond to differences in the location of the cooling tracks of different sources in the flux-temperature (HR) diagram, were first noted by Matsuoka (1986). It is possible that at least part of these differences are caused by differences in the chemical composition. However, the model calculations (see below) indicate that the expected differences are substantially smaller than those observed between the sources, and probably fail to explain the observations.

Also, the shape and location of the cooling track in the flux-temperature diagram can vary appreciably between different bursts from a single source. In 0748–676 (Gottwald *et al.* 1986) and 1705–440 (Gottwald *et al.* 1989) this variation corresponds to differences in the apparent blackbody radius by a factor up to ~2,

and is correlated with the intensity of the persistent X-ray emission (see Sect. 3.8). Damen *et al.* (1989) found that for 1636–536 the location of the cooling track (expressed as the observed colour temperature $kT_{0.1}$ at a flux level corresponding to one tenth of the Eddington limit) is strongly correlated with the duration τ of the burst (defined as the ratio of the burst fluence to peak burst flux). In turn, both $kT_{0.1}$ and τ appear to be correlated with the "state" of the X-ray source, as indicated by the properties of the persistent X-ray spectrum and its fast variability (Van der Klis *et al.* 1990; see also Sect. 3.8 and 4.7). This suggests that both τ and $kT_{0.1}$ are determined by the accretion rate.

As discussed in Sect. 3.8, the burst duration depends on the chemical composition of the flashing layer; bursts which are due to helium flashes in a hydrogen-rich environment last longer than pure helium bursts due to the relatively long time scales involved in proton capture reactions. The relative positions of the cooling tracks for long and short bursts are in qualitative agreement with those of theoretical cooling tracks calculated for hydrogen-rich and hydrogen-poor neutron star atmospheres (Ebisuzaki and Nakamura 1988). This suggests that the underlying reason for the (τ, $kT_{0.1}$) correlation is the chemical composition. However, the shifts in the positions of the cooling tracks observed by Damen *et al.* (1989) are much larger than predicted by these models. Also, it is not obvious that the hydrogen content of the flashing layer and of the neutron star atmosphere necessarily vary in the same manner.

Summarizing the above results, we conclude that some basic properties of X-ray burst spectra have not, so far, been explained in a satisfactory way.

5.5. Discrete Components in X-Ray Burst Spectra

In Sect. 5.5 we were concerned with possibile deviations of the continuum spectra of X-ray bursts from Planckian spectra. We here turn our attention to the possibility that the spectra of neutron stars contain discrete features (lines, edges), whose presence (conditional upon our ability to identify the atomic species that produces them) would entail the interesting possibility to measure the gravitational redshift at the surface of an accreting neutron star (see Sect. 3.3, 4.6.1).

Absorption lines have been detected in the spectra of eight X-ray bursts from 1636–536, 1608–522 and 1746–217 (Waki *et al.* 1984; Nakamura*et al.* 1988; Magnier *et al.* 1989). The lines occur at energies of 5.7 keV or 4.1 keV (in one, and seven cases, respectively). Their equivalent widths are large, up to ~500 eV.

A number of studies have addressed the question whether these lines can be understood as a result of atomic transitions (Foster *et al.* 1987; Magnier*et al.* 1989; Madej 1989b). Since iron is by far the most abundant element with resonance line energies above 4 keV these studies have been focussed on this element.

Foster *et al.* (1987) and Magnier *et al.* (1989) employed a curve-of-growth analysis, with somewhat different assumptions about the line broadening mechanisms and the temperature structure of the atmosphere, to estimate the equivalent width of the resonance lines of helium-like and hydrogenic iron. For assumed solar

elemental abundances they find upper limits to the equivalent width of these lines of ~30 eV (Foster *et al.* 1987), and ~40 eV (Magnier *et al.* 1989). From a more detailed analysis, incorporating the solution of the (LTE) line transfer problem Madej (1989b) found equivalent widths for these lines up to ~100 eV.

Clearly, these theoretical values are too small to explain the observed lines by quite a margin. Moreover, according to non-LTE calculations (London *et al.* 1984, 1986; see also Foster *et al.* 1987) a larger fraction of the Fe atoms are fully stripped of electrons, compared to the LTE case. Therefore the above theoretical estimates should probably be considered as overestimates, which exacerbates the discrepancy.

Various ways have been suggested to account for the large observed equivalent widths (see Magnier *et al.* 1989; Madej 1989b). These include a large (i.e. more than a factor 10) increase of the Fe abundance, differential velocities in an outflowing atmosphere, and Zeeman splitting (or a combination of these), but it is presently unclear how viable these suggestions are; in particular, spalation of heavy elements (Bildsten *et al.* 1992) may cause a problem for the high-abundance interpretation (see also Day *et al.* 1992). Pinto *et al.* (1992) pointed out that problems with the interpretation of the 4.1 keV feature as photospheric absorption (see also Sect. 4.6.1) are avoided if the line is formed in the accretion flow.

6. Theory of Type I X-ray Bursts

6.1. Introduction

Theoretical models for X-ray bursts involve the accretion of matter onto a compact object. The mechanisms deemed responsible for the outburst are classified into two types. One mechanism derives the energy for the outburst from the nuclear energy stored in the accreted matter, and the other mechanism relies on the release of gravitational potential energy associated with the accretion process. There is now compelling evidence that neutron stars are involved in the X-ray burst phenomenon and that the type I X-ray bursts are produced by a thermonuclear shell flash instability in its surface layers. The mechanism involving an instability in the accretion flow, although not responsible for type I X-ray bursts, is very likely responsible for the type II bursts seen in the Rapid Burster (see Chapters 7 and 8). In this chapter we shall concentrate on the description of the thermonuclear flash model for type I X-ray bursts, and postpone the discussion of models involving accretion instabilities as related to theoretical models for the Rapid Burster until Chapter 8.

Historically, Van Horn and Hansen (1974) and Hansen and Van Horn (1975) were the first to point out that nuclear burning in the accreted envelope of a neutron star could be unstable. Although their specific interest centered on the nature of transient X-ray sources (with month long decay timescales), their pioneering studies laid the foundation for the future theoretical development of the thermonuclear hypothesis. In particular, after the discovery of X-ray bursts in 1975, Woosley and

Taam (1976) proposed the thermonuclear instability model involving the burning of helium fuel, and Maraschi and Cavaliere (1977) proposed a model involving hydrogen flashes. The qualitative comparisons of the observations with the expected properties of the model were considered by Joss (1977) and Lamb and Lamb (1978). Contemporaneously detailed numerical work by Joss (1978) and Taam and Picklum (1978, 1979) provided a firm basis for the viability of the model. Subsequently, a number of investigations including those by Ergma and Tutukov (1980), Fujimoto, Hanawa, and Miyaji (1981), Taam (1980, 1981a, 1981b, 1982, 1985), Ayasli and Joss (1982), Paczynski (1983a), Woosley and Weaver (1985), and Fushiki and Lamb (1987b) have significantly contributed to our fundamental understanding of the thermonuclear flash model.

The basic physical picture of the model involves the accretion of potential nuclear fuel, in the form of hydrogen and helium, from the neutron star's stellar companion. As the accreted layer is built up on the neutron star surface, the high pressures exerted by the weight of this matter lead to its fusion to iron nuclei and eventually to neutrons at densities $\gtrsim 10^{11}$ gm cm^{-3}. This transformation to iron is likely to be explosive in a wide range of circumstances because the degree of electron degeneracy in these layers is high. For temperature sensitive nuclear reaction rates these layers are susceptible to a thermal instability driven by the exothermic reactions. The nuclear energy released is eventually transported to the surface which gives rise to the emission of X-rays for a brief time ($\sim$ tens of seconds). It is this phase which we identify as the X-ray burst.

The thermonuclear model has been remarkably successful in reproducing the basic features of the X-ray burst phenomenon. Of note, are the short rise timescales ($\sim$ 1 s), the recurrence timescales ($\sim$ hrs), the energetics ($\sim$ 10^{39}–10^{40} ergs), the ratio of burst to accretion luminosities, and the spectral softening during burst decay. It is this success that provided the strongest theoretical evidence that neutron stars are involved in the phenomenon. Furthermore, the theory suggested that the magnetic fields of these neutron stars are weak ($\lesssim 10^{10}$–10^{11} G) for, otherwise, the thermonuclear instabilities would be suppressed when matter is funnelled to the magnetic poles (Joss 1978); Taam and Picklum 1978; Joss and Li 1980).

The theoretical work published since the previous reviews of this subject by Lewin and Joss (1981, 1983), Joss and Rappaport (1984), and Taam (1985) have led to new developments. Of particular interest are investigations in the area of the long term evolution of the neutron star's accreted envelope in response to repeated thermonuclear shell flashes (Fujimoto *et al.* 1985; Woosley and Weaver 1985), the new insights gleaned from studies of nuclear burning when nonthermal equilibrium effects are included (Fushiki and Lamb 1987b), the possibility that the heavy elements can be destroyed in the accreted matter via nuclear spallation reactions (Bildsten, Salpeter, and Wasserman 1992), and the potential for using X-ray bursts to probe the thermal state of the neutron star interior (Fushiki *et al.* 1992).

We review these more recent investigations and discuss their impact on the

interpretation of the detailed observational data. A number of major discrepancies between observations and theory still remain to be resolved and possible solutions to these problems are suggested.

6.2. Nuclear Processes on Accreting Neutron Stars

The detailed nuclear reactions that take place in the accreted layer of a neutron star have been discussed in detail in Taam (1985). Below we briefly outline the important reactions of interest.

6.2.1. Hydrogen Burning Reactions

Hydrogen burning by itself cannot produce an X-ray burst since the rate at which protons are burned is limited by the β decays associated with the weak interaction process of transforming a proton into a neutron (Joss 1977; Lamb and Lamb 1978). Although the fusion of protons to helium cannot provide a sufficiently rapid energy release, it can profoundly affect the nuclear burning development in the accreted layer since the energy liberated from hydrogen burning can heat the neutron star envelope to such temperatures that other nuclear fuels (not inhibited by the weak interaction process) can ignite and burn rapidly. In the following we discuss the various reactions that can take place.

At low temperatures ($T < 10^6$ K) hydrogen burning will be delayed until sufficient densities are reached ($\sim 1.4 \times 10^7$ gm cm^{-3}) that the electron capture reaction p(e$^-$, ν)n occurs. In this pycnonuclear regime, the fusion of hydrogen to helium follows via the reactions p(n, γ)^{2}H(p,γ)^{3}He(n, γ)^{4}He as outlined by Rosenbluth *et al.* (1973). Provided that the accretion rates are low ($\dot{M} \lesssim 10^{-14} M_\odot$ yr^{-1}), hydrogen burning will be stable.

If the matter is accreted faster or if the temperatures in the envelope are in the range of 10^6–10^7 K, then hydrogen will ignite at lower densities in the thermonuclear regime via the pp chain. Since the rate of the reactions is determined by the reaction p(p,e$^+\nu$)^{2}H, the temperature dependence of hydrogen burning energy generation rate is weak ($\propto T^4$) and the burning remains stable.

At higher temperatures ($T \gtrsim 10^7$ K) hydrogen burning can proceed much faster via the CNO cycle. The temperature sensitivity of the associated energy generation rate can be high ($\sim T^{16}$) and, thus, the hydrogen burning shell can become thermally unstable. However, at high temperatures ($T \sim 10^8$ K) hydrogen burning becomes insensitive to temperature and the rate is limited by the β decays in the hot CNO cycle. In this event, the maximum energy generation rate of the cycle is determined by the sum of the positron lifetimes associated with the ^{14}O(e$^+\nu$)^{14}N (mean lifetime of 102 s) and the ^{15}O(e$^+\nu$)^{15}N (mean lifetime of 176 s) decays (Hoyle and Fowler 1965). Hence, the hydrogen burning shell can be eventually stabilized.

6.2.2. Helium Burning Reactions

A helium rich layer will form beneath the stable hydrogen burning shell or will form directly by the accretion of helium from a companion star which has evolved from the main sequence to become a helium star or a degenerate dwarf. The helium will be ignited under conditions of high electron degeneracy where the density $\gtrsim 10^6$ g cm^{-3}. In contrast to hydrogen burning, helium burning does not require the operation of weak interaction processes and, as a result, the burning shell can become thermally unstable.

Helium will be ignited via the triple alpha reaction. Under the conditions in the neutron star envelope, strong electron screening is important in enhancing the nuclear reaction rate. At sufficiently high densities and low temperatures (less than the Debye temperature, $T_{\rm D}$ where $T_{\rm D} = 10^8(\rho/10^9)^{1/2}$ K) the helium nuclei are bound in a lattice and the reactions take place in the pcynonuclear regime with the rate $\propto \exp(-C\rho^{-1/6})$ (Cameron 1959). This regime is likely to be thermally stable, since the reaction rates are strongly density dependent and independent of temperature.

On the other hand, for $T > T_{\rm D}$, the burning occurs in the thermonuclear regime. Expressions for the burning rate spanning the pycnonuclear to thermonuclear regime have been derived in Fushiki and Lamb (1987a). In the thermonuclear regime the reaction rate is resonant and very temperature sensitive ($\propto T^{30}$). As a consequence, the helium burning shell in the thermonuclear regime is thermally unstable. At sufficiently high temperatures ($T \sim 10^9$ K) the triple alpha reaction rate saturates and other helium burning reactions (e.g., $^{12}{\rm C}(\alpha,\gamma)^{16}{\rm O}(\alpha,\gamma)^{20}{\rm Ne}(\alpha,\gamma)^{24}{\rm Mg}(\alpha,\gamma)^{28}{\rm Si}$ etc.) provide the primary source of nuclear energy. The build up to heavier elements, however, is limited by the helium abundance and the pressures at which the helium is ignited. The higher the pressure and/or the helium abundance, the higher the temperatures achieved before the instability is quenched by the expansion of the layer.

6.2.3. Hydrogen-Helium Burning Reactions

In contrast to nuclear burning in non compact stars helium burning can occur in the presence of hydrogen in the envelopes of neutron stars as first pointed out by Taam and Picklum (1978, 1979). In this regime, the nuclear burning development is described by nonstandard nuclear flows. The complex network of captures that can occur has been described in the works of Wallace and Woosley (1981, 1985) and Hanawa, Sugimoto, and Hashimoto (1983). The dominant nuclear flows for typical conditions in the envelope of a neutron star undergoing a thermonuclear flash is shown in Figure 6.1. The most dramatic change in the nuclear flow from that described above is the break out from the CNO cycle at temperatures exceeding $\sim 4 \times 10^8$ K. This break out is accomplished via the reactions $^{14}{\rm O}(\alpha,{\rm p})^{17}{\rm F}$ and $^{15}{\rm O}(\alpha,\gamma)^{19}{\rm Ne}$. This is especially important for it opens up new reaction channels for hydrogen and helium burning beyond those previously discussed. For example, the reaction chain to iron and neighboring nuclei can be traced to a series of (p,γ)

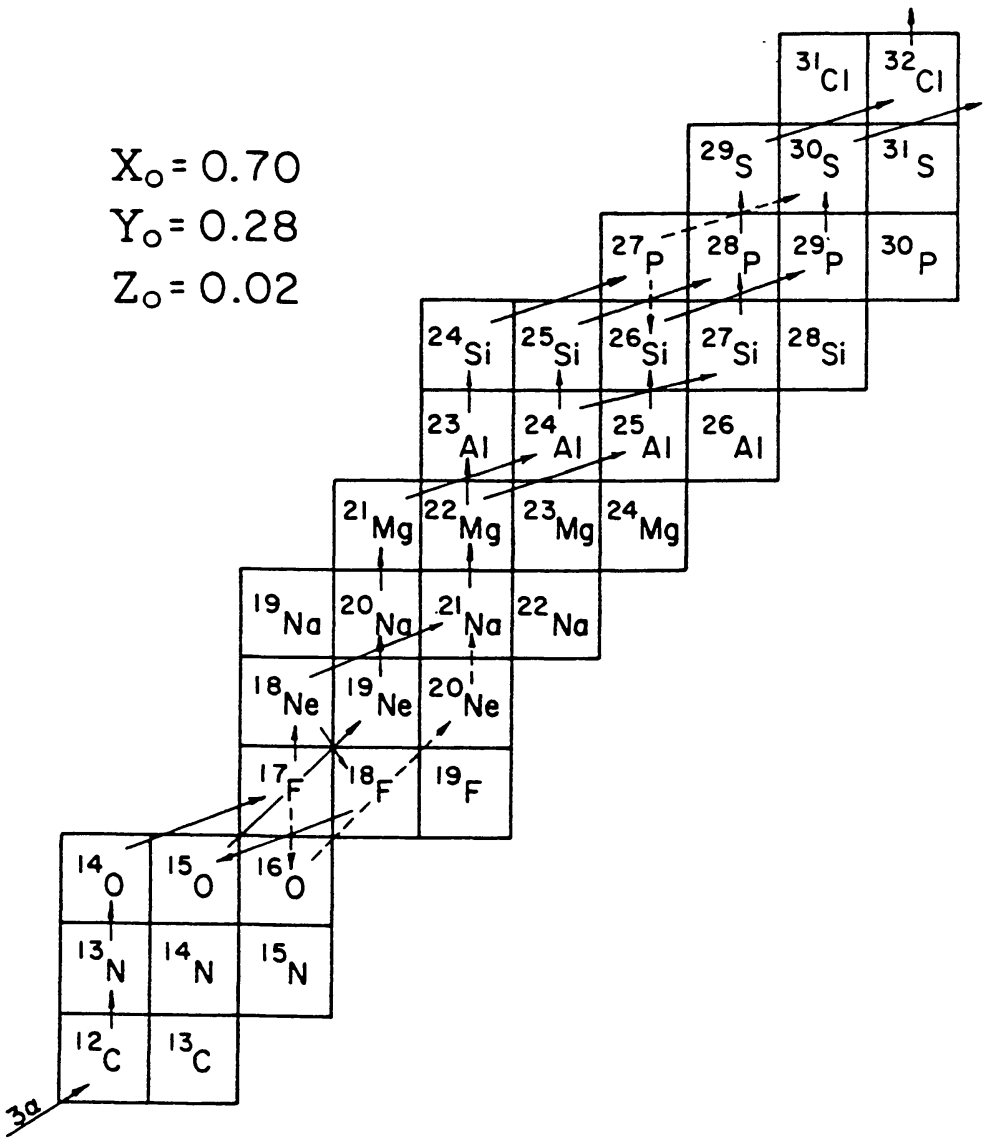

Fig. 6.1. The primary nuclear flows in an accreted layer consisting of hydrogen and helium undergoing a thermonuclear flash at $T \sim 8 \times 10^8$ K and $\rho \sim 6 \times 10^5$ g cm^{-3}. Solid arrows denote flows which are ten times faster than the dashed arrows. From Wallace and Woosley (1981).

reactions followed by positron decays to skew the nuclear flow toward the proton drip line (called the rapid proton or rp process). Modifications to this flow occur at high densities and temperatures where (α,p) reactions can compete with the positron decays. In the latter case, the evolution to iron nuclei is accomplished via a series of (α,p) and (p,γ) reactions.

The amount of iron nuclei produced depends upon the detailed thermodynamic history of the accreted layer during the outburst. For example, if the flash is quenched quickly, it is likely that the nuclear flow to heavier elements will be inhibited by their large Coulomb barriers and that some hydrogen will remain after the outburst (see Sect. 6.5).

6.3. ENVELOPE STRUCTURE

Because the envelope of the neutron star is thin, it can be approximated as plane parallel. The gravity is essentially constant in this layer and general relativity enters into the equations of structure as a numerical factor. For a given mass and radius of the neutron star the envelope structure is determined by the composition of the accreted matter and the primary energy generating processes.

Firstly, the composition of the accreted layer depends upon the evolutionary state of the neutron star's companion. For most binary X-ray sources, the companion is a main sequence-like star and the matter which is transferred will be rich in both hydrogen and helium. In others, such as 4U 1820-30, no hydrogen is expected to be present in the accreted matter. This latter circumstance can arise if the neutron star is a member of an ultra compact binary in which mass is transferred from either a degenerate dwarf or from a helium rich star. In all cases a trace of heavy elements will be transferred. For the nuclear processing discussed in the previous section, the CNO element abundance is particularly important. The mass abundance of these nuclei in the transferred matter can be expected to lie in the range from $\sim 0.0001 - 0.01$ since X-ray burst sources are located in globular clusters as well as in the field of our galaxy. Recently it has been suggested by Bildsten, Salpeter, and Wasserman (1992) that the CNO abundances in the neutron star envelope are much less than these values. They argue that the spallation of these elements in the accretion flow leads to a significant reduction in their abundances. They show that the abundance of CNO nuclei depends on the mass accretion rate and that less than 10^{-3} of these nuclei survive the accretion process. Their results depend very sensitively on the macroscopic properties of the neutron star atmosphere and hence on the treatment of the interaction between the accretion flow and the stellar surface. Much less depletion of the CNO nuclei would be expected if the accretion disk extends to the neutron star surface or if radiative deceleration of the accreting plasma is sufficient to reduce the infall velocities below free fall.

The complete description of the envelope structure is given once the thermal structure is known. In the absence of accretion the thermal structure is determined by the photon and neutrino luminosity emitted from the core region and, hence, is a direct function of the neutron star age. On the other hand, in the presence of accretion the thermal structure is influenced by compressional heating. Here, gravitational energy is released as a given mass element is compressed to higher densities as a result of the increased weight of the overlying matter. This heating is more efficient at higher accretion rates since the energy generation would be localized (i.e., energy would not diffuse out as readily). A more important factor in determining the thermal structure is the energy released by the nuclear burning reactions. This is most effective if the burning is in steady state since then the surface luminosity will be equal to the nuclear luminosity. If the burning is not steady and the energy is released rapidly as in the X-ray burst event, then only a fraction of the energy ($< 10\%$) will be conducted into the core region. In this case,

the thermal structure of the envelope will continually evolve as a consequence of successive thermonuclear flashes (Taam 1980; see also Sect. 6.4.3).

6.4. Steady vs. Non-Steady State Models

The structure and stability of nuclear burning shells in accreting neutron stars can be most simply studied within the steady state approximation where matter is assumed to burn at the same rate it is accreted. In this formulation the nuclear burning luminosity, $L_{\rm nuc}$, is constrained to equal the total luminosity of the neutron star, L. This approach has been fruitfully investigated by Fujimoto *et al.* (1981), Taam (1981b), and Hanawa and Fujimoto (1982). From these analyses an understanding of the behavior of the nuclear burning shells as a function of the column accretion rate, $\dot{\sigma}$, and ignition density, σ, were obtained. In particular stable burning of both hydrogen and helium occurs at accretion rates $\gtrsim \dot{M}_{\rm Edd}$ (where $\dot{M}_{\rm Edd}$ is the Eddington mass accretion rate) for neutron stars at high temperatures ($T \gtrsim 5 \times 10^8$ K) where the degree of electron degeneracy is low and for $\dot{M} \lesssim 10^{-6}\dot{M}_{\rm Edd}$ at low temperatures ($T \lesssim 5 \times 10^6$ K) when the nuclear burning occurs in the pycnonuclear regime. Unstable nuclear burning is classified into three categories, each delineated by a range of mass accretion rates. At high mass accretion rates ($\dot{M}_{\rm Edd} \gtrsim \dot{M} \gtrsim \dot{M}_{c1}$), a helium flash develops in the presence of a hydrogen rich environment; at intermediate accretion rates, hydrogen burning leads to the formation of an underlying unstable helium burning layer; at low accretion rates ($10^{-6}\dot{M}_{\rm Edd} \lesssim \dot{M} \lesssim \dot{M}_{c2}$), the instability in the hydrogen rich layer triggers a helium flash.

By relaxing the steady state assumption, Fushiki and Lamb (1987b) pointed out that the temperature of the envelope can also be an important independent parameter and, therefore, that the behavior of the nuclear burning shells is a function of three parameters. To elucidate the behavior, the concepts of a nuclear ignition surface and a fuel surface were introduced. The former corresponds to a surface at which the nuclear burning is unstable and the latter where the nuclear fuel is exhausted or where the luminosity due to compressional heating and nuclear burning equals that radiated from the neutron star surface. These surfaces are illustrated in Fig. 6.2a and various cuts are shown in Figs. 6.2b, 6.2c, and 6.2d corresponding to the steady state, thermal equilibrium, and the compressional heating case (see Fushiki and Lamb 1987b). It is immediately seen that the steady state approximation is overly restrictive (since the temperature at the bottom of the accreted layer is determined by the mass accretion rate) and severely limits the possible range of available parameter space and nuclear burning shell behaviors that are accessible. The steady state description, for those situations in which bursts occur, is found to be adequate only in the case in which stable hydrogen burning leads to helium shell flashes. This implies that the critical mass accretion rates ($\dot{M}_{c1}$, $\dot{M}_{c2}$) delineating the different unstable nuclear burning shell behaviors are similar in the steady state and nonsteady state models. However, the steady state prescription is inadequate in the phase space corresponding to the occurrence of a combined hydrogen-helium

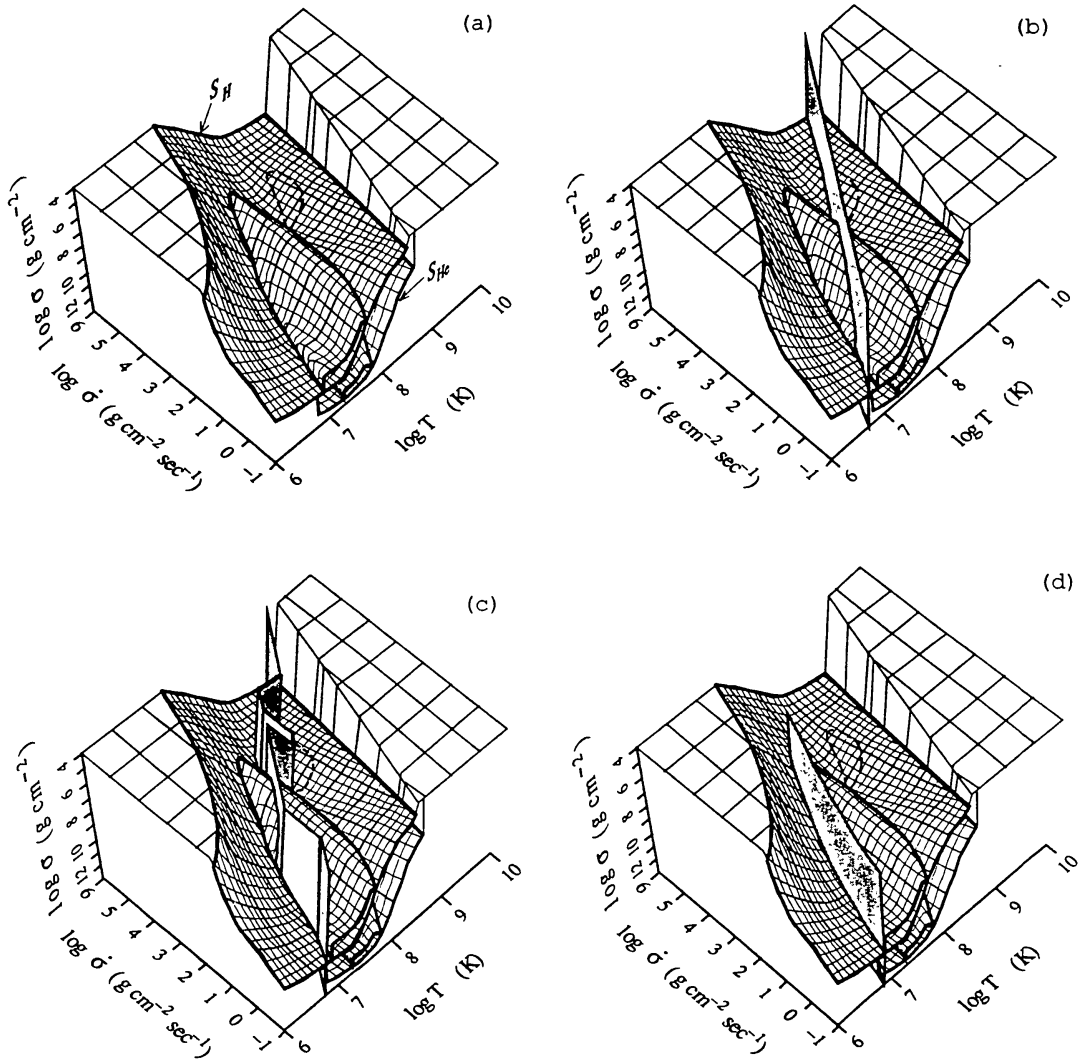

Fig. 6.2. (a) The hydrogen and helium fuel surfaces are denoted by S_H and S_{He} respectively. The ignition surfaces lie just above the fuel surfaces. The plane cutting (a) corresponds to the conditions for a steady state in (b), to the thermal equilibrium case in (c), and the compressional heating case in (d). From Fushiki and Lamb (1987b).

flash. In these cases the considerations of thermal equilibrium (where $L = L_{nuc}$ averaged over a burst cycle) versus nonthermal equilibrium in the envelope, then become important in the determination of the ignition conditions in the nonsteady state approach.

The results obtained from these analyses, for a hydrogen rich composition, are also known to depend upon the abundance of the CNO nuclei, Z_{CNO}, in the accreted matter. These nuclei are catalysts for hydrogen burning via the CNO cycle and dictate the structure of the envelope and the stability of the hydrogen burning shell. The recent work by Bildsten, Salpeter, and Wasserman (1992), which provides a description of the fate of these nuclei, complicates this issue since they show that these nuclei can be destroyed by nuclear spallation reactions prior to their

assimulation in the neutron star envelope (see Sect. 6.3). Hence, the possibility that the metal abundance in the accreted envelope of the neutron star is different than that transferred from the stellar companion makes the structure and stability of the nuclear burning shells an intrinsically four dimensional problem depending on $\dot{\sigma}$, σ, T, and $Z_{\rm CNO}$. One arrives at a similar conclusion when one takes account of the results regarding the compositional evolution of the accreted envelope in which successive thermonuclear flashes are followed numerically. Here, the ignition conditions in the burning shell depend not only on the composition of the accreted matter, but also on the composition profile (of hydrogen, helium and the heavy elements) produced from the previous outburst.

Although the utility of the steady and nonsteady state models is limited due to the large number of parameters and the uncertain relation that exists between them, these studies may still prove useful as guides to the different types of behaviors which can, in principle, be expected. As such we briefly summarize the results obtained from these studies, realizing that the detailed confrontation of theory with observations must rely on theoretical results obtained from full scale time dependent numerical calculations.

6.4.1. Helium Shell Flash

From both the steady and nonsteady state analyses, it is found that the hydrogen burning shell is stabilized at intermediate mass accretion rates. The mass accretion rate where this occurs depends on the metal abundance of the transferred matter and ranges from $10^{-12} M_\odot$ yr^{-1} to $5 \times 10^{-11} M_\odot$ yr^{-1} for $Z = 0.0004$ and $5 \times 10^{-11} M_\odot$ yr^{-1} to $5 \times 10^{-10} M_\odot$ yr^{-1} for $Z = 0.02$. This hydrogen burning development eventually leads to the formation of a helium layer devoid of hydrogen and to its ignition in a region of high electron degeneracy. We note that if the CNO elements are significantly depleted by nuclear spallation reactions as suggested by Bildsten *et al.* (1992) this pure helium flash regime is not expected.

Although the steady and nonsteady analyses are in qualitative agreement, a new behavior was uncovered in the nonsteady state approach. Because the core temperature was not constrained by the mass accretion rate Fushiki and Lamb (1987b) found that at high temperatures (corresponding to young, hot neutron stars) and low mass accretion rates a series of hydrogen flashes could occur which eventually leads to a helium flash. This regime is not accessible to steady state models since the temperatures required are greater than that obtainable in the steady state approximation.

For the mass accretion rates and temperatures which lead to stable hydrogen burning, all the helium at the base of the accreted layer is burned to heavy elements via a series of helium capture reactions. The nuclear energy released in these reactions results in the ratio of persistent emission to time averaged burst emission, α, $\gtrsim 100$ with recurrent timescales no less than 10 hrs. Shorter recurrence timescales must either involve a combined hydrogen-helium burning phase (see Sect. 6.2.3) or involve the accretion of pure helium at a high rate. In the latter case the helium

burning shell is unstable for accretion rates in the range $(10^{-14}$–$10^{-8})M_{\odot}$ yr^{-1}. Because of the rapid release of nuclear energy the rise timescales associated with these flashes can be short ($\lesssim 1$ s).

6.4.2. Combined Hydrogen-Helium Shell Flash

The burning of hydrogen and helium in the same mass layer can occur at high mass accretion rates $\dot{M}_{\rm Edd} \gtrsim \dot{M} \gtrsim \dot{M}_{c1}$ where the hydrogen burning is stabilized by the weak interactions, but the ignition temperature and density is sufficiently high to lead to unstable helium burning. In this case, compressional heating is more effective than in the helium flash case (Sect. 6.4.1) and the helium burns in regions where the hydrogen has been partially depleted. For sufficiently high mass accretion rates ($\gtrsim \dot{M}_{\rm Edd}$) helium is ignited in regions of such low electron degeneracy that the nuclear burning is thermally stable.

The coexistence of hydrogen burning with helium burning is also possible at low mass accretion rates $10^{-6}\dot{M}_{\rm Edd} \lesssim \dot{M} \lesssim \dot{M}_{c2}$ where the ignition densities are high ($\rho \gtrsim 10^6$g cm^{-3}). In this case, compressional heating is unimportant, but the heating associated with hydrogen burning leads to sufficiently high temperatures that the helium is ignited. Here, a hydrogen flash triggers a helium flash.

In these regimes the subsequent nuclear burning involves a series of complex nuclear reactions leading up to iron nuclei (see Sect. 6.2.3). Because of the weak interactions, the nuclear burning development is slower, and the rise time of the burst is correspondingly longer than for a pure helium flash. This aspect of the nuclear burning development may be responsible for the differences in bursts characterized by a fast rise time (< 2 s) and slow rise time (see Murakami *et al.* 1980a; Sect. 3.2). In addition, it is possible that not all of the accreted fuel will be consumed (see Sect. 6.5). As a result the α values are smaller than for the pure helium flash case, but can be no smaller than ~ 20.

6.4.3. Thermal State and Relation to Burst Types

From the analyses in both the steady and nonsteady state approximation the behavior of the nuclear burning shells depends critically on the thermal state of the neutron star. This state depends on the previous history of the star, which may reflect its relatively young age (for a hot neutron star), the effects of compresssional heating associated with the mass accretion process, and the history of the nuclear burning that has previously taken place (on an older neutron star).

Of particular importance is the relation between the thermal state of the envelope and the interior. This subject has been addressed in the study by Fujimoto *et al.* (1984, 1987a) in which it is found that the thermal structure of the envelope is effectively decoupled from the interior provided that the mass accretion rate and abundance of the CNO nuclei are high ($\dot{M} \gtrsim 0.01\dot{M}_{\rm Edd}$, $Z_{\rm CNO} \sim 0.01$). If these conditions are not satisfied, on the other hand, the nuclear burning takes place deep in the conductive region of the neutron star and the envelope thermal structure is significantly influenced by the interior.

The steady state models can approximately describe the thermal state of accreting neutron stars in which the nuclear burning in the envelope is stable. This description is justifiable at very high mass accretion rates where both hydrogen and helium are stable, at intermediate accretion rates where the hydrogen burning shell is stable, and at low accretion rates where both burning shells are stable in the pycnonuclear regime. Such models may apply to those neutron stars in non bursting binary X-ray sources. On the other hand, the mass accretion rate and thermal regimes characterizing the coexistence of hydrogen and helium burning in the neutron star envelope are not well described by the steady state assumption. In this case a small amount of energy is conducted into the core region amounting to $L_{\rm core} \lesssim 0.1 L_{\rm nuc}$ (Ayasli and Joss 1982; Woosley and Weaver 1985; Fujimoto *et al.* 1985) indicating that the temperatures characterizing the accreted envelopes are significantly lower (by about a factor of 2) in comparison with the temperatures obtained from the steady state assumption ($L = L_{\rm nuc}$). Although the nuclear burning behaviors are the same as for the steady state case in this regime, the ignition conditions and, therefore, the resulting burst properties differ. The soft X-ray transients which also exhibit X-ray bursts, such as Aql X-1 and 1608-522, are in such a category where it is likely that the neutron stars in these sources are cool (Fushiki *et al.* 1992).

An example, where the relaxation of the steady state approximation has led to additional insights is provided by the recognition that, whenever the helium and hydrogen ignition surfaces lie close to one another in temperature and density, irregular behavior of burst properties may be expected (Fushiki and Lamb 1987b). Specifically, in the high temperature regime a small variation in the accretion rate can produce a large variation in ignition temperature and, hence, in the properties characterizing the X-ray burst. Lack of correlation of burst behavior with the level of persistent emission is also anticipated in the low temperature regime where a significant variation in the accretion rate results in little change in the ignition temperature and therefore in the properties of the burst. Irregular behavior of the type exhibited by Ser X-1 (Li *et al.* 1977) and 1735-44 (Lewin *et al.* 1980; see also Sect. 3.5) may be a consequence of the near coincidence of these ignition surfaces.

The calculation of the specific properties of X-ray bursts requires the determination of the relationship between the mass accretion rate and thermal state of the neutron star. This aspect of the theory cannot be addressed within the steady state or nonsteady state approximation. To provide understanding of this important relationship, we now turn to the full scale time dependent numerical calculations.

6.5. Numerical Calculations

The comparison of X-ray burst observations with the early numerical calculations of an individual burst provided persuasive evidence for the viability of the thermonuclear flash model. The qualitative estimates and quantitative calculations led to the understanding for the observed α values and reproduced the energetics and properties of X-ray bursts in a natural manner. For example, the calculated bursts

were characterized by peak burst luminosities $\sim 10^{38}$ ergs s^{-1}, burst energies $\sim 10^{39}$–10^{40} ergs, durations $\sim$ 10–100 s, and a spectral softening during burst decay. In addition, two principal burst types were found which were distinguished by a slow rise timescale (> 1 s), and a fast rise timescale (< 1 s).

Although the model was successful in reproducing the gross properties of the X-ray bursts, detailed comparisons between observations and theory were lacking. Progress was made in this direction by Ayasli and Joss (1982) who incorporated the fully relativistic equations of stellar structure in their calculations. They demonstrated that these effects could significantly modify the theoretical X-ray burst properties especially for neutron star models based on soft nuclear-matter equation of state. For example, the peak luminosity and effective temperature is reduced and the burst duration and recurrence time scale are increased relative to a Newtonian calculation. Notwithstanding these effects theoretical models were still incomplete since the thermal state of the neutron star was assumed apriori and not calculated as part of the global analysis. As emphasized in Sect. 6.4.3, the burst properties are sensitive to thermal inertia effects (Taam 1980) reflecting the heating associated with the previous outbursts. Thus, long term studies of the neutron star envelope subject to a number of repeated thermonuclear flashes were required for a complete description of the model. Subsequently, a number of studies were undertaken to investigate such effects (Ayasli and Joss 1982; Woosley and Weaver 1985; Fujimoto *et al.* 1985). Of these studies, the investigations of Woosley and Weaver (1985) are especially noteworthy with respect to the total number of flashes that could be followed. An important outgrowth of this study was the recognition that the burst properties are not only influenced by thermal inertia effects, but also by the compositional profile left from the previous outburst. That is, not all of the accreted fuel is burned in the X-ray burst event (see Ayasli and Joss 1982; Hanawa and Fujimoto 1984; Woosley and Weaver 1985). This result has implications for α values, recurrence timescales, and on the observed burst characteristics. Depending upon the choice of parameters the composition of the accreted layer in the post burst phase may contain a large fraction of hydrogen-rich matter. The presence of this residual fuel significantly modifies the burst properties expected from the steady state and nonsteady state analyses described in Sect. 6.4 and may have important implications for the regularity or lack of regularity of the burst behavior (e.g., 1735-44; see Sect. 3.5). In addition, the possibility of inverted molecular weight gradients and temperature profiles in the immediate post burst state have consequences for bursts which are produced with short recurrent timescales ($\sim 5 - 10$ minutes; see Sect. 3.5).

In the following, we discuss the nuclear burning behaviors outlined in the previous section in the framework of the time dependent analysis with particular emphasis on the resulting X-ray burst properties.

6.5.1. Limit Cycle Behavior

The applicability of the steady state and nonsteady state analyses to observed burst sources relies on the assumption that the bursts display similar properties (i.e., rise time, decay time, recurrence time, and α values) from burst to burst. The first demonstration of a periodic or limit cycle behavior was presented in the paper by Woosley and Weaver (1985) in which 12 successive combined hydrogen-helium flashes were followed over a time interval of $\sim$ 30 hrs. The bursting behavior was regular and the bursts were characterized by similar light curves and recurrence timescales ($\sim$ 2.4 hrs). This behavior was found for CNO abundances, $Z_{\rm CNO}$, $\sim$ 0.02, and mass accretion rates $\sim 2 \times 10^{-9} M_\odot$ yr^{-1}. There is some indication of erratic behavior for lower metallicities or lower mass accretion rates, but this has not yet been demonstrated to the same extent as for the periodic behavior. A complicating issue is related to the fact that a significant fraction of hydrogen remains after a shell flash. In these cases, hydrogen burning via the rapid proton capture process (Wallace and Woosley 1981) is not complete during the X-ray burst event since the positron decay times ($\sim$ seconds) are long. One can anticipate that hydrogen burning will contribute to the quiescent luminosity level during the burst inactive state (Van Paradijs *et al.* 1988a; see also Sect. 3.8) and that this will influence the evolution toward either a limiting cyclic or erratic state.

Regular bursting behavior is also expected in situations where helium ignites in a region where hydrogen is absent. Although it has not been demonstrated by detailed time dependent calculations, such behavior is expected for $\dot{M}_{c1} > \dot{M} > \dot{M}_{c2}$ for the accretion of hydrogen rich matter and for $\dot{M}_{\rm Edd} > \dot{M} > 10^{-6} \dot{M}_{\rm Edd}$ for the accretion of pure helium matter. Note, however, that for helium flashes the recurrence timescales are long ($\sim$ 1 day) unless the accretion rates are high ($\gtrsim 10^{-9} M_\odot$ yr^{-1}).

For those circumstances in which helium is ignited at high densities ($> 10^6$ g cm^{-3}), the nuclear luminosity generated is sufficient to cause photospheric expansion of the neutron star. The surface luminosity reaches the Eddington limit and a wind driven from the neutron star results (Hanawa and Sugimoto 1982; Taam 1982; Wallace, Woosley, and Weaver 1982; Paczynski and Proszynski 1986; Paczynski and Anderson 1986; Joss and Melia 1987; see also Sect. 3.4). A long lasting Eddington limited phase ($\sim$ minutes) associated with a pure helium flash underlying a hydrogen rich region is likely to be responsible for the rapid transients which are accompanied by a presursor (however, it has not yet been demonstrated by detailed numerical calculation). Although the bolometric luminosity is nearly constant, the X-ray precursor can be understood to reflect variations of the neutron star photosphere. Energy is shifted out of the X-ray band to lower energies as the photosphere expands (with a concommitant decrease in color temperature) and shifts back into the X-ray band as the photosphere contracts (see Fig. 3.12; Tawara *et al.* 1984; Lewin, *et al.* 1984). A similar explanation is likely to be applicable to those bursts characterized by high peak fluxes which also exhibit double peaked profiles. The identification with a deep seated helium flash is also consistent with the short rise

time (< 1 s) seen for bursts which show evidence for radius expansion (Lewin *et al.* 1987a). Further support for this interpretation is provided by the X-ray bursts emitted by the ultra compact binary 4U 1820-30 (see Sect. 3.4). In this source all bursts show evidence for radius expansion, and it is likely that the companion to the neutron star is transferring nearly pure helium rich material (see Sect. 6.3).

An important outgrowth of the long term evolutionary studies is the demonstration that compositional inertia effects can significantly affect burst patterns. This is of equal importance to thermal inertia effects in determining the ignition conditions for the thermonuclear flash. A proper description of these effects must be developed before detailed comparisons between theory and observations are attempted. An example where compositional effects may help to improve our understanding of X-ray bursts is its possible relevance to X-ray bursts seen with recurrence timescales as short as $\sim$ 5–10 minutes.

6.5.2. Bursts with Short Time Intervals

X-ray bursts with short time intervals have been reported from a number of sources (e.g., MXB 1743-28, Lewin *et al.* 1976d; EXO 0748-676, Gottwald *et al.* 1986; XB 1745-24 Oda 1982). These bursts have similar burst properties to other type I X-ray bursts, but are of an enigmatic variety since $\alpha \lesssim 10$ (and in several cases < 2). This small value of α cannot be explained within the framework of the simple picture of the thermonuclear model outlined in the steady or nonsteady state analyses since there is insufficient time to accumulate mass to initiate another outburst if all matter accreted in a given burst is burned. As a consequence a number of mechanisms have been suggested for these bursts which rely on the storage of nuclear fuel. Among them are ideas related to the pooling of fuel over the different locations of the neutron star surface (Fujimoto, Hanawa, and Miyaji 1981; Nozakura, Ikeuchi, and Fujimoto 1984) and others wherein the second burst is attributed to the occurrence of mixing during the post burst phase (Woosley and Weaver 1985; Fujimoto *et al.* 1987b). In the former mechanism it is conjectured that the thermonuclear flash originates at a point (because of the high temperature sensitivity of the nuclear reactions) and that a front propagates around the surface of the neutron star. The rate at which energy can be generated is limited by the velocity at which the front propagates. Thus, a burst produced in one pool of fuel may be followed by another when the front reaches the second pool. In the latter mechanism, Fujimoto *et al.* (1987b) suggest that elemental mixing and dissipative heating associated with hydrodynamical instabilities caused by the redistribution of angular momentum in the accreted envelope are responsible for the "premature ignition". However, no detailed calculation exists, at present, to test the viability of this hypothesis.

The most detailed treatment of the mixing conjecture was carried out by Woosley and Weaver (1985) who make use of the fact that an inverted molecular weight gradient forms as a natural consequence of the nuclear burning development during the main outburst. This situation is Rayleigh Taylor unstable; however, during the

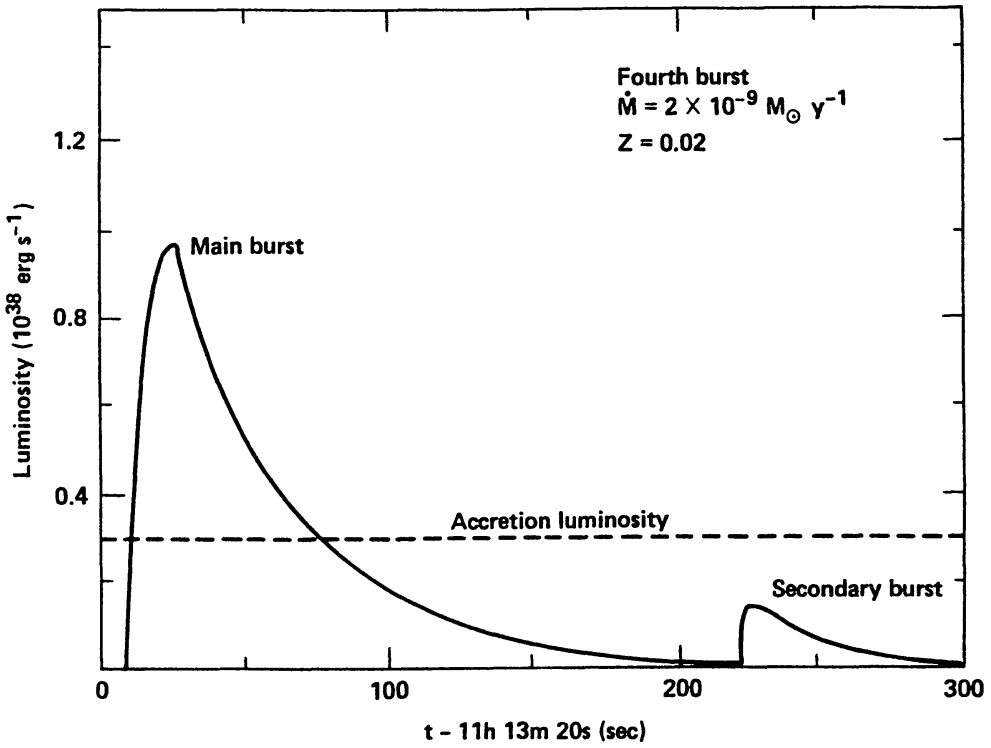

Fig. 6.3. The light curve of the main burst and a recurrent burst at short time intervals caused by convective mixing during the post burst phase. From Woosley and Weaver (1985).

post burst phase an inverted temperature gradient is present which stabilizes this layer. As the envelope cools during the post burst phase the inverted temperature gradient is relieved and the mixing of matter results. The mixing of the residual carbon from the burnt out helium burning region with the residual hydrogen from the overlying layer leads to a rekindling of the fuels with the consequence that a second burst can be produced. The time delay from the main burst to the onset of mixing is determined by the cooling timescale of the envelope and is typically a few minutes. A light curve of the main burst and of the recurrent burst is shown in Figure 6.3. A characteristic of these bursts is that they are much weaker (by a factor of 5) than the main bursts. The energetics and the recurrence time of the weaker X-ray burst are reminiscent of the bursts seen, for example, from 1743-26 (Lewin *et al.* 1976d) and EXO 0748-676 (Gottwald *et al.* 1986; see also Sect. 3.5), but inconsistent with the repetitive bursts exhibiting similar properties seen in XB 1745-24 (Oda 1982). Since the amplitude of the second burst is sensitive to the temperatures achieved in the nuclear burning regions and the extent over which an inverted molecular weight gradient exists and the delay time of the second burst depends upon the depth of the accreted layer, a larger burst might be produced to yield burst properties more in common with those seen in the main bursts if a larger fraction of the burning region or a deeper layer can be involved.

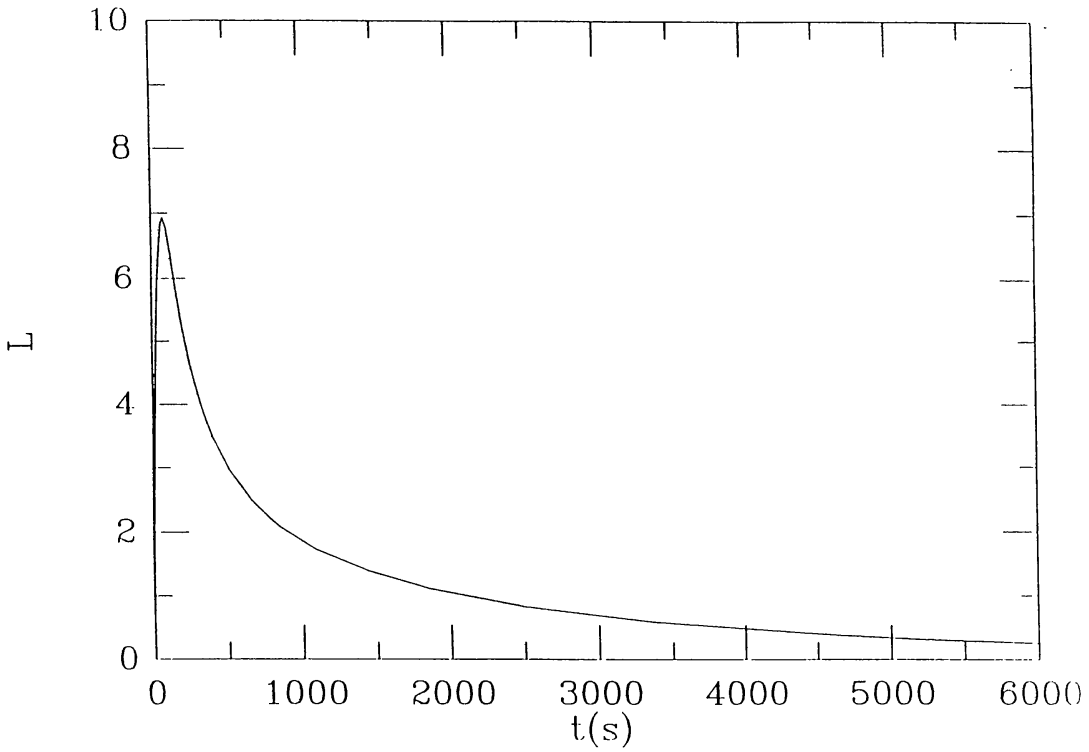

Fig. 6.4. The light curve for the first X-ray burst produced after the onset of accretion. Note the long relatively flat X-ray tail extending out to 6000 s. The luminosity, L, is in units of 10^{37} erg/sec. From Fushiki *et al.* (1992).

6.5.3. Probe of Interior Structure

The properties of the neutron star can, in principle, be constrained by using results obtained from the thermonuclear flash model. As discussed above, this possibility is complicated by effects associated with thermal and compositional inertia. However, if one can observe the first X-ray burst emitted by an object from a transient source then such complications do not play such essential roles. The observations of the unusually long X-ray burst from the recurrent soft X-ray transient Aql X-1 may provide such a testing ground.

In particular, two type I X-ray bursts were detected by Czerny, Czerny and Grindlay (1987) during the 1979 outburst of Aql X-1, the first of which was characterized by a relatively flat X-ray tail lasting for more than 2500 s and another which was observed 4 days later lasting less than $\sim$ 200 s. Based upon detailed numerical computations Fushiki *et al.* (1992) interpreted the long tail of the first burst as an extended phase of hydrogen burning accelerated by electron capture processes in regions at high densities ($\sim 10^7$ gm cm^{-3}). The light curve obtained from the numerical calculation is shown in Figure 6.4. In this interpretation, the neutron star envelope is out of thermal equilibrium. Consequently, only the first X-ray burst emitted by Aql X-1 exhibits such a prolonged X-ray phase. The subsequent bursts, on the other hand, do not exhibit long X-ray tails since the ignition densities are reduced as a result of the thermal inertia effects in the neutron star envelope. The properties of these subsequent bursts vary from burst to burst and are more

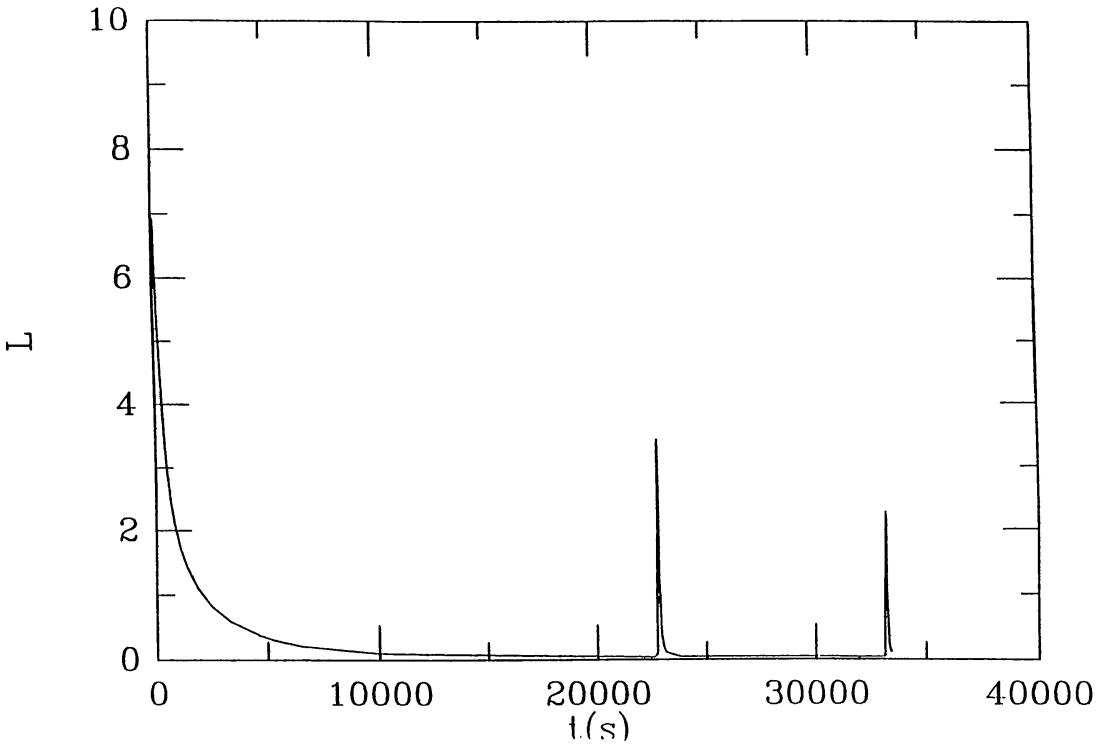

Fig. 6.5. Same as for Fig. 6.4 for the first three bursts. Time has been shifted to the occurrence of the first X-ray burst. Note the relatively short accumulation timescale required to initiate the thermal instability and the low peak luminosity level in successive bursts. From Fushiki *et al.* (1992).

similar to those of typical type I X-ray bursters. Note the appearance of a dwarf-like burst (i.e., bursts with low peak fluxes; see Figure 6.5) in the light curve.

During the X-ray inactive phase the envelope of the neutron star relaxes to its nonbursting thermal state. It is likely that for all recurrent soft X-ray transients which exhibit X-ray bursts (see Sect. 2.2.1, and 3.5) the core temperature is low and that the description of the bursts must involve models out of thermal equilibrium. As a consequence, the burst patterns of these sources are expected to exhibit very irregular behavior not correlated with the properties of the persistent emission. Fushiki *et al.* (1992) place limits on the thermal state of the neutron star and find that for a mass of $1.4 M_{\odot}$ and a radius of 9.1 km the envelope temperatures of the neutron star prior to the onset of burst activity must have been less than 1.5×10^7 K. This interpretation is consistent with the thermal relaxation of the neutron star envelope between major outbursts and with the mass accretion rates inferred for the transient outburst.

6.6. Outlook

A foundation for the interpretation of X-ray bursts has been provided by the thermonuclear flash model, which has been remarkably successful in reproducing the gross properties of the observed bursts. Yet, a number of outstanding discrepancies remain between observation and theory. Among them are the erratic correlations between persistent emission and burst behavior exhibited by such sources as 1735-

44 (Lewin *et al.* 1980; Van Paradijs *et al.* 1988b), Ser X-1 (Li *et al.* 1977; Sztajno *et al.* 1983), 1608-522 (Murakami *et al.* 1980a) and EXO 0748-67 (Gottwald *et al.* 1986), and the nearly identical bursts separated by 10 min seen in XB 1745-24 (Oda 1982).

Among the recent theoretical developments which require further study is the possibility that the CNO abundance of the accreted matter is significantly reduced. Recent work by Tillett and MacDonald (1992) in the steady state approximation reveals that the significant depletion of CNO elements by nuclear spallation as advocated by Bildsten *et al.* (1992) restricts the diversity of nuclear shell burning behavior that the observations suggest is required. For example, the explanation of the gap in the peak fluxes in MXB 1636-536 (Ohashi 1981) of a factor of ~ 1.7 would be difficult to quantify in such a model along the ideas of Sugimoto, Ebisuzaki, and Hanawa (1984) since the surface composition would not change significantly after mass loss for significant CNO depletion. Furthermore, the high α values (~ 300) inferred for EXO 0748-67 and especially 1735-44 (where α can range up to 8000 without a significant change in persistent X-ray flux) would be difficult to quantify. Such observations argue against significant CNO depletion and suggest that the amount of destruction in the accretion flow is overestimated. This would be the case if the accretion disk extends to the neutron star surface and the matter is not accreted at free fall velocities as assumed. Future investigations of spallation in different geometries would be highly desirable.

The comparison of observations with theory has now progressed beyond the general considerations of burst properties. As emphasized in this Chapter, the next step must involve the confrontation of data with detailed numerical models in which successive bursts are followed. It is only in this manner that thermal and compositional inertia effects can be fully evaluated. Although the set of calculations carried out to date are limited to spherical symmetry, they show a great variety of burst properties when such effects are included. The utility of such an approach has demonstrated the interplay between such effects and the resulting burst properties in a way not fully appreciated in the simple description of the thermonuclear model developed in the 1970's. To make comparisons to observations more meaningful, the full power of numerical calculations of series of bursts in the spherical approximation must be brought to bear on future theoretical modeling. As a glimpse of the potential relevance of such studies, the results of Taam *et al.* (1993) suggest that the Rayleigh Taylor mixing mechanism can lead to unstable nuclear burning in an irregular manner manifesting itself in terms of erratic X-ray bursting behavior.

Further theoretical efforts must also be directed toward the construction of more realistic multi-dimensional models. Such models remain largely unexplored due to the numerical complexity, but we can anticipate that with the advances in computer architecture and algorithms the detailed investigation of the ignition, propagation, and evolution of nuclear burning fronts in multi-dimensional circumstances will become realizable in the next decade.

7. The Rapid Burster

7.1. Introduction

The Rapid Burster (RB) was discovered by Lewin *et al.* (1976c). It is located in the highly reddened globular cluster Liller 1 (Liller 1977), at a distance of ~10 kpc (Kleinmann *et al.* 1976). Its behavior is unlike any other source. When the RB is active (see Fig. 7.1), it can produce X-ray bursts in quick succession with intervals as short as ~10 s (see Fig. 7.2). Hoffman, Marshall and Lewin (1978a) discovered that the RB produces two very different types of bursts which led to the classification of type I and type II bursts (Fig. 7.3); this was a turning point in our understanding of bursts (see Sect. 1.3). Hoffman, Marshall and Lewin (1978a) noticed that the ratio of the time-averaged luminosity in the very frequent type II bursts was $\sim 10^2$ times that in the relatively infrequent type I bursts; this led them to conclude that type I bursts are due to thermonuclear flashes in the surface layers of a neutron star (an idea first suggested by Laura Maraschi in early February 1976 in relation to bursts observed from other sources), and that the type II bursts are due to accretion instabilities (gravitational potential energy) as suggested by Lewin *et al.* (1976c). These ideas are now universally accepted.

None of the unusual behavior of the RB, as described in the following sections, is understood. It is very fortunate that the RB emits type I bursts. At least we know that the accreting compact object is a neutron star. In the absence of the type I bursts, the many peculiarities of the RB would undoubtedly have been ascribed by some people to a black hole (an ideal object to bury our ignorance).

We would like to remind the reader who feels encouraged to unravel the mysteries of the RB that in August 1983 this binary system behaved like other "normal" LMXB (Sect. 7.3); instead of type II bursts, a persistent flux of X rays was observed (Kunieda *et al.* 1984b; Barr *et al.* 1987). Thus, the RB with all its idiosyncrasies is almost a "normal" LMXB.

Hereafter, whenever we quote luminosities or burst energies, we have always assumed a source distance to the RB of 10 kpc (Kleinmann *et al.* 1976) and isotropic emission.

7.2. Type I and Type II Bursts

The distinct spectral softening during burst decay is very characteristic for a type I burst (thermonuclear flashes); it is the signature of the cooling of the neutron star surface (Sect. 3.3 and Chap. 4). The type II bursts as observed from the RB lack this signature; they are due to a yet unknown accretion instability (Chap. 8).

Type I bursts from the RB have been detected at intervals of ~1.5–4 h (Hoffman, Marshall and Lewin 1978a; Marshall *et al.* 1979; Kunieda *et al.* 1984b; Kawai 1985; Barr *et al.* 1987; Kaminker *et al.* 1990); type I burst intervals from other sources are typically in the same range (Sect. 3.5). Type II bursts from the RB can have intervals of order ~10 sec (this is quite common; see e.g., Lewin *et al.* 1976c; Mason *et al.* 1976b; White *et al.* 1978a; Marshall *et al.* 1979; Kunieda *et al.* 1984b;

TABLE 7.1

A Summary of Rapid Burster Observations 1981 - Present

Start Date	End Date	Primary Target	Spacecraft	On / Off	Reference
1981 Apr 09	1981 Apr 10	RB	Hakucho	OFF	1
1981 Apr 13	1981 Apr 15	RB	Hakucho	OFF	1
1981 Apr 17	1981 Apr 21	RB	Hakucho	OFF	1
1981 Apr 21	1981 May 12	1702-363	Hakucho	OFF	1
1981 May 12	1981 May 15	1715-321	Hakucho	OFF	1
1981 May 15	1981 May 17	NGC 6441	Hakucho	OFF	1
1981 Aug 02	1981 Aug 02	RB	Hakucho	OFF	1
1981 Aug 03	1981 Aug 04	RB	Hakucho	OFF	1
1982 Apr 24	1982 Apr 27	RB	Hakucho	OFF	1
1983 Jul 31	1983 Aug 05	RB	Tenma	OFF	2
1983 Aug 02	1983 Aug 03	1728-34	EXOSAT	OFF	3
1983 Aug 05	1983 Aug 07	RB	Tenma	ON	2
1983 Aug 07	1983 Aug 07	RB	EXOSAT	ON	3
1983 Aug 10	1983 Aug 22	RB	Hakucho	ON	2
1983 Aug 10	1983 Aug 22	RB	Tenma	ON	2
1983 Aug 13	1983 Aug 13	RB	EXOSAT	ON	3
1983 Aug 15	1983 Aug 15	RB	EXOSAT	ON	3
1983 Aug 22	1983 Aug 31	RB	Hakucho	ON	2
1983 Aug 26	1983 Aug 26	RB	EXOSAT	ON	3
1983 Sep 01	1983 Sep 05	RB	Hakucho	OFF	2
1984 Jul 02	1984 Jul 10	RB	Tenma	ON	4
1984 Jul 17	1984 Jul 17	RB	EXOSAT	ON	3
1984 Sep 13	1984 Sep 13	1728-34	EXOSAT	OFF	3
1985 Apr 20	1985 Apr 21	1728-34	EXOSAT	OFF	3
1985 Aug 27	1985 Aug 28	RB	EXOSAT	ON	3
1985 Aug 28	1985 Aug 28	1728-34	EXOSAT	OFF	3
1985 Aug 30	1985 Aug 31	RB	EXOSAT	ON	3
1985 Sep 10	1985 Sep 10	RB	EXOSAT	ON	3
1985 Sep 13	1985 Sep 13	RB	EXOSAT	ON	3
1987 Mar 28	1987 Mar 28	SLEW	Ginga LAC	OFF	5
1987 Mar 28	1987 Mar 28	SLEW	Ginga LAC	OFF	5
1987 Apr 04	1987 Apr 04	SLEW	Ginga LAC	OFF	5
1987 Apr 06	1987 Apr 06	SLEW	Ginga LAC	OFF	5
1987 Aug 09	1987 Aug 10	RB	Ginga ASM	OFF	9
1987 Aug 26	1987 Aug 26	SLEW	Ginga LAC	OFF	5
1987 Sep 01	1987 Sep 01	SLEW	Ginga LAC	OFF	5
1987 Oct 21	1987 Oct 23	RB	Ginga ASM	OFF	9
1987 Oct 12	1987 Oct 14	1728-34	Ginga LAC	OFF	5
1988 Mar 17	1988 Mar 17	SLEW	Ginga ASM	OFF	7
1988 Mar 27	1988 Mar 27	SLEW	Ginga LAC	OFF	5
1988 Aug 10	1988 Aug 14	RB	Ginga LAC	ON	5
1988 Aug 24	1988 Aug 24	RB	Ginga LAC	OFF	5
1989 Jan 15	1989 Jan 16	RB	Ginga ASM	ON	6
1989 Jan 16	1989 Jan 18	RB	Ginga ASM	OFF	6
1989 Feb 15	1989 Feb 15	RB	Ginga ASM	OFF	6
1989 Mar 02	1989 Mar 02	SLEW	Ginga LAC	OFF	5
1989 Apr 01	1989 Apr 02	SLEW	Ginga ASM	OFF	7
1989 Aug 24	1989 Aug 24	SLEW	Ginga LAC	OFF	5
1989 Aug 26	1989 Aug 26	SLEW	Ginga LAC	OFF	5
1990 Apr 17	1990 Apr 18	SLEW	Ginga ASM	OFF	8
1990 Oct 07	1990 Oct 08	SLEW	Ginga ASM	OFF	8
1991 Feb 27	1990 Feb 28	SLEW	Ginga ASM	OFF	8
1991 Apr 01	1990 Apr 01	SLEW	Ginga ASM	OFF	8

1 = Private Communications, N. Kawai, Nov 18, 1992.
2 = Kunieda *et. al.* PASJ 36, 807.
3 = The EXOSAT Observation Log Book.
4 = Kawai *et. al.* PASJ 42, 115.
5 = Private Communication, T. Dotani, Jun 04, 1990.
6 = Private Communication, H. Tsunemi, Jun 04 1990.
7 = Private Communication, K. Koyama & S. Yamauichi, Jun 06, 1990.
8 = Private Communication, H. Tsunemi, Oct 30 1992.
9 = Private Communication, H. Tsunemi, Dec 02 1992.

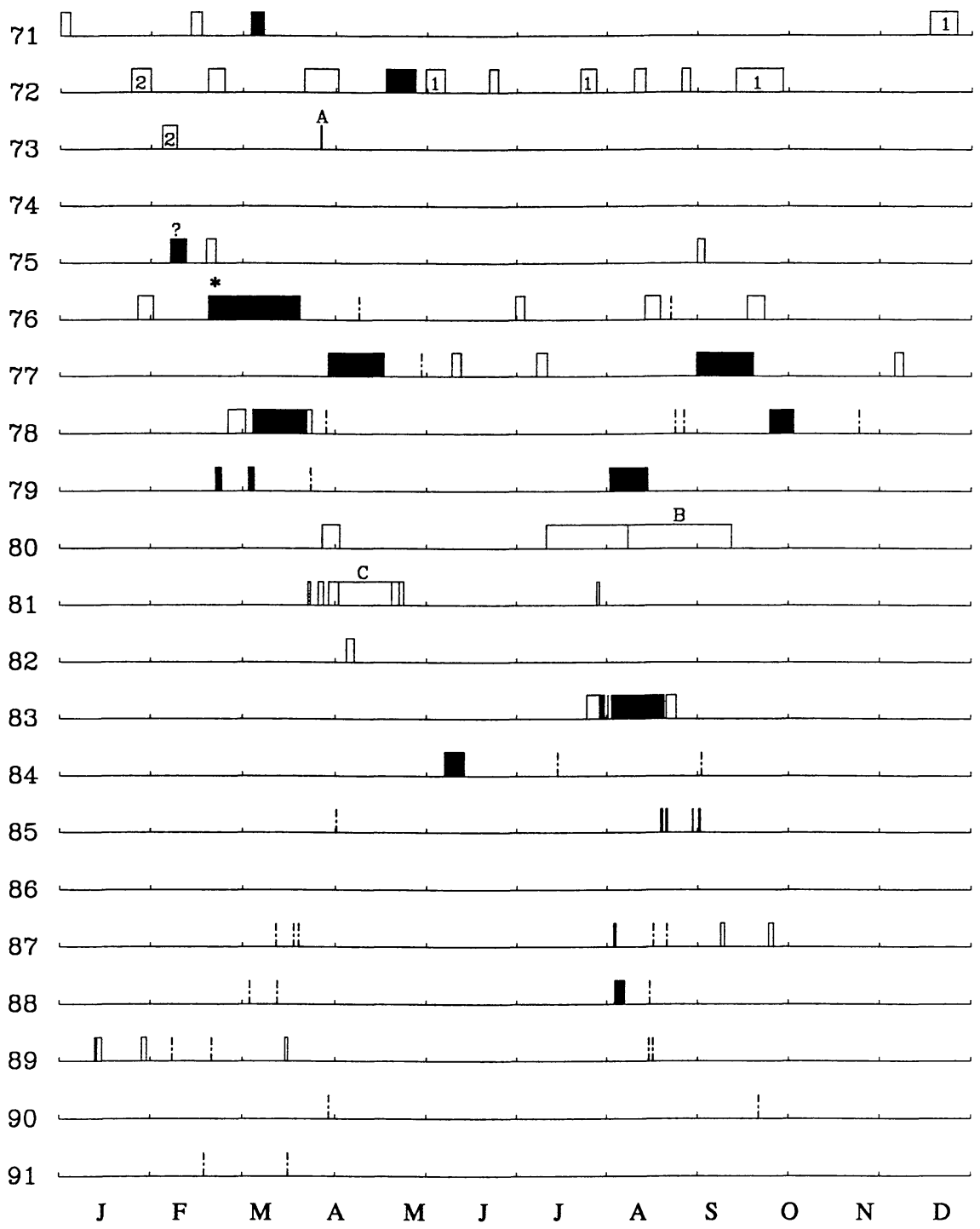

Fig. 7.1. Record of observations of the Rapid Burster. The horizontal scale is one year; the months are indicated. Active periods are indicated by shaded squares; no activity was observed during the open squares. A "1" or "2" in an open square indicate that 1 or 2 type I bursts were observed which were probably from 1728–34. The vertical dashed lines indicate observing periods of less than one day during which no bursts were detected. The periods marked "A" and "?" represent times during which the Rapid Burster may have been active. During the time marked "B" intermittent observations were made with ~3-d intervals. The * indicates the time of discovery of the Rapid Burster. For more details see Fig. 2.18 in Lewin and Joss 1983. This figure was prepared by Eugene Magnier. Some of the information in this figure is from private communications from Drs. H. Tsunemi, N. Kawai, H. Kunieda, and T. Dotani.

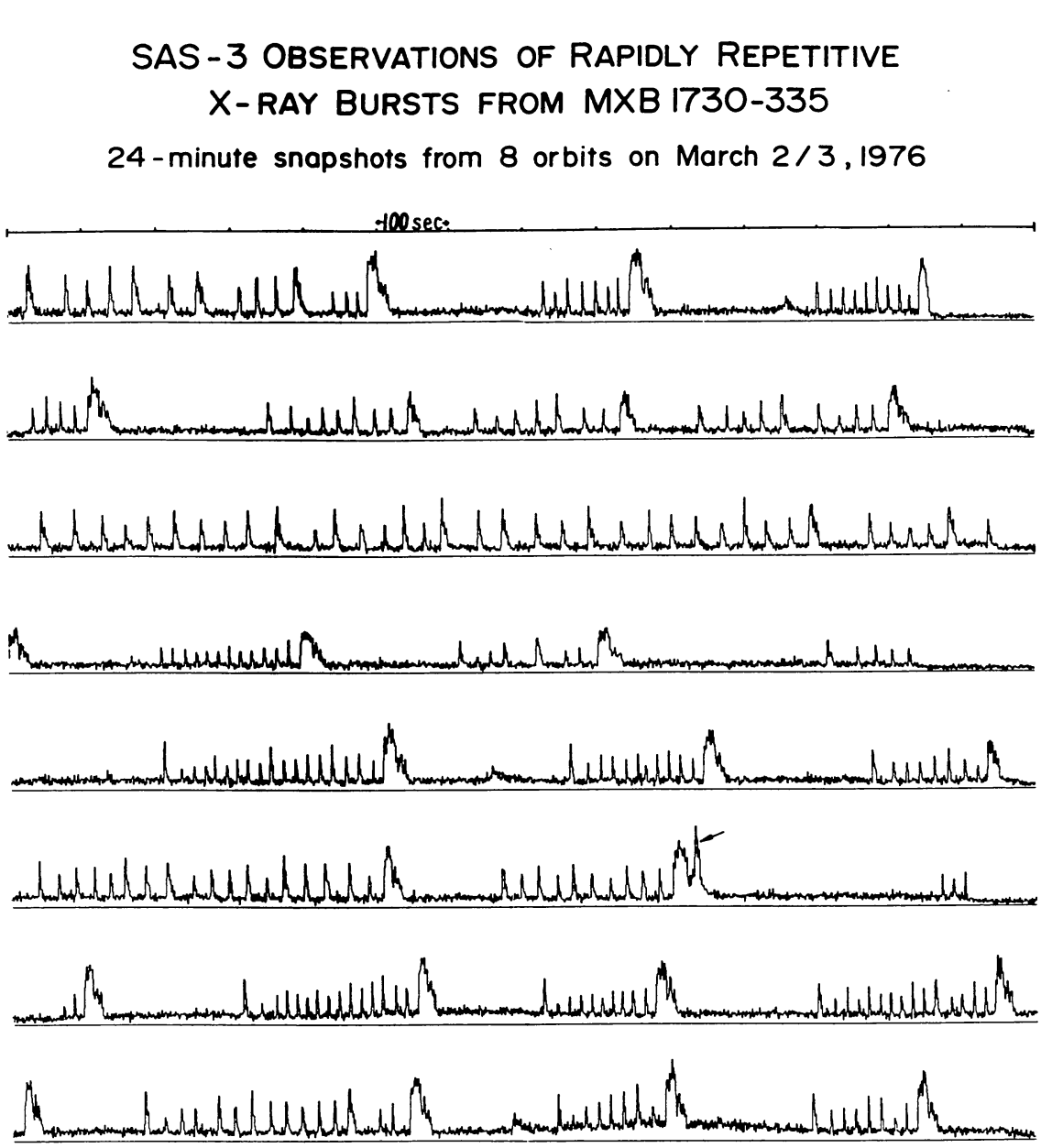

Fig. 7.2. Discovery with SAS–3. Type II bursts from the Rapid Burster in mode I (third curve from above is in mode II). Notice the flat tops in the large bursts; the "ringing" during burst decay of the large bursts is clearly visible. The burst indicated with an arrow is a type I burst from 1728–34. "Anomalous" bursts are visible in the upper curve, the 5th, and the bottom curve. It is possible that these are type I bursts from the Rapid Burster (see text). This figure is from Lewin (1977).

Tawara *et al.* 1985; Barr *et al.* 1987; Dotani 1990; Lubin *et al.* 1991b, 1992a; Tan *et al.* 1991a) and as long as ~1 h (these intervals are rarer; Inoue *et al.* 1980; Kunieda *et al.* 1984a; Stella *et al.* 1988a; Tan *et al.* 1991a).

At the time that the type I/type II classification was introduced, the very short burst intervals (seconds to minutes) were a characteristic of the type II bursts, and the long intervals (hours to days) were a characteristic of the type I bursts, but this is no longer the case. Therefore, of the original two phenomenological differences

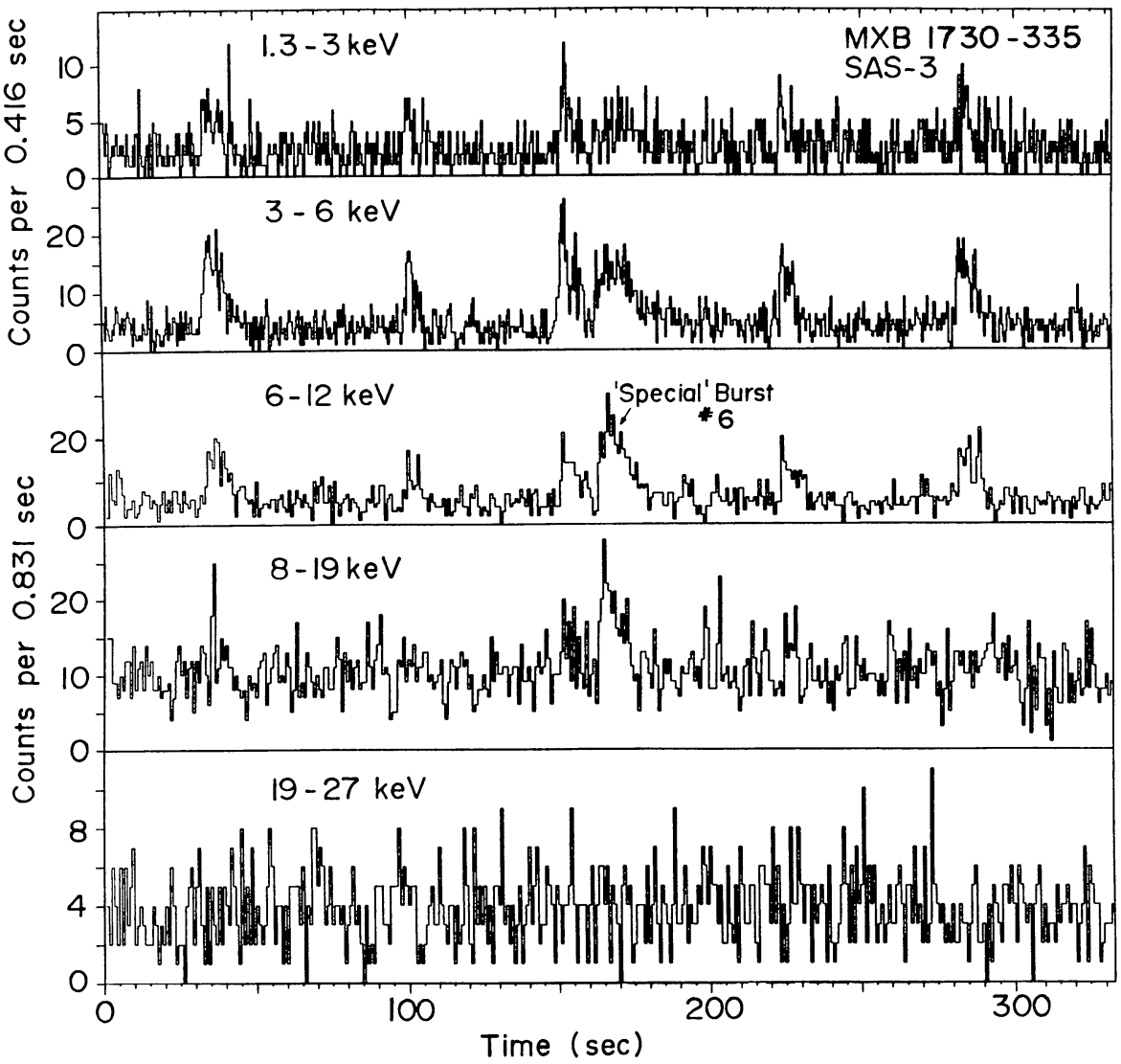

Fig. 7.3. Discovery with SAS–3 of type I X-ray bursts (marked "Special") from the Rapid Burster. They occur independently of the rapidly repetitive type II bursts (numbered separately). This figure is from Hoffman, Marshall and Lewin 1978b). This discovery was a turning point in our understanding of the burst mechanisms (Sect. 1.3).

(Hoffman, Marshall and Lewin 1978a), only the significant difference in spectral softening during burst decay remains; the type II bursts exhibit very little spectral evolution compared to the type I bursts which show a distinct cooling during their decay.

The type II burst mechanism behaves like a relaxation oscillator (Lewin *et al.* 1976c); the fluence in a type II burst is approximately linearly proportional to the interval to the *next* type II burst (Fig. 7.4). This is very characteristic for the type II bursts from the RB.

Whether or not type II bursts have been observed from sources other than the RB depends on taste. There are sources that have shown burst-like events in quick succession whereby the spectrum during the bursts showed little (if any) evolution

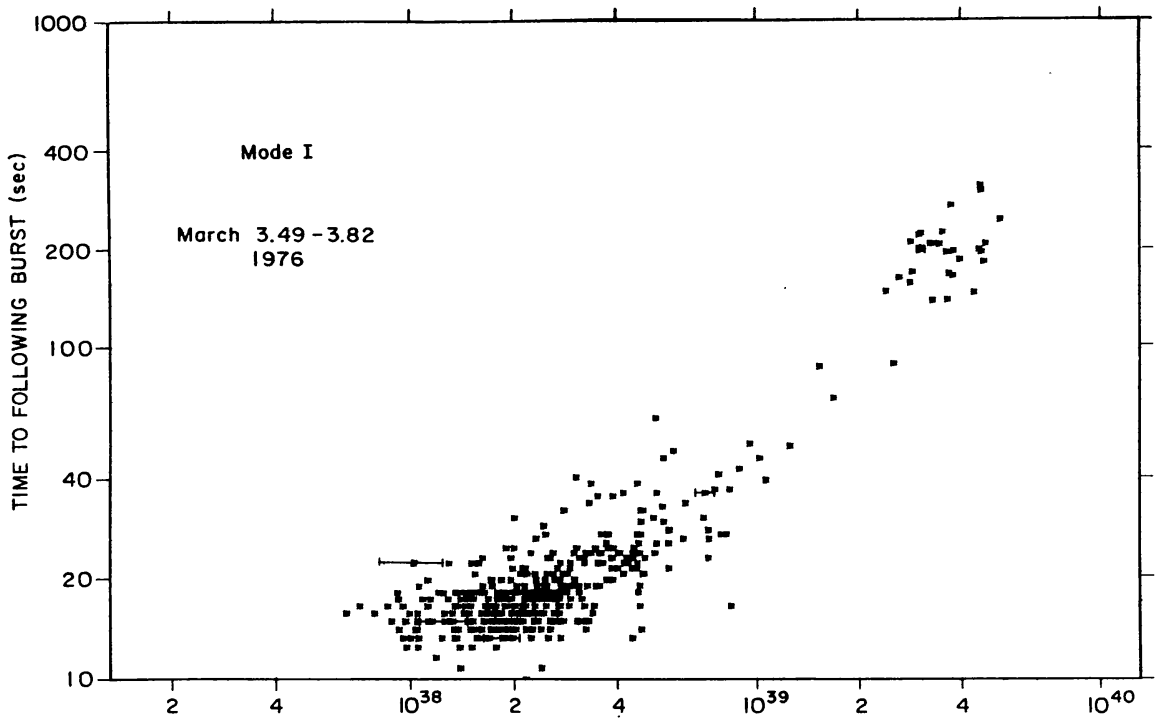

Fig. 7.4. Log-log plot of the type II burst fluence, E, versus the waiting time, Δt, to the next burst for some of the March 3, 1976 data obtained with SAS–3. The data points would lie on a straight line at an angle of 45° if the relation between E and Δt were strictly linear. The bursts were in mode I (see text). This figure is from Marshall *et al.* (1979).

(see, e.g., Lewin and Joss 1983). These events are likely due to sudden changes in the accretion rates (gravitational potential energy), and as such one may want to call them type II bursts. Yet, the very characteristic relaxation-oscillator behavior, as observed from the RB, has not been seen in any other source. It seems possible that the accretion instability that leads to these bursts is only operative in the RB. The question: "yes or no" type II bursts from sources other than the RB is not so interesting. It is our understanding of the physics of the various accretion instabilities that counts; unfortunately, we have made little progress in this respect (Chap. 8).

7.3. Normal and Abnormal Accretion

The most common mode of activity of the RB is type II bursts in combination with type I bursts (for references, see above). No type I bursts were originally reported from the March-April 1976 active period; however, there is now little doubt that the "anomalous" bursts detected during this period (Ulmer *et al.* 1977) are type I bursts (see the discussion in Lubin *et al.* 1991b). The only type II burst active period during which no type I bursts were observed is August-September 1985 (Stella *et al.* 1988a, b; Tan *et al.* 1991a; Lubin *et al.* 1991a).

On one occasion, near August 5, 1983, when the source became active, at first no type II bursts were detected. Instead a strong persistent X-ray flux and type I bursts

(with intervals of $\sim$ 1.5 h) were observed for at least several days but probably for $\sim$ 10 days (Kunieda *et al.* 1984b; Kawai 1985; Barr *et al.* 1987; Kaminker *et al.* 1990).

The behavior in August, 1983 showed that the RB does not always behave abnormally (spasmodic accretion; Chap. 3). The average luminosity of the persistent emission was $\sim 1.3 \times 10^{37}$ erg s^{-1} ($\sim$ 1–9 keV) which is comparable to the time-averaged type II burst luminosities in the early phase of type II burst activity (see below). Near August 19, 1983 type II bursts were observed (Kunieda *et al.* 1984b; Kawai 1985) [possibly already on August 16 (Kaminker *et al.* 1990)], and they continued till the burst activity ceased on August 31, 1983.

7.4. Type-II Burst Patterns – Evolution – Persistent Emission – Average Luminosities

Type II burst intervals vary from $\sim$7 s (Lewin 1977; Marshall *et al.* 1979) to $\sim$1 hour (Stella *et al.* 1988a; Tan *et al.* 1991a). The type II burst patterns vary a great deal. Most striking is the fact that the fluence in a type II burst is approximately proportional to the interval to the *next* type II burst (Lewin *et al.* 1976c; Lewin 1977; White *et al.* 1978a; Marshall *et al.* 1979; Inoue *et al.* 1980; Kunieda *et al.* 1984a,b); this is often referred to as the $E - \Delta t$ relation (see Fig. 7.4).

The *time-averaged* type II burst luminosity ($\sim$2–15 keV) decreases (though not monotonically; Marshall *et al.* 1979) during the active periods which last typically several weeks (see e.g., Marshall *et al.* 1979; Inoue *et al.* 1980; Kunieda *et al.* 1984a, b; Barr *et al.* 1987; Tan *et al.* 1991a). The time-averaged type II burst luminosity was $\sim 1.5 \times 10^{37}$ erg s^{-1} near March 2, 1976, and it had decreased to $\sim 5 \times 10^{36}$ erg s^{-1} by April 3–4. In August, 1979 Kunieda *et al.* (1984a) observed a turn-on in activity; the time-averaged type II burst luminosity increased during the first $\sim$3 days (from $\sim 7 \times 10^{36}$ erg s^{-1} to $\sim 4 \times 10^{37}$ erg s^{-1}) and then decreased by about a factor of 2 during the following week. The time-averaged type II burst luminosity was $\sim 3 \times 10^{37}$ erg s^{-1} on August 28–31, 1985; on September 13, 1985 it had decreased to $\sim 4 \times 10^{36}$ erg s^{-1} (Stella *et al.* 1988a; Tan *et al.* 1991a).

There is a burst pattern (called mode I by Marshall *et al.* 1979) in which a dozen relatively short (lasting several seconds) type II bursts are produced followed by a relatively long burst ($\sim$30–60 seconds long); this pattern repeats (Lewin *et al.* 1976c; Dotani *et al.* 1990a; Lubin *et al.* 1992a; see Fig. 7.2). In this mode the energy distribution of the type II bursts is *distinctly* double-peaked (the ratio of the mean burst fluences in the two peaks is $\sim$20; see Fig. 2 of Marshall *et al.* 1979). [Celnikier (1977) has made an attempt to explain this pattern in terms of deterministic chaos.] There are burst patterns (called mode II by Marshall *et al.* 1979) in which the energy distribution of the type II bursts is not so distinctly double-peaked (Inoue *et al.* 1980; Basinska *et al.* 1980; Stella *et al.* 1988a; Tan *et al.* 1991a; Lubin *et al.* 1992a) [it remains to be seen whether a clear distinction between mode I and II is always possible]. There are even times (in mode II) when the type II bursts intervals are almost regular. Type II burst trains (these trains can

last for tens of minutes with only a few seconds jitter in individual bursts) with quasi-periods between 15 s and 30 s have been observed (Mason *et al.* 1976b; Lewin 1977; Kunieda *et al.* 1984b). During portions of the latest recorded active period in August 1988, very regular type II burst intervals of ~30 s were observed (T. Dotani, private communication). Kunieda *et al.* (1984b) have suggested that there may be a coherent nature to the type II bursts with intervals of ~16 s. In our opinion the quasi-periods in the range ~15–30 s are probably a semi-stable mode of spasmodic accretion unrelated to a stable clock. In any case, intervals of ~15 s are not the shortest (~7 s intervals have been observed; Lewin 1977; Marshall *et al.* 1979).

A full cycle (from turn-on to turn-off) of the active period was only observed (though intermittently) in August 1983 (Kunieda *et al.* 1984b; Kawai 1985). At first no type II bursts were observed, only persistent emission [$\sim 1.3 \times 10^{37}$ erg s^{-1} (~1–9 keV)] in combination with type I bursts (this may have lasted continuously for ~10 days; Kunieda *et al.* 1988b; Kawai 1985; Barr *et al.* 1987; Kaminker *et al.* 1990). When the type II bursts first occurred (near August 18, 1983), they were very long (several minutes), and the average persistent emission between the bursts was near $\sim 8 \times 10^{36}$ erg s^{-1} (~1–9 keV). The type II bursts became shorter (not monotonically) as the active period evolved, and the persistent emission (after August 19) became $< 5 \times 10^{36}$ erg s^{-1} (~1–9 keV). The type II burst intervals were ~100 s near August 20.5, 24.5 and 30.5, 1983, but they were ~25 s near August 23.5 and 26. Burst trains with very regular intervals of ~16 s were observed on August 26. The activity came to an end near August 31.

The turn-on was observed in the August 1979 active period; at first short (< 30 s) type II bursts were observed, the bursts then became longer (~40 s to ~700 s) for about one week after which they became shorter again; the turn-off was not observed (Kunieda *et al.* 1984a).

Due to the rather limited coverage (see Fig. 7.1), it is not clear whether the type II burst pattern evolves in approximately the same way in the course of each active period. It is rather likely, however, that the type II bursts become very short (and approximately regular) near the end of an active period; this was observed in April 1976 (Lewin 1977; Marshall *et al.* 1979), in August 1979 (Kunieda *et al.* 1984a), August 1983 (Kunieda *et al.* 1984b; Kawai 1985), September 1985 (Tan *et al.* 1991a; Lubin *et al.* 1991a) and in August 1988 (T. Dotani, private communication).

7.5. Type II Burst Profiles, Energies, and Luminosities

Type II bursts vary in duration from ~2 s to ~11 min. Their peak luminosities range from $\sim 5 \times 10^{37}$ to $\sim 4 \times 10^{38}$ erg s^{-1}, and the integrated burst energies range from $\sim 1 \times 10^{38}$ erg to $\sim 7 \times 10^{40}$ erg. When the type II burst duration exceeds ~15 s, the type II bursts in general have approximately flat tops whose flux levels, however, can vary greatly from burst to burst (see e.g., Lewin *et al.* 1976c; Inoue *et al.* 1980; Basinska *et al.* 1980; Kunieda *et al.* 1984a,b; Stella *et al.*

1988a, b; Tan *et al.* 1991a). Thus, these flat tops are not the result of an Eddington limit.

Type II bursts which are shorter than ~50 s almost always show successive peaks during their decay which we call "ringing" (Lewin *et al.* 1976c; Lewin 1977; Kawai 1985; Tawara *et al.* 1985; Kawai *et al.* 1990; Tan *et al.* 1991a). Kawai (1985), Tawara *et al.* (1985), and Kawai *et al.* (1990) discussed data in which the type II bursts have nearly identical profiles though the characteristic timescale of the profiles and peak fluxes differs from burst to burst. They defined the characteristic timescale τ as the time between the first and second peak in the decay portion of the type II burst and noticed that the decay portion can be expressed by a single function $F(t/\tau)$ where t is the time since the start of the burst (since the burst peak fluxes differ, the "heights" of the bursts have to be normalized). In other words, their burst profiles were timescale-invariant. This held over their range of timescales τ from ~0.3 s to ~9 s (the corresponding burst durations ranged from ~2 s to ~50 s).

When one explores the entire range of type II burst durations, the profiles are not timescale-invariant (Tan *et al.* 1991a). There is a gradual change in the type II burst profiles as the bursts get longer. Very globally, with increasing burst duration the relative length of the approximately flat top of the type II bursts increases at the expense of the number of oscillations in the ringing during burst decay (Fig. 7.5). Also, as the bursts become long and approximately flat-topped, the peak fluxes become lower (Kunieda *et al.* 1984a; Stella *et al.* 1988a). The long type II bursts occasionally show a burst-like event superimposed on the flat top; this event may not be a type I burst (Kunieda *et al.* 1984a, b).

Type II bursts of very low fluence ($< 1.1 \times 10^{-8}$ erg cm^{-2}; this corrresponds to a total burst energy of less than $\sim 1.3 \times 10^{38}$ erg) can have erratic profiles, showing a series of flares (Fig. 7.6; Lubin *et al.* 1991b). On September 13, 1985, the very low-fluence bursts occur "too early"; the burst intervals to the burst *prior to* the low-fluence bursts are significantly shorter, while at the same time the burst intervals *after* the low-fluence bursts appear to be longer than one would expect on the basis of the observed relaxation oscillator relation between burst fluence and the interval to the *following* burst. It appears in these cases as if the accretion instability responsible for the type II bursts occurs prematurely with only a relatively small amount of matter being accreted on the neutron star (Lubin *et al.* 1991b).

7.6. Radio and Infrared Bursts?

Radio and infrared bursts have been reported from the Rapid Burster (Calla *et al.* 1979, 1980a,b; Apparao *et al.* 1979; Kulkarni *et al.* 1979; Jones *et al.* 1980). However, their believability is in question (see Lewin and Joss 1981, 1983 and Sect. 3.9.2).

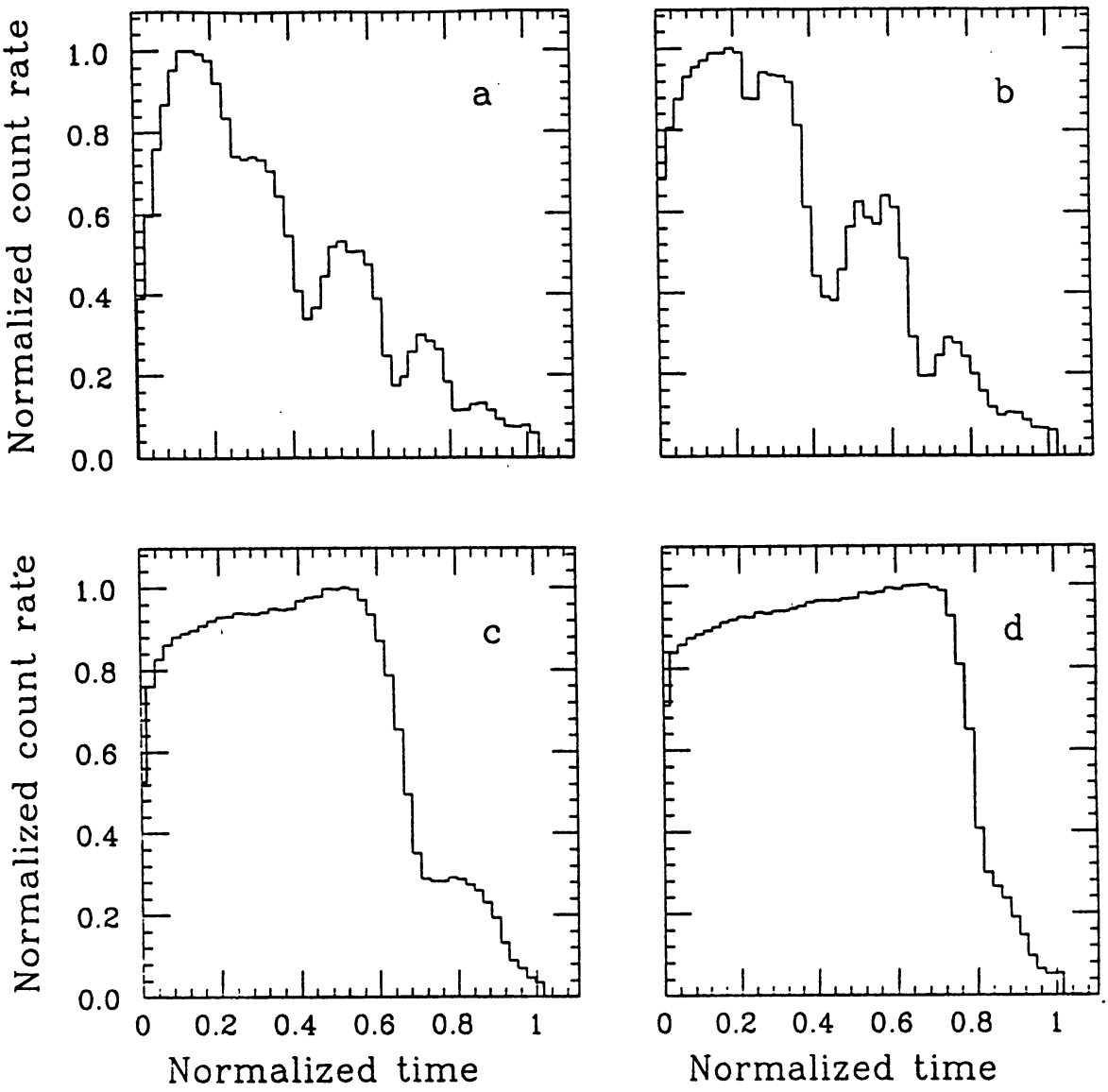

Fig. 7.5. Composite type II burst profiles (1–22 keV). The lengths and heights of the profiles are normalized to 1. (a) 342 bursts with durations from ~2–17 s; (b) 169 bursts with durations ~4–27 s; (c) 49 bursts with durations from ~40–200 s; (d) 39 bursts with durations from ~90–680 s. This figure is from Tan *et al.* (1991a).

7.7. Persistent Emission after Energetic Type II Bursts

Persistent X-ray emission is often observed after type II bursts with a relatively high fluence (this is the case for most bursts which last longer than ~30 sec); persistent emission is not observed after low-fluence type II bursts. This persistent X-ray flux emerges gradually after the type II bursts, and it decreases gradually before the occurrence of the next type II burst; this is often referred to as the "dips" in the persistent emission (Figs. 7.7, 7.10 and 7.14; Marshall *et al.* 1979; Van Paradijs *et al.* 1979b; Kunieda *et al.* 1984a; Stella *et al.* 1988a; Lubin *et al.* 1992b). The disappearance of this persistent emission is not the result of photo-electric

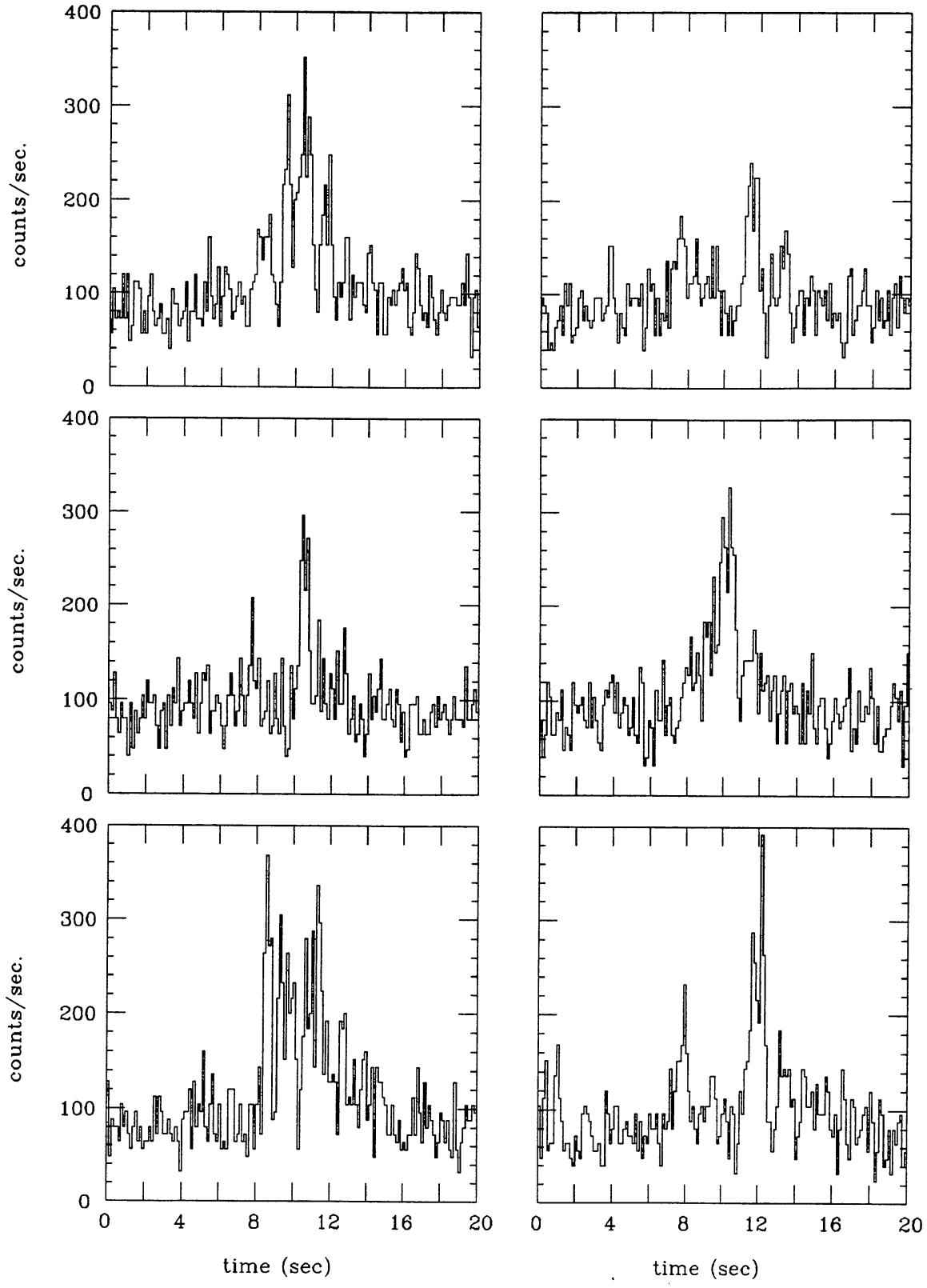

Fig. 7.6. Erratic type II burst profiles. These bursts, with a flare-like structure, are at the extreme low end of the fluence distribution ($< 1.1 \times 10^{-8}$ erg cm^{-2}). The data have not been corrected for background and not for transmission efficiency. This figure was adapted from Lubin *et al.* (1991b).

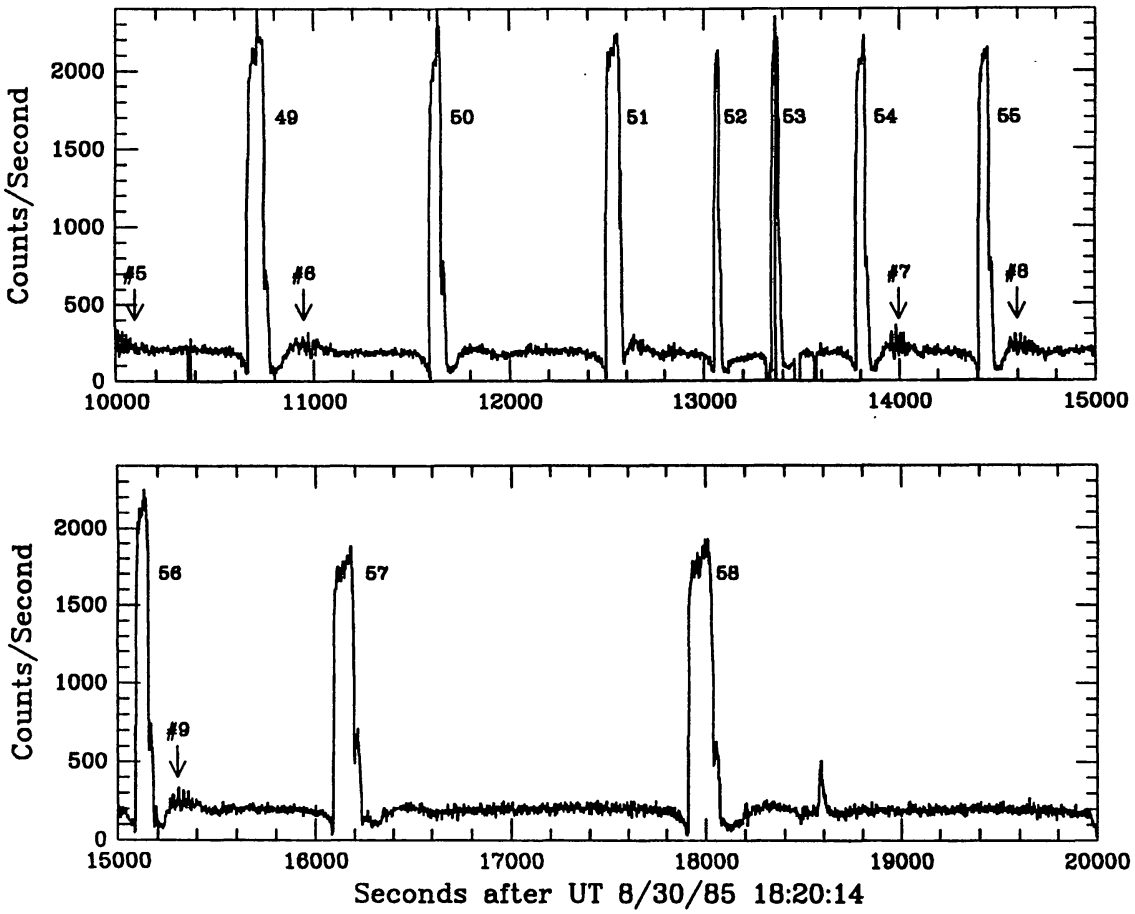

Fig. 7.7. Light curves of the Rapid Burster obtained with EXOSAT on August 30, 1985; the background has been subtracted and the data have been normalized to 7/8 of the total area of the full array; 1 burst count corresponds to $\sim 1.6 \times 10^{-11}$ erg/cm^2 (bolometric), 1 count in the persistent emission corresponds to $\sim 7.8 \times 10^{-12}$ erg/cm^2 (bolometric). Notice the dips in the persistent emission (see also Figs. 7.10 and 7.14, and see text). Arrows indicate times that the ~0.042 Hz oscillations are observed (see text). This figure is from Lubin *et al.* (1992b). An expanded light curve of the interval between bursts #54 and #56 is shown in Fig. 7.8.

absorption (Stella *et al.* 1988a). No satisfying explanation exists for this behavior.

In March 1976, the mean flux in this persistent emission after the long type II bursts (observed with SAS–3) was ~5% of the time-averaged type II burst flux (Van Paradijs *et al.* 1979b). Persistent emission after high fluence type II bursts were observed with HEAO–1 in March 1978 (Hoffman *et al.* 1978c) and with Hakucho in August 1979. During the latter observations, between August 8 and 15, 1979 when long (~40 s–~700s) type II bursts were observed, the average persistent luminosity was $\sim 1.8 \times 10^{37}$ erg s^{-1}; this was ~50% of the time-averaged type II burst luminosity (Kunieda *et al.* 1984a). On August 28–31, 1985 all type II bursts (observed with EXOSAT) were in excess of ~1 min and persistent emission was observed after each burst (Figs. 7.7, 7.10 and 7.14). The average persistent luminosity was $\sim 2.2 \times 10^{37}$ erg s^{-1} which is comparable to the average type II burst luminosity of $\sim 2.8 \times 10^{37}$ erg s^{-1} during the same period.

No persistent emission has been observed to date after type II bursts with durations less than ~20 s. On July 17, 1984 and September 10, 1985 when the type II bursts durations varied between ~2 s and ~17 s, the average persistent luminosity between the bursts was $< 2.5 \times 10^{36}$ erg s^{-1} (2σ upper limit); at those times the time-averaged type II burst luminosity was $\sim 8 \times 10^{36}$ erg s^{-1} (Tan *et al.* 1991a). On September 13, 1985, when the type II bursts were all shorter than 30 s, the time averaged type II burst luminosity had decreased to $\sim 4 \times 10^{36}$ erg s^{-1}, and the 2σ upper limit to the persistent emission between the bursts was $\sim 2 \times 10^{36}$ erg s^{-1}. The persistent flux of X rays between the type II bursts, when observed, varies a great deal (Figs. 7.7, 7.10 and 7.14). The light curves can, at times, be carbon copies of each other, including such fine details as "humps", sharp "glitches" and "bumps" (Lubin *et al.* 1992c). During the 1985 EXOSAT observations the persistent emission which followed type II bursts with integrated fluxes of less than $\sim 4.8 \times 10^{-6}$ erg cm^{-2} in general exhibited a specific pattern which was characterized by a hump in the early portion of the emission. The hump was almost never observed after bursts with fluences greater than this value. It was also absent in cases that the persistent emission lasted less than ~400 s. A hump typically lasted ~200 s and was harder than the average persistent emission (Lubin *et al.* 1992c). The ~0.042 Hz oscillations (see below; Lubin *et al.* 1992b) and ~4 Hz QPO (Sect. 7.10; Stella *et al.* 1988a; see also Rutledge *et al.* 1993) were only observed during this hump. In addition to the characteristic hump and the oscillations, the persistent emission showed distinctive features which included sharp glitches (lasting ~20–30 sec) and small bumps (lasting ~20–100 sec). In several cases a glitch was followed by a bump (Lubin *et al.* 1993).

In ten cases, immediately following a type II burst on August 28–31, 1985, very clear ("naked eye") ~0.042 Hz quasi-periodic oscillations were observed (Figs. 7.7 and 7.8; Lubin *et al.* 1992b). The mean frequency of the oscillations increased (in 7 of the 10 cases) by ~30–50% on a timescale of ~100 s as the oscillations died out (Fig. 7.8). The fractional rms variation of these oscillations ranged from ~5 to 15% (see also Sect. 7.10.2).

7.8. X-Ray Emission during an Inactive Period

Several attempts have been made to measure X rays from the RB during inactive periods. The best upper limit has been reported by Grindlay (1981). On April 10, 1979 the average X-ray luminosity was less than 10^{34} erg s^{-1}.

7.9. Spectral Information

7.9.1. Type I Bursts

The spectrum during type I bursts can be approximated by that of a blackbody with an approximately constant radius and, generally, with a decreasing temperature during burst decay (Sect. 3.3). Marshall *et al.* (1979) reported a maximum blackbody temperature (kT) during type I bursts of ~2 keV and a blackbody radius (for an assumed source distance of 10 kpc and isotropic emission) of 9 ± 2 km;

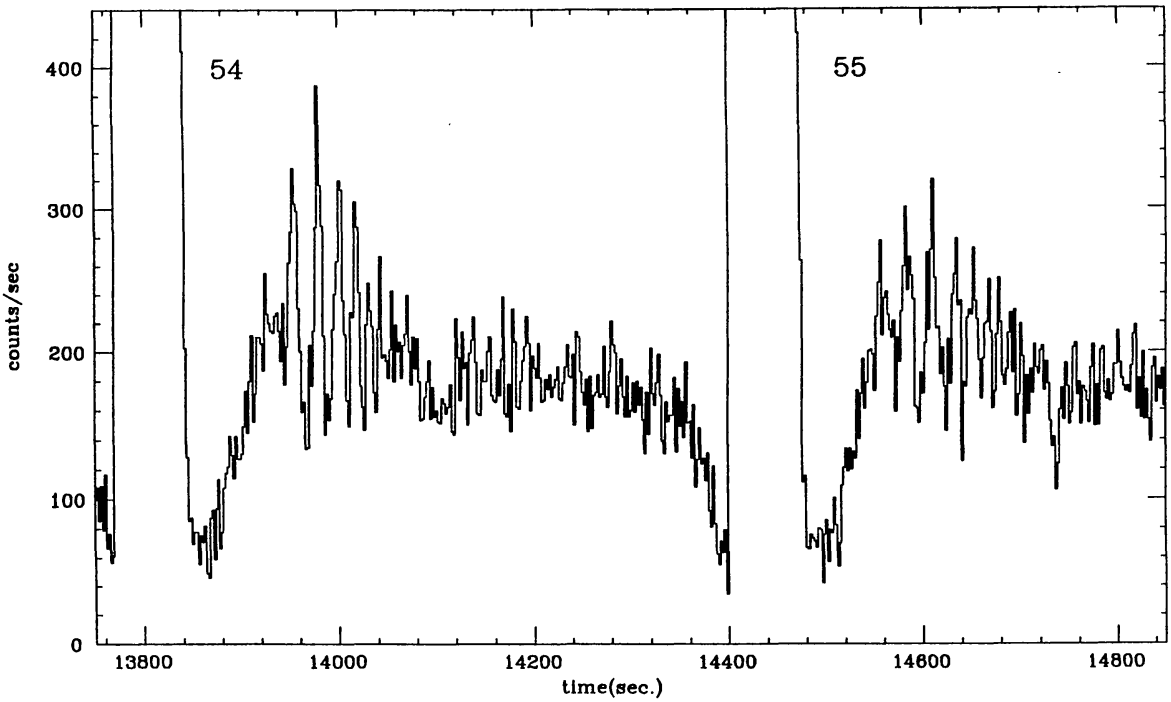

Fig. 7.8. Expanded light curves of the Rapid Burster which show the "naked-eye" ~0.042 Hz quasi-periodic oscillations (see text and Fig. 7.7); the background has been subtracted and the data have been normalized to 7/8 of the total area of the full array (for conversion from counts to flux, see Fig. 7.7). Notice the increasing frequency as the oscillations die out. This figure was adapted from Lubin *et al.* (1992b).

Barr *et al.* (1987) reported a blackbody radius of ~10 km. [We caution that the interpretation of blackbody temperatures and radii is not at all straightforward (see Sect. 4.7)]. Marshall *et al.* (1979) find an average type I burst peak luminosity of $\sim 2 \times 10^{38}$ erg s^{-1} (active period of September-October 1977); Barr *et al.* (1987) report peak type I burst luminosities (2–15 keV) of 9.6×10^{37} erg s^{-1} (August 7, 1983) and 7.2×10^{37} erg s^{-1} (August 14/15, 1983). If the anamolous bursts as reported by Ulmer *et al.* (1977) are type I bursts, as argued by Lubin *et al.* (1991b), their peak luminosities are $\sim 5 \times 10^{36}$ erg s^{-1}.

7.9.2. Type II bursts

The burst peak luminosities in type II bursts range from $\sim 5 \times 10^{37}$ to $\sim 4 \times 10^{38}$ erg s^{-1}, and the integrated burst energies from $\sim 1 \times 10^{38}$ erg to $\sim 7 \times 10^{40}$ erg. The spectra during type II bursts have been approximated by that of a blackbody by various authors (Marshall *et al.* 1979; Kunieda *et al.* 1984a; Barr *et al.* 1987; Kawai *et al.* 1990; Tan *et al.* 1991a; Lubin *et al.* 1992a). Very roughly the blackbody temperature remains constant throughout the type II bursts; the blackbody temperatures (kT) are ~1.8 keV (Marshall *et al.* 1979; Kunieda *et al.* 1984a). Studied in more detail, one finds that there is some temperature evolution during the type II bursts correlated with the ringing during burst decay; blackbody temperatures (kT) vary from ~1.5 keV to ~2 keV (Kawai *et al.* 1990; Tan *et*

al. 1991a). Tan *et al.* (1991a) have shown that the temperature evolution in type II bursts is different for bursts with different profiles (and thus different burst durations). The roughly constant blackbody temperature throughout the type II bursts implies that the size of the emitting region decreases as the bursts decay. The largest blackbody radii are observed early on in the type II bursts. Marshall *et al.* (1979) report an average blackbody radius of $\sim 16\pm 2$ km during the first 15 s of the type II bursts. Kawai *et al.* (1990) and Tan *et al.* (1991a) report maximum radii from ~10 to ~15 km. Marshall *et al.* (1979) and Kawai *et al.* (1990) concluded that the maximum blackbody radii measured during type II bursts are larger than the blackbody radii measured during type I bursts.

Kunieda *et al.* (1984a), using Hakucho data from August 1979, and Tan *et al.* (1991a), using EXOSAT data from August 1985, have shown that there is a correlation between the color temperature, T, and the luminosity, L, as observed during the flat tops of relatively long type II bursts; they find that $L \propto T^6$. This led to the suggestion by Tan *et al.* (1991a) that the radiation during a type II burst comes from a photosphere whose radius is larger for higher type II burst accretion rates. This could explain in a natural way why the blackbody radii during the early part of type II bursts are larger than those observed during type I bursts. Using the Ginga data of August 1988, Lubin *et al.* (1992a) found that the above relation between L and T holds approximately for mode II bursts but not for mode I bursts (Fig. 7.9). [We caution that the interpretation of blackbody temperatures and radii is not at all straightforward (see Sect. 4.7).]

Stella *et al.* (1988a) concluded that blackbody fits to the type II bursts are unacceptably poor; they showed that an unsaturated Comptonization model, approximated by the function $E^{-\Gamma}\ e^{-E/kT}$ (see White *et al.* 1986), with an iron emission line at ~6.7 keV, gives acceptable fits. They derived *average* spectra for the type II bursts and found values of $\Gamma = -0.66\pm 0.06$ and -0.89 ± 0.11, a (color) temperature of $kT = 2.65 \pm 0.06$ keV and 2.20 ± 0.07 keV, and a column density of $N_{\rm H} = (1.7\pm 0.1)\times 10^{22}$ cm^{-2} and $(1.3\pm 0.1)\times 10^{22}$ cm^{-2}, respectively, during the 1.5–2 minute long type II bursts and the very long (> 2 min) bursts. The iron line flux during the type II bursts was $\sim 7.3 \times 10^{-3}$ photons cm^{-2} s^{-1}.

Dotani (1990) has fit the type II burst spectra to a Comptonized blackbody (Kawai 1985) with a fixed electron temperature. He reports blackbody temperatures of ~1.5 and ~1.7 keV and optical depths of 0.22 ± 0.03 and 0.27 ± 0.06 for the initial peak and the following peak in the type II bursts, respectively.

On a timescale of hours, the spectral hardness of the type II bursts and the persistent emission was generally correlated in August 1985 (Rutledge *et al.* 1993).

7.9.3. Persistent Emission

In early August 1983, the RB was active, but it emitted no type II bursts; however, persistent emission and type I bursts were observed (Kunieda *et al.* 1984b; Kawai 1985; Barr *et al.* 1987). The average luminosity of the persistent emission was $\sim 1.3 \times 10^{37}$ erg s^{-1} ($\sim$ 1–9 keV) (see Sect. 7.3). Barr *et al.* (1987) showed that

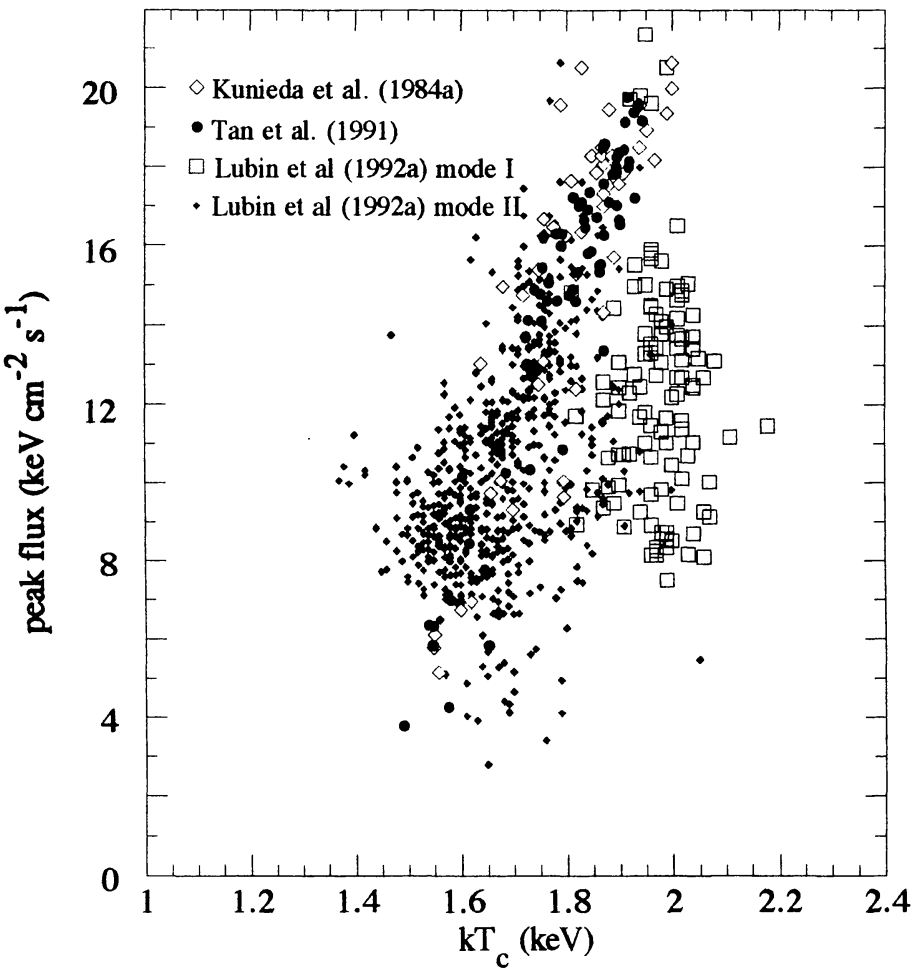

Fig. 7.9. Peak burst flux (bolometric) versus blackbody temperature at the peak of the type II bursts in mode I and in mode II. This is a composite of the results from three different observatories (Hakucho, EXOSAT, and Ginga). It appears that the distribution is very different for the mode I bursts than for the mode II bursts. This figure was adapted from Lubin *et al.* (1992a).

blackbody fits to the data were unacceptably poor. Both power law spectra (photon index $\Gamma = 2.1 \pm 0.2$) and thermal-bremsstrahlung ($kT = 9 + 3/ - 2$ keV) gave acceptable fits.

From August 8–15, 1979, when long (~40 s–~700 s) type II bursts were observed, the time-averaged persistent emission between the bursts was $(1.8 \pm 0.3) \times 10^{37}$ erg s^{-1} (~50% of the time-averaged luminosity in type II bursts observed during the same time). The spectral hardness in terms of the ratio of counting rates in two energy bands (9–22 keV and 1–9 keV) was about equal for the persistent emission and the type II bursts (Kunieda *et al.* 1984a).

In August 1985, very long type II bursts were observed with persistent emission after all the bursts; see Figs. 7.7, 7.10 and 7.14. The average luminosity in the persistent emission between two consecutive type II bursts varied from $\sim 2 \times 10^{37}$ to $\sim 3.4 \times 10^{37}$ erg s^{-1}. Stella *et al.* (1988a) showed that an unsaturated Comptonization model, approximated by the function $E^{-\Gamma}\ e^{-E/kT}$ (see White

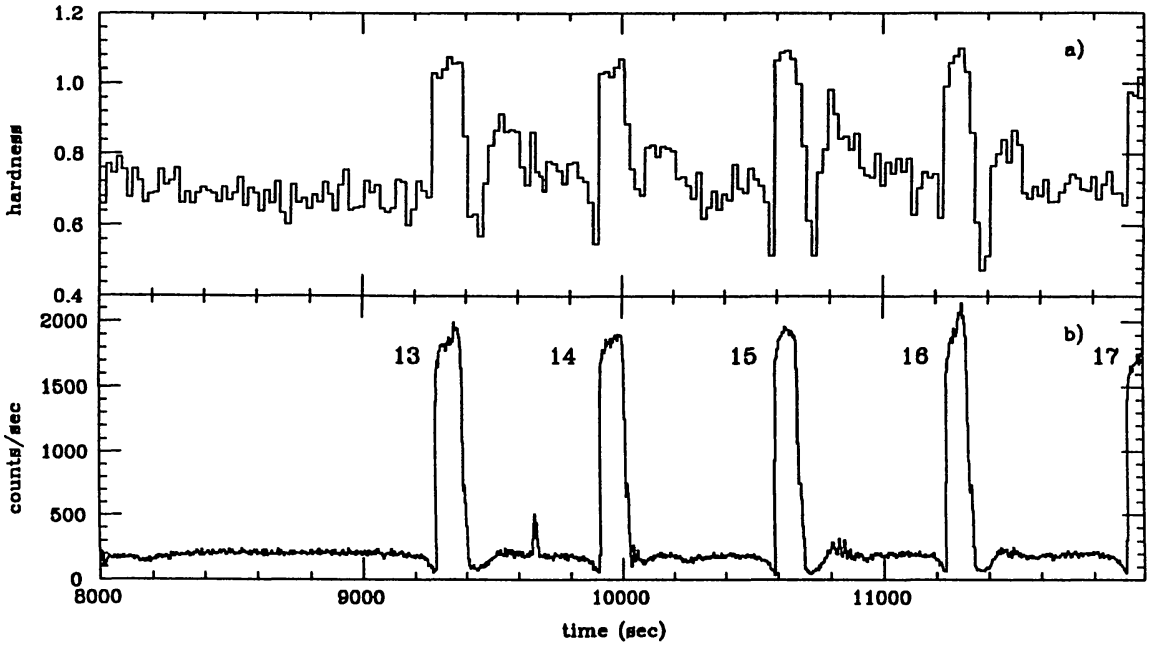

Fig. 7.10. (a) Spectral hardness (5–15 keV/1– 5 keV) versus time. (b) light curve of Rapid Burster data of August 28, 1985; the background has been subtracted and the data have been normalized to 7/8 of the total area of the full array (for the conversion from counts to flux, see Fig. 7.7). The type II bursts are harder than the persistent emission; the dips in the persistent emission are very soft; the persistent emission is hardest after the bursts. Notice the ~0.042 Hz oscillations after burst #15. This figure is from Lubin *et al.* (1992b).

et al. 1986, 1988) with an iron emission line at ~6.7 keV, gives acceptable fits for this persistent emission. They derived *average* spectra and found values of Γ =–0.06 ± 0.21 and –0.30 ± 0.18, a color temperature of $kT = 2.8 \pm 0.3$ keV and 2.4 ± 0.2 keV, and a column density of $N_{\rm H} = (1.2 \pm 0.2) \times 10^{22}$ cm^{-2} and $(0.9 \pm 0.2) \times 10^{22}$ cm^{-2}, respectively, during the intervals after the 1.5–2 minute long type II bursts and after the very long (> 2 min) bursts, respectively. The iron line flux during the persistent emission was $\sim 2.2 \times 10^{-3}$ photons cm^{-2} s^{-1}. A spectral hardness (counting rate ratio in the 5–15 keV and the 1–5 keV energy band) showed that (i) the type II burst spectra are harder then the average spectrum of the persistent emission between the bursts, (ii) the spectra of the dips in the persistent emission just after the type II bursts are much softer than the average persistent emission, and (iii) there is an evolution in the spectral hardness in the persistent emission (Fig. 7.10).

In August 1988, short (<35 s) type II bursts and persistent emission after the relatively long type II bursts were observed (Dotani *et al.* 1990a; Dotani 1990). The average luminosity (1–30 keV) in the persistent emission was $\sim 6 \times 10^{36}$ erg s^{-1}. A power law (with index ~2.5) model gave the best fits to the observed spectra.

On a timescale of several hours, the spectral hardness of the type II bursts and the persistent emission was generally correlated in August 1985 (Rutledge *et al.* 1993).

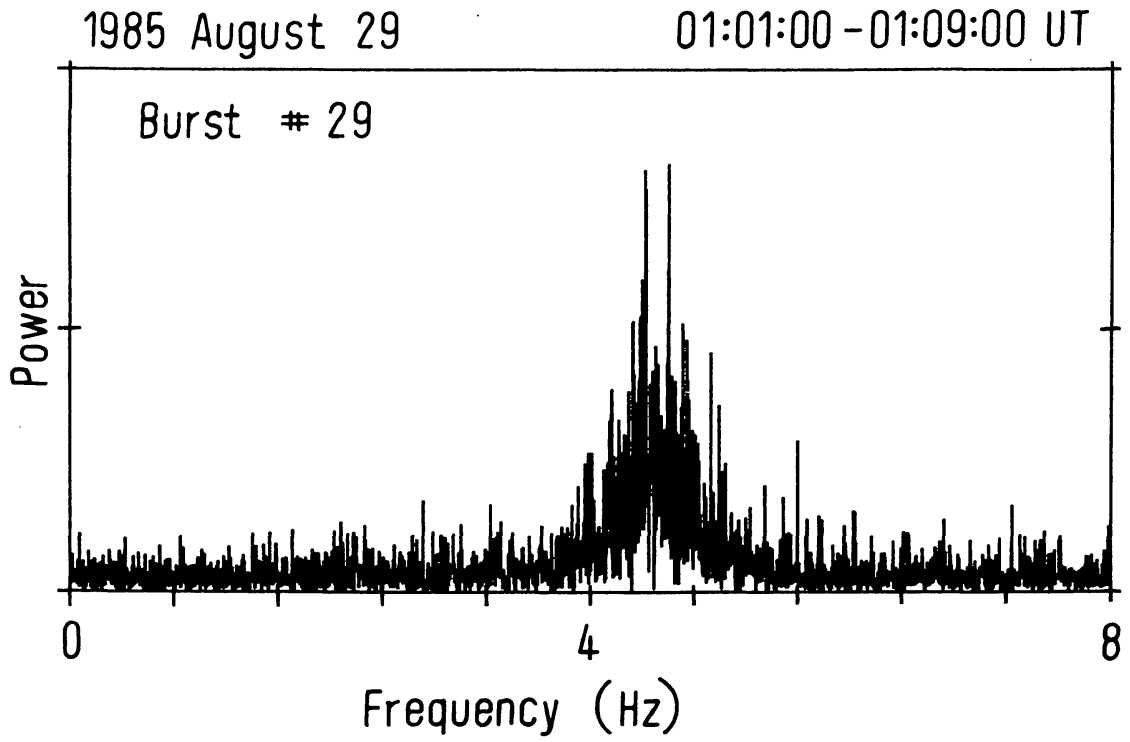

Fig. 7.11. Power density spectrum (2048 frequency bins) from an 8-min interval during a long type II burst observed with EXOSAT on August 29, 1985. The fractional rms variation in the ~4.2 Hz QPO is ~21%. This figure is from Stella *et al.* (1998a).

7.10. Quasi-Periodic Oscillations

7.10.1. Introduction

Quasi-periodic oscillations (QPO) of ~2 Hz were discovered (with Hakucho) in 2 out of 63 long type II bursts observed during the August 1979 active period (Tawara *et al.* 1982). Several years later a very complex QPO behaviour was observed during the August-September 1985 active period. QPO were observed during many (not all) type II bursts and often (not always) during the persistent emission between the type II bursts (Figs. 7.11, 7.12 and 7.14; Stella *et al.* 1988a,b; Lubin *et al.* 1991a). QPO during the type II bursts were also observed during the August 1988 active period (Fig. 7.13; Dotani 1990; Dotani *et al.* 1990a). No QPO have been observed to date in any type I burst from the RB.

It is presently unclear whether the QPO observed in the RB have any relation to other forms of QPO observed in many bright LMXB (see also Sect. 2.5; for reviews on QPO see Lewin, Van Paradijs and Van der Klis 1988; Hasinger and Van der Klis 1989; Van der Klis 1989, 1993; Van der Klis and Lamb 1993). Rutledge *et al.* (1993) have shown that the Rapid Burster is neither an atoll source, nor a Z source [Hasinger and Van der Klis (1989) classification].

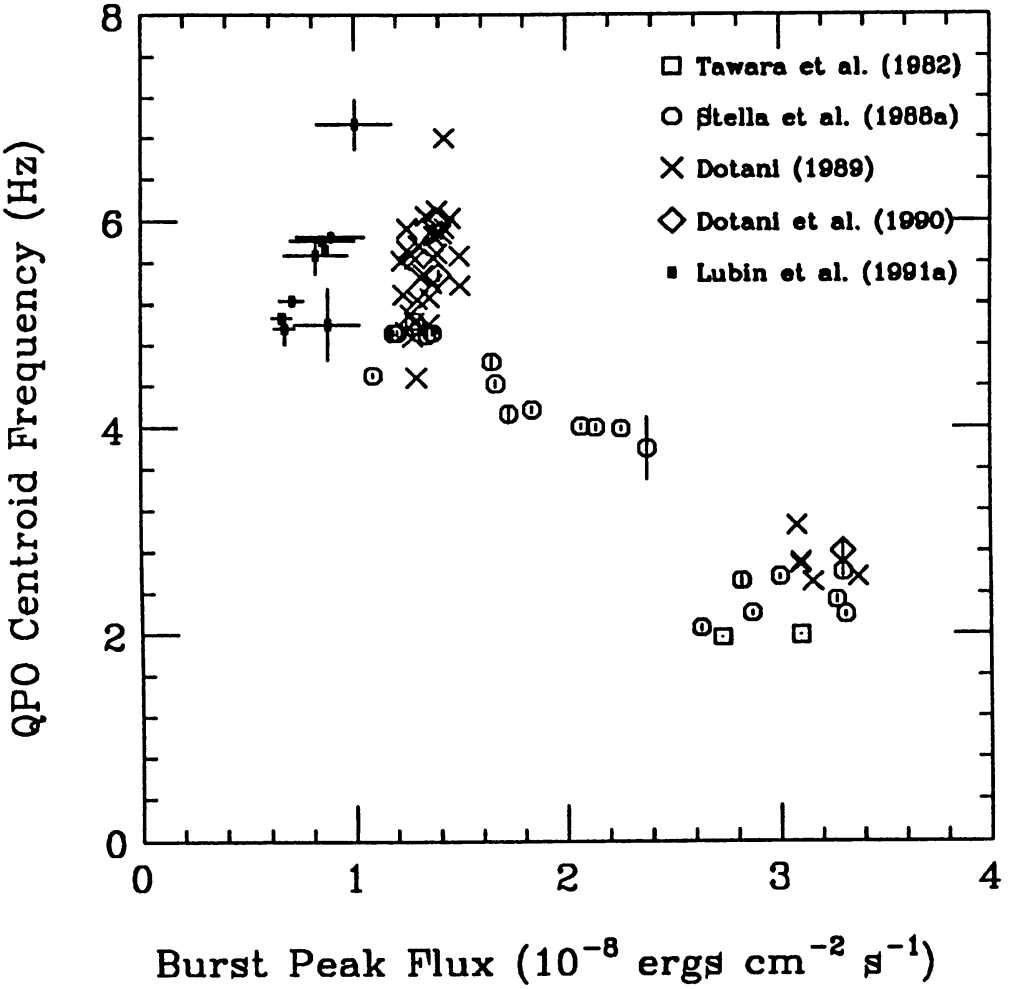

Fig. 7.12. Type II peak burst flux versus the QPO centroid frequency. This figure was adapted from Lubin *et al.* (1991a).

7.10.2. Type II Bursts

Tawara *et al.* (1982) discovered ~2 Hz QPO with a strength of 10% (fractional rms variation) in two of 63 long (~40–600 s) type II bursts. The upper limits to the strength in the other 61 were ~4%.

During August 28–29, 1985 41 type II bursts were detected which lasted between ~1.5 min and ~11 min; the shortest bursts had higher peak fluxes than the longer bursts (Stella *et al.* 1988a). QPO with frequencies between 2 and 5 Hz were observed in 23 (of the 41) type II bursts. The fractional rms variation ranged from <2% (90% confidence level) to ~20% for the longest and most energetic type II bursts (these energetic bursts are the least luminous bursts and have QPO frequencies near 5 Hz). In Fig. 7.11 we show a power density spectrum from an 8 min portion of a type II burst. Lubin *et al.* (1991a) made a study of the QPO in 784 short (<30 s) and low-luminosity type II bursts observed with EXOSAT and found that QPO were only observed in bursts within a certain range of durations. Combining all results, the QPO centroid frequencies in the type II bursts range

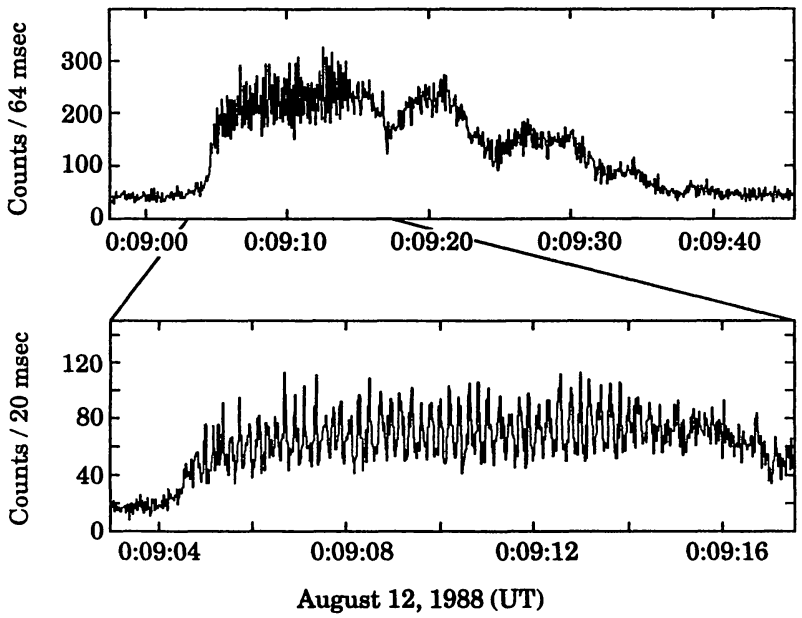

Fig. 7.13. Light curve of a type II burst from the Rapid Burster observed with Ginga on August 12, 1988. Notice the distinct "ringing" during burst decay and the "naked-eye" ~5 Hz QPO (bottom panel). This figure was adapted from Dotani *et al.* (1990).

from ~2 to ~7 Hz, and they are strongly anti-correlated with the average burst peak flux (Fig. 7.12).

During the August 1988 active period relatively short type II bursts (< 35 s) were observed (Dotani *et al.* 1990a; Dotani 1990). Dotani *et al.* (1990a) found evidence that the presence of QPO is correlated with the ringing in the burst profiles. The QPO is very strong during the initial peak in the burst profile, absent in the second peak, and strong again at the onset of the third peak; average fractional rms variations are ~18%, <2% and ~13%, respectively. The strength of the 5 Hz QPO was very large, and the individual oscillations can be seen in the burst profiles (Fig. 7.13). Dotani *et al.* (1990a) showed that, during the large majority of the type II bursts, the oscillations can be described as a periodic modulation without phase jumps whose frequency changes gradually by up to ~25%. The frequency drifts can explain the width of the QPO peaks in the power density spectra.

The oscillations can be described by changes of the temperature of a blackbody emitter with constant apparent area, but they can equally well be described by changes in the photospheric radius and associated temperature changes (Dotani *et al.* 1990a). Lewin *et al.* (1991) have given some arguments why the latter may be more likely (see also Lubin *et al.* 1992a).

The fractional rms variation of the QPO in the type II bursts increases with increasing photon energies. It increases from ~8% near 3 keV to ~13% near 10 keV (Stella *et al.* 1988b; Dotani *et al.* 1990a).

No significant time lags (between high-energy and low-energy photons) were observed in the QPO in the type II bursts (Stella *et al.* 1988b; Dotani *et al.* 1990a).

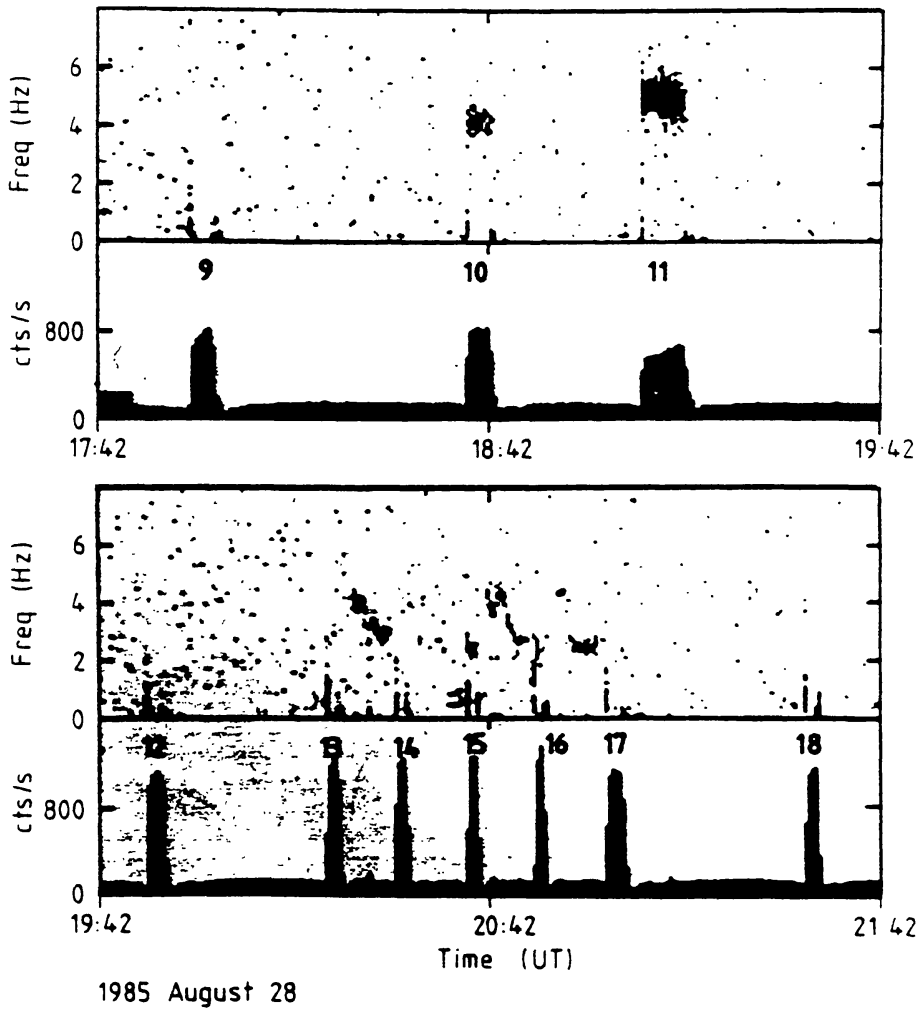

Fig. 7.14. Power density spectra (*upper panel*), and light curves (1–15 keV countrate) of Rapid Burster EXOSAT data from August 28, 1985. The shade of grey in the power density spectra indicates the power; the darker the shade, the higher is the power. Notice the evolution in the QPO frequency in the persistent emission. Relatively high-frequency QPO (~4 Hz) occur when the spectral hardness in the persistent emission is relatively high (see Fig. 7.10); the QPO frequency is lowest (~2.5 Hz) just before a type II burst. This figure is from Stella *et al.* (1988a).

7.10.3. Persistent Emission

In early August 1983 when the RB showed only persistent emission and type I bursts, no QPO were observed in the persistent emission with an upper limit of ~10% in the fractional rms variation (Barr *et al.* 1987). During the active period in August 1985, QPO were occasionally observed in the persistent emission after relatively short (1–2 min) type II bursts. The fractional rms variation could be as high as ~35% (Stella *et al.* 1988a). In several cases the QPO frequency evolved from ~4 Hz after a type II burst to ~2 Hz in 3 to 6 min without a general correlation with the flux of the persistent emission (Fig. 7.14). Variations in the QPO frequencies were positively correlated with the spectral hardness, such that the spectrum of the persistent emission softened as the QPO frequency decreased. The fractional rms variation of the QPO in the persistent emission increases with

increasing photon energies, from ~20% near 2–3 keV to ~35% near 10 keV (Stella *et al.* 1988a).

QPO with frequencies ranging between 0.4 and 1 Hz were also observed occasionally (August 1985) during intervals of 1 to 3 min before type II bursts. On one occasion two QPO peaks (with centroid frequencies of ~0.44 and ~0.88 Hz) were observed simultaneously.

Dotani (1990) report an upper limit of 9% fractional rms variation for QPO in the persistent emission observed after some of the longest type II bursts (in excess of ~25 s) observed in August 1988.

Stella *et al.* (1988b) reported a marginally significant time lag between high-energy and low-energy photons in the QPO in the persistent emission; a reanalysis of the same data showed that this result was not significant (R. E. Rutledge, private communication). No significant time lags have been observed by Dotani *et al.* (1990a).

"Naked eye" quasi-periodic oscillations with centroid frequencies of ~0.042 Hz have been observed in the persistent emission immediately following ten type II bursts (Lubin *et al.* 1992b); they are described in Sect. 7.7 (Figs. 7.7 and 7.8). In 7 out of 10 cases ~4 Hz QPO were observed; therefore, there is a high probability that the occurrence of the ~0.042 Hz and of the ~4 Hz QPO are related (Lubin *et al.* 1992b).

8. Models for the Rapid Burster

8.1. Introduction

Numerous theoretical models have been advanced for the explanation of the Rapid Burster since its discovery in 1976. Since the time averaged type II burst emission can be comparable to or greater than the persistent emission, a common hypothesis in all models is that the bursts are caused by the sudden release of energy associated with the accretion of matter onto the neutron star surface. Despite the continued monitoring of the Rapid Burster over the last decade which have revealed a plethora of new observational results (see Chapter 7) and despite a number of theoretical attempts to model this enigmatic source, the nature of the instability responsible for the type II bursts has yet to be established. Since it is likely that the ultimate model for the Rapid Burster may include some of the essential features of previous models, we shall review the theoretical models for the Rapid Burster in this chapter. Emphasis will be placed on the theoretical developments since the last major review of the Rapid Burster (Lewin and Joss 1981; 1983).

8.2. Instability Picture

The fundamental difficulty in making significant progress in understanding the behavior of the Rapid Burster has been the lack of an identification for the proper gating mechanism. This is not due to the lack of ingenuity by theorists. A simple mathematical representation of the behavior has been proposed by Celnikier (1977)

in a form similar to that encountered in the population dynamics field. Physically, the diversity of burst behavior may be associated with viscous or thermal instabilities in an accretion disk (Taam and Lin 1984; Hayakawa 1985; Meyer 1986), magnetospheric substorms resulting from magnetic reconnection (Davidson 1982), interactions between an accretion disk and a magnetosphere of a rotating neutron star (Michel 1977; Lamb *et al.* 1977; Baan 1977, 1979; Horiuchi *et al.* 1981; Singh and Duorah 1983; Hanami 1988; Hanawa *et al.* 1989; Spruit and Taam 1993), or instabilities in the mass flow in the disk associated with radiation drag effects (Milgrom 1987; Walker 1992). In all models mass is accumulated up to a critical level above which instabilities develop to produce the intermittent accretion.

Accretion disks are a common ingredient in models since there is observational evidence which suggests that they are likely to be relevant in the theoretical interpretation. This follows from the approximate linear relationship between the energy of the burst, E_b, and the waiting time to the next burst, Δt (Lewin *et al.* 1976c). This behavior mimics that of a relaxation oscillator and can be understood if there exists a reservoir where matter is accumulated and stored, suddenly released, and then replenished at a constant rate (see Sect. 7.2). Most workers identify the accretion disk surrounding the neutron star as this temporary storage medium. Accretion disks are an attractive candidate because the wide range of observed timescales finds a natural explanation in terms of the viscous diffusion timescale over different spatial regions in the disk.

Although the Rapid Burster exhibits properties characteristic of "normal" low mass X-ray binaries at times (see Sect. 7.3), it is unique in its burst behavior. What makes the Rapid Burster unique in this regard? A number of possibilities have been discussed including the alignment of the magnetic axis of the neutron star with its rotation axis (Hayakawa 1985), the location of the inner edge of the disk near the innermost marginally stable orbit (Milgrom 1987; Hanawa, Hirotani, and Kawai 1989; Walker 1992), and the location of a magnetospheric boundary at a point where the Keplerian angular velocity is close to the angular velocity of the neutron star (Baan 1977, 1979; Spruit and Taam 1993).

Each of the theoretical models has its own merits, and in the following we shall review them.

8.3. Accretion Disk Models

A promising candidate for the theoretical model of the type II burst phenomenon involves the operation of either viscous or thermal instabilities in an accretion disk to prevent the development of a steady state accretion flow to the neutron star surface. In this case, the mass transfer rate from the companion star to the disk can be constant, but physical processes in the disk lead to the modulation of the flow rate onto the neutron star. For viscous instabilities the density contrasts in the disk are amplified as a consequence of a negative diffusion coefficient (Lightman and Eardley 1974). Here, the viscous stress is inversely proportional to the column density and there is a tendency for the disk to break up into concentric

rings. On the other hand, thermal instabilities result from the inability of the local heating and cooling mechanisms to efficiently maintain a thermal balance (Pringle, Rees, and Pacholczyk 1973). Within the framework of the standard turbulent disk models pioneered by Shakura and Sunyeav (1973) the hot inner regions of accretion disks surrounding neutron stars are susceptible to such instabilities (for $\dot{M} \gtrsim 10^{-9} M_{\odot}$ yr^{-1}) when radiation pressure significantly contributes to the total pressure and when electron scattering is the dominant source of opacity (Lightman and Eardley 1974; Shakura and Sunyeav 1976). These models can, in principle, provide for a theoretical understanding of the observed $E_b - \Delta t$ relation since for the more energetic bursts a larger region of the disk is involved, and the time required to replenish the mass is correspondingly increased.

Taam and Lin (1984) were the first to carry out full scale time dependent calculations of these instabilities and found that the nonlinear development led to burst-like nonsteady accretion behavior. This evolution is a consequence of the net heating which under the action of the enhanced viscosity leads to an increased mass flow rate until the inner region of the disk is sufficiently depleted. This region is eventually replenished on the local viscous diffusion timescale. Although many of the gross properties of the type II bursts (duration, amplitude, and recurrence timescale) were modelled, the $E_b - \Delta t$ relation could not be quantified without requiring a secular variation in the mass input rate into the disk or a variation of the viscosity from burst to burst. Less detailed accretion disk models were advanced by Hayakawa (1985) and Meyer (1986). In the model developed by Hayakawa (1985) a thermal instability in the disk corona is presumed to amplify vertical oscillations in the disk which, in turn, leads to mass ejection from the disk and accretion by the neutron star. Meyer (1986), independent of Taam and Lin (1984), also suggested that the Lightman Eardley instability is responsible for the type II bursts. However, in contrast to Taam and Lin (1984), Meyer assumed that the inner disk inflates into a spherical structure and that the bursts arise from an accretion phase during this temporary state.

A failing of such models is their generality since they would also be applicable to other low mass X-ray binary systems as well as to the Rapid Burster. Thus, it is unclear what ingredient distinguishes the Rapid Burster from all other X-ray sources in these models. One possible difference may be related to the strength of the neutron star's magnetic field. To prevent the formation of a hot inner disk region in other sources, and thus, the thermal or viscous instabilities in the disk, a magnetosphere may be sufficiently large that the inner region is disrupted. Although the existence of such a field alleviates the problem, it does not remove it since, in these models, instability of a different type may be expected (see Sect. 8.4).

Accretion disk models for the Rapid Burster involving physical processes near the innermost stable circular orbit of an accretion disk have also been proposed for producing variability (Paczynski 1987; Milgrom 1987; Walker 1992). The uniqueness of the Rapid Burster in these models is, thus, attributed to the fact that the neutron star has a radius smaller than or close to the innermost stable orbit of

the disk (corresponding to $3R_g$, where R_g is the Schwarzschild radius given as $2GM/c^2$). In addition, as in the previously described models, it is assumed that the magnetic field of the neutron star is sufficiently weak that it does not disrupt the disk (Milgrom 1987; Walker 1992). Within this framework two different mechanisms for the variability have been proposed. One involves the recognition that there do not exist stable stationary disk-like accretion flows which pass through a sonic point for a viscosity parameter greater than 0.03 (Paczynski 1987). The other mechanism relies on the feedback between radiation emitted from the boundary layer of the neutron star and the remaining matter (via radiation torques) in the inner region of the disk (Milgrom 1987; Walker 1992).

With respect to the first possibility, it is well known that the accreting matter in a geometrically thin disk eventually becomes supersonic (see Muchotrzeb 1983; Matsumoto *et al.* 1984) near its innermost stable circular orbit. It was suggested by Muchotrzeb-Czerny (1986) and later confirmed by Kato *et al.* (1988) and Matsumoto *et al.* (1988) by detailed calculation that the transonic region is unstable with respect to axisymmetric perturbations. The instability is viscous in origin and was first discussed by Kato (1978). The detailed nonlinear calculations of Matsumoto, Kato, and Honma (1988) reveal that the innermost region of the disk is, indeed, pulsationally unstable. The period of the radial oscillation is comparable to the local Keplerian timescale in the inner region ($\sim 10^{-3}$ s) and its amplitude is modulated on a longer timescale of $\lesssim 0.1$ s. Such models, unfortunately, are not likely to succeed in explaining the type II burst phenomena since the timescales of variability are orders of magnitude too short.

The models involving radiation feedback (Milgrom 1987; Walker 1992) are, perhaps, more promising. In these models the radiation interaction with gas is most effective in the vicinity of the innermost stable orbit. Here the properties of the disk rapidly vary with radius and the structure and evolution of this region can be very sensitive to additional torque contributions. Under the action of radiation torques the inner disk region is depleted, giving rise to a burst, and subsequently replenished by viscous transport from larger radii. The calculations of Walker (1992) demonstrate that burst-like behavior with properties very similar to those observed in the Rapid Burster can be produced demonstrating the viability of the model. However, very low viscosity parameters ($< 10^{-6}$) are needed to reproduce the largest observed burst energies ($\sim 10^{40}$ ergs), requiring that the disk surrounding the neutron star is massive. Furthermore, the light curve is always strictly periodic. As in the case for the viscous and thermal instability model the relationship between the burst energy and waiting time to the next burst can only be modelled by either varying the global mass transfer rate in the disk or by varying the viscosity parameter from burst to burst.

8.4. Magnetospheric Models

Theoretical models incorporating the effects of magnetic fields are, probably, the most attractive for explaining the type II burst phenomenon. In most models the

magnetosphere acts as the gate with the matter entering the magnetosphere as a consequence of large scale Rayleigh Taylor instabilities (Baan 1977, 1979; Lamb et al 1977; Singh and Duorah 1983). The accretion geometry can be either spherical (Baan 1977, 1979; Lamb *et al.* 1977; Singh and Duorah 1983) or disk-like (Baan 1977, 1979; Horiuchi, Kadonaga, and Tomimatsu 1982; Hanami 1988; Hanawa, Hirotani, and Kawai 1989; Spruit and Taam 1993).

In the spherical case, matter is temporarily accumulated outside the magnetopause until Rayleigh Taylor instabilities transport mass into the magnetosphere. With the opening of the magnetic gate matter accretes onto the neutron star surface thereby producing the X-ray burst. The burst terminates as X-rays emitted from the surface Compton heat the infalling matter to such an extent that further accretion is temporarily prevented (Lamb *et al.* 1977). Although such models are attractive, the time dependent spherical accretion calculations by Cowie, Ostriker, and Stark (1978) do not provide support for this interpretation of the Rapid Burster.

Type II burst models involving the angular momentum of the accreted matter are more promising. In these models the accretion disk is disrupted by the magnetosphere surrounding a rotating neutron star. In most models a plasma Rayleigh Taylor instability (Kruskal and Schwarzschild 1954), perhaps, accompanied by the occurrence of tearing mode instability (Furth, Killeen, and Rosenbluth 1963) is assumed to produce the intermittent phases of accretion. As an example, Hanami (1988) examined the nonlinear motion of the magnetopause by considering the properties of the Rayleigh Taylor instability and found oscillations in the motion of the magnetosphere and the mass accretion rate with periods corresponding to a multiple of the Keplerian rotation period at the magnetopause. The direct application of this model to the Rapid Burster, however, implies field strengths $\sim 10^{15}$ G which rules out such an explanation for the Rapid Burster. On the other hand, Hanawa, Hirotani, and Kawai (1989) argue for a weak magnetic field ($\sim 10^8$ G) in order to explain the lack of type II burst activity at luminosities $\sim 10^{37}$ ergs s^{-1} (Kunieda *et al.* 1984b; Barr *et al.* 1987; see also Sect. 7.1). During this phase, they suggest that the magnetosphere shrinks to become smaller than the neutron star or the radius of the innermost stable orbit of the disk. At lower luminosities the mass flow is assumed to be regulated by an unspecified angular momentum transfer via magnetic torques in the burst phase. The model, in its present version, is difficult to quantify due to the lack of physical understanding of the precise form for the magnetic torque.

A different viewpoint is adopted in the investigations of Baan (1977, 1979) and Spruit and Taam (1993). Specifically, they exploit the variations in the effective gravity at the inner edge of the disk as a means for modulating the mass accretion rate. In this scenario, the mass flow rate through the magnetosphere of a rotating neutron star is inhibited or reduced when the magnetopause is located outside the corotation point as a result of the centrifugal barrier which forms when the magnetosphere rotates more rapidly than the accreting matter (Illianarov and Sunyaev 1975). This phase corresponds to the condition that the fastness parameter, ω_s, is

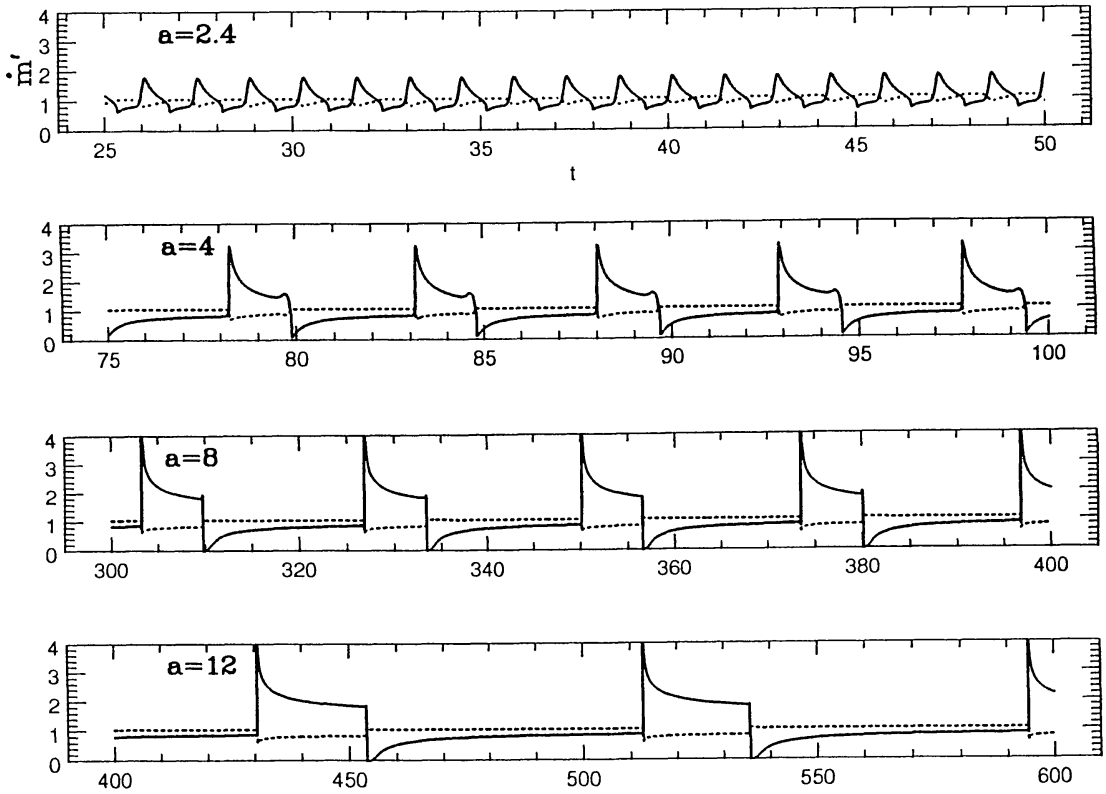

Fig. 8.1. The variation of the mass accretion rate and fastness parameter as a function of time for a steepness parameter of the boundary function ranging from 2.4 to 12. The solid curve corresponds to the accretion rate and the dashed curve to the fastness parameter. The accretion rate is normalized to the rate which places the magnetosphere at the corotation point in the steady state case, and the unit of time is normalized to the viscous diffusion time from the inner edge of the disk.

greater than unity (with ω_s defined as the ratio of the stellar angular velocity to that at the inner edge of the disk; Ghosh and Lamb 1979a,b). In this phase, matter accumulates outside the magnetosphere in the inner region of the disk. Eventually the surface density at the boundary rises to the point where it is sufficient to drive the magnetosphere inside the corotation radius and matter accretes onto the neutron star as a result of the Rayleigh Taylor instabilities (Baan 1977, 1979). To provide for an explanation of the most energetic type II bursts ($\sim 10^{40}$ ergs) magnetic moments comparable to those found for X-ray pulsars are required. The existence of type I bursts (see chapter 6) and the lack of coherent pulsations in the Rapid Burster argues against such an interpretation.

In a recent study Spruit and Taam (1993) have identified an instability associated with the magnetosphere-accretion disk interaction which operates in concert with the centrifugal barrier gating mechanism. In general it is assumed that matter flows into the magnetosphere via transport across field lines (Spruit and Taam 1990) and onto the surface of the neutron star in the absence of the barrier. The requirements imposed on the disk by the presence of the magnetosphere lead to a surface density at the inner edge of the disk that increases rapidly with the fastness

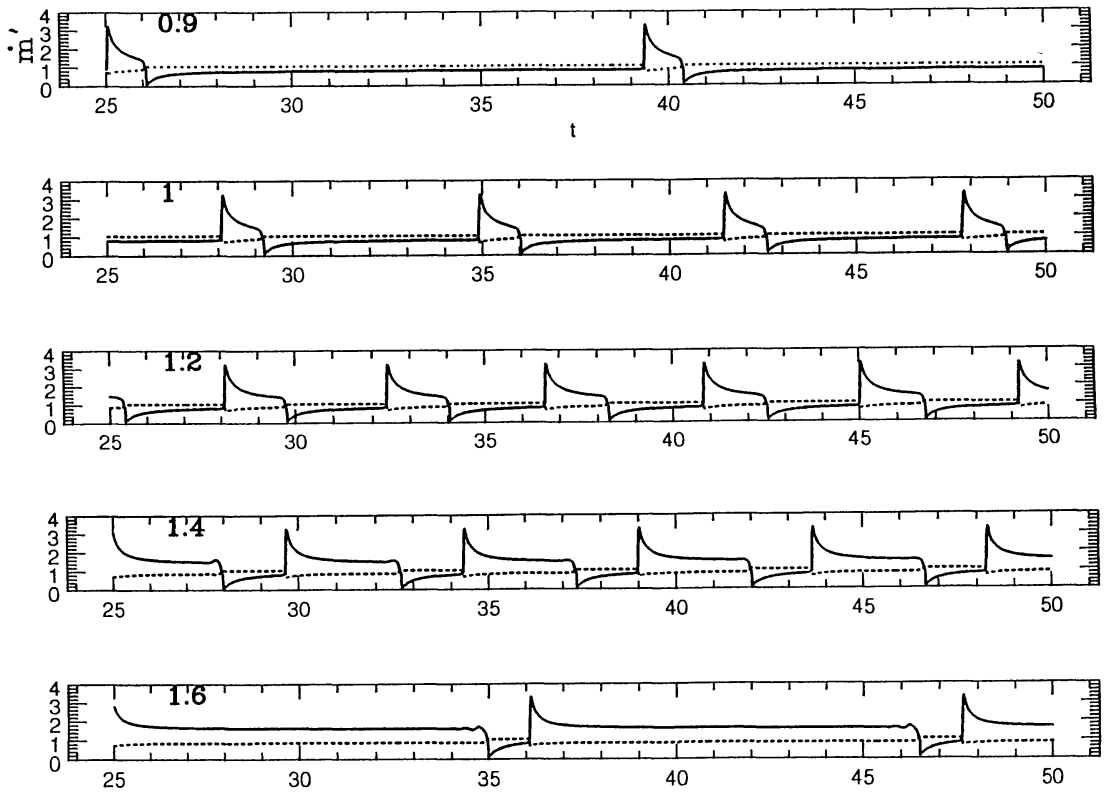

Fig. 8.2. Same as for Fig. 8.1 except that the dependence of the burst properties on the average mass accretion rate ranging from 0.9 to 1.6 is illustrated. The accretion flow in the disk is steady for average accretion rates less than 0.82 and greater than 1.7 in this simulation.

parameter. If the boundary surface density is a sufficiently sensitive function of the fastness parameter, the instability will operate for ω_s close to, but less than unity. The nature of the instability can be understood as follows. Given a slight inward perturbation of the magnetopause, a much lower gas density at the boundary is required. This results in an increase in the mass flux and to a concomittant inward shift of the magnetospause, thus, reinforcing the perturbation. The disk immediately outside the boundary can sustain the mass flow rate above the average, until the depletion of matter requires the displacement of the magnetosphere to beyond the corotation point. Material flow into the magnetosphere is, thus, inhibited by the centrifugal barrier with the matter accumulating on the viscous diffusion timescale. Since the diffusion timescale depends on the spatial extent of the region involved, the corresponding waiting time to the next burst can vary markedly. The cycle repeats when sufficient matter has accumulated in the inner region of the disk to drive the magnetopause inside corotation to initiate the above described instability anew. The burst profiles resulting from the nonlinear evolutionary calculations of the instability (Spruit and Taam 1993) are illustrated in Figures 8.1 and 8.2 for variations in the steepness parameter of the boundary surface density and for variations in the average mass accretion rate respectively. A variety of burst profiles and timescales can be produced. As can be seen the length of the cycle

can be expected to vary and can, in principle, be very long. Since the variation of the magnetopause about the corotation point is essential for the instability Spruit and Taam (1993) suggest that $\omega_s \sim 1$ for some phase in the evolution of the Rapid Burster. It is argued that this parameter distinguishes the Rapid Burster from other low mass X-ray binary systems. Although several properties of the Rapid Burster can be simulated, the model is unable to reproduce the correlation between the burst energy with the time interval to the next burst and the remarkable self similarity observed in the profiles of medium sized bursts (Kawai *et al.* 1990; Tan *et al.* 1991a; see also Sect. 7.5). The failure to explain the $E_b - \Delta t$ relation stems from the fact that, in its present form, the model yields strictly periodic bursts at a given mass accretion rate.

8.5. Areas for Future Work

The theoretical models developed to date are based upon simple considerations of the accretion physics. Although the resultant burst profiles exhibit behavior which is reminiscent of the observed properties of the Rapid Burster, the models should only be regarded as suggestive of the type of phenomena that can be expected. All models are based upon parameterizations of rather complex physical processes and much needed numerical work will be required to understand the interactions between the many processes to place the theoretical basis of the models on a firm foundation. Specific areas for future work will involve multi-dimensional simulations of accretion disks with the goal of identifying the mechanism responsible for the effective viscosity and elucidating the relevance of viscous and thermal instabilities. Equally important will be the large scale studies of the Rayleigh Taylor and Kelvin Helmholtz instabilities in the accretion disk context. The results of such simulations will provide important insights into the global structure of the disk and, in particular, into the detailed structure of the transition region between the magnetosphere and accretion disk. Such studies are expected to be especially fruitful as guides for the future development of models for the Rapid Burster as well as for theoretical models of the quasi-periodic oscillation phenomenon and the secular spin behavior of accreting X-ray pulsars.

9. Individual Burst Sources

9.1. Introduction

In this Chapter we discuss the main results of observations of individual X-ray burst sources, arranged in order of increasing right ascension. Unless noted otherwise burst fluxes and fluences are bolometric. Luminosities given in this Chapter are for isotropic emitters. Several symbols are often used in this Chapter, they have the following meaning. α is the ratio of the average X-ray flux emitted in the persistent emission to that emitted in bursts, either averaged over a time interval much longer than a typical burst interval, or over the time interval since the previous burst (see Sect. 3.7). F_p indicates the persistent X-ray flux, F_{max} the burst peak flux (above the

persistent flux level), E_b the burst fluence (i.e. integrated burst flux). The rise time of a burst is indicated by τ_r, the effective duration of the burst (defined by the ratio $E_b/F_{\max}$) by τ, and the time interval since the previous burst by Δt. γ indicates the ratio of persistent X-ray flux to the peak flux of bursts that show radius expansion (see Sect. 3.8).

9.2. The Sources

9.2.1. 0512–401/NGC 1851

The steady X-ray source 0512–401, located in the globular cluster NGC 1851 (Clark *et al.* 1975; Jernigan and Clark, 1979; Hertz and Grindlay 1983), has been detected in most X-ray surveys, with an average flux of 1.6×10^{-10} erg cm^{-2} s^{-1} [range $(< 1.0$–$4.5) \times 10^{-10}$ erg cm^{-2} s^{-1}]. Variability occurs on a time scale of days; during time scales of the order of hours the source does not vary much (Leahy *et al.* 1983; Ercan *et al.* 1988; Parmar *et al.* 1989b). For a source distance of 10–12 kpc (Alcaino *et al.* 1990) the average persistent X-ray luminosity is $\sim 2 \times 10^{36}$ erg s^{-1}.

Forman and Jones (1976) detected one X-ray burst during an Uhuru scan over the source. During the 15 second transit the flux decreased by a factor 2 (the rise was missed). One burst was detected with SAS–3 (Clark and Li 1977; Cominsky 1980); it had a rise time <0.4 s, a duration of ~10 s, and it reached a peak flux of ~0.2 Crab (corresponding to $\sim 6 \times 10^{37}$ erg s^{-1}). No bursts were seen during 18 hours of EXOSAT observations (Parmar *et al.* 1989b).

9.2.2. 0614 + 091

This is a rather faint source near the galactic anti-center region. Its persistent X-ray flux has been observed to vary between $(0.3$–$2) \times 10^{-9}$ erg cm^{-2} s^{-1}, with an average value of $\sim 8 \times 10^{-10}$ erg cm^{-2} s^{-1} (Davidsen *et al.* 1974; Mason *et al.* 1976a; Forman *et al.* 1978; Warwick *et al.* 1981; Wood *et al.* 1984). Its optical counterpart, V1055 Ori, is an ~19th magnitude blue star whose optical spectrum is typical for a low-mass X-ray binary (Murdin *et al.* 1974; Davidsen *et al.* 1974). A detailed optical study of this star has been made by Machin *et al.* (1990a). Swank *et al.* (1978) observed an X-ray burst with OSO–8 from a 5° circular field of view including 0614 + 091. During their observation, which lasted for ~3 days, the persistent X-ray flux varied between $(5$–$9) \times 10^{-10}$ erg cm^{-2} s^{-1}, on a time scale of a day. The X-ray burst had a rise time of ~5 s, a duration of ~40 s, and reached a peak flux of 3.5×10^{-8} erg cm^{-2} s^{-1}. However, this event looked very different from a normal (type I) X-ray burst in that the color temperature (kT) at the peak was only 0.8 keV, and at no time during the burst exceeded 1.05 keV. Brandt *et al.* (1992) detected an X-ray burst with the WATCH experiment on board the MIR station from an error box (radius $< 1°$) that includes 0614 + 091. The spectral characteristics of this event, which lasted ~100 s, are similar to those of type I X-ray bursts.

9.2.3. 0748–676

This transient source was discovered in 1985 by Parmar *et al.* (1986). The X-ray light curve shows eclipses, lasting ~8 minutes, which occur every orbital cycle of 3.8 h. In addition, intensity dips occur, preferentially in the half orbital cycle preceding the eclipse; these dips are believed to be caused by obscuration of the X-ray source by a thick bulge at the outer edge of the disk where the gas stream from the secondary hits the disk. The orbital period decreases on a time scale of $\sim 5 \times 10^6$ yr, which is two orders of magnitude faster than expected according to simple models of the evolution of low-mass X-ray binaries (Parmar *et al.* 1991; see also Asai *et al.* 1993). Observations of the optical counterpart, UY Vol, showed that the system remained active at least till 1988 (Wade *et al.* 1985; Crampton *et al.* 1986; Schmidtke and Cowley 1987; Van Paradijs *et al.* 1988c).

During nine observations with EXOSAT a total of 37 bursts were detected (Gottwald *et al.* 1986; 1987a). The properties of these bursts, and the intervals between them, were strongly correlated with the persistent X-ray flux, F_p, which varied between $\sim 3 \times 10^{-10}$ and $\sim 2 \times 10^{-9}$ erg cm^{-2} s^{-1}. We can summarize this correlation as follows (Gottwald *et al.* 1986, 1987a).

(i) The average burst interval increased from ~1 h to > 4 h as F_p inceased over the above interval; when F_p was high the burst pattern became irregular. Below $F_p \sim 5 \times 10^{-10}$ erg cm^{-2} s^{-1} bursts occurred on a number of occasions, which were separated by only 10 to 20 minutes (see Sect. 3.5); the second burst in a pair was always at least 3 times less energetic than the first one.

(ii) On average, both $F_{\max}$ and E_b increased with F_p; their average ratio τ decreased from ~25 s to ~8 s when F_p increased over the above interval. All bursts had a rise time of ~6 s, except those that occurred after a waiting time longer than ~5 h, which had $\tau_r \sim 1$ s. When F_p was high, E_b and $F_{\max}$ were correlated. When F_p was low, $F_{\max}$ did not vary much, whereas E_b did; consequently, the range of τ was then rather large [this is similar to what Murakami *et al.* (1980a) observed in 1608–522]. The bursts with the highest peak fluxes showed photospheric radius expansion; their waiting times were all >5 h, and they occurred only when the persistent flux was high.

(iii) Over the above range in F_p the α ratio increased from ~10 to $\sim 10^2$.

(iv) For bursts which occurred when $F_p > 7.5 \times 10^{-10}$ erg cm^{-2} s^{-1} the apparent blackbody radius R_{bb}, taken at an observed colour temperature $kT_c = 1.6$ keV, was 8.7 ± 0.5 km (at an assumed distance of 10 kpc and isotropic emission); for $F_p < 5 \times 10^{-10}$ erg cm^{-2} s^{-1} this value was 4.4 ± 0.5 km. Bursts which came in quick succesion (see above) showed no difference in blackbody radii.

The correlations of α and τ with F_p agree with the overal dependence of these quantities on the persistent luminosity parameter γ (see Sect. 3.8). Since F_p and burst duration τ are correlated, the above dependence of R_{bb} on F_p is related to the correlation between τ and burst temperature $kT_{0.1}$ found by Damen *et al.* (1989) in bursts from 1636–536 (see Sect. 3.8 and 4.7).

9.2.4. 0836–429

This burst source is the northern component of a close pair (separation less than half a degree) of transient sources; the other one is 0834–430, a 12.3 s X-ray pulsar (Aoki *et al.* 1993). 0836–429 is likely the same source as the previouskly detected transient MX0836–42 (Markert *et al.* 1977). Aoki *et al.* (1993) detected 28 X-ray bursts from 0834–429; usually they came at intervals of ~2 hours, but intervals as short as 8 minutes were observed. None of these X-ray bursts showed evidence for photospheric radius expansion.

9.2.5. 1254–690

The orbital period of this source is 3.9 hours as is evident from periodically recurring highly structured dips in the X-ray intensity curve (Courvoisier *et al.* 1986), and from periodic, approximately sinusoidal optical brightness variations (Motch *et al.* 1987). Mason *et al.* (1980) detected an optical burst from the optical counterpart GR Mus (Griffiths *et al.* 1978), which lasted for ~20 s, and rose in 1.7 s to a peak brightness a factor ~2 above the persistent optical flux. During ~52 h of EXOSAT observations Courvoisier *et al.* (1986) detected two X-ray bursts, with rise times of ~1 s, which lasted for ~20 s. At peak fluxes of $\sim 1.1 \times 10^{-8}$ erg cm^{-2} s^{-1} they showed no radius expansion. The average persistent flux $F_p \sim 6 \times 10^{-10}$ erg cm^{-2} s^{-1} corresponds to $\gamma < 0.055$.

9.2.6. 1323–619

This source was detected as a faint source ($\sim 3\mu$Jy) in the Uhuru and Ariel–5 surveys (Forman *et al.* 1978; Warwick *et al.* 1981). In a ~4 h EXOSAT observation Van der Klis *et al.* (1985b) detected a dip in the X-ray intensity curve which lasted for ~1 h. During this dip an (attenuated) X-ray burst occurred. A subsequent 30 h EXOSAT observation showed that the dips occur periodically, at intervals of 2.93 hours, and six more bursts were detected. The burst intervals are very regular (they range between 318 and 326 min), and the bursts are all very similar; none of the bursts show evidence for radius expansion. Since the time resolution of the data was 10 s, a detailed time-resolved spectral analysis of the bursts could not be made. However, from high-time resolution data (without spectral resolution) the rise times of the bursts ($\tau_r = 4.0 \pm 0.6$ s) and the smearing effect on the burst profiles could be estimated. Using this information Parmar *et al.* (1989a) derived a (corrected) average peak burst flux of $(5.2 \pm 0.9) \times 10^{-9}$ erg cm^{-2} s^{-1}, and an average burst duration $\tau = 14 \pm 2$ s. With the average persistent flux $F_p \sim 1.7 \times 10^{-10}$ erg cm^{-2} s^{-1} one finds $\alpha \sim 80$ and $\gamma < 0.033$.

9.2.7. 1455–314/Cen X–4

Cen X–4 was discovered in 1969 as a bright transient source which became twice as bright as Sco X–1 by Conner *et al.* (1969) and Evans *et al.* (1970). The source disappeared on a time scale of ~2 months. Before the outburst a precursor occurred (Belian *et al.* 1972) which had all the properties of a type I X-ray burst. It reached

a maximum flux of 1.4×10^{-6} erg cm^{-2} s^{-1}, and disappeared after a few minutes. No persistent emission was detected from the precursor location.

A second outburst was detected in 1979 by Kaluzienski *et al.* (1980), with a peak brightness only one-fifth of that in 1969, and an ~2.5 times shorter duration (cf. Bouchacourt *et al.* 1984). Matsuoka *et al.* (1980) detected a type I X-ray burst which occurred during the decay of this outburst; this burst had a peak flux of $\sim 1.0 \times 10^{-6}$ erg cm^{-2} s^{-1} ($\gamma \leq 0.018$), and a duration $\tau \sim 7$ s. From the assumption that during the peak of this burst the luminosity does not exceed the Eddington limit a distance <1.2 kpc follows.

Coincident with the 1979 outburst was an optical nova, which reached $V_{\max} \sim 12.8$, and then decreased to a quiescent magnitude $V \sim 18.5$ (Canizares *et al.* 1980). This correlated optical brightness increase is caused by reprocessing of X rays in the accretion disk (cf. Blair *et al.* 1984). During the outburst the optical spectrum was very similar to that of steady LMXB. When the optical magnitude had returned to the quiescent level the optical spectrum showed the presence of late-type stellar absorption features, indicating a K-type secondary star (Van Paradijs *et al.* 1980).

During quiescence Cen X–4 has been detected with EXOSAT at a luminosity level between $(0.2–1.0) \times 10^{33}$ erg s^{-1} (Van Paradijs *et al.* 1987; assumed distance 1.2 kpc). This indication for continued accretion during quiescence is supported by the observation of low-level optical acivity in quiescence (Chevalier *et al.* 1989). The optical observations of Chevalier *et al.* (1989) [see also Cowley *et al.* 1988; McClintock and Remillard 1990] also led to a more accurate spectral classification (K7), and revealed ellipsoidal optical brightness variations with an (orbital) period of 15.1 hours which are caused by the rotational and tidal distortion of the Roche-lobe filling secondary. From the optical data, and the distance limit (<1.2 kpc) Chevalier *et al.* (1989) and McClintock and Remillard (1990) infer a secondary mass $< 0.2\ M_{\odot}$, which indicates that the secondary is probably a very evolved star which has lost most of its hydrogen envelope.

9.2.8. 1516–569/Cir X–1

For some time Circinus X–1 has been considered a black-hole candidate because its erratic intensity variations were somewhat similar to those of Cygnus X–1 (see e.g. Dower *et al.* 1982, for a review of much of the older literature on Cir X–1).

Kaluzienski *et al.* (1976) discovered that the large variability of Cir X–1 contained a periodic component, in the form of flares which were terminated by a very sudden intensity drop (in some cases within a minute) to a low-intensity state. The intensity drops occurred regularly, at intervals of 16.6 days. The radio and infra-red fluxes of Cir X–1 also vary with this 16.6 day period (Glass 1978; Nicolson *et al.* 1980). Subsequent observations showed that there are long-term changes in the 16.6 day X-ray, infra-red and radio intensity curves (see, e.g. Murdin *et al.* 1980; Nicolson *et al.* 1980; Tennant 1987). The 16.6 day period is generally accepted to reflect the orbital period. Murdin *et al.* (1980) proposed a highly eccentric

($e > 0.7$) binary model, in which the sudden turn-offs of the X-ray flux are caused by enhancements in the column density of cold absorbing material along the line of sight, and the long-term X-ray variations are the result of apsidal motion.

A lower limit to the distance of Cir X–1 of 8 kpc has been inferred from an interpretation of the 21 cm hydrogen absorption line profile in terms of a galactic kinematic model (Goss and Mebold 1977). The optical counterpart is a heavily reddened very faint star (Moneti 1992). Cir X–1 is a QPO source (Tennant 1987, 1988).

Tennant *et al.* (1986a) detected 8 X-ray bursts with EXOSAT, at intervals between ~25 and ~45 minutes. The bursts rose in ~3 s to a maximum flux of (3–6) $\times 10^{-9}$ erg cm^{-2} s^{-1}; they had a duration $\tau = 25 \pm 3$ s. The α value during this observation was ~30. There was relatively little softening of the burst spectrum during decay (kT_c decreased from ~2.2 keV to 1.8 keV), therefore Tennant *et al.* (1986a) could not rule out the possibility that these events are not type I X-ray bursts. Because the saturation temperature at the end of burst decay is rather high, it is unlikely that the lack of pronounced softening is caused by the presence of a persistent blackbody component originating from the neutron star (see Sect. 3.3).

Tennant *et al.* (1986b) detected three more X-ray bursts during a later one-day EXOSAT observation, in which the persistent emission gradually rose from $\sim 6 \times 10^{-11}$ to 2×10^{-9} erg cm^{-2} s^{-1}. These three bursts are without doubt type I X-ray bursts, and this showed convincingly that Cir X–1 is a neutron star. One of the bursts showed evidence for radius expansion of the photosphere. Tennant *et al.* (1986b) obtained average values for τ and α of ~10 s, and ~100, respectively. The change in τ and α compared to the previously observed bursts follow the observed general pattern (see Sect. 3.8); however, there is no clear corresponding change in the average persistent flux.

9.2.9. 1608–522

The first observed outburst of the transient source 1608–522 occurred in 1971 (Tananbaum *et al.* 1976; Markert *et al.* 1977), and the source has been undergoing outbursts ever since. These outbursts often recur at intervals of order a year, with peak fluxes up to ~1 mJy, and decay time scales of ~2 months ; however, in some cases the source remained detectable for hundreds of days (Fabbiano *et al.* 1978; White *et al.* 1984). During the 1977 outburst the optical counterpart was identified with an $m_I \sim 18.2$ star (Grindlay and Liller 1978).

Between 1969 and 1976 Belian *et al.* (1976) detected many brief strong X-ray events with the Vela 5 satellites, ten of which were consistent with an origin in one source, whose position coincided with that of the above transient. These events reached peak fluxes in excess of 10^{-7} erg cm^{-2} s^{-1}; since 1608–522 is one of the very few burst sources with maximum burst fluxes this high it is virtually certain that the events discussed by Belian *et al.* (1976) originated from this source.

Grindlay and Gursky (1976b) retrieved four X-ray bursts from the Uhuru data, whose occurrence times indicated that 1608–522 had burst-active and burst-

inactive periods; during the former the bursts recurred at intervals of the order of hours.

Murakami *et al.* (1980a) detected 22 X-ray bursts with Hakucho, whose properties showed a strong correlation with the persistent X-ray flux. When the persistent flux was high ($\sim 300\mu$Jy) the burst peak fluxes were generally high, and variable; the bursts rose within $\sim$2 s, and had a duration $\tau \sim 8$ s. When the persistent source was not detectable ($F_p < 60\mu$Jy) the bursts had low peak fluxes, rise times $\tau_r > 2$ s, and durations τ between 10 and 30 s. The burst frequency did not differ much between these two periods. One of the bursts occurred after a waiting time of only 10 minutes (Murakami *et al.* 1980b). Murakami *et al.* (1980a) drew the remarkable conclusion that "... the persistent flux exerts no direct influence ... on the rate of energy release in the form of bursts." (see also Sect. 3.8).

In one of 22 bursts detected during another Hakucho observation which showed radius expansion, a 0.6 s oscillation was found during the phase of slow contraction of the photosphere (Murakami *et al.* 1987). During this oscillation the high-energy and low-energy fluxes were anti-correlated, consistent with an explanation of the oscillations in terms of radius variations at a constant luminosity.

Tenma observations of 1608–522 confirmed the strong correlation between the properties of the bursts and the persistent emission (Nakamura *et al.* 1989). Apart from the correlation with the persistent flux level, the burst properties (particularly τ and α) appear to be related to the spectral hardness of the persistent source, similar to the results found for 1636–536 and 1705–442 (see Sect. 3.8 and 4.7). When the persistent flux was low the burst spectra showed a high-energy (>10 keV) excess relative to a blackbody fit. This excess was interpreted by Nakamura *et al.* (1989) as the result of comptonization of the burst emission in hot plasma around the neutron star (cf. Mitsuda *et al.* 1989).

Nakamura *et al.* (1988) detected an absorption line in the X-ray spectra during the decay parts of three bursts observed with Tenma; none of these bursts showed evidence for radius expansion. The centroid freqencies of the absorption were all consistent with a single value 4.07 ± 0.07 keV.

EXOSAT observations, during which two bursts were detected, have been discussed by Gottwald *et al.* (1987b) and Penninx *et al.* (1989a).

9.2.10. 1636–536

X-ray bursts were first detected from a 1 square degree region of the sky that included the persistent source 1636–536 with OSO–8 by Swank *et al.* (1976a). Bursts detected with SAS–3 allowed Hoffman, Lewin and Doty (1977a) to define the location of the burst source to be within $\sim 6'$ of that of the persistent source. The bursts observed with OSO–8 and SAS–3 came at intervals between 2.7 and 12.2 hours, and 1636–536 has remained one of the more "reliable" burst sources, which has been extensively observed with Hakucho, Tenma and EXOSAT. Its persistent flux is fairly strong, ranging between $\sim$ (0.7–6) $\times 10^{-9}$ erg cm^{-2} s^{-1}. Optical observations of stars in the SAS–3 error box of 1636–536 led to the identification

of an ~18th magnitude star (V801 Ara) as the optical counterpart (McClintock *et al.* 1977).

Hakucho observations showed (Ohashi *et al.* 1982; see also Ohashi 1981) that the burst profiles vary a lot with respect to peak flux, fluence and rise time. There is a good correlation between the former two quantities, corresponding to burst durations between 6 and 11 s. These variations do not show an obvious relation with properties of the persistent emission. Ohashi (1981) found evidence for a gap in the distribution of peak fluxes, which was confirmed by later observations (see Inoue *et al.* 1984b; Fujimoto *et al.* 1988). Acccording to Sugimoto *et al.* (1984) the fluxes above the gap are equal to the Eddington limit for hydrogen-poor matter, those below the gap are bounded by the Eddington limit for matter with normal composition (see Sect. 3.8).

Part of the Hakucho observations were correlated with optical observations (Pedersen *et al.* 1982a, b; Lawrence *et al.* 1983b; Matsuoka *et al.* 1984). A total of 41 optical bursts were observed, of which 10 were coincident with X-ray bursts (there was no X-ray coverage during the remaining 31 optical bursts). The optical bursts were delayed with respect to the X-ray bursts by $\sim 2.5 \pm 0.6$ s on average; in one case there is evidence that the delay was significantly smaller. The average ratio of optical to X-ray burst energy (corrected for interstellar absorption) is $\sim 6 \times 10^{-4}$. One of the optical/X-ray bursts was observed simultaneously in three optical passbands (Lawrence *et al.* 1983b). The results of these simultaneous observations are consistent with the idea that all optical emission is due to reprocessing of X rays within ~1.5 light-seconds of the neutron star; likely sites for the reprocessing are the accretion disk and a part of the companion star not shielded from X rays by the disk. There is a positive correlation between the strength of the optical bursts and the waiting time since the previous burst.

The optical observations also led to the discovery of a 3.8 hour period in the optical brightness of V801 Ara, which is most likely the orbital period (Pedersen, Van Paradijs and Lewin 1981); this result has been confirmed by subsequent observations (Smale and Mukai 1988; Van Paradijs *et al.* 1990b).

Waki *et al.* (1984) detected a discrete absorption feature at 4.1 keV in the spectra of three X-ray bursts they observed from 1636–536 with Tenma (see also Waki 1984). They interpreted these as a redshifted Lyman α line of a highly ionized atomic species; in the case of helium-like or hydrogenic iron the inferred gravitational redshift factor $(1 + z) \sim 1.6$.

Lewin *et al.* (1987a) observed 27 bursts from 1636–536 during an ~80 hours uninterrupted EXOSAT observation (see also Turner and Breedon 1984, and Breedon *et al.* 1986). They found a good correlation between peak fluxes and fluences of the bursts and the waiting time since the previous burst, which for the weaker bursts is approximately linear, but which flattens off for very long waiting times. No obvious connection was visible between the burst behaviour and the properties of the persistent emission.

Some of the bursts from 1636–536 observed with EXOSAT had complicated

profiles, showing two (Sztajno *et al.* 1985), and even three peaks (Van Paradijs *et al.* 1986a). The peak luminosities of these bursts were below the Eddington limit and they showed no evidence for radius expansion. It is likely that these profiles reflect variations in the rate of generation or release of nuclear energy (see also Melia 1987, and Penninx *et al.* 1987).

From a spectral analysis of all bursts from 1636–536 observed with EXOSAT Damen *et al.* (1989) found a strong correlation between the duration of the bursts and the blackbody radius measured during the burst decay. The origin of the correlation is unclear, but is arguably related to the chemical profile of the neutron star envelope. Van der Klis *et al.* (1990) showed that both the burst duration and the blackbody radius are correlated with the spectral state of the persistent source as indicated by the location of the source in an X-ray color-color diagram (see Fig. 3.16).

9.2.11. 1658–298

Lewin *et al.* (1976e) detected 24 X-ray bursts at regular intervals (2.1 to 2.6 hours) from this source with SAS–3 in October 1976; 17 more bursts were detected in June 1977 (Cominsky 1980). Persistent emission was not detected during either of these observations (this corresponds to $\alpha < 25$). In March 1978 the persistent source was bright, at $\sim 5 \times 10^{-10}$ erg cm^{-2} s^{-1}, but bursts were then not detected (Lewin *et al.* 1978; Share *et al.* 1978; Lewin 1978). HEAO–1 observations showed that during the low state persistent flux is present at a level of $\sim 10^{-10}$ erg cm^{-2} s^{-1} (Cominsky and Wood 1984). High and low states occur in the optical brightness as well, with V ranging between 18.3 (Doxsey *et al.* 1979) and >23 (Cominsky *et al.* 1983). The X-ray intensity curve shows irregular dips (Lewin 1979; Cominsky *et al.* 1983) and eclipses; the orbital period is 7.1 hours (Cominsky and Wood 1984).

9.2.12. 1702–429

In 55 days of Hakucho observations in 1979 (~6 hours net coverage per day) Makishima *et al.* (1982) detected 14 X-ray bursts from a 0.1 deg^2 region of the sky consistent with the position of the persistent X-ray source 4U1702–42 (Forman *et al.* 1978; Jernigan *et al.* 1978). During 40 days of similar observations in April–July 1980 only 2 bursts were detected from this source (Makishima *et al.* 1982). The burst had peak fluxes between 1.0 to 1.8 mJy (3–10 keV), their average duration was ~10 s. The average persistent flux was $\sim 100\mu$Jy; the corresponding value of $\alpha \sim 400$. Oosterbroek *et al.* (1991) detected three X-ray bursts from 1702–429 during one of two EXOSAT observations. They concluded that 1702–429 is an atoll source; the characteristics of the bursts are similar to those of 1636–536 in the banana state. Three X-ray bursts have been observed from 1702–429 by Patterson *et al.* (1989) with TTM/Kvant on board the Mir station. A burst observed with OSO–8 (Swank *et al.* 1976c) may have come from 1702–429. It is possible, but by no means certain, that the burst reported by Marshall *et al.* (1976) came from 1702–429.

9.2.13. 1705–440

During ~68 hours of EXOSAT observations 24 X-ray bursts were detected from 1705–440 (Langmeier *et al.* 1987). The source shows high and low states (range in persistent flux F_p from 3×10^{-10} to 10^{-8} erg cm^{-2} s^{-1}); these states may recur regularly with a period of 223 days (Priedhorsky 1986). The burst intervals and the properties of the bursts depend on F_p, in a way that is similar as observed for 0748–676 (Langmeier *et al.* 1987; Gottwald *et al.* 1989). No bursts were seen in the high state ($F_p \sim 10^{-8}$ erg cm^{-2} s^{-1}). At intermediate persistent flux levels the bursts pattern was irregular, with average intervals of ~5 hours. In the low state ($F_p \sim 2 \times 10^{-9}$ erg cm^{-2} s^{-1}) the bursts occurred at regular intervals of 2.1 to 2.6 hours; three bursts were then observed after very short waiting times (<10 min). None of the bursts showed evidence for radius expansion during the peak. The average peak flux, the effective burst duration τ, and the α ratio vary from $\sim 1.3 \times 10^{-8}$ to 2.0×10^{-8} erg cm^{-2} s^{-1}, from ~20 s to ~6 s, and from ~60 to ~600, respectively, between the low and intermediate states. The blackbody radii R_{bb} observed during the low and intermediate states are $\sim$ 8 and $\sim$ 11 km, respectively (assumed distance 10 kpc, and isotropic emission).

9.2.14. 1715–321

During about a month of Hakucho observations in 1979 (coverage ~6 hours per day) Makishima *et al.* (1981a) detected 3 X-ray bursts from within $\sim 0.5^\circ$ of the position (Jernigan *et al.* 1978) of the rather faint X-ray source 1715–321 (measured 2–10 keV flux values between 15–45μJy, see Markert *et al.* 1976). These bursts rose rather slowly, and had effective durations $\tau \sim 15$ s. No persistent emission was seen above the detection limit of $\sim 100\mu$Jy. The burst activity is low: only one more burst was seen during another ~4 months of similar observations, corresponding to an average burst interval of ~10 days (this includes a correction for bursts that are missed because of limited coverage). This fourth burst (see Tawara *et al.* 1984a) lasted ~150 s, and had a "precursor" separated from the main event by ~6 s. The peak flux and fluence of the burst were $(6.7 \pm 0.4)10^{-8}$ erg cm^{-2} s^{-1}, and $(1.0 \pm 0.1)10^{-5}$ erg cm^{-2}, respectively. The persistent flux was then $< 20\mu$Jy. A similar "fast transient with precursor" (i.e. a very energetic X-ray burst with strong radius expansion, see Sect. 3.4), which lasted for ~150 s, was observed (likely from this source) by Hoffman *et al.* (1978b). Previously, Markert *et al.* (1976) reported the observation with OSO–8 of an ~10 minute flare from a 1.5 deg^2 error box containing 1715–321; it is likely that they observed a similar event.

9.2.15. 1724–307/Ter 2

Swank *et al.* (1977) detected a very long X-ray burst with OSO–8 from an $\sim$ 0.8 deg^2 positional error box that includes the globular cluster Terzan 2. The peak flux and fluence of the burst were 6×10^{-8} erg cm^{-2} s^{-1}, and 5×10^{-6} erg cm^{-2}, respectively. No persistent flux was detected ($F_p < 30\mu$Jy). Since the satellite scanned the source once every 10 s, the burst profile could not be studied

in detail; however, it is likely that this burst was similar to the "fast transients with a precursor" observed, e.g., from 1715–321 and 2127 + 119. During a 30 minute Einstein observation Grindlay *et al.* (1980) detected an X-ray burst from a persistent source ($\gamma = 0.012$) located in the core of Ter 2. The burst had a peak flux $\sim 4 \times 10^{-8}$ erg cm^{-2} s^{-1}, and duration $\tau \sim 15$ s; radius expansion probably occurred during this burst. The burst activity of Ter 2 is sporadic: Makishima *et al.* (1981a) did not detect X-ray bursts during several months of Hakucho coverage (on average 6 hours per day) of a region of the sky including this source. During a 12 hour continuous EXOSAT observation no X-ray bursts were detected; the persistent flux was quite stable at 2.2×10^{-10} erg cm^{-2} s^{-1} (Parmar *et al.* 1989b).

9.2.16. 1728–337

X-ray bursts from 1728–337 were first detected with SAS–3 in March 1976 (Lewin 1976b; Hoffman *et al.* 1976). RMC observations with SAS–3 and Ariel 5 established the connection of the burst source with a source of persistent emission (Hoffman *et al.* 1976; Carpenter *et al.* 1976). In spite of an earlier report (Grindlay and Hertz 1981) this source is not located in a globular cluster (Van Paradijs and Isaacman 1989). An optical counterpart has not yet been found. Further observations of 1728–337 have been made with HEAO–1 (Hoffman *et al.* 1979), Einstein (Grindlay and Hertz 1981), EXOSAT (Foster *et al.* 1986), Astron (Kaminker *et al.* 1989), Ginga (Day and Tawara 1990), and TTM/Kvant (Patterson *et al.* 1989). The time intervals between bursts are fairly regular, but on a time scale of days the average burst intervals drift by a factor ~2. Hoffman, Lewin and Doty (1977b) found a general correlation between the average burst frequency and sizes of bursts. A study of all 96 bursts detected during 48 days of SAS–3 observations spread over 1976 and 1977 was made by Basinska *et al.* (1984). For relatively weak bursts they found a linear relation between burst peak flux $F_{\max}$ and fluence E_b; for stronger bursts this relation saturates at a level $F_{\max} = 7.5 \times 10^{-8}$ erg cm^{-2} s^{-1}, which is also reached by one very energetic burst which showed radius expansion (Hoffman, Cominsky and Lewin 1980). The rise times are generally between 1.0 and 2.5 s, but smaller and larger values also occur. The persistent flux varied between $\sim 2 \times 10^{-9}$ and $\sim 4.5 \times 10^{-9}$ erg cm^{-2} s^{-1}. Except for an anti-correlation between E_b and F_p there is no evidence for a dependence of the burst properties on the strength of the persistent emission. The average value of $\alpha = 110$, with only ~15% variation between different observations. The duration of the burst is well defined; the average value of τ equals 7.8 ± 2.4 (s.d.) s. Sadeh *et al.* (1982) reported the presence of ~12 ms coherent pulsations during and just before one burst observed with HEAO–1 (see Sect. 3.10).

9.2.17. 1730–335 (Rapid Burster)

For extensive information on this source we refer to Chapter 7.

9.2.18. 1731–260

Three bursts were observed from this transient source in August 1989 with the TTM/Kvant camera on board the Mir station by Sunyaev *et al.* (1990). The persistent emission varied between ~50–100 μJy. The bursts lasted 10–20 s, and reached peak intensities of ~0.6 Crab.

9.2.19. 1732–304/Ter 1

Two X-ray bursts were detected with Hakucho from a $0.3^\circ \times 0.2^\circ$ region of the sky containing the globular cluster Terzan 1 (Makishima *et al.* 1981b). The bursts rose and decayed rather slowly; they had peak fluxes $(7.4 \pm 1.0) \times 10^{-8}$ erg cm^{-2} s^{-1} (Inoue *et al.* 1981), and effective duration $\tau \sim 10$ s. Ter 1 was in the field of view of Hakucho for about a month in 1979, and between July 22 and early September 1980, but no further bursts were detected from this source; apparently the burst activity of Ter 1 is sporadic. The persistent X-ray flux was below the detection limit of $\sim 5 \times 10^{-10}$ erg cm^{-2} s^{-1} ($\gamma < 0.007$). No bursts were detected during an ~13 hour continuous EXOSAT observation (Parmar *et al.* 1989b); the persistent flux varied little (average value 2.5×10^{-10} erg cm^{-2} s^{-1}). The persistent source was detected by Skinner *et al.* (1987) at a level of $\sim (1\text{–}3) \times 10^{-10}$ erg cm^{-2} s^{-1}).

9.2.20. 1735–444

The persistent X-ray flux of 1735–444 varies by typically a factor 2 around an average value of 5×10^{-9} erg cm^{-2} s^{-1}. X-ray bursts were discovered by Lewin *et al.* (1977a) using SAS–3. Optical observations of stars in the SAS–3 error box of 1735–444 led to the identification of a V ~17.5 star (V926 Sco) with a UV excess as the optical counterpart of the X-ray source (McClintock *et al.* 1977). The optical and UV properties of this star are remarkably similar to those of the optical counterpart of Sco X–1 (McClintock *et al.* 1978; Canizares *et al.* 1979; Hammerschlag-Hensberge *et al.* 1982; see also White *et al.* 1980). During simultaneous X-ray and optical observations a coincident X-ray/optical burst was observed from 1735–444 (Grindlay *et al.* 1978). The optical burst was delayed with respect to the X-ray burst by ~2.8 s (McClintock *et al.* 1979). Periodic optical brightness variations of V926 Sco show that the orbital period of the system is 3.65 hours (Corbet *et al.* 1986; Smale *et al.* 1986; Van Amerongen *et al.* 1987).

With SAS–3 a total of 57 bursts were detected (Lewin *et al.* 1980). They occurred very irregularly, and their properties did not show a correlation with those of the persistent emission. There is an indication that the average burst interval was correlated with the size of the bursts. The peak fluxes and fluences of the bursts were strongly correlated, corresponding to a mean duration $\tau = 4.4$ s. The average α ratio varied between 380 and 1580.

During an 80 hours continuous EXOSAT observation five bursts were detected (Van Paradijs *et al.* 1988b). The burst intervals varied between ~1 and ~57 hours; however, the fluences hardly increased for intervals above one hour. The α ratio varied between 250 and ~8000. These results indicate that between the bursts not

only hydrogen, but also helium is stably burned. There is a tendency for the bursts to come in clusters (this is also noticeable in the SAS–3 observations, see Lewin *et al.* 1980), which suggests that perhaps the bursts themselves create conditions that quench further burst activity for a while.

The fast-variability characteristics of 1735–444 were studied by Penninx *et al.* (1989b); it is an atoll source (Hasinger and Van der Klis 1989).

9.2.21. 1741–293

Two bursts from this source were observed in August 1989 by In 't Zand *et al.* (1991) using the TTM coded-mask camera on board the Mir station. The peak intensities ranged up to $\sim 30\mu$Jy.

9.2.22. Galactic Center Region

Lewin *et al.* (1976d) detected a total of 28 X-ray bursts from the galactic center region. Most of these bursts came from three distinct sources, MXB 1742–29, MXB 1743–29, and MXB 1743–28, all located within a degree of the galactic center. The positions of 1742–29 and 1743–29 are consistent with those of the transient sources A1742–294 and A1742–289, respectively (Eyles *et al.* 1975; Branduardi *et al.* 1976; Proctor *et al.* 1978; Cruddace *et al.* 1978). A1742–294 remained bright since the 1975 outburst (Watson *et al.* 1981; Skinner *et al.* 1990); A1742–289 decayed to a flux level at most 10^{-3} that of its peak value (Watson *et al.* 1981).

The bursts observed by Lewin *et al.* (1976d) from 1742–29 and 1743–29 came quite regularly, at intervals of 0.55 days (jitter 5.9%), and 1.46 days (jitter 3.4%), respectively. Probably all bursts from 1743–29 showed evidence for photospheric radius expansion. Three bursts were observed from 1743–28; they came at intervals of 18 and 4 minutes.

Proctor *et al.* (1978) reported the detection of three bursts from three different sources in the galactic center region (not coincident with the sources discovered by Lewin *et al.* 1976d); these bursts were much less energetic than those observed by Lewin *et al.* The error box of one of these bursts was consistent with that of a persistent X-ray source (GX + 0.2, –0.2) which probably is a transient (Watson *et al.* 1981; Skinner *et al.* 1987). Two bursts were detected by Watson *et al.* (1981) from the galactic center region; their positional accuracy ($1^\circ \times 1^\circ$) is not sufficient to ascribe them to any of the above burst sources.

Skinner *et al.* (1990) detected an X-ray burst from the source 1744–300, which is the southern component of two X-ray sources, separated by $\sim 3'$. Seven bursts were detected by Warwick *et al.* (1988); all can be accounted for by the sources discovered by Lewin *et al.* (1976d) and 1744–300 (Skinner *et al.* 1987). X-ray bursts from 1742–294 and 1744–300 observed with TTM/Kvant have been reported by Patterson *et al.* (1989) and Sunyaev *et al.* (1991).

9.2.23. 1744–265/GX 3+1

The persistent X-ray flux of the bright galactic-bulge source GX 3 + 1 varies by a factor ~3 around an average value of $\sim 10^{-8}$ erg cm^{-2} s^{-1}. Its fast-variability behaviour has been described by Lewin *et al.* (1987b) and Hasinger and Van der Klis (1989) on the basis of EXOSAT data; GX 3 + 1 is an atoll source. No optical counterpart has been detected so far, due to the high interstellar reddening of GX 3 + 1 (see Naylor *et al.* 1991). During 1979, when the X-ray flux of GX 3+1 was particularly low ($\sim 5 \times 10^{-9}$ erg cm^{-2} s^{-1}), nine X-ray bursts were detected with Hakucho (Makishima *et al.* 1983). The bursts reached peak fluxes of $(4–8) \times 10^{-8}$ erg cm^{-2} s^{-1}, and had fluences of $\sim 3 \times 10^{-7}$ erg cm^{-2}. The occurrence of X-ray bursts when the persistent X-ray flux was low supports the idea that a very high accretion rate inhibits thermonuclear flashes. X-ray bursts from GX 3 + 1 have also been observed by Sunyaev *et al.* (1991) with TTM/Kvant.

9.2.24. 1745–248/Ter 5

Makishima *et al.* (1981b) detected 14 bursts with Hakucho from an $\sim 0.1^\circ \times 0.1^\circ$ region of the sky that includes the globular cluster Terzan 5. The average burst intervals were ~5 hours; two of the bursts were separated by only ~8 min (Inoue *et al.* 1984a). The peak fluxes ranged from $\sim 2 \times 10^{-8}$ to $(6.1 \pm 0.7) \times 10^{-8}$ erg cm^{-2} s^{-1}; the average burst duration was ~10 s (see also Inoue *et al.* 1981). No persistent emission was observed above the detection limit of $\sim 10^{-9}$ erg cm^{-2} s^{-1} ($\gamma < 0.016$). Burst activity of this source is sporadic: the globular cluster was in the field of view of Hakucho from July 15 till early September 1980 (and also for a month in 1979), but bursts were only detected between 1980 August 5–21. The persistent source was not detected during imaging observations with Einstein (Hertz and Grindlay 1983), with an upper limit to its flux of $\sim 2 \times 10^{-12}$ erg cm^{-2} s^{-1}. It was detected during the EXOSAT galactic-plane survey at a flux level of 3×10^{-9} erg cm^{-2} s^{-1} (Warwick *et al.* 1988); this suggests that 1745–248 is a transient source.

9.2.25. 1746–370/NGC 6441

The persistent flux of 1746–370 is in the range 13–80 μJy. Based on a rather large positional error box derived from Uhuru data Giacconi *et al.* (1974) suggested that the X-ray source is associated with the globular cluster NGC 6441. This suggestion was confirmed by subsequent, more accurate positions (Clark *et al.* 1975; Grindlay *et al.* 1976b; Jernigan and Clark 1979; Hertz and Grindlay 1983). NGC 6441 is one of the most metal rich globular clusters (Zinn 1980; Burstein *et al.* 1984), and is located at a distance between 7.4 and 10.2 kpc (Sztajno *et al.* 1987).

Li and Clark (1977) observed two brief X-ray bursts with SAS–3 from a source whose error box included 1746–370. Sztajno *et al.* (1987) detected two X-ray bursts ($\tau_r \sim 1.5$ s, $\tau \sim 5$ s) , separated by 8.5 hours, during a continuous 12 hour EXOSAT observation. Both bursts showed photospheric radius expansion [$F_{\max} = (9.5 \pm 1.0) \times 10^{-9}$ erg cm^{-2} s^{-1}]. With the source distance known

Sztajno *et al.* derived constraints on the mass-radius relation of the neutron star in 1746–370 (see Ch. 4). Parmar *et al.* (1989b) suggested that the X-ray intensity curve (average flux $F_p = 5 \times 10^{-10}$ erg cm^{-2} s^{-1}, $\gamma = 0.05$, $\alpha = 280$) contains two absorption dips, separated by ~5 hours.

9.2.26. 1747–214

This transient source was detected in April 1985 by Parmar *et al.* (1985) with EXOSAT, at a persistent flux level of $\sim 70\mu$Jy; the source was also active about a year earlier during the EXOSAT galactic-plane survey (Warwick *et al.* 1988). During about 9 hours of EXOSAT observations two X-ray bursts were detected (Parmar *et al.* 1985). During the rise part of the second burst the burst spectrum showed an absorption feature at 4.05 ± 0.12 keV, with an equivalent width of 570 ± 87 eV (Magnier *et al.* 1989). The line energy is equal, to within the accuracy of its determination, to those of absorption lines seen in burst spectra from 1636–536 and 1608–522 (Waki *et al.* 1984; Nakamura *et al.* 1988; see Sect. 3.3, 4.6.1, 5.5).

9.2.27. 1811–171/GX 13+1

This bright galactic-bulge source (X-ray flux typically 200–300 μJy, Forman *et al.* 1978; Warwick *et al.* 1981; Wood *et al.* 1984) has recently been classified as an atoll-type source (Hasinger and Van der Klis 1989). GX 13 + 1 is a radio source (Grindlay and Seaquist 1986), and a (heavily reddened) infrared counterpart has been proposed by Garcia *et al.* (1992) and Naylor *et al.* (1991). Garcia *et al.* (1988) found that during a simultaneous VLA-EXOSAT observation the radio and X-ray intensity variations showed no correlations.

Fleischman (1985) reported the detection of an X-ray burst with SAS–3 from a circular area with 3.4 degree FWHM, which included 1812–12 and GX 13+1. Two X-ray bursts were detected from GX 13 + 1 in 1990 with Ginga (W. Lewin, private communication).

9.2.28. 1812–12

Three X-ray bursts from this source were detected in 1982 with Hakucho by Murakami *et al.* (1983). They had rise times $\tau_r \sim 5$ s, and durations $\tau \sim 20$ s. Two of the bursts showed clear evidence for photospheric radius expansion during the peak of the burst ($F_{\max} = 1.7 \times 10^{-7}$ erg cm^{-2} s^{-1}). No persistent source was detected ($F_p < 20\mu$Jy; $\gamma < 0.028$). It is possible that the bursts originate from the persistent source 1H1812–12 (Wood *et al.* 1984; Forman *et al.* 1978; Warwick *et al.* 1981). Murakami *et al.* (1983) suggested that the burst source is associated with the transient Ser X–2, observed once in 1965 (Friedman *et al.* 1967). Fleischman (1985) reported the detection of an X-ray burst with SAS–3 from a circular area with 3.4 degree FWHM, which included 1812–12 and GX 13 + 1.

9.2.29. 1813–140/GX 17 + 2

GX 17 + 2 is a bright Z-type source [average F_p between (1–4) $\times 10^{-8}$ erg cm^{-2} s^{-1}]. Its radio flux is correlated with its X-ray spectral state (Hasinger and Van der Klis 1989; Penninx *et al.* 1988; 1990; cf. White *et al.* 1978b). A V ~17 G star in the radio error box (Tarenghi and Reina 1972; Davidsen *et al.* 1976) is unlikely to be the companion (Van Paradijs and Lewin 1985a; Naylor *et al.* 1991).

Kahn and Grindlay (1984) observed one burst-like event with the MPC on Einstein which lasted ~10 s and reached a peak flux ~50% above the persistent level. Their data did not allow them to make a time-resolved spectral analysis of the burst, and it is unclear whether this event is a type I burst (Kahn and Grindlay preferred an interpretation of the event as a type II burst).

Tawara *et al.* (1984b) observed four X-ray bursts from GX 17 + 2 with Hakucho. All reached a maximum flux of only ~50–70% above the persistent flux, and they lasted very long (τ between 80 and 360 s). Tawara *et al.* could not decide whether these events are type I bursts since they did not show a pronounced softening during the decay, and they differed from previously observed very long type I bursts in not showing evidence for photospheric radius expansion.

Sztajno *et al.* (1986) detected two bursts during four separate EXOSAT observations, lasting between 6.5 and 24 hours. The first burst (rise time ~1 s, duration ~10 s) was similar to the event observed by Kahn and Grindlay (1984). The second burst, which lasted more than 5 minutes, was similar to the bursts observed by Tawara *et al.* (1984b). Both bursts rose to ~40% above the persistent flux level. During the decay of the long burst the blackbody temperature of the burst spectra decreased by only 20%, and the blackbody radius strongly decreased. Sztajno *et al.* showed that this is the result of a contribution to the persistent emission of a blackbody-like component originating from the same neutron star atmosphere which transfers the burst emission (Van Paradijs and Lewin 1985b; see Sect. 3.3). They made a time-resolved two-component spectral analysis of the combined burst and persistent emission, and took account of the deviations of the spectra of neutron stars from Planckian curves (see Chapter 5). They found that the blackbody radius of this spectral component does not vary significantly, and has the same value as in the persistent emission. This analysis showed convincingly that the long bursts from GX 17 + 2 are genuine type I bursts.

The non-standard properties of the long bursts from GX 17 + 2 are likely related to the fact that the accretion rate of this Z-type source is higher than for most other burst sources which are atoll sources (the bursts may have been ignited in a hydrogen-rich environment).

9.2.30. 1820–303/NGC 6624

This source is located in NGC 6624 (Giacconi *et al.* 1974; Jernigan and Clark 1979; Hertz and Grindlay 1983), one of the most metal rich globular clusters in the Galaxy (Zinn 1980; Burstein *et al.* 1984). X-ray bursts from this source were discovered by Grindlay *et al.* (1976a).

From EXOSAT observations Stella *et al.* (1987a) discovered a 685-second periodicity in the X-ray intensity variations of 1820–303, whose long-term stability (Morgan *et al.* 1988; Smale *et al.* 1987) confirms their idea that it reflects the orbital period of the system. The extremely short orbital period implies that the secondary star is a low-mass helium-rich degenerate star (see Rappaport *et al.* 1987). Subsequent observations with Ginga showed that the 685-s period is decreasing on a time scale of $\sim 10^7$ years (Sansom *et al.* 1989; Tan *et al.* 1991b; Van der Klis *et al.* 1992), likely caused by gravitational acceleration in the cluster potential or by a distant third companion in a hierarchical triple (Tan *et al.* 1991b; see also Tavani 1991).

From a decade of observations with Vela 5B Priedhorsky and Terrell (1984b) found that the X-ray flux of 1820–303 shows a 176-day periodic variation with a factor ~2 (average) amplitude. Burst activity is related to the low-intensity state (see below). 1820–30 is an atoll source (Stella *et al.* 1987b; Hasinger and Van der Klis 1989).

In September 1975 Grindlay *et al.* (1976a) detected two X-ray bursts from 1820–303 with ANS, when the persistent X-ray source was in a low state. The bursts rose within a second to their peaks, their duration was less than 10 s. During the bursts the X-ray spectrum was found to become harder, which was initially interpretated in terms of reverberation of a sharp input X-ray signal in a cloud of hot matter surrounding the source, and led to the idea that X-ray bursts originate from black holes (Grindlay and Gursky 1976a; see, however, Canizares 1976; see also Sect. 1.3). We now know (Vacca, Lewin and Van Paradijs 1986) that this hardening is caused by the very rapid photospheric radius expansion (see Sect. 3.4), not resolved in the ANS data.

Clark *et al.* (1977) observed 10 bursts with SAS–3 in May 1975 and 22 in March 1976. During the first observation the average burst interval was ~4.4 h. During the first four days of the second observation the intervals decreased from an average of ~3.4 h to ~2.2 h as the persistent X-ray flux inceased by a factor ~5. During the remaining four days of the observation no additional bursts were observed. This was the first example of a transition from a burst active to a burst-inactive state correlated with the increase of the persistent X-ray flux.

From a detailed analysis of a subset of six of these bursts Vacca, Lewin and Van Paradijs (1986) concluded that all six showed radius expansion during their peaks, and that with the source distance of 6.4 kpc their peak luminosities were consistent with the Eddington limit for a neutron star with a hydrogen-poor envelope.

During most subsequent observations (see Stella *et al.* 1984) the source was in a high state, and bursts were not observed until August 1985, when 7 bursts were detected during a 20 h continuous EXOSAT observation (Haberl *et al.* 1987). These bursts occurred at very regular intervals of 3.21 ± 0.04 hr. They all showed radius expansion by a factor ~20, with a peak luminosity of 2.6×10^{38} erg s^{-1}, for a source distance of 6.4 kpc (Vacca, Lewin and Van Paradijs 1986). As the radius contracted the spectrum hardened, and the blackbody temperature reached

a maximum value of ~3 keV. Based on Haberl *et al.* 's results Van Paradijs and Lewin (1987) attempted to derive constraints on the mass-radius relation of the neutron star in 1820–303 (see also Miyaji 1988; Damen *et al.* 1990b).

9.2.31. 1837 + 049/Ser X–1

Ser X–1 is a relatively bright X-ray source [average persistent X-ray flux $\sim (3\text{–}6) \times 10^{-9}$ erg cm^{-2} s^{-1}] (Forman *et al.* 1978; Warwick *et al.* 1981; Priedhorsky and Terrell 1984a). A 3.4-day periodicity in its persistent X-ray flux was reported by Ponman (1984); this result, in our opinion, needs confirmation. Radio emision has not been detected (Ulmer *et al.* 1978).

X-ray bursts were first detected with OSO–8 from a source within a 5° radius error circle containing Ser X–1 by Swank *et al.* (1976b). Li *et al.* (1977) detected 22 bursts from this source with SAS–3 ; they came from within 10′ of the persistent source Ser X–1 (Doxsey *et al.* 1977a). Based on this position Thorstensen *et al.* (1980) eventually identified the optical counterpart, which enabled Hackwell *et al.* (1979) to detect coincident optical/X-ray bursts (see Sect. 3.9.1).

A detailed analysis of 57 bursts observed during a total of ~28 days of SAS–3 observations between July 1976 and September 1978 was made by Sztajno *et al.* (1983). During these observations the persistent flux of Ser X–1 varied by a factor ~2 around an average value of $\sim 6 \times 10^{-9}$ erg cm^{-2} s^{-1} on a time scale of days. The X-ray bursts came very irregularly, at intervals between ~1 and 38 hours (unlikely to be only the result of bursts being missed by Earth occultations). None of them show evidence for photospheric radius expansion. The burst rise times are rather short, half of them less than 0.4 s, in 10% of the cases longer than 3 s. Sztajno *et al.* found a good correlation between the peak flux $F_{\max}$ and fluence E_b of the bursts, with an average duration $\tau = 6.8 \pm 2.1$ (1 s.d.) s. The variations in burst intervals are not correlated with properties of the persistent emission. However, $F_{\max}$ increases with the persistent flux F_p; since the correlation between E_b and F_p is weak, there is an anti-correlation between F_p and burst duration τ (see also Sect. 3.8).

9.2.32. 1850–087/NGC 6712

Based on Ariel–5 scanning observations Seward *et al.* (1976) suggested that 1850–087 is located in the globular cluster NGC 6712. Their suggestion was confirmed by subsequent observations (Cominsky *et al.* 1977; Grindlay *et al.* 1977; Doxsey *et al.* 1977a; Hertz and Grindlay 1983). The faint blue optical counterpart proposed by Cudworth (1988) is composite (Lehto *et al.* 1990; Nieto *et al.* 1990; Machin *et al.* 1990b); component S is the likely counterpart (Auriere and Koch-Miramond 1992). The persistent X-ray flux varies from $< 8 \times 10^{-11}$ to $\sim 5 \times 10^{-10}$ erg cm^{-2} s^{-1}, with a long-term average value of 2×10^{-10} erg cm^{-2} s^{-1} (Cominsky *et al.* 1977; Forman *et al.* 1978; Warwick et al. 1981; Priedhorsky and Terrell 1984a), which at a distance of 6.5 kpc (Cudworth 1988) corresponds to an X-ray luminosity of $\sim 3 \times 10^{35}$ erg s^{-1}. The burst activity of 1850–087 is sporadic: in 14 days of

SAS–3 observations in 1978 three bursts were detected; two of these occurred at an interval of 17 hours. The third one showed photospheric radius expansion; it reached a maximum flux of $(5.5 \pm 0.5) \times 10^{-8}$ erg cm^{-2} s^{-1}; its duration was 34 s (see Hoffman *et al.* 1980). Swank *et al.* (1976c) detected one burst (peak flux ~1.5 Crab units) with OSO–8 from within a few degrees of NGC 6712. During Uhuru scans Cominsky *et al.* (1977) detected a flare, in which the intensity rose by a factor of 40 in less than 5.5 minutes, and then decayed with an e-folding time of ~3 minutes. It is unlikely that this event was a "fast transients with a precursor" (see Sect. 3.4), since the peak luminosity was only a few times 10^{37} erg s^{-1}, i.e. much smaller than the Eddington limit. No bursts were detected during a 13 hour continuous EXOSAT observation; the persistent flux was stable, at 1.4×10^{-10} erg cm^{-2} s^{-1} (Parmar *et al.* 1989b).

9.2.33. 1905+000

The persistent X-ray flux of 1905 + 000 is in the range $(2\text{–}7) \times 10^{-10}$ erg cm^{-2} s^{-1}, but is most often found near $\sim 3 \times 10^{-10}$ erg cm^{-2} s^{-1} (see Chevalier and Ilovaisky 1990, for references). Lewin *et al.* (1976b) discovered five bursts from 1905+000 at average intervals of ~5 hours ($\alpha \sim 80$). These bursts had risetimes of less than 0.8 s. Matsuoka (1980) reported on the observation with Hakucho of an X-ray burst which showed evidence for photospheric radius expansion. Chevalier and Ilovaisky (1990) made a time-resolved spectral analysis of one radius-expansion burst detected during a continuous 19 hour EXOSAT observation. This burst had a rise time of ~2.5 s, a peak flux of 3.2×10^{-8} erg cm^{-2} s^{-1} ($\gamma \sim 0.02$, $\alpha > 50$), and a fluence of 8.4×10^{-7} erg cm^{-2}. It showed a substantial spectral hardening, when its luminosity approached the Eddington limit, with a colour temperature of 3.5 ± 0.7 keV. The optical counterpart (Chevalier *et al.* 1985) is substantially less luminous than that of the average low-mass X-ray binary (Van Paradijs 1981, 1983; Van Paradijs and McClintock 1993).

9.2.34. 1908 + 005/Aql X–1

Aql X–1 is a recurrent soft X-ray transient, with outburst intervals of roughly a year (Kaluzienski *et al.* 1977; Charles *et al.* 1980; Priedhorsky and Terrell 1984a). The outbursts last typically a month, and peak fluxes as high as 4×10^{-8} erg cm^{-2} s^{-1} have been reached in some of them. Czerny *et al.* (1987) reported the detection of Aql X–1 in quiescence with the Einstein MPC, with a (1–10 keV) flux of $(2.1 \pm 0.2) \times 10^{-11}$ erg cm^{-2} s^{-1}. Aql X–1 was not detected with the low-energy telescope on EXOSAT, with an upper limit to the (1–4.5 keV) flux of $(1.4\text{–}3.0) \times 10^{-12}$ erg cm^{-2} s^{-1} (Van Paradijs *et al.* 1987). If the signal detected by Czerny *et al.* (1987) originated from Aql X–1 this would indicate that in quiescence the source varies by at least a factor 3. The optical counterpart of Aql X–1 is a variable star (V1333 Aql) whose brightness is correlated with the X-ray outbursts (Margon *et al.* 1978; Thorstensen *et al.* 1978; Charles *et al.* 1980). In quiescence (V1333 Aql) has a late-type (G7–K3) spectrum (Thorstensen

et al. 1978). Chevalier and Ilovaisky (1991) discovered a 19-hour periodicity in the optical brightness variations of V1333 Aql, which likely reflects the orbital period.

Two X-ray bursts were observed in May 1980 with Hakucho (Koyama *et al.* 1981), and two in April 1979 with Einstein (Czerny *et al.* 1987), during the decay parts of outbursts. The first pair of bursts occurred when the persistent flux had decayed to $\sim 2 \times 10^{-9}$ erg cm^{-2} s^{-1}; they reached peak fluxes $\sim 1.1 \times 10^{-7}$ erg cm^{-2} s^{-1}, and their duration $\tau \sim 10$ s. For the second pair of bursts these numbers are (5–8) $\times 10^{-9}$ erg cm^{-2} s^{-1}, $\sim 7 \times 10^{-8}$ erg cm^{-2} s^{-1}, and ~10 and ~18 s, respectively. After one of the latter bursts the persistent emission was enhanced by ~25% compared to the pre-burst level for 2500 s after the burst. Acording to Fushiki *et al.* (1992) this is caused by a long phase of hydrogen burning , which occurs only after the first thermonuclear flash in a transient outburst. One burst detected with SAS–3 from Aql MXB (Lewin *et al.* 1976b) likely originated from Aql X–1 (Lewin, private comm.).

Schoelkopf and Kelley (1991) detected a 7.6-Hz coherent oscillation at a 4.1σ confidence level during an X-ray burst from Aql X–1 observed with Einstein, which they argue reveals the spin period of the neutron star .

9.2.35. 1916–053

Eleven X-ray bursts were detected in April 1976 with OSO–8 from a 15 sq. deg. region containing the source 1916–053 (Swank *et al.* 1976c; Becker *et al.* 1977). SAS–3 burst observations in June 1977 refined the error box to 0.07 sq. deg. and confirmed 1916–053 as burst source (Lewin*et al.* 1977c). Bursts have subsequently been observed with HEAO–1 (Swank *et al.* 1984) and EXOSAT (Smale *et al.* 1988). Bursts intervals are typically 4 to 6 hours; however, no X-ray bursts were seen by Smale *et al.* (1989) during 14 hours of Ginga observations. Radius expansion was not observed in these bursts; however, in some bursts very high color temperatures (~3 keV) occurred near the peak, and it is likely that in these bursts the peak luminosity was close to the Eddington limit.

Interpretating this peak flux as the Eddington limit of a 1.4 $M_\odot$ object Smale *et al.* (1988) derived a distance to 1916–053 of ~10 kpc. Then the absolute magnitude of the optical counterpart (Grindlay *et al.* 1988), corrected for interstellar absorption ($A_V \sim 1$; Smale *et al.* 1988) is $M_V \sim 4$. This is much fainter than the average value for LMXB ($M_V \sim 1$; Van Paradijs 1981, 1983; Van Paradijs and McClintock 1993).

The persistent X-ray flux (outside dips) is in the range (0.5–6) $\times 10^{-10}$ erg cm^{-2} s^{-1} (Forman *et al.* 1978; Warwick *et al.* 1981; γ ~0.01). The α ratio varies between ~ 120 (Swank *et al.* 1984) and 170 (Smale *et al.* 1988). Most of the bursts have durations $\tau \sim 5$ s, but some bursts last up to a factor 2 longer. The persistent X-ray flux shows long-term variability which may be periodic (Priedhorsky and Terrell 1984a). The X-ray intensity curve shows recurrent irregular dips, with a period of 3005.0 ± 6.6 s (White and Swank 1982; Walter *et al.* 1982; Smale *et al.* 1988, 1989), which is different from the period (3027.4 ± 0.4s) observed in the

optical brightness variations (Schmidtke 1988; Grindlay *et al.* 1988). This has been explained in terms of a triple model (Grindlay 1989), and as the LMXB equivalent of superhumps (Whitehurst 1988).

9.2.36. 1940–04

Murakami *et al.* (1983) detected a small X-ray flare from a region of the sky at $\alpha = 19^{h}40^{m} \pm 4^{m}$, $\delta = -4 \pm 1°$, which lasted for ~30 s. This may have been a type I burst. No persistent flux was detected ($F_X < 50$ μJy). There is no catalogued X-ray source in the error box.

9.2.37. 2127 + 119/M15

The X-ray source 2127 + 119 is located in the globular cluster M15 (Giacconi *et al.* 1974; Jernigan and Clark 1979; Hertz and Grindlay 1983). The optical counterpart has been identified with the star AC 211 on the basis of positional coincidence and colours (Auriere *et al.* 1984) and the presence of the He II λ 4686 emission line in its spectrum (Charles *et al.* 1986). The orbital period of 8.5 hours has been detected in optical and X-ray variations (Ilovaisky *et al.* 1987; Naylor *et al.* 1988; Hertz 1987; Callanan *et al.* 1989). One very energetic X-ray burst has been observed from 2127+119, which showed very strong photospheric radius expansion leading to a "fast transient with precursor" profile (Dotani *et al.* 1990b; Van Paradijs *et al.* 1990a; see Sect. 3.4). The burst reached a peak flux of $\sim 4 \times 10^{-8}$ erg cm^{-2} s^{-1}, its fluence was 5.0×10^{-6} erg cm^{-2}, and it lasted for ~150 s. During the first 30 s of the burst a series of slow oscillations of the photospheric radius were observed whose termination may signify the transition from an outflowing neutron star wind to a static extended (but slowly shrinking) envelope (see Sect. 3.4). From a time-resolved spectral analysis of the burst it appears that the burst spectra deviate from a blackbody in a way that cannot be described in terms of a spectral hardening alone (Van Paradijs *et al.* 1990a).

9.2.38. 2129+470

Optical brightness variations show that 2129 + 470 has an orbital period of 5.24 hours (Thorstensen *et al.* 1979; McClintock *et al.* 1981). This period has also been observed in variations of the X-ray intensity (McClintock *et al.* 1982; White and Holt 1982) and the radial velocity (Thorstensen and Charles 1982; Horne *et al.* 1986). The shape of the X-ray eclipse indicates that the observed X rays come from an extended source, most likely an accretion-disk corona which scatters a small fraction of the X rays over the edge of the accretion disk; the compact X-ray source itself is always occulted by the disk (McClintock *et al.* 1982; White and Holt 1982). 2129 + 470 was a moderately bright X-ray source until the mid 1980's, after which it went into a low state (Pietsch *et al.* 1986). During this low state the optical counterpart does not show the expected ellipsoidal brightness variations (Thorstensen *et al.* 1988). It is likely that the optical light in the low state is dominated by another star in the line of sight; 2129+470 may be a triple system

(Thorstensen *et al.* 1988).

Garcia and Grindlay (1987) detected one type I X-ray burst from 2129 + 470 which reached a peak luminosity of a few 10^{35} erg s^{-1}; this result supports the accretion-disk corona model in which the direct emission from the neutron star (thus also the burst emission) is obscured by the disk.

9.2.39. 2142 + 380/Cyg X–2

Cyg X–2 is a Z-type LMXB (Hasinger and Van der Klis 1989; Hasinger *et al.* 1990); according to current ideas this implies that the X-ray luminosity is near the Eddington limit (Hasinger 1987; Lamb 1989, 1991). Optical spectroscopic and photometric observations show that the orbital period of Cyg X–2 is 9.8 days (Cowley *et al.* 1979). Kahn and Grindlay (1984) detected a burst-like event from Cyg X–2, which lasted ~5 s, and reached a peak flux $F_{max} = 1.1 \times 10^{-8}$ erg cm^{-2} s^{-1} (corresponding to an increase of only a factor 2 above the persistent flux). The spectrum of the whole event was consistent with that of a 2 keV blackbody (the statistical accuracy of the data did not allow a time-resolved spectral analysis of the event). It is unclear whether this event is a type I X-ray burst; if it is, its rarity may be related to the high persistent luminosity of Cyg X–2 (see Sect. 3.8).

9.3. X-Ray Bursts from Unknown Sources

A number of bursts have been reported with very uncertain locations. For several of these the error boxes include known persistent X-ray sources, but identification with one of these is not well possible.

Doty (1976) reported the detection of a burst from a direction centered on $\alpha = 114°$, $\delta = -50°$. The error circle of 13° radius includes the transient source 0836–429 (see Sect. 9.2.4.). The large error box for the burst centered on $\ell^{II} = 315°$, $b^{II} = -4°$ (listed by Lewin and Joss 1983) includes the burst source 1254–690 (see Sect. 9.2.5.). Swank *et al.* (1976c) reported the detection of four X-ray bursts from a region, centered on $\ell^{II} = 4°$, $b^{II} = -4°$, which contains the globular cluster NGC 6553. The 8° × 8° error box for two bursts detected by Becker *et al.* (1976) includes five globular clusters (NGC 6638, NGC 6642, NGC 6656, NGC 6716, and Pal 8), and the transient X-ray source 1826–240 (Makino *et al.* 1988; In 't Zand *et al.* 1989). The event from a region centered on $\ell^{II} = 200°$, $b^{II} = -5°$ may have originated from 0614 + 091 (see Sect. 9.2.2.). According to Swank (as quoted by Lewin 1979) the event from a region centered on $\ell^{II} = 79°$, $b^{II} = -9°$, is suspect. Hoffman *et al.* (1978b) detected two very strong X-ray bursts ("fast transients with precursors", see Sect. 3.4). One event likely originated from 1715–321 (see Sect. 9.2.14); the very large error box of the other event includes 4U1708–23, but it is uncertain whether this source is the origin for the burst.

Acknowledgements

This work was supported in part by the National Aeronautics and Space Administration under Grants NAGW–2526, NAGW–2935 and NAG8–700, and by the National Science Foundation under Grant No. PHY89–04035. This manuscript was written in part at the Institute for Theoretical Physics in Santa Barbara and at the Aspen Center for Physics. WHGL thanks L.M. Lubin for her valuable contributions. We thank T. Oosterbroek, L.M. Lubin, R. Rutledge, and E.I. Favery for their assistence in preparing many figures.

References

Abramenko, A. N., Gershberg, R. E., Pavlenko, E. E., Prokof'eva, V. V., Lewin, W. H. G., Van Paradijs, J., Hoffman, J. A., and Li, F. K.: 1978, *Monthly Notices Roy. Astron. Soc.* **184**, 27P.

Alcaino, G., Liller, W., Alvarado, F., and Wenderoth, E.: 1990, *Astron. J.* **99**, 817.

Alpar, M. A. and Shaham, J.: 1985, *Nature* **316**, 239.

Alpar, M. A., Hasinger, G., Shaham, J., and Yancopoulos, S.: 1992, *Astron. Astrophys.* in press, and in E. P. J. van den Heuvel and S. A. Rappaport (eds) *X-ray Binaries and Recycled Pulsars* (Kluwer Academic Publ.), NATO ASI Series C, **377**, 527.

Aoki, T., Dotani, T., Ebisawa, K., Itoh, M., Makino, F., Nagase, F., Takeshima, T., Mihara, T., and Kitamoto, S.: 1993, *Publ. Astron. Soc. Japan* **45**, in press.

Apparao, K. V. M. and Chitre, S. M.: 1980, *Astrophys. Space Sci.* **72**, 127.

Apparao, K. M. V., Chitre, S. M., Ashok, N. M., and Kulkarni, P. V.: 1979, *IAU Circular* No. 3344.

Arnett, W. D. and Bowers, R. L.: 1977, *Astrophys. J. Suppl.* **33**, 415.

Asai, K., Dotani, T., Nagase, F., Corbet, R. H. D., and Shaham, J.: 1993, *Publ. Astron. Soc. Japan* **45**, in press.

Auriere, M. and Koch-Miramond, L.: 1992, *Astron. Astrophys.* **263**, 82.

Auriere, M., Le Fevre, O., and Terzan, A.: 1984, *Astron. Astrophys.* **138**, 415.

Ayasli, S. and Joss, P. C.: 1982, *Astrophys. J.* **256**, 637.

Baan, W. A.: 1977, *Astrophys. J.* **214**, 245.

Baan, W. A.: 1979, *Astrophys. J.* **227**, 987.

Babul, A. and Paczynski, B.: 1987, *Astrophys. J.* **323**, 582.

Barr, P., White, N. E., Haberl, F., Stella, L., Pollard, G., Gottwald, M., and Parmar, A. N.: 1987, *Astron. Astrophys.* **176**, 69.

Basinska, E. M., Lewin, W. H. G., Cominsky, L. R., Van Paradijs, J., and Marshall, F. J.: 1980, *Astrophys. J.* **241**, 787.

Basinska, E. M., Lewin, W. H. G., Sztajno, M., Cominsky, L., and Marshall, F. J.: 1984, *Astrophys. J.* **281**, 337.

Baym, G. and Pethick, C.: 1979, *Ann. Rev. Astron. Astrophys.* **17**, 415.

Becker, R. H., Pravdo, S. H., Serlemitsos, P. J., and Swank, J. H.: 1976, *IAU Circular* No. 2953.

Becker, R. H., Smith, B. W., Swank, J. H., Boldt, E. A., Holt, S. S., Pravdo, S. H., and Serlemitsos, P. J.: 1977, *Astrophys. J.* **216**, L101.

Belian, R. D., Conner, J. P., and Evans, W. D.: 1972, *Astrophys. J.* **171**, L87.

Belian, R. D., Conner, J. P., and Evans, W. D.: 1976, *Astrophys. J.* **206**, L135.

Bernacca, P. L., Bianchini, A., Walker, A., Backman, D., Canizares, C. R., Van Paradijs, J., Hoffman, J. A., Doty, J., Marshall, H., Wheaton, W., Jernigan, J. G., and Lewin, W. H. G.: 1979, *Monthly Notices Roy. Astron. Soc.* **186**, 287.

Bhattacharya, D. and Srinivasan, G.: 1986, *Current Sci.* **55**, 327.

Bhattacharya, D. and Srinivasan, G.: 1991, in J. Ventura and D. Pines (eds), *Neutron Stars: Theory and Observation*, (Kluwer Academic Publ.), NATO ASI Series C, **344**, 219.

Bhattacharya, D. and Srinivasan, G.: 1993, in W. H. G. Lewin, J. van Paradijs, and E. P. J. van den Heuvel (eds.), *X-ray Binaries*, Cambridge University Press (Cambridge), in press.

Bhattacharya, D. and Van den Heuvel, E. P. J.: 1991, *Physics Reports* **203**, 1.

Bildsten, L., Salpeter, E. E., and Wasserman, I.: 1992, *Astrophys. J.* **384**, 143.
Bionta, R. M., Blewitt, G., Bratton, C. B., Casper, D., Ciocio, A., Claus, R., Cortez, B., Crouch, M., Dye, S. T., Errede, S., Foster, G. W., Gajewski, W., Ganezer, K. S., Goldhaber, M., Haines, T. J., Jones, T. W., Kielczewska, D., Kropp, W. R., Learned, J. G., LoSecco, J. M., Matthews, J., Miller, R., Mudan, M. S., Park, H. S., Price, L. R., Reines, F., Schultz, J., Seidel, S., Shumard, E., Sinclair, D., Sobel, H. W., Stone, J. L., Sulak, L. R., Svoboda, R., Thornton, G., Van der Velde, J. C., and Wuest, C.: 1987, *Phys. Rev. Lett.* **58**, 1494.
Bisnovatyi-Kogan, G. S. and Komberg, B. V.: 1974, *Sov. Astron.* **18**, 217.
Blair, W. P., Raymond, J. C., Dupree, A. K., Wu, C. C., Holm, A. V., and Swank, J. H.: 1984, *Astrophys. J.* **278**, 270.
Bohlin, R. C., Savage, B. D., and Drake, J. F.: 1978, *Astrophys. J.* **224**, 132.
Bouchacourt, P., Chambon, G., Niel, M., Refloch, A., Estulin, I. V., Kuznetsov, A. V., and Melioransky, A. S.: 1984, *Astrophys. J.* **285**, L67.
Bowyer, S., Byram, E. T., Chubb, T. A., and Friedman, H.: 1964, *Science* **146**, 912.
Brandt, S., Castro-Tirado, A. J., Lund, N., Dremin, V., Lapshov, I., and Sunyaev, R.: 1992, *Astron. Astrophys.* **262**, L15.
Branduardi, G., Ives, J. C., Sanford, P. W., Brinkman, A. C., and Maraschi, L.: 1976, *Monthly Notices Roy. Astron. Soc.* **175**, 47P.
Breedon, L. M., Turner, M. J. L., King, A. R., and Courvoisier, T. J. -L.: 1986, *Monthly Notices Roy. Astron. Soc.* **218**, 487.
Burbidge, G.: 1963, *Astrophys. J.* **137**, 995.
Burbidge, G.: 1972, *Comm. Astrophys. Space Sci.* **4**, 105.
Burstein, D., Faber, S. M., Gaskell, C. M., and Krumm, N.: 1984, *Astrophys. J.* **287**, 586.
Calla, O. P. N., Barathy, S., and Snagal, A. K.: 1980a, *IAU Circular* No. 3458.
Calla, O. P. N., Barathy, S., and Snagal, A. K.: 1980b, *IAU Circular* No. 3467.
Calla, O. P. N., Bhandari, S. M., Deshpande, M. R., and Vats Hari, O. M.: 1979, *IAU Circular* No. 3347.
Callanan, P. J., Charles, P. A., Hassall, B. J. M., Machin, G., Mason, K. O., Naylor, T., Smale, A. P., and Van Paradijs, J.: 1990, *Monthly Notices Roy. Astron. Soc.* **238**, 25P.
Callanan, P. J., Naylor, T., and Charles, P. A.: 1989, *Proc. 11th North American Workshop on Low-mass X-ray Binaries and Cataclysmic Variables*, Santa Fe, N.M. October 1989.
Cameron, A. G. W.: 1959, *Astrophys. J.* **130**, 916.
Canizares, C. R.: 1976, *Astrophys. J.* **207**, L101.
Canizares, C. R., McClintock, J. E., and Grindlay, J. E.: 1979, *Astrophys. J.* **234**, 556.
Canizares, C. R., McClintock, J. E., and Grindlay, J. E.: 1980, *Astrophys. J.* **236**, L55.
Carpenter, G. F., Skinner, G. K., Wilson, A. M., and Willmore, A. P.: 1976, *Nature* **262**, 473.
Castor, J. I.: 1974, *Astrophys. J.* **189**, 273.
Celnikier, L. M.: 1977, *Astron. Astrophys.* **60**, 421.
Charles, P. A., Jones, D. C., and Naylor, T.: 1986, *Nature* **323**, 417.
Charles, P. A., Thorstensen, J. R., Bowyer, S., Clark, G. W., Li, F. K., Van Paradijs, J., Remillard, R., Holt, S. S., Kaluzienski, L. J., Junkkarinen, V. T., Puetter, R. C., Smith, H. E., Pollard, G. S., Sanford, P. W., Tapia, S., and Vrba, F. J.: 1980, *Astrophys. J.* **237**, 154.
Chevalier, C. and Ilovaisky, S. A.: 1990, *Astron. Astrophys.* **228**, 119.
Chevalier, C. and Ilovaisky, S. A.: 1991, *Astron. Astrophys.* **251**, L11.
Chevalier, C., Ilovaisky, S. A., and Charles, P. A.: 1985, *Astron. Astrophys.* **147**, L3.
Chevalier, C., Ilovaisky, S. A., Van Paradijs, J., Pedersen, H., and Van der Klis, M.: 1989, *Astron. Astrophys.* **210**, 114.
Chiu, H. Y.: 1964, *Ann. Phys.* **26**, 364.
Chiu, H. Y. and Salpeter, E. E.: 1964, *Phys. Rev. Lett.* **12**, 413.
Clark, G. W.: 1965, *Phys. Rev. Lett.* **14**, 91.
Clark, G. W. and Li, F. K.: 1977, *IAU Circular* No. 3092.
Clark, G. W., Li, F. K., Canizares, C., Hayakawa, S., Jernigan, G., and Lewin, W. H. G.: 1977, *Monthly Notices Roy. Astron. Soc.* **179**, 651.
Clark, G. W., Markert, T. H., and Li, F. K.: 1975, *Astrophys. J.* **199**, L93.
Clayton, D. D.: 1968, *Principles of Stellar Evolution and Nucleosynthesis* (McGraw-Hill Book Cy).

Cominsky, L. R.: 1980, Ph. D. Thesis, Massachusetts Institute of Technology.
Cominsky, L. R. and Wood, K. S.: 1984, *Astrophys. J.* **283**, 765.
Cominsky, L., Forman, W., Jones, C., and Tananbaum, H.: 1977, *Astrophys. J.* **211**, L9.
Cominsky, L., Ossman, W., and Lewin, W. H. G.: 1983, *Astrophys. J.* **270**, 226.
Conner, J. P., Evans, W. D., and Belian, R. D.: 1969, *Astrophys. J.* **157**, L157.
Corbet, R. H. D., Thorstensen, J. R., Charles, P. A., Menzies, J. W., Naylor, T., and Smale, A. P.: 1986, *Monthly Notices Roy. Astron. Soc.* **222**, 15P.
Cordova, F.: 1993, in W. H. G. Lewin, J. van Paradijs, and E. P. J. van den Heuvel (eds), *X-ray Binaries*, Cambridge University Press, in press.
Courvoisier, T. J. -L., Parmar, A. N., Peacock, A., and Pakull, M.: 1986, *Astrophys. J.* **309**, 265.
Cowie, L. L., Ostriker, J. P., and Stark, A. A.: 1978, *Astrophys. J.* **226**, 1041.
Cowley, A. P., Crampton, D., and Hutchings, J. B.: 1979, *Astrophys. J.* **231**, 539.
Cowley, A. P., Hutchings, J. B., Schmidtke, P. C., Hartwick, F. D. A., Crampton, D., and Thompson, I. B.: 1988, *Astron. J.* **95**, 1231.
Crampton, D., Cowley, A. P., Stauffer, J., Ianna, P., and Hutchings, J. B.: 1986, *Astrophys. J.* **306**, 599.
Cruddace, R. G., Fritz, G., Shulman, S., Friedman, H., McKee, J., and Johnson, M.: 1978, *Astrophys. J.* **222**, L95.
Cudworth, K. S.: 1988, *Astron. J.* **96**, 105.
Czerny, M. and Sztajno, M.: 1983, *Acta Astron.* **33**, 213.
Czerny, M., Czerny, B., and Grindlay, J. E.: 1987, *Astrophys. J.* **312**, 122.
Damen, E.: 1990, Ph.D. Thesis, University of Amsterdam.
Damen, E., Jansen, F., Penninx, W., Oosterbroek, T., Van Paradijs, J., and Lewin, W. H. G.: 1989, *Monthly Notices Roy. Astron. Soc.* **237**, 523.
Damen, E., Magnier, G., Lewin, W. H. G., Tan, J., Penninx, W., and Van Paradijs, J.: 1990b, *Astron. Astrophys.* **237**, 103.
Damen, E., Wijers, R. A. M. J., Van Paradijs, J., Penninx, W., Oosterbroek, T., Lewin, W. H. G., and Jansen, F.: 1990a, *Astron. Astrophys.* **233**, 121.
Datta, B.: 1988, *Fundam. Cosmic Phys.* **12**, 151.
Davidsen, A., Malina, R., and Bowyer, S.: 1976, *Astrophys. J.* **203**, 448.
Davidsen, A., Malina, R., Smith, H., Spinrad, H., Margon, B., Mason, K., Hawkins, F., and Sanford, P.:1974, *Astrophys. J.* **193**, L25.
Davidson, G. T.: 1982, *Astrophys. J.* **255**, 705.
Day, C. and Tawara, Y.: 1990, *Monthly Notices Roy. Astron. Soc.* **245**, 31P.
Day, C. S. R. and Dove, C.: 1991, *Monthly Notices Roy. Astron. Soc.* **253**, 35P.
Day, C. S. R., Fabian, A. C., and Ross, R. R.: 1992, *Monthly Notices Roy. Astron. Soc.* **257**, 471.
Dennerl, K.: 1991, Ph.D. Thesis Ludwig-Maximilians University, Munich, MPE Report 232.
Dotani, T.: 1990: Ph.D. Thesis, University of Tokyo, *ISAS Research Note* **418**.
Dotani, T., Inoue, H., Murakami, T., Nagase, F., Tanaka, Y., Tsuru, T., Makishima, K., Ohashi, T., and Corbet, R. H. D.: 1990b, *Nature* **347**, 534.
Dotani, T., Mitsuda, K., Inoue, H., Tanaka, Y., Kawai, N., Tawara, Y., Makishima, K., Van Paradijs, J., Penninx, W., Van der Klis, M., Tan, J., and Lewin, W. H. G.: 1990a, *Astrophys. J.* **350**, 395.
Doty, J.: 1976, *IAU Circular* No. 2922.
Dower, R. G., Bradt, H. V., and Morgan, E. H.: 1982, *Astrophys. J.* **261**, 228.
Doxsey, R. E., Apparao, K. M. V., Bradt, H. V., Dower, R. G., and Jernigan, J. G.: 1977a, *Nature* **269**, 112.
Doxsey, R. E., Apparao, K. M. V., Bradt, H. V., Dower, R. G., and Jernigan, J. G.: 1977b, *Nature* **270**, 586.
Doxsey, R., Grindlay, J., Griffiths, R., Bradt, H., Johnston, M., Leach, R., Schwartz, D., and Schwarz, J.: 1979, *Astrophys. J.* **228**, L67.
Ebisuzaki, T.: 1987, *Publ. Astron. Soc. Japan* **39**, 287.
Ebisuzaki, T. and Nakamura, N.: 1988, *Astrophys. J.* **328**, 251.
Ebisuzaki, T. and Nomoto, K.: 1986, *Astrophys. J.* **305**, L67.
Ebisuzaki, T., Hanawa, T., and Sugimoto, D.: 1983, *Publ. Astron. Soc. Japan* **35**, 17.
Ebisuzaki, T., Hanawa, T., and Sugimoto, D.: 1984, *Publ. Astron. Soc. Japan* **36**, 551.

Ercan, N., Branduardi-Raymont, G., and Kiziloglu, Ü.: 1988, *Astrophys. Lett. Comm.* **26**, 349.
Ergma, E. V. and Tutukov, A. V.: 1980, *Astron. Astrophys.* **84**, 123.
Evans, W. D., Belian, R. D., and Conner, J. P.: 1970, *Astrophys. J.* **159**, L57.
Eyles, J. C., Skinner, G. K., Willmore, A. P., and Rosenberg, F. D.: 1975, *Nature* **257**, 291.
Fabbiano, G., Bradt, H. V., Doxsey, R. E., Gursky, H., Schwartz, D. A., and Schwarz, J.: 1978, *Astrophys. J.* **221**, L49.
Faulkner, J.: 1971, *Astrophys. J.* **170**, L99.
Faulkner, J., Flannery, B. P., and Warner, B.: 1972, *Astrophys. J.* **175**, L79.
Finley, J. P., Ögelman, H., and Kiziloglu, Ü.: 1992, *Wisconsin Astrophysics Preprint* 419.
Finzi, A.: 1964, *Astrophys. J.* **139**, 1398.
Fleischman, J. R.: 1985, *Astron. Astrophys.* **153**, 106.
Forman, W. and Jones, C.: 1976, *Astrophys. J.* **207**, L177.
Forman, W., Jones, C., Cominsky, L., Julien, P., Murray, S., Peters. G., Tananbaum, H., and Giacconi, R.: 1978, *Astrophys. J. Suppl.* **38**, 357.
Fortner, B. F., Lamb, F. K. and Miller, G. S.: 1989, *Nature* **342**, 775.
Fortner, B. F., Lamb, F. K. and Miller, G. S.: 1993, *Astrophys. J.* in press.
Foster, A. J., Ross, R. R., and Fabian, A. C.: 1986, *Monthly Notices Roy. Astron. Soc.* **221**, 409.
Foster, A. J., Ross, R. R., and Fabian, A. C.: 1987, *Monthly Notices Roy. Astron. Soc.* **228**, 259.
Fraser, G.: 1989, *X-ray Detectors in Astronomy* (Cambridge University Press).
Friedman, H., Byram, E. T., and Chubb, T. A.: 1967, *Science* **156**, 374.
Friedman, J. L., Ipser, J. R., and Parker, L.: 1986, *Astrophys. J.* **304**, 115.
Fujimoto, M. Y.: 1985, *Astrophys. J.* **293**, L19.
Fujimoto, M. Y.: 1988, *Astrophys. J.* **324**, 995.
Fujimoto, M. Y. and Taam, R. E.: 1986, *Astrophys. J.* **305**, 246.
Fujimoto, M. Y., Hanawa, T. and Miyaji, S.: 1981, *Astroph. J.* **247**, L17.
Fujimoto, M. Y., Hanawa, T., Iben, I., Jr., and Richardson, M. B.: 1984, *Astrophys. J.* **278**, 813.
Fujimoto, M. Y., Hanawa, T., Iben, I., Jr., and Richardson, M. B.: 1985, in S. E. Woosley (ed), *High Energy Transients in Astrophysics*, AIP Conf. Proc. No. 115, (New York, AIP Press), 302.
Fujimoto, M. Y., Hanawa, T., Iben, I., Jr., and Richardson, M. B.: 1987a, *Astrophys. J.* **315**, 198.
Fujimoto, M. Y., Sztajno, M., Van Paradijs, J., and Lewin, W. H. G.: 1987b, *Astrophys. J.* **319**, 902.
Fujimoto, M. Y., Sztajno, M., Lewin, W. H. G., and Van Paradijs, J.: 1988, *Astron. Astrophys.* **199**, L9.
Furth, H. P., Killeen, J., and Rosenbluth, M. N.: 1963, *Phys. Fluids* **6**, 459.
Fushiki, I. and Lamb, D. Q.: 1987a, *Astrophys. J.* **317**, 368.
Fushiki, I. and Lamb, D. Q.: 1987b, *Astrophys. J.* **323**, L55.
Fushiki, I., Taam, R. E., Woosley, S. E., and Lamb, D. Q.: 1992, *Astrophys. J.* **390**, 634.
Gallagher, J. S. and Starrfield, S.: 1978, *Ann. Rev. Astron. Astrophys.* **16**, 171.
Garcia, M. R. and Grindlay, J. E.: 1987, *Astrophys. J.* **313**, L59.
Garcia, M. R., Grindlay, J. E., Bailyn, C. D., Pipher, J. L., Shure, M. A., and Woodward, C. E.: 1992, *Astron. J.* **103**, 1325.
Garcia, M. R., Grindlay, J. E., Molnar, L. A., Stella, L., White, N. E., and Seaquist, E. R.: 1988, *Astrophys. J.* **328**, 552.
Ghosh, P. and Lamb, F. K.: 1979a, *Astrophys. J.* **232**, 259.
Ghosh, P. and Lamb, F. K.: 1979b, *Astrophys. J.* **234**, 296.
Ghosh, P. and Lamb, F. K.: 1992, in E. P. J. van den Heuvel and S. A. Rappaport (eds) Proceedings of the NATO Advanced Research Workshop on *"X-ray Binaries and the Formation of Binary and Millisecond Radio Pulsars"*, (Kluwer Academic Publ., Dordrecht), p. 487.
Giacconi, R., Gursky, H., and Waters, J. R.: 1965, *Nature* **207**, 572.
Giacconi, R., Gursky, H., Paolini, F. R., and Rossi, B.: 1963, *Phys. Rev. Letters* **9**, 439.
Giacconi, R., Murray, S., Gursky, H., Kellogg, E., Schreier, E., Matilsky, T., Koch., D., and Tananbaum, H.: 1974, *Astrophys. J. Suppl.* **27**, 37.
Ginzburg, V. L.: 1990, *Annual Rev. Astron. Astrophys.* **28**, 1.
Glass, I. S.: 1978, *Monthly Notices Roy. Astron. Soc.* **183**, 335.
Goldman, I.: 1979, *Astron. Astrophys.* **78**, L15.
Gorenstein, P.: 1975, *Astrophys. J.* **198**, 95.

Goss, W. M. and Mebold, U.: 1977, *Monthly Notices Roy. Astron. Soc.* **181**, 255.
Gottwald, M., Haberl, F., Langmeier, A., Hasinger, G., Lewin, W. H. G., and Van Paradijs, J.: 1989, *Astrophys. J.* **339**, 1044.
Gottwald, M., Haberl, F., Parmar, A. N., and White, N. E.: 1986, *Astrophys. J.* **308**, 213.
Gottwald, M., Haberl, F., Parmar, A. N., and White, N. E.: 1987a, *Astrophys. J.* **323**, 575.
Gottwald, M., Stella, L., White, N. E., and Barr, P.: 1987b, *Monthly Notices Roy. Astron. Soc.* **229**, 395.
Griffiths, R. E., Gursky, H., Schwartz, D. A., Schwarz, J., Bradt, H., Doxsey, R. E., Charles, P. A., and Thorstensen, J. R.: 1978, *Nature* **276**, 247.
Grindlay, J. E.: 1978, *Astrophys. J.* **221**, 234.
Grindlay, J. E.: 1981, in R. Giacconi (ed.), *X-ray Astronomy with the Einstein Satellite*, Reidel, Dordrecht, p. 79.
Grindlay, J. E.: 1989, in J. Hut and B. Battrick (eds), *Proc. 23rd ESLAB Symposium*, Vol. 1 (ESA SP–296), p. 121.
Grindlay, J. and Gursky, H.: 1976a, *Astrophys. J.* **205**, L131.
Grindlay, J. and Gursky, H.: 1976b, *Astrophys. J.* **209**, L61.
Grindlay, J. E. and Hertz, P.: 1981, *Astrophys. J.* **247**, L17.
Grindlay, J. E. and Liller, W.: 1978, *Astrophys. J.* **220**, L127.
Grindlay, J. E. and Seaquist, E. R.: 1986, *Astrophys. J.* **310**, 172.
Grindlay, J. E., Bailyn, C. D., Cohn, H., Lugger, P. M., Thorstensen, J. R., and Wegner, G.: 1988, *Astrophys. J.* **334**, L25.
Grindlay, J. E., Gursky, H., Parsignault, D. P., Cohn, H., Heise, J., and Brinkman, A. C.: 1977, *Astrophys. J.* **212**, L67.
Grindlay, J. E., Gursky, H., Schnopper, H., Parsignault, D. R., Heise, J., Brinkman, A. C., and Schrijver, J.: 1976a, *Astrophys. J.* **205**, L127.
Grindlay, J. E., Marshall, H. L., Hertz, P., Soltan, A., Weisskopf, M. C., Elsner, R. F., Ghosh, P., Darbo, W., and Sutherland, P. G.: 1980, *Astrophys. J.* **240**, L121.
Grindlay, J. E., McClintock, J. E., Canizares, C. R., Van Paradijs, J., Cominsky, L., Li, F. K., and Lewin, W. H. G.: 1978, *Nature* **274**, 567.
Grindlay, J. E., Schnopper, H., Schreier, E., Gursky, H., and Parsignault, D. P.: 1976b, *Astrophys. J.* **206**, L23.
Gunn, J. E. and Ostriker, J. P.: 1969, *Nature* **222**, 813.
Haberl, F., Stella, L., White, N. E., Priedhorsky, W. C., and Gottwald, M.: 1987, *Astrophys. J.* **314**, 266.
Hackwell, J. A., Grasdalen, G. L., Gehrz, R. D., Van Paradijs, J., Cominsky, L., and Lewin, W. H. G.: 1979, *Astrophys. J.* **233**, L115.
Hameury, J. M., Bonazzolla, S., Heyvaerts, J., and Lasota, J. P.: 1983, *Astron. Astrophys.* **128**, 369.
Hammerschlag-Hensberge, G., McClintock, J. E., and Van Paradijs, J.: 1982, *Astrophys. J.* **254**, L1.
Hanami, H.: 1988, *Monthly Notices Roy. Astron. Soc.* **233**, 423.
Hanawa, T. and Fujimoto, M. Y.: 1982, *Publ. Astron. Soc. Japan* **34**, 495.
Hanawa, T. and Fujimoto, M. Y.: 1984, *Publ. Astron. Soc. Japan* **36**, 119.
Hanawa, T., Hirotani, K., and Kawai, N.: 1989, *Astrophys. J.* **336**, 920.
Hanawa, T. and Sugimoto, D.: 1982, *Publ. Astron. Soc. Japan* **34**, 1.
Hanawa, T., Sugimoto, D., and Hashimoto, M.: 1983, *Publ. Astron. Soc. Japan* **35**, 491.
Hansen, C. J. and Van Horn, H. M.: 1975, *Astrophys. J.* **195**, 735.
Hasinger, G.: 1987, *Astron. Astrophys.* **186**, 153.
Hasinger, G. and Van der Klis, M.: 1989, *Astron. Astrophys.* **225**, 79.
Hasinger, G., Van der Klis, M., Ebisawa, K., Dotani, T., and Mitsuda, K.: 1990, *Astron. Astrophys.* **235**, 131.
Hayakawa, S.: 1981, *Space Sci. Rev.* **29**, 221.
Hayakawa, S.: 1985, *Physics Reports* **121**, 317.
Hertz, P.: 1987, *Astrophys. J.* **315**, L119.
Hertz, P. and Grindlay, J. E.: 1983, *Astrophys. J.* **275**, 105.
Hertz, P. and Wood, K. S.: 1988, *Astrophys. J.* **331**, 764.
Hirata, K., Kajita, T., Koshiba, M., Nakahata, M., Oyama, Y., Sato, N., Suzuki, A., Takita, M.,

Totsuka, Y., Kifune, T., Suda, T., Takahashi, K., Tanimori, T., Miyano, K., Yamada, M., Beier, E. W., Feldscher, L. R., Kim, S. B., Mann, A. K., Newcomer, F. M., Van Berg, R., Zhang, W., and Cortez, B. G.: 1987, *Phys. Rev. Lett.* **58**, 1490.
Hoffman, J. A., Cominsky, L., and Lewin, W. H. G.: 1980, *Astrophys. J.* **240**, L27.
Hoffman, J. A., Lewin, W. H. G., and Doty J.: 1977a, *Astrophys. J.* **217**, L23.
Hoffman, J. A., Lewin, W. H. G., and Doty J.: 1977b, *Monthly Notices Roy. Astron. Soc.* **179**, 57P.
Hoffman, J. A., Lewin, W. H. G., Doty, J., Hearn, D. R., Clark, G. W., Jernigan, G., and Li, F. K.: 1976, *Astrophys. J.* **210**, L13.
Hoffman, J. A., Lewin, W. H. G., Doty, J., Jernigan, J. G., Haney, M., and Richardson, J. A.: 1978b, *Astrophys. J.* **221**, L57.
Hoffman, J. A., Lewin, W. H. G., Primini, F. A., Wheaton, W. A., Swank, J. H., Boldt, E. A., Holt, S. S., Serlemitsos, P. J., Share, G. H., Wood, K., Yentis, D., Evans, W. D., Matteson, J. L., Gruber, D. F., and Peterson, L. E.: 1979, *Astrophys. J.* **233**, L51.
Hoffman, J. A., Marshall, H. L., and Lewin, W. H. G.: 1978a, *Nature* **271**, 630.
Hoffman, J. A., Wheaton, W. A., Primini, F. A., Campbell, P., Dobson, C. A., Howe, S. K., Tsiang, E. Y., Scheepmaker, A., Lewin, W. H. G., Matteson, J. L., Gruber, D. E., Peterson, L. E., Swank, J. H., Boldt, E. A., Holt, S. S., Rothschild, R. E., and Serlemitsos, P.: 1978c, *Nature* **276**, 587.
Horiuchi, R., Kodonaga, T., and Tominatsu. A.: 1981, *Prog. Theor. Phys.* **66**, 172.
Horne, K., Verbunt, F., and Schneider, D. P.: 1986, *Monthly Notices Roy. Astron. Soc.* **218**, 63.
Hoshi, R.: 1981, *Astrophys. J.* **247**, 628.
Hoyle, F. and Fowler, W. A.: 1965, in I. Robinson et al. (eds) *Quasi-Stellar Sources and Gravitational Collapse*, (Chicago: Univ. of Chicago Press), 62.
Illarionov, A. F. and Sunyaev, R. A.: 1975, *Astron. Astrophys.* **39**, 185.
Ilovaisky, S. A., Auriere, M., Chevalier, C., Koch-Miramond, L., Cordoni, J. P., and Angebault, L. P.: 1987, *Astron. Astrophys.* **179**, L1.
In 't Zand, J. J. M., Heise, J., Brinkman, A. C., Jager, R., Skinner, G. K., Patterson, T. G., Pan, H. -C., Nottingham, M. R., Willmore, A. P., Al-Emam, O., Sunyaev, R. A., Churazov, E. M., Gilfanov, M. R. and Yamburenko, N. S.: 1991, *Adv. Space Res.* **11** (8), 187.
In 't Zand, J. J. M., Patterson, T. G., Brinkman, A. C., Heise, J., Jager, R., Skinner, G. K., Willmore, A. P., Al-Emam, O., Sunyaev, R., Churazov, E., Gilfanov, M. R., and Yamburenko, N.: 1989, in J. Hut and B. Battrick (eds), *Proceedings 23rd ESLAB Symp.*, Vol 1 (ESA SP–296), p. 693.
Inoue, H., Koyama, K., Makino, F., Makishima, K., Matsuoka, M., Murakami, T., Oda, M., Ogawara, Y., Ohashi, T., Shibazaki, N., Tanaka, Y., Hayakawa, S., Kunieda, H., Masai, K., Nagase, F., Tawara, Y., Miyamoto, S., Tsunemi, H., Yamashita, K., and Kondo, I.: 1984a, *Publ. Astron. Soc. Japan* **36**, 855.
Inoue, H., Koyama, K., Makishima, K., Matsuoka, M., Murakami, T., Oda, M., Ogawara, Y., Ohashi, T., Shibazaki, N., Tanaka, Y., Kondo, I., Hayakawa, S., Kunieda, H., Makino, F., Masai, K., Nagase, F., Tawara, Y., Miyamoto, S., Tsunemi, H., and Yamashita, K.: 1981, *Astrophys. J.* **250**, L71.
Inoue, H., Koyama, K., Makishima, K., Matsuoka, M., Murakami, T., Oda, M., Ogawara, Y., Ohashi, T., Shibazaki, N., Tanaka, Y., Tawara, Y., Kondo, I., Hayakawa, S., Kunieda, H., Makino, F., Masai, K., Nagase, F., Miyamoto, S., Tsunemi, H., and Yamashita, K.: 1980, *Nature*, **283**, 358.
Inoue, H., Waki, I., Koyama, K., Matsuoka, M., Ohashi, T., Tanaka, Y., and Tsunemi, H.: 1984b, *Publ. Astron. Soc. Japan* **36**, 831.
Jernigan, J. G. and Clark, G. W.: 1979, *Astrophys. J.* **231**, L125.
Jernigan, J. G., Apparao, K. M. V., Bradt, H. V., Doxsey, R. E., Dower, R. G., and McClintock, J. E.: 1978, *Nature* **272**, 701.
Johnson, A. M., Catura, R. C., Lamb, P. A., White, N. E., Sanford, P. W., Hoffman, J. A., Lewin, W. H. G., and Jernigan, J. G.: 1978, *Astrophys. J.* **222**, 664.
Jones, A. W., Selby, M. J., Mountain, C. M., Wade, R., Magro, C. S., and Munoz, M. P.: 1980, *Nature* **283**, 550.
Joss, P. C.: 1977, *Nature* **270**, 310.
Joss, P. C.: 1978, *Astrophys. J.* **225**, L123.
Joss, P. C. and Li, F. K.: 1980, *Astrophys. J.* **238**, 287.
Joss, P. C. and Melia, F.: 1987, *Astrophys. J.* **312**, 700.

Joss, P. C. and Rappaport, S. A.: 1984, *Ann. Rev. Astr. Ap.* **22**, 537.
Kahn, S. M. and Grindlay, J. E.: 1984, *Astrophys. J.* **281**, 826.
Kaluzienski, L. J., Holt, S. S., and Swank, J. H.: 1980, *Astrophys. J.* **241**, 779.
Kaluzienski, L. J., Holt, S. S., Boldt, E. A., and Serlemitsos, P. J.: 1976, *Astrophys. J.* **208**, L71.
Kaluzienski, L. J., Holt, S. S., Boldt, E. A., and Serlemitsos, P. J.: 1977, *Nature* **265**, 606.
Kaminker, A. D., Pavlov, G. G., Shibanov, Y. A., Kurt, V. G., Smirnov, A. S., Shamolin, V. M., Kopaeva, I. F., and Sheffer, E. K.: 1989, *Astron. Astrophys.* **220**, 117.
Kaminker, A. D., Pavlov, G. G., Shibanov, Yu. A., Kurt, V. G., Shafer, E.Yu., Smirnov, A. S., Shamolin, V. M., Kopaeva, I. F., and Sheffer, E. K.: 1990, *Astrophys. Space Sci.*, **173**, 171.
Kaminker, A. D., Pavlov, G. G., Shibanov, Yu. A., Kurt, V. G., Shafer, E. Yu., Smirnov, A. S., Shamolin, V. M., Kopaeva, I. F. and Sheffer, E. K.: 1990, *Astrophys. Sp. Sci.* **173**, 189.
Kapoor, R. C. and Datta, B.: 1984, *Monthly Notices Roy. Astron. Soc.* **209**, 895.
Kato, M.: 1983, *Publ. Astron. Soc. Japan* **35**, 33.
Kato, S.: 1978, *Monthly Notices Roy. Astron. Soc.* **185**, 629.
Kato, S., Honma, F., and Matsumoto, R.: 1988, *Monthly Notices Roy. Astron. Soc.* **231**, 37.
Kawai, N.: 1985, *ISAS Research Note*, **302**, PhD Thesis, University of Tokyo.
Kawai, N., Matsuoka, M., Inoue, H., Ogawara, Y., Tanaka, Y., Kunieda, H., and Tawara, Y.: 1990, *Publ. Astron. Soc. Japan*, **42**, 115.
Kleinmann, D. E., Kleinmann, S. G., and Wright, E. L.: 1976, *Astrophys. J.* **210**, L83.
Kluzniak, W.: 1989, *Astrophys. J.* **336**, 367.
Koyama, K., Inoue, H., Makishima, K., Matsuoka, M., Murakami, T., Oda, M., Ogawara, Y., Ohashi, T., Shibazaki, N., Tanaka, Y., Marshall, F. J., Hayakawa, S., Kunieda, H., Makino, F., Masai, K., Nagase, F., Tawara, Y., Miyamoto, S., Tsunemi, H., and Yamashita, K.: 1981, *Astrophys. J.* **247**, L27.
Kraft, R. P., Mathews, J., and Greenstein, J. L.: 1962, *Astrophys. J.* **136**, 212.
Kruskal, M. and Schwarzschild, M.: 1954, *Proc. Roy. Soc.* **A223**, 348.
Kulkarni, P. V., Ashok, N. M., Apparao, K. V. M., and Chitre, S. M.: 1979, *Nature* **280**, 819.
Kulkarni, S. R.: 1986, *Astrophys. J.*, **306**, L85.
Kulkarni, S. R., Djorgovski, S. G., and Klemola, A. R.: 1991, *Astrophys. J.* **367**, 221.
Kunieda, H., Tawara, Y., Hayakawa, S., Masai, K., Nagase, F., Inoue, H., Koyama, K., Makino, F., Makishima, K., Matsuoka, M., Murakami, T., Oda, M., Ogawara, Y., Ohashi, T., Shibazaki, N., Tanaka, Y., Kondo, I., Miyamoto, S., Tsunemi, H., and Yamashita, K.: 1984a, *Publ. Astron. Soc. Japan* **36**, 215.
Kunieda, H., Tawara, Y., Hayakawa, S., Nagase, F., Inoue, H., Kawai, N., Makino, F., Makishima, K., Matsuoka, M., Murakami, T., Oda, M., Ogawara, Y., Ohashi, T., Tanaka, Y., and Waki, I.: 1984b, *Publ. Astron. Soc. Japan* **36**, 807.
Lamb, D. Q. and Lamb, F. K.: 1978, *Astrophys. J.* **220**, 291.
Lamb, F. K.: 1991, in J. Ventura and D. Pines (eds), *Neutron Stars : Theory and Observations*, (Kluwer Academic Publ.), NATO ASI Series C, **344**, p. 445.
Lamb, F. K., Fabian, A. C., Pringle, J. E., and Lamb, D. Q.: 1977, *Astrophys. J.* **217**, 197.
Lamb, F. K., Shibazaki, N., Shaham, J., and Alpar, M. A.: 1985, *Nature*, **317**, 681.
Langmeier, A., Sztajno, M., Hasinger, G., Trümper, J., and Gottwald, M.: 1987, *Astrophys. J.* **323**, 288.
Lapidus, I. I. and Sunyaev, R. A.: 1985, *Monthly Notices Roy. Astron. Soc.* **217**, 291.
Lapidus, I. I., Sunyaev, R. A., and Titarchuk, L. G.: 1986, *Sov. Astron. J. (Letters)* **12**, 383.
Lawrence, A., Cominsky, L., Engelke, C., Jernigan, J., Lewin, W. H. G., Matsuoka, M., Mitsuda, K., Oda, M., Ohashi, T., Pedersen, H., and Van Paradijs, J.: 1983b, *Astrophys. J.* **271**, 793.
Lawrence, A., Cominsky, L., Lewin, W. H. G., Oda, M., Ogawara, Y., Inoue, H., Koyama, K., Makishima, K., Matsuoka, M., Murakami, T., Ohashi, T., Shibazaki, N., Tanaka, Y., Kondo, I., Hayakawa, S., Kunieda, H., Makino, F., Masai, K., Nagase, F., Tawara, Y., Miyamoto, S., Tsunemi, H., Yamashita, K., Dashido, T., Oka, R., Ohkawa, T., Maruyama, T., Yokoyama, T., Nicholson, G., Balonek, T., Dent, W. A., Glass, I. S., Carter, B. S., Jones, A. W., Selby, M. J., Martinez Roger, C., Sanchez Magro, C., Giles, A. B., Duldig, M., Pramesh Rao, A., Venugopal, V. R., Haynes, R. F., Jauncey, D. L., Okuda, H., Sato, S., Kobayashi, Y., Jugaku, J., Backman, D., Pogge, R., Hodge, P. E., Aller, H. D., and Van Paradijs, J.: 1983a, *Astrophys. J.* **267**, 301.

Leahy, D. A., Darbro, W., Elsner, R. F., Weisskopf, M. C., Sutherland, P. G., Kahn, S., and Grindlay, J. E.: 1983, *Astrophys. J.* **266**, 160.
Lehto, H., Machin, G., McHardy, I. M., and Callanan, P.: 1990, *Nature* **347**, 49.
Levine, A., Ma, C. P., McClintock, J., Rappaport, S., Van der Klis, M., and Verbunt, F.: 1988, *Astrophys. J.*, **327**, 732.
Lewin, W. H. G.: 1976a, *IAU Circular* No. 2918.
Lewin, W. H. G.: 1976b, *IAU Circular* No. 2922.
Lewin, W. H. G.: 1977, *Annals New York Acad. Sci.* **302**, 210.
Lewin, W. H. G.: 1978, *IAU Circular* No. 3193.
Lewin, W. H. G.: 1979, in W. A. Baity and L. E. Peterson (eds), *X-ray Astronomy*, Oxford – Pergamon Press, Vol. 3, p. 133.
Lewin, W. H. G.: 1984, in S. E. Woosley (ed.), *High Energy Transients in Astrophysics*, AIP Conference Proc. 115 (American Inst. Physics), p. 249.
Lewin, W. H. G. and Joss, P. C.: 1977, *Nature* **270**, 211.
Lewin, W. H. G. and Joss, P. C.: 1981, *Space Sci. Rev.* **28**, 3.
Lewin, W. H. G. and Joss, P. C.: 1983, in W. H. G. Lewin and E. P. J. van den Heuvel (eds), *Accretion Driven Stellar X-ray Sources*, Cambridge University Press, Cambridge, p. 41.
Lewin, W. H. G. and Van Paradijs, J.: 1986, *Comments on Astrophys.* **11**, No. 3, 469.
Lewin, W. H. G., Doty, J., Clark. G. W., Rappaport, S. A., Bradt, H. V., Doxsey, R., Hearn, D. R., Hoffman, J. A., Jernigan, J. G., Li, F. K., Mayer, W., McClintock, J. E., Primini, F., and Richardson, J.: 1976c, *Astrophys. J.* **207**, L95.
Lewin, W. H. G., Hoffman, J. A., and Doty, J.: 1976e, *IAU Circular* No. 2994.
Lewin, W. H. G., Hoffman, J. A., and Doty, J.: 1977c, *IAU Circular* No. 3087.
Lewin, W. H. G., Hoffman, J. A., Doty, J., Clark, G. W., Swank, J. H., Becker, R. H., Pravdo, S. H., and Serlemitsos, P. J.: 1977b, *Nature* **267**, 28.
Lewin, W. H. G., Hoffman, J. A., Doty, J., Hearn, D. R., Clark, G. W., Jernigan, J. G., Li, F. K., McClintock, J. E., and Richardson, J: 1976d, *Monthly Notices Roy. Astron. Soc.* **177**, 83P.
Lewin, W. H. G., Hoffman, J. A., Doty, J., Li, F. K., and McClintock, J. E.: 1977a, *IAU Circular* No. 3075.
Lewin, W. H. G., Hoffman, J. A., Marshall, H. L., Primini, F., Wheaton, W. A., Cominsky, L., Jernigan, G., and Osman, W.: 1978, *IAU Circular* No. 3190.
Lewin, W. H. G., Li, F. K., Hoffman, J. A., Doty, J., Buff, J., Clark, G. W., and Rappaport, S.: 1976b, *Monthly Notices Roy. Astron. Soc.* **177**, 93P.
Lewin, W. H. G., Lubin, L. M., Van Paradijs, J., and Van der Klis, M.: 1991, *Astron. Astrophys.* **248**, 538.
Lewin, W. H. G., Penninx, W., Van Paradijs, J., Damen, E., Sztajno, M., Trümper, J., and Van der Klis, M.: 1987a, *Astrophys. J.* **319**, 892.
Lewin, W. H. G., Ricker, G. R., and McClintock, J. E.: 1971, *Astrophys. J.*, **169**, L17.
Lewin, W. H. G., Vacca, W. D., and Basinska, E. M.: 1984, *Astrophys. J.* **277**, L57.
Lewin, W. H. G., Van Paradijs, J., Cominsky, L., and Holzner, S.: 1980, *Monthly Notices Roy. Astron. Soc.* **193**, 15.
Lewin, W. H. G., Van Paradijs, J., Hasinger, G., Penninx, W. H., Langmeier, A., Van der Klis, M., Jansen, F., Basinska, E. M., Sztajno, M., and Trümper, J.: 1987b, *Monthly Notices Roy. Astron. Soc.* **226**, 383.
Lewin, W. H. G., Van Paradijs, J., and Van der Klis, M.: 1988, *Space Sci. Rev.*, **46**, 273.
Li, F. K. and Clark, G. W.: 1977, *IAU Circular* No. 3095.
Li, F.K., Lewin, W. H. G., Clark, G. W., Doty, J., Hoffman, J. A., and Rappaport, S. A.: 1977, *Monthly Notices Roy. Astron. Soc.* **179**, 21P.
Liang, E. T.: 1986, *Astrophys. J.* **304**, 682.
Lightman, A. P. and Eardley, D. M.: 1974, *Astrophys. J.* **187**, L1.
Liller, W.: 1977, *Astrophys. J.* **213**, L21.
Livio, M. and Bath, G. T.: 1982, *Astron. Astrophys.* **116**, 286.
London, R. A., Taam, R. E., and Howard, W. M.: 1984, *Astrophys. J.* **287**, L27.
London, R. A., Taam, R. E., and Howard, W. M.: 1986, *Astrophys. J.* **306**, 170.
Loredo, T. and Lamb, D. Q.: 1989, *Ann. New York Acad. Sci.* **571**, 601.

Lubin, L. M., Lewin, W. H. G., Dotani, T., Oosterbroek, T., Mitsuda, K., Magnier, E., Van Paradijs, J., Van der Klis, M.: 1992a, *Monthly Notices Roy. Astron. Soc.*, **256**, 624.
Lubin, L. M., Lewin, W. H. G., Rutledge, R. E., Van Paradijs, J., Van der Klis, M., and Stella, L.: 1992b, *Monthly Notices Roy. Astron. Soc.* **258**, 759.
Lubin, L. M., Lewin, W. H. G., Van Paradijs, J., Van der Klis, M.: 1993, *Monthly Notices Roy. Astron. Soc.* **261**, 149.
Lubin, L. M., Lewin, W. H. G., Tan, J., Van Paradijs, J., and Van der Klis, M.: 1991b, *Monthly Notices Roy. Astron. Soc.* **252**, 190.
Lubin, L. M., Stella, L., Lewin, W. H. G., Tan, J., Van Paradijs, J., Van der Klis, M., and Penninx, W.: 1991a, *Monthly Notices Roy. Astron. Soc.*, **249**, 300.
Machin, G., Callanan, P. J., Charles, P. A., Thorstensen, J., Brownsberger, K., Corbet, R. H. D., Hamwey, R., Harlaftis, E. T., Mson, K. O., and Mukai, K.: 1990a, *Monthly Notices Roy. Astron. Soc.* **247**, 205.
Machin, G., Lehto, H. J., McHardy, I. M., Callanan, P., and Charles, P. A.: 1990b, *Monthly Notices Roy. Astron. Soc.* **246**, 237.
Madej. J.: 1974, *Acta Astron.* **24**, 327.
Madej, J.: 1989a, *Astrophys. J.* **339**, 386.
Madej, J.: 1989b, *Astron. Astrophys.* **209**, 226.
Madej, J.: 1991, *Astrophys. J.* **376**, 161.
Magnier, E., Lewin, W. H. G., Van Paradijs, J., Tan, J., Penninx, W., and Damen, E.: 1989, *Monthly Notices Roy. Astron. Soc.*, **237**, 729.
Makino, F. and the Ginga Team: 1988, *IAU Circular* 4653.
Makishima K. and Mihara, T.: 1992, in K. Koyama and Y. Tanaka (eds), Proceedings of the 28th Yamada Conference in Japan, p. 23.
Makishima, K., Inoue, H., Koyama, K., Matsuoka, M., Murakami, T., Oda, M., Ogawara, Y., Ohashi, T., Shibazaki, N., Tanaka, Y., Hayakawa, S., Kunieda, H., Makino, F., Masai, K., Nagase, F., Tawara, Y., Miyamoto, S., Tsunemi, H., Yamashita, K., and Kondo, I.: 1981a, *Astrophys. J.* **244**, L79.
Makishima, K., Inoue, H., Koyama, K., Matsuoka, M., Murakami, T., Oda, M., Ogawara, Y., Ohashi, T., Shibazaki, N., Tanaka, Y., Hayakawa, S., Kunieda, H., Makino, F., Masai, K., Nagase, F., Tawara, Y., Miyamoto, S., Tsunemi, H., Yamashita, K., and Kondo, I.: 1982, *Astrophys. J.* **255**, L49.
Makishima, K., Mitsuda, K., Inoue, H., Koyama, K., Matsuoka, M., Murakami, T., Oda, M., Ogawara, Y., Shibazaki, N., Tanaka, Y., Marshall, F. J., Hayakawa, S., Kunieda, H., Makino, F., Nagase, F., Tawara, Y., Miyamoto, S., Tsunemi, H., Yamashita, K., and Kondo, I.: 1983, *Astrophys. J.* **267**, 310.
Makishima, K., Ohashi, T., Inoue, H., Koyama, K., Matsuoka, M., Murakami, T., Oda, M., Ogawara, Y., Shibazaki, N., Tanaka, Y., Kondo, I., Hayakawa, S., Kunieda, H., Makino, F., Masai, K., Nagase, F., Tawara, Y., Miyamoto, S., Tsunemi, H., and Yamashita, K.: 1981b, *Astrophys. J.* **247**, L23.
Maraschi, L. and Cavaliere, A.: 1977, in: E. A. Müller (ed), *Highlights in Astronomy*, Reidel, Dordrecht, Vol. 4, Part I, 127.
Margon, B., Bowyer, S., Lampton, M., and Cruddace, R.: 1971, *Astrophys. J.* **169**, L45.
Margon, B., Katz, J. I., and Petro, L. D.: 1978, *Nature* **271**, 633.
Markert, T. H., Backman, D. E., and McClintock, J. E.: 1976, *Astrophys. J.* **208**, L115.
Markert, T. H. Canizares, C. R., Clark, G. W., Hearn, D. R., Li, F. K., Sprott, G. F., and Winkler, P. F.: 1977, *Astrophys. J.* **218**, 801.
Marshall, H. L.: 1982, *Astrophys. J.* **260**, 815.
Marshall, H. L., Li, F. K., and Rappaport, S.: 1976, *IAU Circular* No. 3134.
Marshall, H. L., Ulmer, M. P., Hoffman, J. A., Doty, J., and Lewin, W. H. G.: 1979, *Astrophys. J.* **227**, 555.
Mason, K., Bell-Burnell, J., and White, N. E.: 1976b, *Nature* **262**, 474.
Mason, K. O., Charles, P. A., White, N. E., Culhane, J. L., Sanford, P. J., and Strong, K. T.: 1976a, *Monthly Notices Roy. Astron. Soc.* **177**, 513.
Mason, K. O., Middleditch, J., Nelson, J. E., and White, N. E.: 1980, *Nature* **287**, 516.

Matsumoto, R., Kato, S., Fukue, J., and Okazaki, A. T.: 1984, *Publ. Astron. Soc. Japan* **36**, 71.
Matsumoto, R., Kato, S., and Honma, F.: 1988, in Y. Tanaka (ed), *Physics of Neutron Stars and Black Holes*, (Tokyo: Universal Academic Press), 155.
Matsuoka, M.: 1980, in: *Symposium on Space Astrophysics*, Tokyo, July 29, 1980 (ISAS), p. 88.
Matsuoka, M.: 1985, in: Y. Tanaka and W. H. G. Lewin (eds), *Japan-US Seminar on Galactic and Extragalactic Compact X-ray Sources*, (ISAS, Tokyo), p. 45.
Matsuoka, M.: 1986, in: J. Trümper, W. H. G. Lewin and W. Brinkmann (eds), *The Evolution of Galactic X-ray Binaries*, NATO ASI Series C, Vol. 167, p. 301.
Matsuoka, M., Inoue, H., Koyama, K., Makishima, K., Murakami, T., Oda, M., Ogawara, Y., Ohashi, H., Shibazaki, N., Tanaka, Y., Kondo, I., Hayakawa, S., Kunieda, H., Makino, F., Masai, K., Nagase, F., Tawara, Y., Miyamoto, S., Tsunemi, H., and Yamashita, K.: 1980, *Astrophys. J.* **240**, L137.
Matsuoka, M., Mitsuda, K., Ohashi, T., Inoue, H., Koyama, K., Makino, F., Makishima, K., Murakami, T., Oda, M., Ogawara, Y., Shibazaki, N., Tanaka, Y., Tsuno, K., Miyamoto, S., Tsunemi, H., Yamashita, K., Hayakawa, S., Kunieda, H., Masai, K., Nagase, F., Tawara, Y., Kondo, I., Cominsky, L., Jernigan, J. G., Lawrence, A., Lewin, W. H. G., Pedersen, H., Motch, C., and Van Paradijs, J.: 1984, *Astrophys. J.* **283**, 774.
Mauder, H.: 1981, *ESO Messenger* **24**, 13.
McClintock, J. E. and Remillard, R. E.: 1990, *Astrophys. J.* **350**, 386.
McClintock, J. E., Canizares, C., and Backman, D. E.: 1978, *Astrophys. J.* **223**, L75.
McClintock, J. E., Canizares, C. R., Bradt, H. V., Doxsey, R. E., Jernigan, J. G., and Hiltner, W. A.: 1977, *Nature* **270**, 320.
McClintock, J. E., Canizares, C. R., Van Paradijs, J., Cominsky, L., Li, F. K., Lewin, W. H. G., and Grindlay, J. E.: 1979, *Nature* **279**, 47.
McClintock, J. E., London, R. A., Bond, H. E., and Grauer, A. D.: 1982, *Astrophys. J.* **258**, 245.
McClintock, J. E., Remillard, R. A., and Margon, B.: 1981, *Astrophys. J.* **243**, 900.
Meegan, C. A., Fishman, G. J., Wilson, R. B., Paciesas, W. S., Pendleton, G. N., Horack, J. N., Brock, M. N., and Kouveliotou, C.: 1992, *Nature* **355**, 143.
Melia, F.: 1987, *Astrophys. J.* **315**, L43.
Meyer, F.: 1986, in D. Mihalas and K. H. A. Winkler (eds.), *Radiation Hydrodynamics in Stars and Compact Objects*, Springer Verlag, Berlin, 249. Michel, F. C.: 1977, *Astroph. J.* **216**, 838.
Michel, F. C.: 1977, *Astrophys. J.* **216**, 838.
Middleditch, J., Mason, K. O., Nelson, J. E., and White, N. E.: 1981, *Astrophys. J.* **244**, 1001.
Mihalas, D.: 1978, *Stellar Atmospheres*, 2nd Ed. (Freeman and Cy, San Francisco).
Milgrom, M.: 1987, *Astron. Astrophys.* **172**, L1.
Misner, C., Thorne, K. S., and Wheeler, J. A.: 1973, *Gravitation* (Freeman and Cy).
Mitsuda, K., Inoue, H., Koyama, K., Makishima, K., Matsuoka, M., Ogawara, Y., Shibazaki, N., Suzuki, K., Tanaka, Y., and Hirano, T.: 1984, *Publ. Astron. Soc. Japan* **36**, 741.
Mitsuda, K., Inoue, H., Nakamura, N., and Tanaka, Y.: 1989, *Publ. Astron. Soc. Japan* **41**, 97.
Miyaji, S.: 1988, in M. P. Ulmer (ed.) *13th Texas Symposium on Relativistic Astrophysics*, (World Scientific), p. 545.
Moneti, A.: 1992, *Astron. Astrophys.* **260**, L7.
Morgan, E. H., Remillard, R. A., and Garcia, M. R.: 1988, *Astrophys. J.* **324**, 851.
Morrisson, R. and McCammon, D.: 1983, *Astrophys. J.* **270**, 119.
Morton, D. C.: 1964, *Astrophys. J.* **140**, 460.
Motch, C., Pedersen, H., Beuermann, K., Pakull, M. W., and Courvoisier, T. J. -L.: 1987, *Astrophys. J.* **313**, 792.
Muchotrzeb, B.: 1983, *Acta Astron.* **33**, 79.
Muchotrzeb-Czerny, B.: 1986, *Acta Astron.* **36**, 1.
Murakami, T., Inoue, H., Koyama, K., Makishima, K., Matsuoka, M., Oda, M., Ogawara, Y., Ohashi, T., Makino, F., Shibazaki, N., Tanaka, Y., Hayakawa, S., Kunieda, H., Masai, K., Nagase, F., Tawara, Y., Miyamoto, D. S., Tsunemi, H., Yamashita, K., and Kondo, I.: 1983, *Publ. Astron. Soc. Japan* **35**, 531.
Murakami, T., Inoue, H., Koyama, K., Makishima, K., Matsuoka, M., Oda, M., Ogawara, Y., Ohashi, T., Shibazaki, N., Tanaka, Y., Tawara, Y., Hayakawa, S., Kunieda, H., Makino, F., Masai, K.,

Nagase, F., Miyamoto, D. S., Tsunemi, H., Yamashita, K., and Kondo, I.: 1980a, *Astrophys. J.* **240**, L143.
Murakami, T., Inoue, H., Koyama, K., Makishima, K., Matsuoka, M., Oda, M., Ogawara, Y., Ohashi, T., Shibazaki, N., Tanaka, Y., Hayakawa, S., Kunieda, H., Makino, F., Makino, F., Masai, K., Nagase, F., Tawara, Y., Miyamoto, D. S., Tsunemi, H., Yamashita, K., and Kondo, I.: 1980b, *Publ. Astron. Soc. Japan* **32**, 543.
Murakami, T., Inoue, H., Makishima, K., and Hoshi, R.: 1987, *Publ. Astron. Soc. Japan* **39**, 879.
Murdin, P., Jauncey, D. L., Haynes, R. F., Lerche, I., Nicolson, G. D., Holt, S. S., and Kaluzienski, L. J.: 1980, *Astron. Astrophys.* **87**, 292.
Murdin, P., Penston, M. J., Penston, M. V., Glass, I. S., Sanford, P. W., Hawkins, F. J., Mason, K. O., and Willmore, A. P.: 1974, *Monthly Notices Roy. Astron. Soc.* **169**, 25.
Nagase, F.: 1989, *Publ. Astron. Soc. Japan*, **41**, 1.
Nakamura, N., Dotani, T., Inoue, H., Mitsuda, K., Tanaka, Y., and Matsuoka, M.: 1989, *Publ. Astron. Soc. Japan* **41**, 617.
Nakamura, N., Inoue, H., and Tanaka, Y.: 1988, *Publ. Astron. Soc. Japan* **40**, 209.
Naylor, T., Charles, P. A., and Longmore, A. J.: 1991, *Monthly Notices Roy. Astron. Soc.* **252**, 203.
Naylor, T., Charles, P. A., Drew, J. E., and Hassall, B. J. M.: 1988, *Monthly Notices Roy. Astron. Soc.* **233**, 285.
Nelson, L. A., Rappaport, S. A., and Joss, P. C.: 1986, *Astrophys. J.*, **304**, 231.
Nicolson, G. D., Feast, M. W., and Glass, I. S.: 1980, *Monthly Notices Roy. Astron. Soc.* **191**, 293.
Nieto, J. L., Auriere, M., Sebag, J., Arnaud, J., Lelievre, G., Blazit, A., Foy, R., Bonaldo, S., and Thouvenot, E.: 1990, *Astron. Astrophys.* **239**, 155.
Nozakura, T., Ikeuchi, S., and Fujimoto, M. Y.: 1984, *Astrophys. J.* **286**, 221.
Oda, M.: 1982, in R. E. Lingenfelter, H. S. Hudson, and D. M. Worrall (eds), *Gamma Ray Transients and Related Astrophysical Phenomena*, AIP Conf. Proc. 77, (New York: AIP Press), 319.
Ohashi, T.: 1981, Ph. D. Thesis, Univ. Tokyo (*ISAS Research Note* No. 141).
Ohashi, T., Inoue, H., Koyama, K., Makishima, K., Matsuoka, M., Murakami, T., Oda, M., Ogawara, Y., Shibazaki, N., Tanaka, Y., Tawara, Y., Hayakawa, S., Kunieda, H., Makino, F., Masai, K., Nagase, F., Miyamoto, S., Tsunemi, H., and Yamashita, K.: 1982, *Astrophys. J.* **258**, 254.
Onyejuba, P. E. and Gaustad, J. E.: 1967, *Astrophys. J.* **147**, 806.
Oosterbroek, T.: 1989, Master's thesis, Univ. Amsterdam.
Oosterbroek, T., Penninx, W., Van der Klis, M., Van Paradijs, J., and Lewin, W. H. G.: 1991, *Astron. Astrophys.* **250**, 389.
Orszag, S. A.: 1965, *Astrophys. J.* **142**, 473.
Paczynski, B.: 1967, *Acta Astronomica* **17**, 287.
Paczynski, B.: 1971, *Ann. Rev.* **9**, 183.
Paczynski, B.: 1983a, *Astrophys. J.* **264**, 282.
Paczynski, B.: 1983b, *Astrophys. J.* **267**, 315.
Paczynski, B. and Anderson, N.: 1986, *Astrophys. J.* **302**, 1.
Paczynski, B. and Proszynski, M.: 1986, *Astrophys. J.* **302**, 519.
Paczynski, B. and Sienkiewicz, R.: 1981, *Astrophys. J.* **248**, L27.
Paczynski, B. and Sienkiewicz, R.: 1983, *Astrophys. J.*, **268**, 825.
Parmar, A. N., Gottwald, M., Van der Klis, M., and Van Paradijs, J.: 1989a, *Astrophys. J.* **338**, 1024.
Parmar, A. N., Smale, A. P., Verbunt, F., and Corbet, R. H. D.: 1991, *Astrophys. J.* **366**, 253.
Parmar, A. N., Stella, L., and Giommi, P.: 1989b, *Astron. Astrophys.* **222**, 96.
Parmar, A. N., White, N. E., Giommi, P., and Gottwald, M.: 1986, *Astrophys. J.* **308**, 199.
Parmar, A. N., White, N. E., Giommi, P., Stella, L., and White, N. E.: 1985, *IAU Circular* No. 4058.
Patterson, T. G., Skinner, G. K., Willmore, A. P., Emam, O., Brinkman, A. C., Heise, J., In 't Zand, J. J. M., Jager, R., Sunyaev, R., Churazov, E., Gilfanov, M. R., and Yamburenko, N.: 1989, in J. Hut and B. Battrick (eds), *Proceedings 23rd ESLAB Symp.*, Vol 1 (ESA SP–296), p. 567.
Pavlov, G. G., Shibanov, Yu. A., and Zavlin, V. E.: 1991, *Monthly Notices Roy. Astron. Soc.* **253**, 193.
Pedersen, H., Lub, J., Inoue, H., Koyama, K., Makishima, K., Matsuoka, M., Mitsuda, K., Murakami, T., Oda, M., Ogawara, Y., Ohashi, H., Shibazaki, N., Tanaka, Y., Hayakawa, S., Kunieda, H., Makino, F., Masai, K., Nagase, F., Tawara, Y., Miyamoto, S., Tsunemi, H., Yamashita, K., Kondo, I., Jernigan, J. G., Van Paradijs, J., Beardsley, A., Cominsky, L., Doty, J., and Lewin, W. H. G.:

1982a, *Astrophys. J.* **263**, 325.
Pedersen, H., Van Paradijs, J., and Lewin, W. H. G.: 1981, *Nature* **294**, 725.
Pedersen, H., Van Paradijs, J., Motch, C., Cominsky, L., Lawrence, A., Lewin, W. H. G., Oda, M., Ohashi, T., and Matsuoka, M.: 1982b, *Astrophys. J.* **263**, 340.
Penninx, W., Damen, E., Tan, J., Lewin, W. H. G., and Van Paradijs, J.: 1989a, *Astron. Astrophys.* **208**, 146.
Penninx, W., Hasinger, G., Lewin, W. H. G., Van Paradijs, J., and Van der Klis, M.: 1989b, *Monthly Notices Roy. Astron. Soc.* **238**, 851.
Penninx, W., Lewin, W. H. G., Mitsuda, K., Van Paradijs, J., Van der Klis, M., and Zijlstra, A. A.: 1990, *Monthly Notices Roy. Astron. Soc.* **243**, 114.
Penninx, W., Lewin, W. H. G., Zijlstra, A. A., Mitsuda, K., Van Paradijs, J., and Van der Klis, M.: 1988, *Nature* **336**, 146.
Penninx, W., Van Paradijs, J., and Lewin, W. H. G.: 1987, *Astrophys. J.* **321**, L67.
Pietsch, W., Steinle, H., Gottwald, M., and Graser, U.: 1986, *Astron. Astrophys.* **157**, 23.
Pines, D.: 1991 in J. Ventura and D. Pines (eds), *Neutron Stars: Theory and Observation*, NATO ASI Series C, **344**, 57.
Pinto, P. A., Taam, R. E., and Laming, J. M.: 1992, *Astrophys. J.* in press.
Ponman, T.: 1984, *Monthly Notices Roy. Astron. Soc.* **201**, 769.
Predehl, P., Hasinger, G., and Verbunt, F.: *Astron. Astrophys.* **246**, L21.
Priedhorsky, W.: 1986, *Astrophys. Sp. Sci.* **126**, 89.
Priedhorsky, W. and Terrell, J.: 1984b, *Astrophys. J.* **284**, L17.
Priedhorsky, W. C. and Terrell, J.: 1984a, *Astrophys. J.* **280**, 661.
Pringle, J. E., Rees, M. J., and Pacholczyk, A. G.: 1973, *Astron. Astrophys.* **29**, 179.
Proctor, R. J., Skinner, G. K., and Willmore, A. P.: 1978, *Monthly Notices Roy. Astron. Soc.* **185**, 745.
Rappaport, S. A. and Joss, P. C.: 1983, in W. H. G. Lewin and E. P. J. van den Heuvel (eds), *Accretion Driven Stellar X-ray Sources* (Cambridge University Press), p. 1.
Rappaport, S. A., Nelson, L. A., Ma, C. P., and Joss, P. C.: 1987, *Astrophys. J.* **322**, 842.
Reynolds, A. P., Bell, S. A., and Hilditch, R. W.: 1992, *Monthly Notices Roy. Astron. Soc.* **256**, 631.
Romani, R.: 1987, *Astrophys. J.* **313**, 718.
Romani, R. W.: 1990, *Nature* **347**, 741.
Rosenbluth, M. N., Ruderman, M., Dyson, F., Bahcall, J., Shaham, J., and Ostriker, J.: 1973, *Astrophys. J.* **184**, 907.
Rutledge, R. E., Lubin, L. M., Lewin, W. H. G., Van Paradijs, J., and Van der Klis, M.: 1993, *Monthly Notices Roy. Astron. Soc.*, submitted.
Ryba, M. F. and Taylor, J. H.: 1991, *Astrophys. J.* **371**, 739.
Rybicki, G. B. and Lightman, A. P.: 1979, *Radiative Processes in Astrophysics* (J. Wiley and Sons).
Ryter, C., Cesarsky, C. R., and Audouze, J.: 1975, *Astrophys. J.* **198**, 103.
Sadeh, D., Byram, E. T., Chubb, T. A., Friedman, H., Hedler, R. L., Meekins, J. F., Wood, K. S., and Yentis, D. J.: 1982, *Astrophys. J.* **257**, 214.
Salpeter, E. E.: 1964, *Astrophys. J.* **140**, 796.
Sansom, A. E., Watson, M. G., Makishima, K., and Dotani, T.: 1989, *Publ. Astron. Soc. Japan* **41**, 591.
Sato, S., Kawara, K., Kobayashi, Y., Maihara, T., Okuda, H., and Jugaku, J.: 1980, *Nature* **286**, 668.
Schaefer, B.: 1990, *Astrophys. J.* **354**, 720.
Schmidtke, P. C.: 1988, *Astron. J.* **95**, 1528.
Schmidtke, P. C. and Cowley, A. P.: 1987, *Astron. J.* **93**, 374.
Schoelkopf, R. J. and Kelley, R. L.: 1991, *Astrophys. J.* **375**, 696.
Seward, F. D., Page, C. G., Turner, M. J. L., and Pounds, K. A.: 1976, *Monthly Notices Roy. Astron. Soc.* **175**, 39P.
Shakura, N. I. and Sunyaev, R. A.: 1973, *Astron. Astrophys.* **24**, 337.
Shakura, N. I. and Sunyaev, R. A.: 1976, *Monthly Notices Roy. Astron. Soc.* **175**, 613.
Shapiro, S. L. and Teukolsky, S. A.: 1983, *Black Holes, White Dwarfs and Neutron Stars* (John Wiley and Sons).
Share, G., Wood, K., Yentis, D., Johnson, N., Shulman, S., Meekins, J., Evans, W., Byram, E., Chubb, T., and Friedman, H.: 1978, *IAU Circular* No. 3190.

Shibazaki, N., and Lamb, F. K.: 1987, *Astrophys. J.*, **318**, 767.
Shibazaki, N., Murakami, T., Shaham, J., and Nomoto, K.: 1989, *Nature* **342**, 656.
Shklovsky, I. S.: 1967, *Astrophys. J.* **148**, L1.
Singh, L. M. and Duorah, H. L.: 1983, *Astrophys. Space Sci.* **92**, 143.
Skinner, G. K., Foster, A. J., Willmore, A. P., and Eyles, C. J.: 1990, *Monthly Notices Roy. Astron. Soc.* **243**, 72.
Skinner, G. K., Willmore, A. P., Eyles, J. C., Bertram, D., Church, M. J., Harper, P. K. S., Herring, J. R. H., Peden, J. C. M., Pollock, A. M. T., Ponman, T. J., and Watt, M. P.: 1987, *Nature* **330**, 544.
Smale, A. P. and Mukai, K.: 1988, *Monthly Notices Roy. Astron. Soc.* **231**, 663.
Smale, A. P., Corbet, R. H. D., Charles, P. A., Menzies, J. W., and Mack, P.: 1986, *Monthly Notices Roy. Astron. Soc.* **223**, 207.
Smale, A. P., Mason, K. O., and Mukai, K.: 1987, *Monthly Notices Roy. Astron. Soc.* **225**, 7P.
Smale, A. P., Mason, K. O., White, N. E., and Gottwald, M.: 1988, *Monthly Notices Roy. Astron. Soc.* **232**, 647.
Smale, A. P., Mason, K. O., Williams, O. R., and Watson, M. G.: 1989, *Publ. Astron. Soc. Japan* **41**, 607.
Spruit, H. C. and Taam, R. E.: 1990, *Astron. Astrophys.* **229**, 475.
Spruit, H. C. and Taam, R. E.: 1993, *Astrophys. J.* in press.
Srinivasan, G., Bhattacharya, D., Muslimov, A. G., and Tsygan, A. I.: 1990, *Current Sci.* **59**, 31.
Stella, L., Haberl, F., Lewin, W. H. G., Parmar, A., Van der Klis, M., and Van Paradijs, J.: 1988b, *Astrophys. J.* **327**, L13.
Stella, L., Haberl, F., Lewin, W. H. G., Parmar, A., White, N. E., and Van Paradijs, J.: 1988a, *Astrophys. J.* **324**, 379.
Stella, L., Kahn, S. M., and Grindlay, J. E.: 1984, *Astrophys. J.* **282**, 713.
Stella, L., Priedhorsky, W., and White, N. E.: 1987a, *Astrophys. J.* **312**, L17.
Stella, L., White, N. E., and Priedhorsky, W.: 1987b, *Astrophys. J.* **315**, L49.
Stock, R.: 1989, *Nature* **337**, 319.
Sugimoto, D., Ebisuzaki, T., and Hanawa, T.: 1984, *Publ. Astron. Soc. Japan* **36**, 839.
Sunyaev, R. A., Titarchuk, L. G: 1986, *Sov. Astron. J. (Letters)* **12**, 359.
Sunyaev, R., Churazov, E., Gilfanov, M. R., Pavlinsky, M., Grebenev, S., Dekhanov, I., Kuznetsov, A., Yamburenko, N. S., Skinner, G. K., Patterson, G. T., Willmore, A. P., Al-Emam, O., Pan, H. C., Nottingham, M. R., Brinkman, A. C., Heise, J., In 't Zand, J. J. M., Jager, R., Ballet, J., Laurent, P., Salotti, L., Nataklucci, L., Niel, M., Roques, J. P., and Mandrou, P.: 1991, *Adv. Space Res.* **11** (8), 177.
Sunyaev, R. A., Gilfanov, M. R., Churazov, E. M., Loznikov, V., Yamburenko, N. S., Skinner, G. K., Patterson, G. T., Willmore, A. P., Al-Emam, O., Brinkman, A. C., Heise, J., In 't Zand, J. J. M., and Jager, R.: 1990, *Sov. Astron. J. Lett.* **16**, 59.
Swank, J. H., Becker, R. H., Boldt, E. A., Holt, S. S., Pravdo, S. H., and Serlemitsos, P. J.: 1977, *Astrophys. J.* **212**, L73.
Swank, J. H., Becker, R. H., Boldt, E. A., Holt, S. S., and Serlemitsos, P. J.: 1978, *Monthly Notices Roy. Astron. Soc.* **182**, 349.
Swank, J. H., Becker, R. H., Pravdo, S. H., Saba, J. R., and Serlemitsos, P. J.: 1976a, *IAU Cirular* 3000.
Swank, J. H., Becker, R. H., Pravdo, S. H., Saba, J. R., and Serlemitsos, P. J.:1976c, *IAU Cirular* 3010.
Swank, J., Becker, R., Pravdo, S., and Serlemitsos, P.: 1976b, *IAU Circular* 2963.
Swank, J. H., Taam, R. E., and White, N. E.: 1984, *Astrophys. J.* **277**, 274.
Sztajno, M., Basinska, E. M., Cominsky, L., Marshall, F. J. and Lewin, W. H. G.: 1983, *Astrophys. J.* **267**, 713.
Sztajno, M., Fujimoto, M. Y., Van Paradijs, J., Vacca, W. D., Lewin, W. H. G., Penninx, W., and Trümper, J.: 1987, *Monthly Notices Roy. Astron. Soc.* **226**, 39.
Sztajno, M., Trümper, J., and Langmeier, A.: 1984, in: M. Oda and R. Giacconi (eds) *X-ray Astronomy '84*, (ISAS), p. 111.
Sztajno, M., Van Paradijs, J., Lewin, W. H. G., Langmeier, A., Trümper, J., and Pietsch, W.: 1986, *Monthly Notices Roy. Astron. Soc.* **222**, 499.

Sztajno, M., Van Paradijs, J., Lewin, W. H. G., Trümper, J., Stollman, G., Pietsch, W., and Van der Klis, M.: 1985, *Astrophys. J.* **299**, 487.
Taam, R. E.: 1980, *Astrophys. J.* **241**, 351.
Taam, R. E.: 1981a, *Astrophys. J.* **247**, 257.
Taam, R. E.: 1981b, *Ap. Space Sci.* **77**, 257.
Taam, R. E.: 1982, *Astrophys. J.* **258**, 761.
Taam, R. E.: 1985, *Ann. Rev. Nuc. Part. Sci* **35**, 1.
Taam, R. E. and Lin, D. N. C.: 1984, *Astrophys. J.* **287**, 761.
Taam, R. E. and Picklum, R. E.: 1978, *Astrophys. J.* **224**, 210.
Taam, R. E. and Picklum, R. E.: 1979, *Astrophys. J.* **233**, 327.
Taam, R. E. and Van den Heuvel, E. P. J.: 1986, *Astrophys. J.* **305**, 235.
Taam, R. E., Woosley, S. E., Weaver, T. A., and Lamb, D. Q.: 1993, submitted to *Astrophys. J.*
Takagishi, K., Nagareda, K., Matsuoka, M., Fujii, M., Sato, S., Van Paradijs, J., Hoffman, J. A., Jernigan, G., Wheaton, W., Primini, F., and Lewin, W. H. G.: 1978, *ISAS Research Note* 60.
Tan, J., Lewin, W. H. G., Lubin, L. M., Van Paradijs, J., Penninx, W., Damen, E., and Stella, L.: 1991a, *Monthly Notices Roy. Astron. Soc.* **251**, 1.
Tan, J., Morgan, E., Lewin, W. H. G., Penninx, W., Van der Klis, M., Van Paradijs, J., Makishima, K., Inoue, H., Dotani, T., and Mitsuda, K.: 1991b, *Astrophys. J.* **374**, 291.
Tanaka, Y. and Lewin, W. H. G.: 1993, in W. H. G. Lewin, J. van Paradijs, and E. P. J. van den Heuvel (eds), *X-ray Binaries*, Cambridge University Press, in press.
Tananbaum, H., Chaisson, L. J., Forman, W., Jones, C., and Matilsky, T. A.: 1976, *Astrophys. J.* **209**, L125.
Tarenghi, M. and Reina, C.: 1972, *Nature Phys. Sci.* **240**, 53.
Tavani, M.: 1991, *Nature* **351**, 39.
Tawara, Y., Hayakawa, S., and Kii, T.: 1984c, *Publ. Astron. Soc. Japan* **36**, 845.
Tawara, Y., Hayakawa, S., Kunieda, H., Makino, F., and Nagase, F.: 1982, *Nature* **299**, 38.
Tawara, Y., Hirano, T., Kii, T., Matsuoka, M., and Murakami, T.: 1984b, *Publ Astron. Soc. Japan* **36**, 861.
Tawara, Y., Kawai, N., Tanaka, Y., Inoue, H., Kunieda, H., and Ogawara, Y.: 1985, *Nature* **318**, 545.
Tawara, Y., Kii, T., Hayakawa, S., Kunieda, H., Masai, K., Nagase, F., Inoue, H., Koyama, K., Makino, F., Makishima, K., Matsuoka, M., Murakami, T., Oda, M., Ogawara, Y., Ohashi, T., Shibazaki, N., Tanaka, Y., Miyamoto, S., Tsunemi, H., Yamashita, K., and Kondo, I.: 1984a, *Astroph. J.* **276**, L41.
Taylor, J. H. and Weisberg, J. M. 1989, *Astrophys. J.* **345**, 434.
Tennant, A. F.: 1987, *Monthly Notices Roy. Astron. Soc.* **226**, 971.
Tennant, A. F.: 1988, *Monthly Notices Roy. Astron. Soc.* **230**, 403.
Tennant, A. F., Fabian, A. C., and Shafer, R. A.: 1986a, *Monthly Notices Roy. Astron. Soc.* **219**, 871.
Tennant, A. F., Fabian, A. C., and Shafer, R. A.: 1986b, *Monthly Notices Roy. Astron. Soc.* **221**, 27P.
Thomas, R. M., Duldig, M. L., Haynes, R. F., Simons, L. W., Murdin, P., Hoffman, J. A., Lewin, W. H. G., Wheaton, W., and Doty, J.: 1979, *Monthly Notices Roy. Astron. Soc.* **187**, 299.
Thorne, K. S.: 1977, *Astrophys. J.* **212**, 825.
Thorstensen, J. R. and Charles, P. A.: 1982, *Astrophys. J.* **253**, 756.
Thorstensen, J. R., Brownsberger, K. R., Mook, D. E., the Off-Campus Program Students, Remillard, R. A., McClintock, J. E., Koo, D. C., and Charles, P. A.: 1988, *Astrophys. J.* **334**, 430.
Thorstensen, J., Charles, P., and Bowyer, S.: 1978, *Astrophys. J.* **220**, L131.
Thorstensen, J. R., Charles, P. A., and Bowyer, S.: 1980, *Astrophys. J.* **238**, 964.
Thorstensen, J., Charles, P., Bowyer, S., Briel, U. G., Doxsey, R. E., Griffiths, R. E., and Schwartz, D. A.: 1979, *Astrophys. J.* **233**, L57 [err.: **237**, L25].
Tillett, J. C. and MacDonald, J.: 1992, *Astrophys. J.* **388**, 555.
Titarchuk, L. G.: 1988, *Sov. Astron. J. (Letters)* **14**, 229.
Trümper, J., Pietsch, W., Reppin, C., Secco, B., Kendziorra, E., and Staubert, R.: 1977, *Ann. New York Acad. Sci.* **302**, 538.
Trümper, J., Van Paradijs, J., Sztajno, M., Lewin, W. H. G., Krautter, J., Stollman, G., and Van der Klis, M.: 1985, *Space Sci. Rev.* **40**, 255.
Tsuruta, S.: 1986, *Comm. Astrophys.* **11**, 51.

Turner, M. J. L., and Breedon, L. M.: 1984, *Monthly Notices Roy. Astron. Soc.* **208**, 29P.
Turner, M. J. L., Breedon, L. M., Ohashi, T., Courvoisier, T., Inoue, H., Matsuoka, M., Pedersen, H., Van Paradijs, J., and Lewin, W. H. G.: 1985, *Space Sci. Rev.* **40**, 249.
Ulmer, M. P., Hjellming, R. M., Lewin, W. H. G., Hoffman, J. A., Jernigan, J. G., Wheaton, W., Primini, F., Doty, J., and Marshall, H.: 1978, *Nature* **276**, 799.
Ulmer, M. P., Lewin, W. H. G., Hoffman, J. A., Doty, J., and Marshall, H.:1977, *Astrophys. J.* **214**, L11.
Vacca, W. D., Lewin, W. H. G., and Van Paradijs, J.: 1986, *Monthly Notices Roy. Astron. Soc.* **220**, 339.
Van Amerongen, S., Pedersen, H., and Van Paradijs, J.: 1987, *Astron. Astrophys.* **185**, 147.
Van den Heuvel, E. P. J. and Verbunt, F.: 1993, in W. H. G. Lewin, J. van Paradijs, and E. P. J. van den Heuvel (eds), *X-ray Binaries*, Cambridge University Press, Cambridge, in press.
Van den Heuvel, E. P. J., Van Paradijs, J., and Taam, R. E.: 1986, *Nature* **322**, 153.
Van der Klis, M.: 1989, *Ann. Rev. Astron. Astrophys.* **27**, 517.
Van der Klis, M.: 1993, in W. H. G. Lewin, J. van Paradijs, and E. P. J. van den Heuvel (Eds), *X-ray Binaries* (Cambridge University Press), in press.
Van der Klis, M. and Lamb, F. K.: 1993, *Astron. Astrophys. Rev.* (in press).
Van der Klis, M., Hasinger, G., Damen, E., Penninx, W., Van Paradijs, J., and Lewin, W. H. G.: 1990, *Astrophys. J.* **360**, L19.
Van der Klis, M., Hasinger, G., Dotani, T., Mitsuda, K., Verbunt, F., Murphy, B. W., Van Paradijs, J., Belloni, T., Makishima, K., Morgan, E., and Lewin, W. H. G. : 1993, *Monthly Notices Roy. Astron. Soc.* **260**, 686.
Van der Klis, M., Jansen, F., Van Paradijs, J., Lewin, W. H. G., Van den Heuvel, E. P. J., Trümper, J. E., and Sztajno, M.: 1985a, *Nature* **316**, 225.
Van der Klis, M., Jansen, F., Van Paradijs, J., and Stollman, G.: 1985b, *Space Sci. Rev.* **40**, 287.
Van Horn, H. M. and Hansen, C. J.: 1974, *Astrophys. J.* **191**, 479.
Van Kerkwijk, M., Van Paradijs, J., Zuiderwijk, E. J., Hammerschlag-Hensberge, G., Kaper, L., and Sterken, C.: 1993, *Astron. Astrophys.* (in press).
Van Paradijs, J.: 1978, *Nature* **274**, 650.
Van Paradijs, J.: 1979, *Astrophys. J.* **234**, 609.
Van Paradijs, J.: 1981, *Astron. Astrophys.* **103**, 140.
Van Paradijs, J.: 1982, *Astron. Astrophys.* **107**, 51.
Van Paradijs, J.: 1983, in W. H. G. Lewin and E. P. J. van den Heuvel (eds), *Accretion Driven Stellar X-ray Sources* (Cambridge University Press), p. 191.
Van Paradijs, J.: 1985, in Y. Tanaka and W. H. G. Lewin (eds), *Japan-US Seminar on Galactic and Extragalactic Compact X-ray Sources* (ISAS), p. 79.
Van Paradijs, J.: 1991, in J. Ventura and D. Pines (eds), *Neutron Stars : Theory and Observations*, (Kluwer Academic Publ.), NATO ASI Series C, **344**, p. 245.
Van Paradijs, J.: 1993, in W. H. G. Lewin, J. van Paradijs, and E. P. J. van den Heuvel (Eds), *X-ray Binaries* (Cambridge University Press), in press.
Van Paradijs, J. and Isaacman, R.: 1989, *Astron. Astrophys.* **222**, 129.
Van Paradijs, J. and Lewin, W. H. G.: 1985a, *Astron. Astrophys.* **142**, 361.
Van Paradijs, J. and Lewin, W. H. G.: 1985b, *Astron. Astrophys.* **157**, L10.
Van Paradijs, J. and Lewin, W. H. G.: 1987, *Astron. Astrophys.* **172**, L20.
Van Paradijs J. and McClintock, J.E.: 1993, in W. H. G. Lewin, J. van Paradijs, and E. P. J. van den Heuvel (eds), *X-ray Binaries*, Cambridge University Press, in press.
Van Paradijs, J. A., Cominsky, L., and Lewin, W. H. G.: 1979b, *Monthly Notices Roy. Astron. Soc.* **189**, 387.
Van Paradijs, J., Dotani, T., Tanaka, Y., and Tsuru, T.: 1990a, *Publ. Astron. Soc. Japan* **42**, 633.
Van Paradijs, J., Joss, P. C., Cominsky, L., and Lewin, W. H. G.: 1979a, *Nature* **280**, 375.
Van Paradijs, J., Pedersen, H., and Lewin, W. H. G.: 1981, *IAU Circular* No. 3626.
Van Paradijs, J., Penninx, W., and Lewin, W. H. G.: 1988a, *Monthly Notices Roy. Astron. Soc.* **233**, 437.
Van Paradijs, J., Penninx, W., Lewin, W. H. G., Sztajno, M., and Trümper, J.: 1988b, *Astron. Astrophys.* **192**, 147.

Van Paradijs, J., Sztajno, M., Lewin, W. H. G., Trümper, J., Vacca, W. D., and Van der Klis, M.: 1986a, *Monthly Notices Roy. Astron. Soc.* **221**, 617.
Van Paradijs, J., Van der Klis, M., and Pedersen, H.: 1988c, *Astron. Astrophys. Suppl.* **76**, 185.
Van Paradijs, J., Van der Klis, M., Van Amerongen, S., Pedersen, H., Smale, A. P., Mukai, K., Schoembs, R., Haefner, R., Pfeiffer, M., and Lewin, W. H. G.: 1990b, *Astron. Astrophys.* **234**, 181.
Van Paradijs, J., Verbunt, F., Shafer, R. A., and Arnaud, K. A.: 1987, *Astron. Astrophys.* **182**, 47.
Van Paradijs, J., Verbunt, F., Van der Linden, T., Pedersen, H., and Wamsteker, W.: 1980, *Astrophys. J.* **241**, L161.
Van Riper, K. A.: 1988, *Astrophys. J.* **329**, 339.
Verbunt, F. and Zwaan, C.: 1981, *Astron. Astrophys.* **100**, L17.
Verbunt, F., Hasinger, G., Johnston, H. M., and Bunk, W.: 1993, *Proceedings of Cospar Meeting*, Washington, DC, September 1992.
Verbunt, F., Wijers, R. A. M. J., and Burm, H.: 1990, *Astron. Astrophys.* **234**, 195.
Wade, R. A., Quintana, H., Horne, K., and Marsh, T. R.: 1985, *Publ. Astron. Soc. Pacific* **97**, 1092.
Waki, I.: 1984, Ph.D. Thesis, University of Tokyo (*ISAS Research Note* 277).
Waki, I., Inoue, H., Koyama, K., Matsuoka, M., Murakami, T., Ogawara, Y., Ohashi, T., Tanaka, Y., Hayakawa, S., Tawara, Y., Miyamoto, S., Tsunemi, H., and Kondo, I.: 1984, *Publ. Astron. Soc. Japan*, **36**, 819.
Walker, M. A.: 1992, *Astrophys. J.* **385**, 651.
Walker, M. A. and Meszaros, P.: 1989, *Astrophys. J.* **346**, 844.
Wallace, R. K. and Woosley, S. E.: 1981, *Astroph. J. Suppl.* **45**, 389.
Wallace, R. K. and Woosley, S. E.: 1985, in S. E. Woosley (ed) *High Energy Transients in Astrophysics*, AIP Conf. Proc. No. 115, (New York, AIP Press), 319.
Wallace, R. K., Woosley, S. E. and Weaver, T. A.: 1982, *Astrophys. J.* **258**, 696 (err. **264**, 746).
Walter, F. M., Bowyer, S., Mason, K. O., Clarke, J. T., Henry, J. P., Halpern, J., and Grindlay, J. E.: 1982, *Astrophys. J.* **253**, L67.
Warner, B.: 1976, in P. Eggleton, S. Mitton, and J. Whelan (eds), *Structure and Evolution of Close Binary Stars* , IAU Symp. No. 73 (Reidel Publ. Cy), p. 85.
Warwick, R. S., Marshall, N., Fraser, G. W., Watson, M. G., Lawrence, A., Page, G. C., Pounds, K. A., Ricketts, M. J., Sims, M. R., and Smith, A.: 1981, *Monthly Notices Roy. Astron. Soc.* **197**, 865.
Warwick, R. S., Norton, A. J., Turner, M. J. L., Watson, M. G., and Willingdale, R.: 1988, *Monthly Notices Roy. Astron. Soc.* **232**, 551.
Wasserman, I. and Shapiro, S. L.: 1983, *Astrophys. J.* **265**, 1036.
Watson, M. G., Willingdale, R., Grindlay, J. E., and Hertz, P.: 1981, *Astrophys. J.* **250**, 142.
White, N. E. and Holt, S. S.: 1982, *Astrophys. J.* **257**, 318.
White, N. E. and Swank, J. H.: 1982, *Astrophys. J.* **253**, L61.
White, N. E., Charles, P. A., and Thorstensen, J. R.: 1980, *Monthly Notices Roy. Astron. Soc.* **193**, 731.
White, N. E., Kaluzienski, L., Swank, J. H.: 1984, in S. E. Woosley (ed.), *High Energy Transients in Astrophysics*, AIP Conf. Proceedings No. 115, p. 41.
White, N. E., Mason, K. O, Carpenter, G. F., and Skinner, G. K.: 1978a, *Monthly Notices Roy. Astron. Soc.* **184**, 1P.
White, N. E., Mason, K. O., Huckle, H. E., Charles, P. A., and Sanford, P. W.: 1976, *Astrophys. J.* **209**, L119.
White, N. E., Mason, K. O., Sanford, P. W., Johnson, H. M., and Catura, R. C.: 1978b, *Astrophys. J.* **220**, 600.
White, N. E., Nagase, F., and Parmar, A.: 1993, in W. H. G. Lewin, J. van Paradijs, and E. P. J. van den Heuvel (eds), *X-ray Binary Stars*, Cambridge University Press, in press.
White, N. E., Peacock, A., Hasinger, G., Mason, K. O., Manzo, G., Taylor, B. G., and Branduardi-Raymont, G.: 1986, *Monthly Notices Roy. Astron. Soc.* **218**, 129.
White, N. E., Stella, L., and Parmar, A. N.: 1988, *Astrophys J.* **324**, 363.
Whitehurst, R.: 1988, *Monthly Notices Roy. Astron. Soc.* **232**, 35.
Wolszczan, A.: 1991, *Nature* **350**, 688.

Wood, K. S., Meekins, J. F., Yentis, D. J., Smathers, H. W., McNutt, D. P., Bleach, R. D., Byram, E. T., Chubb, T. A., Friedman, H., and Meidav, M.: 1984, *Astrophys. J. Suppl.* **56**, 507.
Woosley, S. E. and Taam, R. E.: 1976, *Nature* **263**, 101.
Woosley, S. E. and Weaver, T. A.: 1985, in S. E. Woosley (ed) *High Energy Transients in Astrophysics*, AIP Conf. Proc. No. 115, (New York, AIP Press), 273.
Zel'dovich, Ya. B.: 1964, *Soviet Phys.* Vol. 9, reprinted in: R. Giacconi and R. Ruffini, *Neutron Stars, Black Holes and Binary X-ray Sources*, Astrophys. and Space Sci. Library Vol. 48 (Reidel Publ. Cy), p. 329.
Zel'dovich, Ya. B. and Shakura, N. I.: 1969, *Sov. Astron. J.* **13**, 175.
Zinn, R.: 1980, *Astrophys. J. Suppl.* **42**, 19.

BOOK REVIEWS

Space Science Reviews **62:** 391, 1993.